Optimal Supply Chain and Product Design of Biofuels

A DISSERTATION
SUBMITTED TO THE FACULTY OF THE GRADUATE SCHOOL
OF THE UNIVERSITY OF MINNESOTA
BY

William Alexander Marvin

IN PARTIAL FULFILLMENT OF THE REQUIREMENTS
FOR THE DEGREE OF
Doctor of Philosophy

Advised by Prodromos Daoutidis and Lanny D. Schmidt

August 2013

Acknowledgments

I would like to thank my advisers, Professor Prodromos Daoutidis and Professor Lanny D. Schmidt, for providing me the opportunity to work on these projects and for being so supportive of the research direction. They have helped me become the researcher I am now through countless hours of meetings and presentations, by pushing me to consider the bigger picture and the usefulness of my findings, while also urging that I "don't worrying about it" (as Prodromos would often say with a wink and a nod, followed by "And we'll go from there."). I also thank Professor Saif Benjaafar for his excellent course on inventory control that inspired me to study supply chain optimization, and Douglas G. Tiffany for his feedback and technical expertise on biomass.

Additionally, I would like to thank my Daoutidis group office-mates over the years Dr. Fernando V. Lima, Dr. Milana Trifkovic, Dr. Sujit Jogwar, Ana I. Torres, Dimitris Georgis, Srinivas Rangarajan, Seongmin Heo, Adam Kelloway, Abdulla Malek, Nahla Al Amoodi, Michael Zachar, Udit Gupta, and Mustafa Caglayan. I have been incredibly fortunate to work alongside such wonderful people. In particular, I've enjoyed collaborating with Srinivas on biofuel product design, Adam on biorefinery process design, and Milana on microgrid energy system control and real-time optimization. I will miss our group's lively discussions and 2pm coffee time "caffeination for researchination".

Also, I want to thank all my friends in CEMS who have enriched my graduate student life, particularly Garrett Swindlehurst and Bryan Paulsen. Lastly, I am indebted to my family and loved ones, especially my mother, sister and Samia Ilias, for the unconditional love and encouragement.

To My Family

Executive Summary

Growth of a biomass-to-biofuels industry has the potential to reduce oil imports, support agriculture and forestry growth, foster a domestic biorefinery industry, and reduce greenhouse gas emissions compared to gasoline. Unfortunately, relative to petroleum, biomass is a distributed and low energy density resource that can be costly to collect. Furthermore, biomass is a complicated set of feedstocks each with non-uniform composition including grains, crop residues, wood, municipal waste and landfill gas. Nonetheless, biomass is the only renewable source of carbon and a potential resource to substitute fossil hydrocarbons in the production of fuels and chemicals. Biomass can therefore play a key role in mitigating the heavy dependence on fossil carbon.

Successful development of biofuels involves Process Systems Engineering challenges at various scales, including elucidation of complex chemical systems for upgrading biomass in terms of mechanisms, kinetics and thermochemistry, design of novel reactors and reactor networks, synthesis and optimization of novel process flow sheets, and supply chain optimization at the enterprise level. These scales are interdependent, as shown in Figure 1. None of these aspects exist in isolation; each choice impacts the others and has an important role in the overall economic potential.

This thesis addresses important practical problems related to the feasibility of converting biomass that is plentiful in the Midwest into valuable biofuels and coproducts. The two fronts of supply chain and chemistry are investigated to determine (i) important parameters, (ii) optimal decisions, (iii) robustness of decisions given parameter uncertainty, and (iv) best case estimates for economics and environmental impact. These

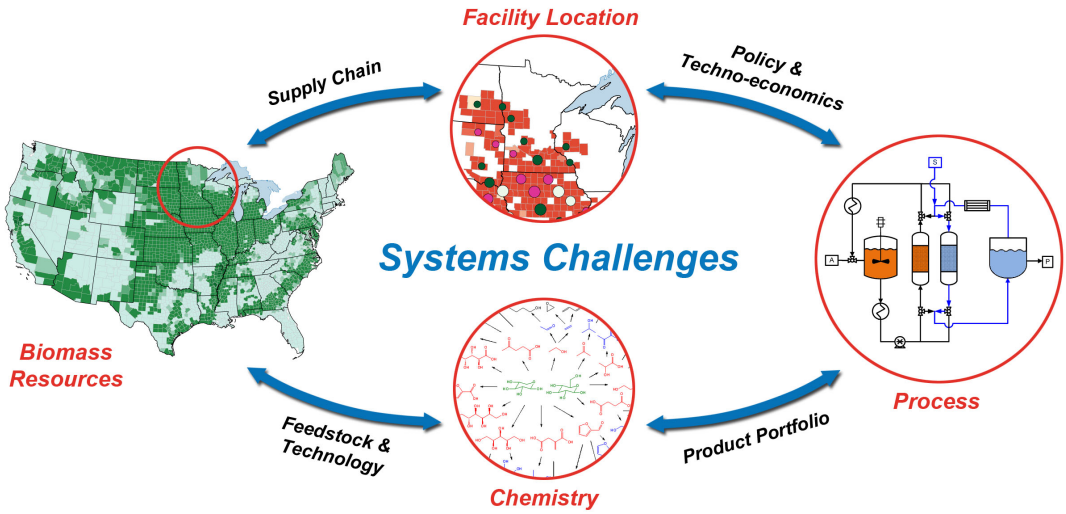

Figure 1: Relationship between various scales of the Process Systems Engineering analysis of biofuels (reprinted from the January 2013 cover of the *AIChE Journal* by Daoutidis et al. [1]).

fronts are unified by the development and application of mathematical optimization models, specifically mixed integer linear programs.

The biofuel supply chain optimization problems were formulated to determine economical and environmentally efficient biomass processing facility locations and capacities, simultaneously with biomass harvest and distribution. Focus was put on the production of biofuels in the Midwestern United States from grain, agricultural residues, energy crops and wood resources, and the feasibility of meeting governmental biofuel mandates in 2015. Sensitivity analysis was performed to elucidate the impact of price uncertainty on the robustness of the supply chain and whether or not the proposed biorefineries will be built or will fail financially after being built. Seven biomass processing technologies that are expected to be commercialized in the near-term are available for construction at each candidate facility site. A detailed cash flow analysis that includes capital depreciation and taxation is embedded into the model formulation to give insights into the minimum biofuel selling price for each facility site. Pareto optimal supply chain configurations were identified for the two objectives of maximizing net present value and minimizing greenhouse gas emissions of the entire supply chain. This enables the identification of supply chain decisions that greatly reduce greenhouse gas emissions for minimal economic losses.

The product design problem investigated was for the production of blended gasoline with biomass-derived components. It involved the simultaneous product design and chemistry selection to exploit the chemical structure of biomass (e.g. carbohydrate-rich with C:O ratio of 1:1, lipids, and oxygen present in different functional forms, such as hydroxyl, ether and carbonyl groups). The strategy consists of i) constructing an exhaustive network of reactions consistent with an input set of chemistry rules and ii) using the network information to formulate and solve an optimization problem that yields an optimal product distribution and the sequence of reactions that synthesize them. We used this strategy to identify potential renewable oxygenates and hydrocarbons obtained from heterogeneous catalysis of biomass that can be blended with gasoline to satisfy ASTM specifications. Multiple objectives (energy loss, catalyst requirement and absolute heat duty) were considered and multiple alternative solutions were found in each case. We identified that both oxygenates and hydrocarbons are components of optimal blends for the energy loss objective, but the other two objectives produce only oxygenates. The proposed strategy is flexible enough to be applicable for any problem involving concurrent product and chemistry selection.

Contents

Acknowledgments **i**

Executive Summary **iii**

Table of Contents **vi**

List of Tables **x**

List of Figures **xii**

1 Introduction **1**

1.1 Biomass and biofuels 1

1.2 Current biofuel industry 3

1.3 Policy 4

1.4 Chemistry and Biofuel Products 6

1.5 Thesis scope and organization 7

2 Background on Optimization **9**

2.1 Linear programming 9

2.2 Mixed integer linear programming 12

3 Economic Supply Chain Optimization for Cellulosic Ethanol **16**

3.1 Summary 16

3.2 Introduction 16
3.3 Optimization problem formulation 21
3.4 Case study parameters 26
3.4.1 Biomass supply 26
3.4.2 Biomass producing locations 28
3.4.3 Biorefinery locations 28
3.4.4 Biomass transportation distance and cost 29
3.4.5 Biomass cost 29
3.4.6 Ethanol sale price 30
3.4.7 Biorefinery costs and capacities 31
3.4.8 Internal Rate of Return (IRR) 33
3.5 Software 35
3.6 Results 35
3.6.1 Base case 35
3.6.2 Sensitivity analysis 37
3.6.3 Monte Carlo analysis 38
3.7 Conclusions 42

4 Economic Supply Chain Optimization with Competing Biorefinery Technologies and Diverse Biomass Feedstocks 45
4.1 Summary 45
4.2 Supply chain overview 46
4.3 Mathematical formulation 47
4.3.1 Objective function 47
4.3.2 Material flow constraints 50
4.3.3 Cash flow and facility capacity constraints 53
4.4 Case study parameters 58
4.4.1 Biomass resources 58
4.4.2 Existing facilities 59
4.4.3 Candidate sites 64
4.4.4 Biomass processing technologies 64
4.4.5 Markets 71
4.4.6 Transportation 72
4.5 Results 73
4.5.1 No RFS2 mandates 73

4.5.2 Mandated biofuel production 82
4.6 Conclusions 87
4.7 Supporting information 87
4.7.1 Objective function parameters 87
4.7.2 Biofuel technology parameters 92
4.7.3 Facility capacities 95
4.8 Notation 104

5 Multiobjective Supply Chain Optimization for Biofuels 109
5.1 Summary 109
5.2 Multiobjective optimization and Pareto optimality 109
5.3 Mathematical formulation 113
5.4 Solution strategy 115
5.5 Life cycle analysis 116
5.6 Emission parameters 118
5.7 Results 120
5.7.1 Pareto Frontiers 120
5.7.2 Key Pareto points 121
5.8 Conclusions 131

6 Automated Generation and Optimal Selection of Biofuel-Gasoline Blends and Their Synthesis Routes 133
6.1 Summary 133
6.2 Introduction 134
6.3 Product and chemistry selection strategy 135
6.3.1 Reaction network construction 135
6.3.2 Optimization framework 139
6.3.3 Objective functions 139
6.3.4 Constraints 141
6.3.5 Optimization program and solution strategy 145
6.4 Results: gasoline blend alternatives 146
6.4.1 Oxygenates 147
6.4.2 Hydrocarbons and oxygenates 150
6.4.3 Other objective functions 152
6.5 Discussion 152

6.6 Conclusions 154
6.7 Supporting information 155
6.7.1 Reaction network construction 155
6.7.2 Reaction cycle enumeration algorithm 155
6.7.3 Alternative solution algorithm 156
6.7.4 Other objective function results 158
6.7.5 Sensitivity analysis 162

7 Future Work **165**
7.1 Supply chain optimization future work 165
7.1.1 Optimization under uncertainty 167
7.2 Product design future work 169

Bibliography **171**

List of Tables

3.1 Subscripts. 23
3.2 Parameters. 24
3.3 Decision variables. 24
3.4 Crop to residue ratio and moisture content of selected crops. 27
3.5 Biomass collection and local storage costs. 30
3.6 Biorefinery capital costs. 32
3.7 Biorefinery operating costs. 33
3.8 Sugar conversions by mass fraction. 34
3.9 Feedstock composition by mass fraction and predicted ethanol yield. . . 34
3.10 Base case result breakdown of cost sources. 37
3.11 Base case model biomass utilization. 38
3.12 Variability of model parameters. 41

4.1 Biomass processing technologies 67
4.2 Reference facility capacity and economics 68
4.3 Coproduct and other variable costs 68
4.4 Economic analysis assumptions 69
4.5 NPV scaling factors 70
4.6 FCI linearization parameters $CF_{l,j}^{\text{linear,FCI}}$ in \$M 71
4.7 Transportation parameters: distance variable and fixed cost 73

4.8 Fraction of feedstock used by each technology for the case of no RFS2 mandates. 77
4.9 Total biomass utilization and costs for the case of no RFS2 mandates. . 77
4.10 Total biofuel production and costs for the case of no RFS2 mandates. . 78
4.11 Total biomass utilization and costs for the case of strict biofuel mandates. 83
4.12 Total biofuel production and costs for the case of strict biofuel mandates. 83
4.13 MACRS depreciation schedules 91
4.14 Biofuel production in mgy at existing facilities 96
4.15 Biofuel production in mgy at candidate sites 102

5.1 A priori methods for multiobjective optimization problems. 112
5.2 Emission parameter values for biomass production. 118
5.3 Emission parameter values for biomass transportation. 119
5.4 Emission parameter values for biorefinery operation. 119
5.5 Emission parameter values for biofuel transportation. 119
5.6 Emission parameter values for market/customer product use (e.g. biofuel combustion). 119

6.1 Blend properties and required specifications 144
6.2 Alternative solutions of (MP) with $Z = \Delta E$ when the set of allowed outputs are 15 oxygenate compounds. 149
6.3 Alternative solutions of (MP) with $Z = \Delta E$ when the set of allowed outputs are 15 oxygenates and 157 hydrocarbons. 151
6.4 Cycles identified in the reaction network. 156
6.5 Alternative solutions with $Z = R^{\text{cat}}$ when the set of allowed outputs are 15 oxygenate compounds. 160
6.6 Alternative solutions with $Z = H^{\text{abs}}$ when the set of allowed outputs are 15 oxygenate compounds. 161
6.7 Alternative solutions with $Z = R^{\text{cat}}$ when the set of allowed outputs are 15 oxygenates and 157 hydrocarbons. Water absorption is limited to 2 wt%. 162
6.8 Alternative solutions with $Z = R^{\text{cat}}$ when the set of allowed outputs are 15 oxygenates and 157 hydrocarbons. LHV must be higher than 32 kJ/mL. 164

List of Figures

1 Relationship between various scales of the Process Systems Engineering analysis of biofuels. iv

1.1 U.S. corn use from 1980 to 2011. 4
1.2 Renewable fuel standard (RFS) mandate, by type, 2008-2022. 5

2.1 Example LP with inequality, equality and nonnegative constraints shown. A basic solution is shown at (4,3). 11
2.2 Branch and bound tree example. 14

3.1 DOE supported integrated biorefinery projects by capacity and conversion technology. 18
3.2 Crop residue availability in the United States by county. 22
3.3 The 535 biomass producing counties and 69 candidate biorefinery locations included in the case study. 27
3.4 Base case optimal supply chain with installed biorefinery capacity in million gallons per year (MGY). Total biomass harvest in thousand dry metric tons per year (kdt/year). 36
3.5 Effect of varying ethanol sale price with other base case parameters fixed. 39
3.6 Effect of varying biorefinery capital investment and operating cost with other base case parameters fixed. 39

3.7 Effect of varying conversion efficiency with other base case parameters fixed. 40
3.8 Monte Carlo method sampling of the parameter space for the base case optimum supply chain configuration. 41
3.9 Percentage of trials in which each candidate biorefinery location was selected in 200 model runs, each using a randomly sampled parameter set. Biomass producing counties are shaded. 43
3.10 Internal Rate of Return for 200 model optimization trials sampled from the parameter space. 44
3.11 Total number of installed NREL SOT 2008 biochemical benchmark biorefineries for 200 model optimization trials sampled from the parameter space. 44

4.1 Simplified supply chain schematic for a biomass producer. 51
4.2 Simplified supply chain schematic for a facility site. 51
4.3 Simplified supply chain schematic for a market. 53
4.4 Piecewise linearization of fixed capital investment (FCI). 55
4.5 Maximum biomass resource availability. Farmgate price for each county not shown. 63
4.6 The 159 existing facilities considered in the case study. Installed capacity in million gallons per year (mgy). 65
4.7 The 98 candidate sites with none nearer than 50 miles. 66
4.8 Optimum supply chain configuration for the case of no RFS2 mandates. Installed facility capacity shown in million gallons per year (mgy). Renewable fuel (RF), advanced biofuel (AB) and cellulosic biofuel (CB) are produced. Perennial grasses were available but were not utilized in the optimum supply chain. 76
4.9 Breakdown of cost sources for installed technologies. Existing facilities are denoted by an asterisk (*). New facilities of technologies $l = \{1, 3, 4, 7\}$ were not constructed in the optimum supply chain. 79
4.10 Minimum biofuel selling price. 80
4.11 Biofuel production curve. Advanced biofuel (AB) price and cellulosic biofuel (CB) price are 0.475 and 0.675 $/gal higher than the RF price, respectively. 81
4.12 Biofuel production curve for cellulosic biofuel only. The national RFS2 mandate for 2015 is also shown. 82

4.13 Optimum supply chain configuration for the case of strict biofuel mandates. Installed facility capacity shown in million gallons per year (mgy). Renewable fuel (RF), advanced biofuel (AB) and cellulosic biofuel (CB) are produced. Perennial grasses were available but were not utilized in the optimum supply chain. 86

5.1 Example Pareto Frontier for maximization of TNPV and minimization of TGHG. The feasible region for the optimization problem is shown with its efficient boundary being the Pareto Frontier. Point (a) is infeasible, point (b) is a Pareto point, and point (c) is feasible but is dominated by point (b). 110
5.2 System boundary of the biofuel life cycle analysis. 117
5.3 Pareto Frontiers for the scenarios of no biofuel mandates and strict mandates. 120
5.4 Total biofuel production for each Pareto point. 122
5.5 Optimum supply chain configuration for the lowest TGHG Pareto point in the case of strict biofuel mandates with fuel credits. Installed facility capacity shown in million gallons per year (mgy). Renewable fuel (RF), advanced biofuel (AB) and cellulosic biofuel (CB) are produced. 126
5.6 Breakdown of cost sources for installed technologies for the lowest TGHG Pareto point in the case of strict biofuel mandates with fuel credits. Existing facilities are denoted by an asterisk (*). New facilities of technologies $l = \{5, 6\}$ were not constructed in the optimum supply chain. 127
5.7 Breakdown of emission sources for installed technologies for the lowest TGHG Pareto point in the case of strict biofuel mandates with fuel credits. Net emissions per gallon of produced biofuel is also shown. Existing facilities are denoted by an asterisk (*). New facilities of technologies $l = \{5, 6\}$ were not constructed in the optimum supply chain. 128
5.8 Optimum supply chain configuration for the "Balanced" Pareto point in the case of strict biofuel mandates with fuel credits. Installed facility capacity shown in million gallons per year (mgy). Renewable fuel (RF), advanced biofuel (AB) and cellulosic biofuel (CB) are produced. Forestry resources and perennial grasses were available but were not utilized in the optimum supply chain. 130

5.9 Breakdown of cost sources for installed technologies for the "Balanced" Pareto point in the case of strict biofuel mandates with fuel credits. Existing facilities are denoted by an asterisk (*). New facilities of technologies $l = \{4, 5, 6, 7\}$ were not constructed in the optimum supply chain. 131
5.10 Breakdown of emission sources for installed technologies for the "Balanced" Pareto point in the case of strict biofuel mandates with fuel credits. Net emissions per gallon of produced biofuel is also shown. Existing facilities are denoted by an asterisk (*). New facilities of technologies $l = \{4, 5, 6, 7\}$ were not constructed in the optimum supply chain. 132

6.1 Proposed strategy for connecting automated network generation and optimization. 136
6.2 Initial reactants input into RING. 137
6.3 Parity plot of experimental and predicted heat of formation and reaction values of a representative set of hydrocarbons and oxygenates. All values are in kJ/mol. Prediction is based on group additivity method in RING. See Supporting Information for more details. 138
6.4 Chemical process envisioned to convert biomass-derived platform chemicals to gasoline. The decision variables for the optimization problem are shown. 139
6.5 An example of reactions that must occur together – the dehydration of a diol molecule. These two reactions are $j = \{2396, 2397\}$ in the reaction network. 142
6.6 An example of reactions which are related such that if the reaction occurs, some other reaction(s) must also occur. If the top reaction (an aldol condensation) occurs, the bottom reaction (a self-condensation) must also occur, because the reactant molecule (acetaldehyde) can undergo self-condensation. These two reactions are $j = \{59, 62\}$ in the reaction network. 142
6.7 The 15 oxygenate molecules that are allowed outputs. 145
6.8 Some alternative solutions of (MP) with $Z = \Delta E$ when the set of allowed outputs are 15 oxygenate compounds. 148
6.9 Alternative solutions of (MP) with $Z = \Delta E$ when the set of allowed outputs are 15 oxygenates and 157 hydrocarbons. Sources of hydrogen are not shown in the figure as they are identical to those in Figure 6.8. . 151

6.10 Some alternative solutions with $Z = R^{\text{cat}}$ when the set of allowed outputs are 15 oxygenate compounds. 159
6.11 Some alternative solutions with $Z = H^{\text{abs}}$ when the set of allowed outputs are 15 oxygenate compounds. 159
6.12 Some alternative solutions with $Z = R^{\text{cat}}$ when the set of allowed outputs are 15 oxygenates and 157 hydrocarbons. LHV must be higher than 32 kJ/mL. 163

CHAPTER 1

Introduction

The objective of this chapter is to provide a motivational background to the thesis. Basic terminology for biomass and biofuels is defined, along with a brief summary of the history of biofuels in the United States, up to the present day. Advantages of biofuels as a substitute for petroleum-based fuels are introduced, along with a discussion of the associated challenges. Biorefineries that produce biofuels must be designed with efficient choices across many scales, ranging from the chemistry of the conversion processes, to reactor and process design, and to supply chain analysis. Such challenges motivate the need for mathematical programming tools with a Process Systems Engineering perspective that take the competing forces in biorefinery design into consideration when making economic and environmental choices.

1.1 Biomass and biofuels

Transportation (aircraft, boats, trains and automobiles) requires high energy density fuels that have been conventionally produced from petroleum. Production of equivalent fuels on a national scale from renewable resources (solar, wind, hydroelectric, geothermal and biomass) poses a significant challenge. Biomass (crops, grasses, agricultural waste, wood, municipal waste and landfill gas) has particular importance among renewable resources as the only currently demonstrated alternative to replace petroleum for

the production of fuels for transportation. A variety of fuels, referred to as biofuels, can be produced from biomass, including solid fuels (e.g. charcoal), liquid fuels (e.g. ethanol, biodiesel, bio-gasoline) and gaseous fuels (e.g. hydrogen and methane). Growth of a biomass-to-biofuel industry could reduce petroleum imports, support agriculture and forestry growth, foster a domestic biorefinery industry, and reduce greenhouse gas emissions [2].

It is important to acknowledge that biofuels have long been recognized as the only domestic, sustainable and renewable alternative for liquid transportation fuel. Some may incorrectly believe that biofuels are a late twentieth century development. Although the rapid escalation of oil prices after the Arab oil embargoes of the 1970s did cause vocal and renewed interest in domestic renewable fuels [3], the reality is that ethanol was being used as a transportation fuel before the discovery of petroleum by Edwin Drake in 1859. Ethanol, sometimes blended with turpentine (a biofuel refined from pine trees), was the fuel for the early internal combustion engines of Samuel Morey in 1826 and Nicholas Otto in 1860 [4]. Unfortunately, in 1861 the U.S. enacted a tax of $2.08/gal on ethanol to fund the Civil War. This is equivalent to $35/gal in 2007, and the law applied to both drinking and fuel alcohol. It continued well past the war's conclusion and was finally removed in 1906. The 1906 issues of the New York Times include the headlines:

> "ALCOHOL FOR AUTOS MAY DISPLACE GASOLINE; Motor Car Owners Awaiting Coming Tests with Great Interest." [5]

and

> "LAUNCHING A GREAT INDUSTRY; THE MAKING of CHEAP ALCOHOL; Government Commission at Columbia University Concludes its Tests and Announces that all American Engines can Burn de-naturized Spirit." [6]

In fact both Henry Ford and Alexander Graham Bell were proponents of ethanol from cellulosic (non-food) biomass. Ford's 1908 Model T contained an adjustable carburetor so that it was capable of running on gasoline, kerosene or ethanol. This fuel flexibility was desired, because petroleum reserves seemed to be scarce at the time. Bell was quoted in a 1917 issue of National Geographic Magazine saying:

> "In relation to coal and oil, the world's annual consumption has become so enormous that we are now actually within measurable distance of the end of the supply. What shall we do when we have no more coal or oil!

> [...] Alcohol can also be manufactured from corn stalks, and in fact from almost any vegetable matter capable of fermentation. Our growing crops and even weeds can be used. The waste products of our farms are available for this purpose and even the garbage from our cities. We need never fear the exhaustion of our present fuel supplies so long as we can produce an annual crop of alcohol to any extent desired." [7]

Rationing of raw materials during the World Wars lead to increased ethanol production, with 60 million gallons produced in 1919 and 600 million gallons produced in 1945. As cheap petroleum returned to the market, biofuel production decreased. However, ethanol was a valuable gasoline additive as an oxygenate and antiknock (i.e. octane enhancer). It was replaced by the cheaper tetraethyl lead in 1921, which was banned by the U.S. EPA in the 1980s following leaded gasoline health concerns. Methyl tertiary butyl ether (MTBE) was then used, but was later replaced by ethanol following groundwater contamination concerns. The question has not been if fuels could be made from biomass, but rather if (a) biofuels can be produced more cheaply than other fuels of the day or (b) new high-value markets can be accessed by biomass products and coproducts (e.g. specialty materials, animal feed or food).

1.2 Current biofuel industry

The current U.S. biofuel industry is dominated by ethanol (mainly produced from corn grain starch) and biodiesel (mainly produced from soybean oil and recycled cooking oils), but cellulosic biofuels (based on non-food resources such as agricultural waste, grasses and woody crops) are predicted to play a large role in the future. Annual ethanol production has quickly expanded from 83 million gallons in 1981 to 14 billion gallons in 2011, and biodiesel production has similarly grown to 700 million gallons. Biofuels became controversial during this rapid growth for influencing the price of food by acting as a competing outlet for agricultural commodities. About a third of U.S. corn production is used to produce ethanol, as shown in Figure 1.1, resulting in ethanol comprising 9.5% of finished gasoline blends in the U.S.. Alternatively, cellulosic biofuels are produced from low resource-intensive biomass, and can provide much greater supplies and environmental benefits than food-based biofuels [8]. The U.S. EPA predicts that 8.7 million gallons of cellulosic biofuel will be produced this year [9], while government mandates require the use of 16 billion gallons of cellulosic biofuel in motor-vehicle fuel

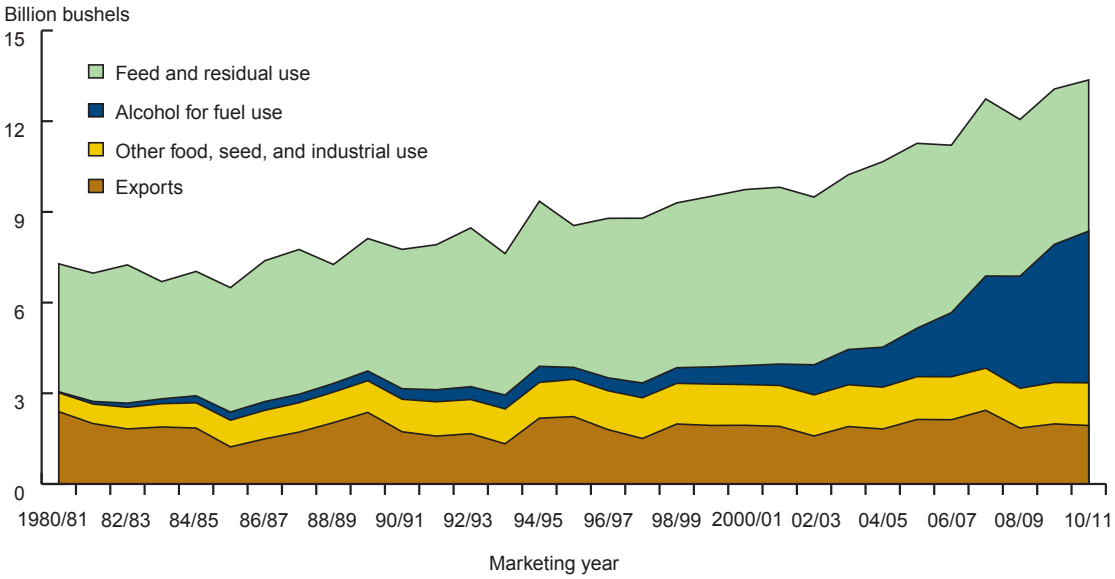

Figure 1.1: U.S. corn use from 1980 to 2011 [10].

by 2022.

Development of the cellulosic biofuel industry to meet these mandates will impose significant logistical challenges at each stage of the biofuel supply chain (biomass production, harvesting, storage, processing and transportation, and biofuel distribution). This industry will require about a billion tons of biomass annually from a variety of sources that each may be seasonally available, with uncertainty in composition, quantity and price. Furthermore, there are many proposed technologies (e.g. crop residue fermentation and biomass gasification with syngas upgrading) competing for biomass processing, and their adoption will determine the economic and environmental impacts of the industry as a whole.

1.3 Policy

Government policy cannot be neglected in an analysis of biofuels, and its impact is summarized here. On the feedstock side, the cost of biomass delivered to a biorefinery can be reduced by biomass production incentives. For example, corn production incentives for farmers lower the feedstock cost for dry-grind ethanol facilities, and also lower the cost of corn stover for cellulosic biofuel facilities. There may also be biofuel production incentives.

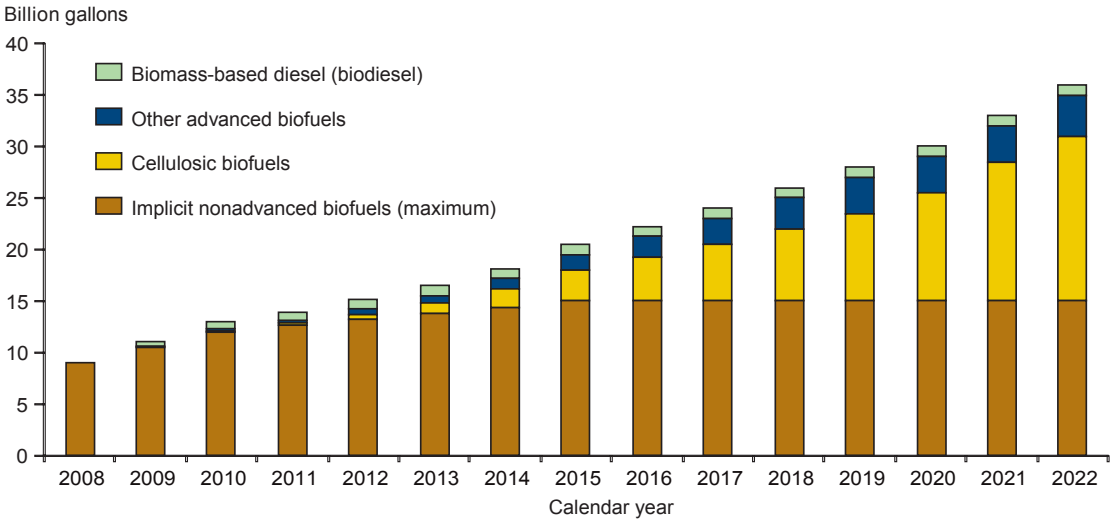

Figure 1.2: Renewable fuel standard (RFS) mandate, by type, 2008-2022 [10].

The Renewable Fuel Standard (RFS) [11] mandates the increased blending of renewable fuel into transportation fuels, as shown in Figure 1.2, up to 36 billion gallons of biofuels annually in the U.S. by 2022. Biofuels are classified as cellulosic biofuel, biomass-based diesel, advanced biofuel and renewable fuel, based on degree of greenhouse gas reduction compared to 2005 gasoline baseline. The classifications are nested so that cellulosic biofuels count as advanced biofuel and renewable fuels. Corn ethanol is classified as a renewable fuel and cannot be counted towards cellulosic or advanced biofuel requirements. RFS is enforced by the Renewable Identification Number (RIN) system, a traded market system that provides incentives to obligated parties (e.g. fuel blenders or importers) that purchase biofuels [10]. The U.S. EPA determines fuel blending percentages each year by dividing the RFS2 requirement by the expected transportation fuel usage that year. Obligated parties must follow these blending percentages by acquiring RINs (i.e. buying biofuels and obtaining RINs directly, or buying RINs from other obligated parties) and presenting them to the EPA or face fines.

Incentives and regulations for the use of biorefinery products are also present. For example, fuel requirements (i.e. ASTM-D4814) on oxygen content and engine emissions favor the blending of oxygenates like ethanol in fuels. Government policies have a direct influence on the supply chain decisions of the biorefinery industry by decreasing biomass and biorefinery costs, increasing biorefinery profit or increasing renewable product demand.

1.4 Chemistry and Biofuel Products

Product design of biofuels requires knowledge of biomass attributes and chemical composition, available chemical transformation steps to other molecules, and desirable product characteristics. Lignocellulosic and carbohydrate-rich biomass contains oxygen, in contrast to crude oil and hydrocarbon fuels. Furthermore, the oxygen is present in different functional forms, such as hydroxyl, ether and carbonyl groups. New chemical transformations and reactor configurations are therefore necessary to utilize biomass as a renewable substitute for fossil hydrocarbons in the production of fuels and chemicals. This has motivated the development of several processes involving biochemical and thermochemical steps.

Biochemical processes have been developed that utilize cell cultures (e.g. metabolically engineered strains of bacteria like *E. Coli* or yeast like *S. Cerevisiae*) to convert biomass such as starch, lignocellulosic sugars, fatty acids and glycerol to alcohols, isoprenoids, fatty acid esters, alkanes, terpenes, and platform chemicals [12,13]. Chemicals from sugar fermentation processes include lactic acid, succinic acid, 3-hydroxypropionic acid and 5-hydroxymethylfurfural (HMF) [14]. HMF has been the subject of process design and control work in Professor Daoutidis' group [15, 16], and can be converted to the liquid biofuel 2,5-dimethylfuran (DMF) or to the nylon-line polymer precursor levulinic acid.

Thermochemical processes include a thermolytic step that converts biomass by gasification to syngas (a gas mixture primarily of hydrogen and carbon monoxide) or by fast pyrolysis to bio-oil, and at least one catalytic step where the thermolytic products are upgraded to alcohols, ethers, esters and hydrocarbons [17]. A variety of chemical processes, spanning gas phase free-radical pyrolysis to homogeneous and heterogeneous acid, metal and base catalysis have been developed [18]. Research in Professor Schmidt's group has focused on production of syngas in short contact time reactors by catalytic partial oxidation, which is useful for small-scale distributed biofuels production [19].

Available chemical transformation steps can be represented as a reaction network of reactions and species. An important characteristic of biomass conversion is that the underlying reaction network can be large and complex. Consequently, a large number of desirable biomass-derived compounds may exist, each with multiple chemical routes to synthesize them. Product design for biofuels must then (a) identify compounds or blends of compounds that satisfied desired properties, and (b) determine efficient synthesis routes to produce these compounds from biomass feedstocks.

1.5 Thesis scope and organization

The aim of this thesis has been to solve important practical problems on the two fronts of supply chain and product design of biofuels. This work is motivated by the opportunity converting biomass that is plentiful in the Midwestern U.S. into valuable biofuels and coproducts. The supply chain problems investigate the economics and environmental impact of biofuel production by determining optimal biomass harvest, transportation and conversion, and biorefinery technology choice, scale and location. The product design problem is to determine optimal product portfolio and synthesis chemistry for fuel, namely blended gasoline. The supply chain and product design fronts are unified by the development and application of mathematical optimization models, specifically mixed integer linear programs (MILP). A description of the general form of these models and their solution techniques are described in Chapter 2, with a focus on the Simplex algorithm for solving linear programming, and branch and bound method for solving MILP problems.

Chapters 3, 4 and 5 describe supply chain problems investigated for the Midwestern United States. Chapter 3 is reprinting with permission from [20] with an expanded background section of biofuel supply chain optimization. This chapter focuses on cellulosic ethanol production from agricultural residues. Sensitivity and Monte Carlo analysis is performed to evaluate the robustness of supply chain choices to uncertainties in costs and technology parameters.

Chapter 4 is reprinted with permission from [21] with summary and introduction modified to highlight differences and expansions from Chapter 3. This chapter includes seven biofuel technologies competing for eight biomass types with existing facilities and candidate sites for new construction. A detailed cash flow analysis that includes piecewise-linear capital cost, capital depreciation and taxation is embedded into the model formulation to give insights into the minimum biofuel selling price for each facility site. Equilibrium market cost for each of the Renewable Fuel classifications (renewable fuel, advanced biofuel and cellulosic biofuel), that is directly related to the Renewable Identification Number market price, is determined through sensitivity analysis of the delivered biofuel price.

Chapter 5 is unpublished and expands the previous chapter to include a competing objective of minimizing greenhouse gas emissions. The resulting multiobjective mixed integer linear program is solved using an ε-constraint approach that yields the Pareto

Frontier of efficient supply chain designs. This allows for the identification of supply chain decisions that greatly reduce greenhouse gas emissions for minimal economic losses.

The biofuel product design problem is described in Chapter 6, and is reprinted with permission from [22]. The proposed strategy of combining reaction network generation with optimization is applied to the heterogeneous catalysis of biomass to oxygenates and hydrocarbons, such that the resulting blend satisfies ASTM specifications for gasoline. Algorithms are proposed for reaction cycle detection and alternative solution enumeration.

Chapter 7 presents conclusions and proposals for future work on the fronts of supply chain and product design of biofuels.

CHAPTER 2

Background on Optimization

The objective of this chapter is to provide a theoretical background on the main optimization techniques applied in this thesis. Developed mathematical programming tools, particularly for mixed integer linear programming (MILP) problems, were utilized for both the biofuel supply chain optimization and biofuel product design problems. The standard form of such mathematical programs will be described, along with the main algorithms devised for their solution.

2.1 Linear programming

Linear programming (LP), namely the Simplex algorithm developed by George Dantzig in 1947 [23], is described first as it is used with MILP algorithms. The LP discussion presented here is adopted from [24, sections 5.1 and 5.3]. The LP standard form is [24]:

$$\begin{aligned} \min \quad & c^T x \\ \text{s.t.} \quad & Ax = b \\ & x \geq 0 \end{aligned}$$

where x is a vector of decision variables.

Notice that no inequality constraint is present in this standard form. Slack variables

are introduced for each inequality constraint to write the LP in standard form. For example, an inequality constraint such as $x_1 + 2x_2 \leq 10$ can easily be converted into an equality constraint by introducing a nonnegative slack variable $x_3 \geq 0$ and declaring $x_1 + 2x_2 + x_3 = 10$.

Note that if a LP has any optimal solution, it has one at an extreme point of its feasible region. The Simplex algorithm detects and then searches through the extreme points for a global optimum. Each extreme point, often referred to as a *basic solution*, is found by fixing enough decision variables to 0 (*nonbasic* variables) such that the remaining decision variables (*basic* variables) can be solved for uniquely. For example, if the LP constraints are as shown in Figure 2.1:

$$x_1 + 2x_2 + x_3 = 10$$
$$x_1 - x_2 = 1$$

then choosing *nonbasic* $x_3 = 0$ results in:

$$x_1 + 2x_2 = 10$$
$$x_1 - x_2 = 1$$

which is easy solved to yield the *basic solution* $(x_1, x_2, x_3) = (4, 3, 0)$.

After finding the first basic solution, phase II of the algorithm begins. To move from a basic solution, simplex directions Δx can be found that point along edges of the feasible polytope toward other basic solutions. These are found by solving $A\Delta x = 0$ when one of the nonbasic variables is increased to 1. In the present example, the nonbasic variable $x_3 = 1$ and $A\Delta x = 0$ then becomes:

$$\Delta x_1 + 2\Delta x_2 + 1 = 10$$
$$\Delta x_1 - \Delta x_2 = 1$$

which leads to the simplex direction $\Delta x = [11/3, 8/3, 1]^T$.

The algorithm moves along the simplex direction that improves the objective function the most. The improvement of the objective function for a movement along the simplex direction Δx corresponding to increasing the nonbasic variable x_j is known as the reduced cost c_j:

$$c_j = c^T \Delta x \tag{2.1}$$

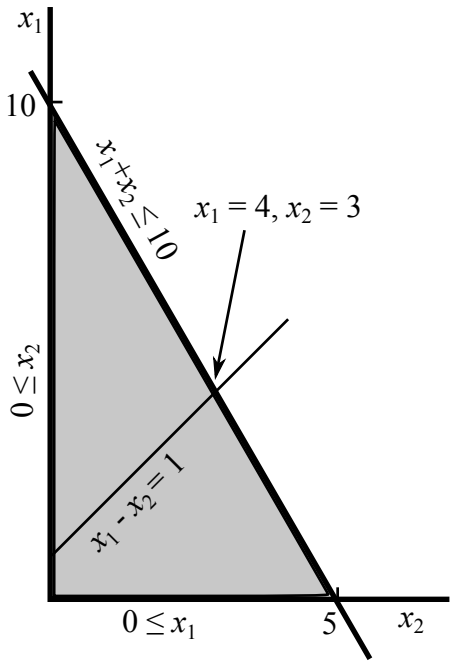

Figure 2.1: Example LP with inequality, equality and nonnegative constraints shown. A basic solution is shown at (4,3).

For a minimization LP, the simplex direction is desirable if $c_j < 0$. Simplex then moves from the current basic solution $x^{(t)}$ at iteration t to a new basic solution $x^{(t+1)} = x^{(t)} + \lambda \Delta x$, where the maximum step size is chosen such that at least one variable $x_j^{(t)}$ is forced to zero (i.e. just before a non-negativity constraint violation along the simplex direction). Thus:

$$\lambda = \min \left\{ \frac{x_j^{(t)}}{-\Delta x_j} : \Delta x_j < 0 \right\} \tag{2.2}$$

Then the nonbasic variable generating the chosen simplex direction enters the basis (set of basic variables) and any one of the basic variables leaves the basis. New simplex directions are found at a new basic solution $x^{(t+1)}$ and the process continues until no simplex direction is improving. Then the global optimum is found to be the current basic solution and the LP is solved.

2.2 Mixed integer linear programming

Several algorithms are available for solving MILP problems [25], including branch and bound methods, cutting planes methods, decomposition methods, and logic-based methods. Branch and bound methods are the most commonly used algorithms in large-scale MILP solvers such as CPLEX by IBM, the solver used in this research. The branch and bound method for solving MILP algorithms uses the Simplex algorithm, because some of the integer requirements are relaxed to create an LP at each node. The MILP discussion presented here is adopted from [24, sections 12.2-5]. The MILP standard form is:

$$\begin{aligned} \min \quad & c^T x \\ \text{s.t.} \quad & Ax = b \\ & x \geq 0 \\ & x_j \in \mathbb{Z}, \text{for some } j \end{aligned}$$

where $\mathbb{Z}$ is the set of integers.

A simple example that is limited to only binary decision variables y is discussed here with the form:

$$\begin{aligned} \min \quad & c^T y \\ \text{s.t.} \quad & Ay \leq b \\ & y_i \in \{0, 1\} \end{aligned}$$

This discussion can easily be extended to maximization MILP by minimizing the negative objective function. Continuous variables could also be included, but this only complicates the LP relaxation calculation and not the branch and bound strategy. Recall that the inequality constraints $Ay \leq b$ are reduced to equality constraints in the Simplex Search by introducing slack variables. Thus there does not need to be a distinction between inequality and equality constraints here.

During an LP relaxation, the decision variables are allowed to be continuous between 0 and 1. Then the optimization is performed using Simplex Search. Look at the following

discrete optimization problem:

$$\begin{aligned} \min \quad & v = 10y_1 + 8y_2 + 18y_3 \\ \text{s.t.} \quad & 2y_1 + 4y_2 + 7y_3 \geq 5 \\ & y_1 + y_2 + y_3 \geq 1 \\ & y_i \in \{0, 1\} \end{aligned}$$

which has the relaxed solution $\tilde{y} = [0, 1, 1/7]^T$ with objective function $\tilde{v} = 74/7 \approx 10.57$.

Note that the true optimum, when all the binary constraints are included, cannot have an objective function as good as this one. Thus we can define the lower bound $v \geq 74/7$. Furthermore, the objective function increases in y_3 and y_3 is not constrained to be less than 1. Thus if we round up $\tilde{y}_3 = 1/7$ to an integer value $\hat{y}_3 = 1$, then the integer-feasible solution $\hat{y} = [0, 1, 1]^T$ has objective function $\hat{v} = 26$. Any integer-feasible solution to a minimizing MILP provides an upper bound, therefore $v \leq 26$.

Branch and bound algorithms use LP relaxation to avoid complete enumeration (performing a LP optimization for each of the 2^N possible combinations of the N binary variables). The optimization strategy is a tree structure as shown in Figure 2.2. At each node t in the tree, an LP relaxation problem is solved to give a relaxed solution $\tilde{y}^{(t)}$ with corresponding objective $\tilde{v}^{(t)}$. If the binary constraints are not satisfied by the relaxed solution, then one of the non-integers (normally the largest) is selected for branching. In the above example, y_3 would be selected for branching because $1/7$ is not an integer. Then two children partial solution problems are formed, where y_3 is fixed to a value of 1 or 0.

Notice that at node 1 the LP relaxation solution satisfies the binary constraint, therefore the incumbent solution $\hat{y} = \tilde{y}^{(1)} = [0, 0, 1]^T$ and the corresponding objective $\hat{v} = \tilde{v}^{(1)} = 18$ is saved. Any subsequently explored node t that produces LP relaxation objective $\tilde{v}^{(t)} \geq \hat{v}$ is removed (along with its explored children) by bounding, because it cannot produce children with a lower objective function. Node 2 has a lower LP relaxation objective of 13, but the solution is not binary ($y_1 = 1/2$). Branching is done on y_1 to produce node 3 and node 4 (removed for not having a feasible LP relaxation solution). At node 3, the LP relaxation produces a non-binary solution for y_2. Branching on y_2 produces an incumbent solution $\hat{y} = \tilde{y}^{(5)} = [1, 1, 0]^T$, which interestingly has the same objective value as the previous incumbent solution. Thus the global optimum objective is $\hat{v} = 18$ for two points $\hat{y} = [0, 0, 1]^T$ and $[1, 1, 0]^T$.

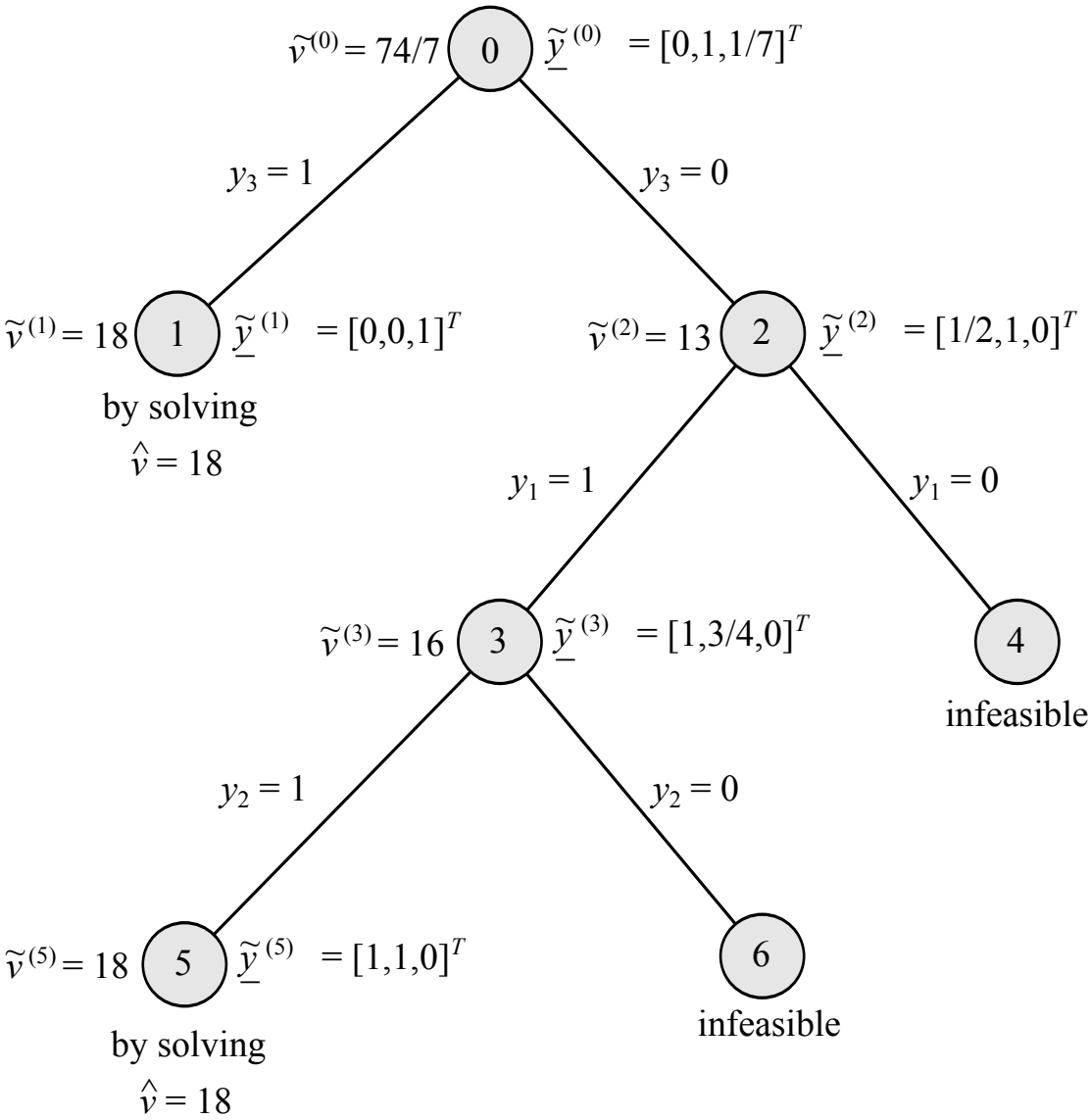

Figure 2.2: Branch and bound tree example.

Most branch and bound algorithms do not explore the tree fully to prove global optimality, as was shown above. Instead, the current candidate solution is returned when the best LP relaxation (lower bound) is within a specified tolerance of the least integer-feasible rounded solution (upper bound).

CHAPTER 3

Economic Supply Chain Optimization for Cellulosic Ethanol*

3.1 Summary

This chapter presents an optimization study of the net present value of a biomass-to-ethanol supply chain in a 9-state region in the Midwestern United States. The study involves formulating and solving a mixed integer linear programming problem. A biochemical technology is assumed for converting five types of agricultural residues into ethanol utilizing dilute acid pretreatment and enzymatic hydrolysis. Optimal locations and capacities of biorefineries are determined simultaneously with biomass harvest and distribution. Sensitivity analysis is performed to elucidate the impact of price uncertainty on the robustness of the supply chain and whether or not the proposed biorefineries will be built or will fail financially after being built.

3.2 Introduction

Growth of a biomass-to-biofuel industry has the potential to reduce oil imports, support agriculture and forestry growth, foster a domestic biorefinery industry [2] and reduce

*Reprinted with permission from W. Alex Marvin, Lanny D. Schmidt, Saif Benjaafar, Douglas G. Tiffany, and Prodromos Daoutidis, *Chemical Engineering Science*, 67(1):68–79, 2012 [20].

greenhouse gas emissions by an estimated 86% over gasoline [26]. For these reasons, many nations have set biofuels targets. The United States Renewable Fuels Standard program (RFS2), as amended by the Energy Independence and Security Act of 2007, mandates that by 2022, at least 36 billion gallons per year (BGY) of renewable fuel be blended into motor vehicle fuel, including 16 BGY from cellulosic biofuel [11]. Using the Biofuels Deployment Model, researchers at Sandia National Labs determined that 21 BG of cellulosic ethanol could be produced per year by 2022 in the U.S. without displacing current crops [27]. Similarly, the European Union has set a minimum target to replace 10% of overall consumption of petrol and diesel in transport with biofuels by 2020 [28].

Cellulosic ethanol is produced from biomass (wood, grasses, non-edible parts of plants, and municipal wastes) and is the only currently demonstrated renewable liquid transportation fuel [29]. If the 1.3 billion dry tons of forestry and agricultural residues produced annually in the US [2] were collected and converted into ethanol, it would replace over one-third of the current US demand for transportation fuel [27]. As of January 2010, there were 187 ethanol refineries operating in the U.S. producing a total of 12.9 BGY ethanol almost exclusively from maize (corn) grain [30]. Cellulosic ethanol production represented only 3 million gallons per year (MGY). Only demonstration cellulosic ethanol biorefineries are operational. DOE-supported project that are currently funded, under construction or operational are shown in Figure 3.1.

One of the major hurdles that must be overcome to increase cellulosic biofuel production in the U.S. by three orders of magnitude to meet the 2022 mandates is to collect and transport biomass efficiently, for it is inherently a distributed resource. Many previous studies have addressed various aspects of delivering biomass for further processing. The distribution of available biomass was quantified in [2, 32], the environmental and economic impacts of an ethanol economy were examined in [27, 29], and the cost of delivered biomass was estimated in [33, 34]. The cost of delivered biomass feedstock constitutes 35-50% of the total ethanol production cost with logistical costs making up 50-75% of those feedstock costs [35]. This is one reason why small-scale biorefineries may be competitive with larger facilities that benefit from economies of scale. Indeed, such small-scale facilities are the norm in the existing bioethanol and biodiesel industry. Small-scale biorefineries and local biomass processing can reduce unwanted/tare transport (e.g. retain water, minerals, weeds and soil at the farm), allow for local use of products (e.g. as fertilizer and feed), and improve safety (e.g. decentralized storage) and

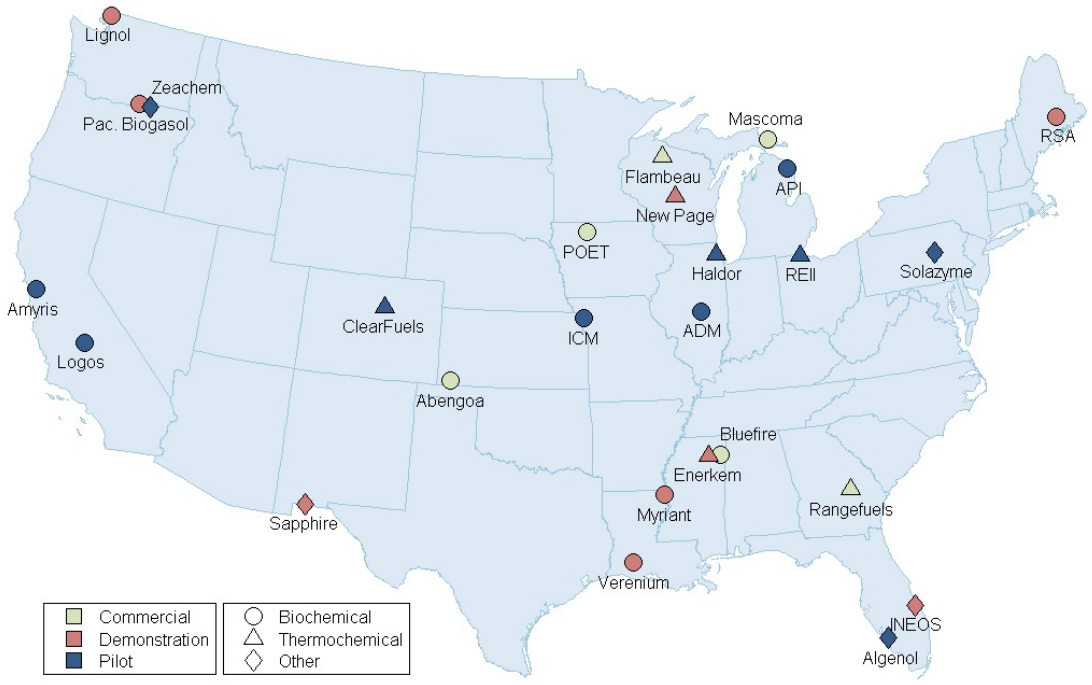

Figure 3.1: DOE supported integrated biorefinery projects by capacity and conversion technology (redrawn from [31])).

environmental impact (e.g. reduced transportation emissions) [36]. Some products may also present unique logistical challenges or opportunities. For example, biofuels must be transported to blending stations and then to fueling stations, whereas biomass-derived fertilizer might be used at nearby fields. The prospect of such a distributed industry, dominated by local supply and demand, represents a drastic departure from the current oil-based industry model. These supply chain considerations must be fully evaluated as they are critical to the success of the entire industry.

Biofuel supply chain optimization (SCO) has become a popular method for understanding the expected expansion of the biofuel industry. Biofuel SCO seeks to determine the optimum supply chain that maximizes a desired performance index (e.g. profitability, greenhouse gas emissions, water use and net energy use) by efficiently utilizing biomass resources while satisfying the biofuel market demand. An et al. [37] provided a review of research in this area, as well as the related field of petroleum and chemical operations research. Floudas et al. [38] provided a review of the more broad area of hybrid energy systems for liquid transportation fuels, including process design and supply chain optimization. In what follows, we provide a concise review of the most relevant biofuel SCO literature, organized by the type of model formulated: linear programs, mixed integer programs, and multiobjective programs.

Linear program formulations for SCO are convex, continuous and solved quickly, and are thus well suited for case studies where having a large supply chain scope (many decision variables) is more important than having binary decisions. Morrow et al. [39] modeled the distribution of cellulosic ethanol produced from switchgrass in the U.S. by formulating a LP to minimize total ethanol transportation distance. Ethanol facility locations and capacities were determined through prescreening of cities based on nearby switchgrass availability. Suh et al. [40] formulated a series of transportation minimization LPs to determine locations for identical ethanol facilities utilizing corn stover in Minnesota.

Binary or integer variables must be included for problems where logical decisions (e.g. to construct a facility or not) are important, resulting in mixed integer programs. Elia et al. [41] proposed a cost minimization MILP to locate facilities of a novel hybrid coal, biomass and natural gas to liquid technology in the U.S. to supply transportation fuels. This technology was designed to economically produced fuels with an estimate 50% emission reduction compared to petroleum [42, 43]. Additional plant designs were included in their expanded SCO study that considered varying levels of

petroleum replacement [44]. Tembo et al. [45] formulated a MILP to determine locations for gasification-fermentation facilities using multiple cellulosic biomass species in Oklahoma. Discrete facility capacity options were considered. Mapemba et al. [46] expanded the Oklahoma study to determine the number of harvest machines for each facility. Shastri et al. [47] examined scheduling switchgrass production and processing near one facility in southern Illinois. Options for switchgrass farming and storage practices were considered. Kang et al. [48] proposed a multiperiod MILP to minimize total costs to meet co-product and ethanol market demand using corn, corn stover and perennial grasses in Illinois. Two biorefinery technologies were considered and existing corn ethanol plants were included. Leduc et al. [49] formulated a MILP to determine low cost supply chains for ethanol production from woody biomass in Sweden. Parker et al. [50] proposed a MILP to determine biofuel supply curves in the Western U.S. as a function of marginal cost of biofuel with a wide range of feedstocks and multiple biorefinery technologies considered. Kim et al. [51] examined two-step biomass processing (bio-oil intermediate) in the Southeastern U.S. with parameter sensitivity analysis and Monte Carlo sampling to estimate supply chain uncertainty. Bai et al. [52] formulated a mixed integer quadratic program (MIQP) to examine the effects of non-cooperative firms and determine feedstock market equilibrium in northern Illinois.

Multiobjective programs are considered when environmental and economic (or other objective functions) are simultaneously important. You et al. [53] determined optimum facility locations of two biorefinery technologies to satisfy cellulosic biofuel mandates in Illinois as a multiperiod multiobjective MILP. A large environmental improvement was identified for a small loss in economies of scale. You and Wang [54] proposed a multiperiod multiobjective MILP to examine the trade-off between economic and environmental performance for biomass gasification to Fischer-Tropsch liquids with options for distributed biomass preconversion in Iowa. They identified a significant emission improvements through the use of distributed processing for a small increase in cost. In a two part paper, Zamboni et al. [55,56] examined ethanol demand satisfaction in northern Italy using a multiobjective MILP to identify low cost supply chains that maintained an estimated 55% emission reduction compared to gasoline. One biorefinery technology was considered with transportation modeled as neighborhood flow within a grid. Akgul et al. [57] expanded upon the cost minimization study with a more detailed neighborhood flow model. Giarola et al. [58] created a multiperiod multiobjective MILP that considered multiple competing technologies to utilize corn and corn stover in northern

Italy.

This chapter presents a MILP that can be applied at the regional or national level to optimize a biomass-to-biofuel supply chain when biomass producers and candidate biorefinery locations are specified. A case study of a 9 state region in the Midwestern U.S. (Illinois, Indiana, Iowa, Minnesota, Missouri, Nebraska, North Dakota, South Dakota, and Wisconsin) is presented which may be useful as a tool for determining national biofuel policies as most of the agricultural residues in the U.S. are located there, as shown in Figure 3.2. The residues of barley, corn, oats and wheat are included with a collection and densification scheme that decouples the biorefinery from the variability of biomass supply. A biochemical technology for biomass-to-ethanol conversion was assumed that is expected to be commercialized in the short-term (within 5 years), allowing for the use of recent agricultural data. The economic parameters for this developing industry are inherently uncertain. Single parameter sensitivity analysis and Monte Carlo simulation are performed to determine the supply chain robustness.

3.3 Optimization problem formulation

The optimization problem is to determine where to place biorefineries and of what capacity, how much biomass to harvest and to which biorefineries to ship it to maximize the Net Present Value (NPV) of the entire supply chain. NPV is calculated as the sum of a time series of cash flows that have been discounted back to the present. For annual cash flows $\{R_m\}$ that occur over a project lifetime T_L,

$$\text{NPV} = \sum_{m=1}^{T_L} \frac{R_m}{(1+i)^m} \tag{3.1}$$

where i is the discount rate (or annual rate of return of a competing investment) [59].

For the optimization problem, we assume that all capital investment R_{invest} occurs in the present year and that the total of all other cash flows R_{annual} are identical for each year of the project lifetime. This leads to the simplification:

$$\text{NPV} = \theta \cdot R_{\text{annual}} - R_{\text{invest}} \tag{3.2}$$

where the scaling factor θ arrives from the simplification of the geometric series with

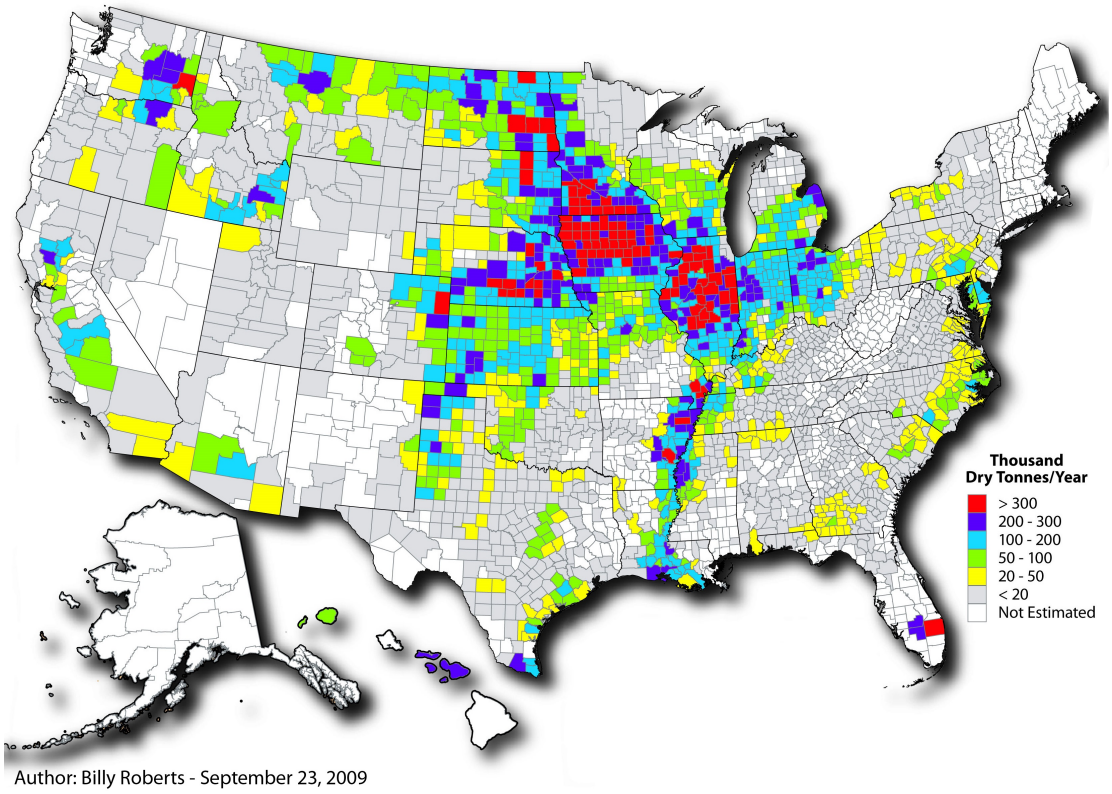

Figure 3.2: Crop residue availability in the United States by county (adapted from [32]).

Table 3.1: Subscripts.

Symbol	Description
$n \in \{1, \ldots, N\}$	biomass producing locations
$r \in \{1, \ldots, R\}$	candidate biorefinery locations
$l \in \{1, \ldots, L\}$	allowed biorefinery capacities
$b \in \{1, \ldots, B\}$	biomass feedstocks
$p \in \{1, \ldots, P\}$	products (e.g. ethanol)

constant ratio $(1+i)^{-1} \neq 1$ and is defined as:

$$\theta = \frac{(1+i)^{T_L} - 1}{i \cdot (1+i)^{T_L}} \tag{3.3}$$

Optimizing the NPV ensures that all biorefinery infrastructure investments meet or exceed a rate of return over the project lifetime. In this biomass-to-ethanol supply chain, R_{annual} includes cash flows for product (ethanol) sales, costs of harvest and transportation of biomass. Biorefinery investment and operating costs are included in R_{invest}, so the objective function and the optimization problem can be stated as follows:

$$\begin{aligned} \max \quad \text{NPV} = \theta \cdot \Bigg\{ & \sum_{r=1}^{R} \sum_{p=1}^{P} \sigma_p \cdot a_{r,p} - \sum_{n=1}^{N} \sum_{b=1}^{B} \rho_b \cdot h_{n,b} \\ & - \sum_{n=1}^{N} \sum_{r=1}^{R} \sum_{b=1}^{B} \tau_{n,r} \cdot y_{n,r,b} \Bigg\} - \Bigg\{ \sum_{r=1}^{R} \sum_{l=1}^{L} \psi_l \cdot x_{r,l} \Bigg\} \end{aligned} \tag{3.4}$$

where the notations for the subscripts, parameters and variables are defined in Tables 3.1, 3.2 and 3.3, respectively.

Notice that NPV is a linear function of continuous ($a_{r,p}$, $h_{n,b}$ and $y_{n,r,b}$) and binary ($x_{r,l}$) variables, making this biomass-to-ethanol supply chain optimization problem a MILP. The MILP is completely defined with the set of linear constraints described below.

The first set of constraints limits the amount of biomass harvested to the amount that is available annually in each biomass producing location n for each type of biomass b:

$$h_{n,b} \leq \lambda_{n,b}, \quad \forall\, n, b \tag{3.5}$$

Once harvested, the biomass is put into local storage where a fraction is lost due to

Table 3.2: Parameters.

Symbol	Description
i	annual discount rate
T_L	project lifetime (y)
θ	NPV scaling factor
σ_p	unit sale price for product p (\$/gal)
ρ_b	unit feedstock cost for biomass b (\$/gal)
$\tau_{n,r}$	unit biomass transportation cost from n to r (\$/gal)
ϕ_l	investment and lifetime operating cost for a biorefinery of size l (\$)
$\lambda_{n,b}$	amount of biomass b harvestable at n annually (dt/y)
α_b	fractional deterioration of biomass b in local storage
$\beta_{b,p}$	biorefinery conversion of biomass b to product p (gal/dt)
$\xi_{l,p}$	annual production capacity of product p for biorefinery of size l (gal/y)

Table 3.3: Decision variables.

Symbol	Description
$a_{r,p}$	amount of product p producted at r annually (gal/y)
$h_{n,b}$	amount of biomass b harvested at n annually (dt/y)
$y_{n,r,b}$	amount of biomass b transported from n to r annually (dt/y)
$x_{r,l}$	biorefinery of size l installed at r (binary variable)

deterioration. A mass balance around the local storage sites of each biomass producing location can be written to account for shipments of biomass to biorefinery sites:

$$-h_{n,b} + (1+\alpha_b) \cdot \sum_{r=1}^{R} y_{n,r,b} \leq 0, \quad \forall\, n, b \tag{3.6}$$

where losses in local storage due to deterioration are defined such that an additional fraction α_b of biomass b must be collected and put into storage than can be removed and shipped to biorefineries.

Each biorefinery in this formulation utilizes the same technology, thus has an equal yield of ethanol per dry metric ton (dt). Any biomass shipped to a biorefinery location is proportional to the product produced there:

$$a_{r,p} - \sum_{b=1}^{B} \sum_{n=1}^{N} \beta_{b,p} \cdot y_{n,r,b} \leq 0, \quad \forall\, r, p \tag{3.7}$$

where the product yield per dt biomass may depend on the biomass type.

A biorefinery of capacity l is optimally placed at site r if the corresponding binary variable $x_{r,l}$ is one. If the binary variable is zero, that biorefinery size is not constructed there. The binary variables are therefore defined as:

$$x_{r,l} \in \{0, 1\}, \quad \forall\, r, l \tag{3.8}$$

The amount of biomass that can be processed at a biorefinery site is limited by the total biorefinery capacity there. If a biorefinery of size $l = 2$ is installed at candidate biorefinery site $r = 3$, then the production of ethanol $a_{3,1}$, for example, cannot exceed the nameplate capacity $\xi_{2,1}$. In general,

$$a_{r,p} - \sum_{l=1}^{L} \xi_{l,p} \cdot x_{r,l} \leq 0, \quad \forall\, r, p \tag{3.9}$$

A maximum of one biorefinery can be placed at each candidate biorefinery location:

$$\sum_{l=1}^{L} x_{r,l} \leq 1, \quad \forall\, r \tag{3.10}$$

All harvests, shipments and productions must be non-negative quantities:

$$a_{r,p}, h_{n,b}, y_{n,r,b} \geq 0, \quad \forall\, n, r, b, p \tag{3.11}$$

This MILP formulation is a Facility Location Problem and is thus NP-Hard [60]. For relatively small sized problems, it is possible to obtain an optimal solution in a reasonable amount of time using standard algorithms. For large problems, an approximate solution approach might be needed (see, for example, [61–63]). The problems considered in this chapter, including the case study of Section 3.4, are solvable to optimality using the commercial software IBM ILOG CPLEX Optimization Studio [64].

3.4 Case study parameters

3.4.1 Biomass supply

The case study examined the use of agricultural residue as feedstock from the following five grains: barley, corn, oats, spring wheat (including durum), and winter wheat. These crops were chosen for their relative abundance in the Midwestern U.S. region and because agricultural residues of this type can be easily processed in a fermentation biorefinery.

Annual grain production per county was determined as the mean of the 2007 to 2009 figures reported to the U.S. Department of Agriculture and available online on the National Agricultural Statistics Service (NASS) website [65]. NASS Quickstats web service was used to collect grain production data for the 779 counties in Illinois, Indiana, Iowa, Minnesota, Missouri, Nebraska, North Dakota, South Dakota, and Wisconsin.

A method from [32] was used to convert these total grain production figures to dry tons (dt) of each crop residue available per county. Specifically, bushels of grain were converted to an equivalent volume of residue and then corrected for average moisture content. Conversions used are shown in Table 3.4. Spring and winter wheat are assumed to have the same properties. The study included the 535 counties highlighted in Figure 3.3 that are within 100 miles of any candidate biorefinery location. Harvesting of specific residues in counties producing less than one thousand dry metric tons per year was not allowed.

A number of factors limit the amount of crop residue that can physically be collected. Technical harvest efficiency on the field is never 100%, some residues are required to

Table 3.4: Crop to residue ratio and moisture content of selected crops [32].

Crop	Residue to grain ratio (by volume)	Moisture content (%)	Bushel weight (lb)
Barley	1.2	14.5	48
Corn	1.0	15.5	56
Oats	1.3	14.0	32
Wheat	1.3	13.5	60

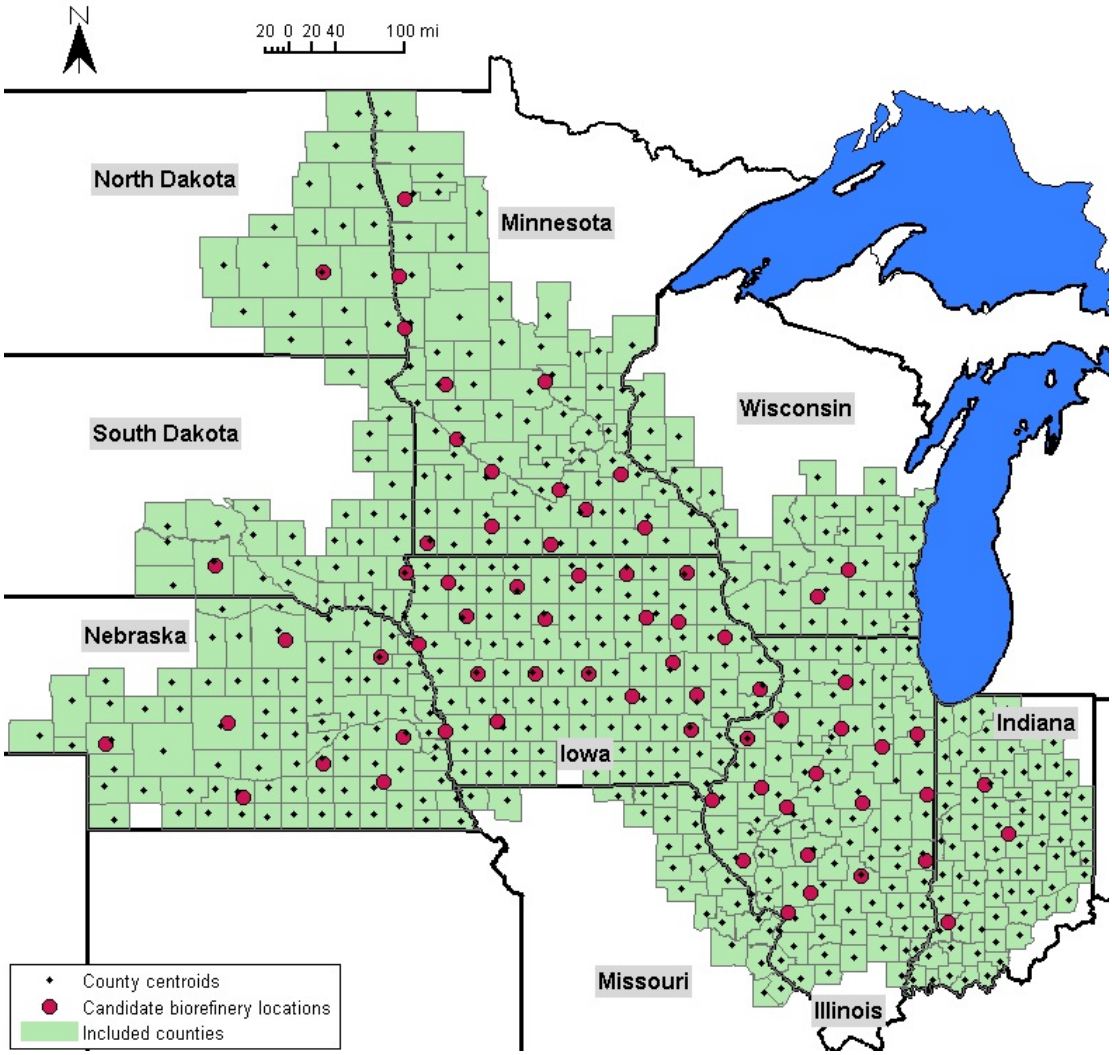

Figure 3.3: The 535 biomass producing counties and 69 candidate biorefinery locations included in the case study.

remain on the field to mitigate soil erosion based on tillage procedure, a portion may be used for grazing or bedding, and there are losses during transportation to central storage. One study assumed that 30% of crop residues are required for soil protection, 2025% are consumed by grazing animals and 1015% are used for other purposes, allowing for 35% of available residues to be collected [32]. Most studies that propose a round bale collection scheme assume 3035% collection efficiency [27, 33, 66, 67]. The present case study allows for an average collection of 35% of available residues (70% of residues removed every other year to reduce harvest operational costs) for all feedstocks and assumes a round bale technology.

3.4.2 Biomass producing locations

Counties are modeled as point sources of biomass due to the availability of biomass resource data. Shipments of agricultural residues will originate from local storage sites distributed within each county, but it is a reasonable assumption that an average biomass shipment will originate from the county geographical center. Some studies that model counties as point sources of biomass use county seats as transportation origins [66]. Others selected a city centered within each county [68]. In this study, the geographical county center (centroid) was used. The county centroids were calculated in MATLAB from each countys boundary using equal area bins. A shapefile of geospatial vector data describing the 2001 county boundaries was downloaded from the NationalAtlas.gov website [69] and was originally compiled by the U.S. Geological Survey.

3.4.3 Biorefinery locations

Candidate biorefinery locations were restricted to cities in Illinois, Indiana, Iowa, Minnesota, Missouri, Nebraska, North Dakota, South Dakota and Wisconsin with U.S. Census 2000 population between three thousand and ten thousand with a maximum of one city per county. Geographic information system (GIS) data for city center coordinates and population was downloaded from the NationalAtlas.gov website [69]. Cities not located near biomass producing counties were removed, namely the urban areas around Chicago and the Twin Cities. See Figure 3.3 for the 69 candidate refinery locations.

Many approaches have been taken in similar studies to determine potential refinery locations. Some studies prefer to allow current corn starch ethanol facilities to expand and utilize cellulosic feedstocks [39]. Others allow a central city from each county in the model that produces biomass to be a candidate plant location [46,68,70]. Another study

allows biorefineries near the centers of biomass production or fuel consumption [71]. Some even perform a preliminary study with an evenly spaced coordinate grid of candidate locations over the region of study to determine a smaller set of locations for the full model [72]. The population cutoff was chosen for this study to ensure that the locations have an adequate employment pool, utility and highway infrastructure, and demand for power produced at the biorefinery.

3.4.4 Biomass transportation distance and cost

In this model roll-press compacted biomass is transported from local county-level storage sites to biorefineries in 22.7 wet metric ton load semi-trucks. A dedicated semi-truck transport is $800 per day and can drive 260 round-trip miles per day [33]. So the cost of the transportation scheme is $0.136 per wet metric ton per round-trip mile or $0.160 per dry metric ton per round-trip mile for 15% moisture content load.

To calculate the matrix of transportation costs $\tau_{n,r}$ from any biomass producing location to any candidate biorefinery location a corresponding matrix of travel distances was determined. Shortest path highway travel distance was found using Google Maps [73]. For simplicity, each biomass type has equivalent transportation costs. Sourcing of biomass from farther than 100 miles was discouraged in the model.

3.4.5 Biomass cost

Economists have studied the economic feasibility of utilizing crop residues for fuel production and process heating for decades with attention placed on the delivered cost of biomass. The use of crop residue in Iowa as an auxiliary fuel in coal-fired power plants to reduce sulfur emissions has been examined [74]. They found a total delivered cost of $69/t (converted to 2009 dollars using the Consumer Price Index) that included the costs for farm production, transportation, processing and handling. A number of National Renewable Energy Laboratory reports in recent years have found delivered biomass feedstock costs of $39/dt [29], $72/dt [75], and $83/dt [76]. The variability here is due to differences in collection technology. The present study focuses on more near-term collection methods.

The system of collection and densification of biomass in this study was proposed in [33] for corn stover only, but is assumed the same for all feedstocks. This method achieves a bulk density of 15 lb/ft^3 and allows for truck transportation to be limited by weight rather than volume. Crop residues are shredded and spread onto the field

Table 3.5: Biomass collection and local storage costs [33].

Source	Cost ($/t)	Cost ($/dt) [a]
Nitrogen replacement	3.68	4.33
Phosphorous replacement	2.04	2.40
Potassium replacement	13.55	15.94
Participation payment to farmer	7.50	8.82
Stalk shredding	2.54	2.99
Raking	1.54	1.81
Baling	21.16	24.89
Bale transportation to local storage	5.51	6.48
Local storage land rent	0.36	0.42
Local storage loss	2.88	3.38
Tub grinding of bales	7.26	8.54
Roll-press compacting	2.48	2.92
Payment to aggregator	3.75	4.41
Total	74.25	87.35

[a] Assuming 15% moisture content for all agricultural residues.

following grain harvest, then raked, and net-wrapped into large round bales (1250 lbs) at 15% moisture. The bales are transported from the field to local storage within a 2 mile radius. They are stored uncovered on level ground in lines running north-south to minimize water gain. A land rent charge of $0.42/dt is incurred annually for crop residue inventory at local storage sites, assuming 15% moisture content. Average fractional deterioration during storage is assumed to be 5% for all feedstocks. Thus the cost of local storage loss is equal to 5% of the sum of the costs incurred to get the biomass to local storage.

Portable 22.7 t/h capacity processing units move around to the local storage sites to grind and densify the residue bales by roll-press compaction into a bulk material transportable by 22.7 metric ton load trucks. Table 3.5 specifies costs for each of these steps in addition to nutrient replacement and other farmer incentives on a dry metric ton basis. Feedstock cost is $87.35/dt and does not include the cost of transporting densified biomass from local storage to a biorefinery.

3.4.6 Ethanol sale price

In October 2010, the average at-the-pump sales price of E85 in the Midwestern U.S. was $2.42/gal and the average gasoline price was $2.78/gal [77]. Thus, the equivalent

average price of 100% ethanol was $2.36/gal. This is the price observed at the fuel station after tax incentives have been applied and is not the sale price from a biorefinery. We assume our example biorefinery qualifies for the Cellulosic Biofuel Producer Tax Credit of $0.46 per gallon ethanol [78] and that the Volumetric Ethanol Excise Tax Credit which expires December 31, 2011 is not renewed. The effective ethanol sale price σ_1 seen at the biorefinery is $2.82/gal. Other incentives, such as the Small Ethanol Producer Tax Credit ($0.10/gal discount up to 15 MGY production) or programs from the USDA and DOE, are not considered.

Ethanol shipment scheduling is not determined by the model as the customer is not necessarily defined and the cost of shipping ethanol is relatively low compared to shipping biomass. Ethanol from a biorefinery is often sold to a central gasoline blending facility that then distributes the common ethanol blends, like E10 and E85, to local fuel stations. To account for the local fuel station demand, Morrow et al. [39] modeled cellulosic ethanol production in the U.S. by including ethanol shipments to Metropolitan Statistical Areas. In that study, the cost of delivering biomass to the biorefinery was found to be relatively high compared to the cost to deliver ethanol to the customer.

3.4.7 Biorefinery costs and capacities

The two main process platforms for cellulosic ethanol production are biochemical (enzymatic hydrolysis and acid hydrolysis) and thermochemical (gasification). National laboratories have focused more on the biochemical platform [27, 75, 76, 79, 80] with the thermochemical platform expected to be demonstrated at the pilot-unit level by 2012 [81]. This study utilizes a biochemical platform that is expected to be commercialized first. In particular, a dilute acid pretreatment with enzymatic hydrolysis of cellulose to simple sugars followed by fermentation to ethanol is thought to be a commercialized technology in the short-term (5 years) [82]. In fact, in a final rule making report by the U.S. EPA regarding RFS2 volume requirements for calendar year 2011, four companies are cited in the U.S. with the potential to produce cellulosic alcohol and make it commercially available in 2011. Three of those companies utilize an enzymatic hydrolysis to sugars followed by fermentation to ethanol technology [83].

Pretreatment of the lignocellulosic biomass is essential to improve ethanol yield for biochemical platform processes. Solvents, acids and bases, or high temperature can be used to remove hemicelluloses and lignin from cellulose. Common pretreatment processes include dilute-acid pretreatment, hot water pretreatment, steam explosion,

Table 3.6: Biorefinery capital costs [75].

Installed equipment	Investment ($)
Pretreatment	25,300,000
Neutralization and conditioning	11,400,000
Saccharification and fermentation	22,200,000
Distillation and solids removal	27,100,000
Wastewater treatment	5,700,000
Storage	4,200,000
Boiler and turbogenerator	55,000,000
Utilities	6,500,000
Total Installed Equipment cost	157,300,000
Added costs [a]	115,200,000
Total Project Investment	272,500,000

[a] Added costs include indirect costs (engineering and supervision, construction expenses, legal and contractor fees) and contingency.

ammonia fiber explosion (AFEX), and treatment with organic solvents [84]. The economic competitiveness of different pretreatment and separation techniques for a cellulase enzymatic hydrolysis process were evaluated in [76]. The cost analysis was performed assuming n^{th}-plant (proven) technology and first-of-kind (pioneer plant) economics for processes published in literature. They determined that dilute acid pretreatment with cellulase saccharification, and cofermentation of C5 and C6 sugars with recombinant Zymomonas mobilis is most economical with an ethanol product value of $3.40/gal for the n^{th}-plant. Added expenses and risks for a pioneer plant increased the ethanol product value to $5.76/gal.

The National Renewable Energy Laboratory 2008 State of Technology (SOT) Model for biochemical production of ethanol has a similar process design and is used in this study for biorefinery economic parameters, because it contains only experimentally determined data [75]. No commercial cellulosic ethanol plants exist today, but the SOT is meant to reflect the best estimate of n^{th}-plant ethanol production costs. Capital investment and operating costs for a 56 million gallon per year (MGY) biorefinery are shown in Tables 3.6 and 3.7, respectively. Minimum ethanol selling price for an Internal Rate of Return of 10% was $2.61/gal [75].

Ethanol yield in the [75] model was 72.6 gallons per dry US ton corn stover with

Table 3.7: Biorefinery operating costs [75].

Source	Cost ($/y)
Corn steep liquor (CSL) nutrient	8,700,000
Cellulase	19,600,000
Other raw material	15,500,000
Waste disposal	1,200,000
Electricity [a]	–7,400,000
Total Operating Cost	37,600,000

[a] Evaporator syrup, lignin, digester solids and biogas are combusted for process heat and to generate excess electricity.

details given in an earlier model [79]. Important unit operation conversions are summarized in Table 3.8. These conversions are assumed equal for all feedstocks, allowing for process yields to be calculated from feedstock sugar composition as shown in Table 3.9. Oat straw is assumed to have the same yield as corn stover.

Biorefinery capacities included in the present model are $\xi_{l,1} = \{$ 56 MGY, 112 MGY, 168 MGY, 224 MGY $\}$ ethanol ($p = 1$). At each candidate biorefinery location there can then be up to four of the benchmark NREL SOT biochemical facilities. Locating five of the facilities at one location for a combined capacity of 280 MGY is not economical at any of the candidate biorefinery locations with base case parameters. Total project investment (TPI) and annual operating costs (AOC) are scaled accordingly to calculate the biorefinery lifetime cost $\psi_l = (\text{TPI})_l + \theta \cdot (\text{AOC})_l$.

3.4.8 Internal Rate of Return (IRR)

Internal Rate of Return (IRR) is the interest rate at which the Net Present Value, calculated in equation (3.2), is zero and is calculated for the optimum supply chain configuration. This gives a measure of the desirability of making all of those supply chain choices together. It does not measure the desirability of choosing each of the candidate biorefinery locations, for example. The estimated lifetime T_L in equation (3.3) is assumed to be 20 years.

Table 3.8: Sugar conversions by mass fraction [75].

Unit operation	Reaction	Conversion (mass fraction)
Pretreatment [a]	$(\text{Xylan})_n + n\ \text{H}_2\text{O} \rightarrow n$ Xylose	0.75
Saccharification [b]	$(\text{Glucan})_n + n\ \text{H}_2\text{O} \rightarrow n$ Glucose	0.90
	sugar loss to contamination	0.07
Conditioning [c]	Glucose loss	0.01
	Xylose loss	0.02
Fermentation [d]	Glucose $\rightarrow$ 2 Ethanol + 2 CO_2	0.90
	3 Xylose $\rightarrow$ 5 Ethanol + 5 CO_2	0.80
	minor sugars $\rightarrow$ Ethanol	0

[a] 1.1% sulfuric acid @ 190 °C, 12.1 atm.
[b] 5 days with 20 mg cellulase per g cellulose.
[c] (ammonia loading)
[d] 2 days.

Table 3.9: Feedstock composition by mass fraction and predicted ethanol yield.

Feedstock	Cellulose (glucan)	Xylan	Ethanol yield (gal/dt)
Barley straw [85]	0.375	0.15	66.2
Corn stover [75]	0.374	0.211	72.6
Wheat straw [86]	0.376	0.195	71.1

3.5 Software

Software used in this project included MATLAB [87] and CPLEX [64]. The IBM ILOG CPLEX Connector for MATLAB was used to interface between MATLAB and CPLEX. Optimization results were processed and displayed in MATLAB using the Mapping Toolbox.

Optimization time was reduced by taking advantage of the geography of the problem. Single-state optimization sub-problems with a reduced set of decision variables were solved quickly for each state. The combination of these sub-problem solutions was used as an initial guess for the combined regional problem as it is an integer feasible solution for the entire region problem. The branch and bound algorithm utilized in CPLEX takes advantage of such integer feasible solutions to trim branches of the search tree by bounding. This sub-problem solution strategy reduced the total runtime by about a third compared to having no initial guess. A solution was returned when the gap between lower and upper bounds on the optimal value of the objective function was less than 0.5%.

3.6 Results

3.6.1 Base case

The maximum Net Present Value supply chain network for the base case model is shown graphically in Figure 3.4. The base case model contains 5557 constraint equations governing 187,595 decision variables, including 276 binary variables that accommodate the possibility of one of four biorefinery capacities at each of the 69 candidate biorefinery locations. The matrix of constraint coefficients contains 375,190 nonzero entries (0.036% nonzero elements). The base case model required about 65.7 s (the 9 sub- problems required a combined runtime of 3 s) to solve on a quad core Intel Xeon 3.20 GHz 64-bit processor.

Our analysis identified biorefineries that are optimally located in 65 of the 69 allowed biorefinery locations. Total capacity of the system is 4.7 BGY of ethanol, which is equivalent to 83 of the NREL SOT 2008 biochemical benchmark biorefineries. The expected Net Present Value is $7.07 BB over a 20-year estimated plant lifewith an annual discount rate of 10%. The Internal Rate of Return is 12.1% annually. Costs by source are described in Table 3.10.

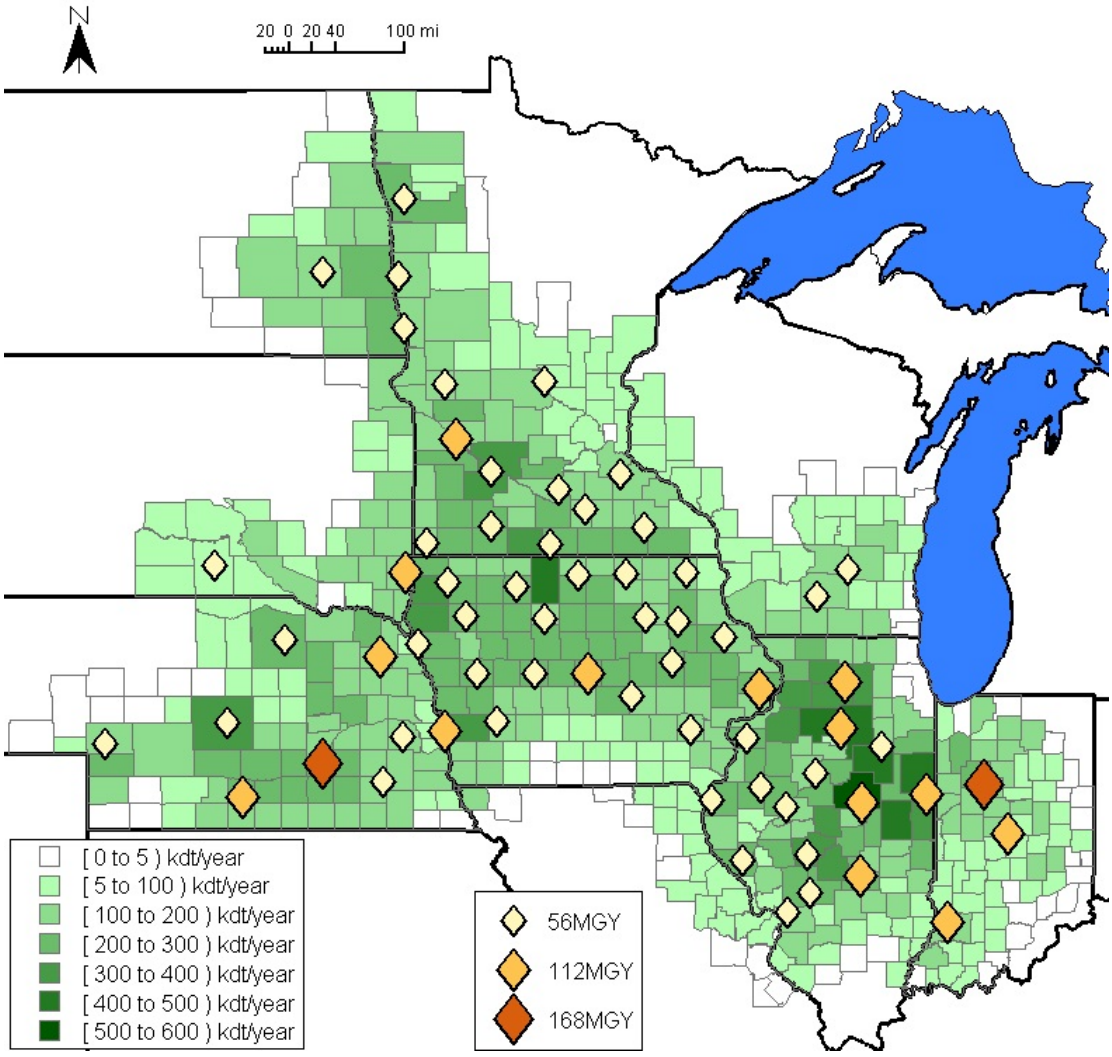

Figure 3.4: Base case optimal supply chain with installed biorefinery capacity in million gallons per year (MGY). Total biomass harvest in thousand dry metric tons per year (kdt/year).

Table 3.10: Base case result breakdown of cost sources.

Cash flow source	Annual cash flow (MM $/y) [a]	Sum of discounted cash flows (MM $) [b]	Percentage [c]
Ethanol sales	+ 13,091	+ 111,451	N/A
Biomass farming [d]	– 4,118	– 35,053	33.6%
Biomass local storage [e]	– 693	– 5,897	5.7%
Biomass densification	– 1,068	– 9,092	8.7%
Biomass transportation	– 605	– 5,151	4.9%
Biorefinery investment and operation	N/A	– 49,187	47.1%
	Net Present Value:	+ 7,070	

[a] Annual cash flow is assumed equal for each year of the 20 year project lifetime.
[b] Determined by discounting each year of the project lifetime.
[c] Contribution to the total production cost of ethanol.
[d] Includes farmer payment, nutrient replacement and baling.
[e] Includes bale transportation, local storage land rent and deterioration losses.

Agricultural residue biomass is more densely available in Illinois and Iowa. In Iowa, biomass availability is limited almost exclusively to corn stover. Illinois has some winter wheat, but is also dominated by corn stover. Wheat becomes prevalent in the Dakotas and northwestern Minnesota.

Of the 35% of crop residues that can be removed annually, about 94% is harvested for the base case model. Table 3.11 summarizes the biomass utilization by feedstock. This finding may be misleading in that the model assumed fixed economic and technological parameters. The economic variability inherent in the real world may make certain regions too risky for a biorefinery investment. Thus, parameter sensitivity must be used to determine the biorefinery supply chain robustness.

3.6.2 Sensitivity analysis

Certain variability exists in the base case economic parameters because they specify volatile prices or characteristics of technology not demonstrated at this scale. Many studies have examined how biomass utilizing systems can be affected by economic parameter uncertainty. The logistic challenges for fossil fuel substitution with biomass for energy production were explored in [88]. The sensitivity of ethanol production cost was compared across multiple technologies in [82].

Table 3.11: Base case model biomass utilization.

Crop	Amount of residue that can be removed (MM dt/y)	Amount of residue harvested (MM dt/y)	Utilization
Barley	0.127	0.040	31.8%
Corn	67.0	64.2	95.7%
Oats	0.113	0.105	92.4%
Wheat (spring)	1.87	1.46	78.5%
Wheat (winter)	2.24	1.52	67.7%
Total	71.4	67.3	94.3%

Analyzing the effects of a single parameter change on the model optimum supply chain while the other base case parameters are fixed gives an intuitive understanding of that parameters effect on profitability. This may be useful to policy makers interested in encouraging this technology. For example, when the ethanol sale price σ_1 seen by the biorefinery is varied as in Figure 3.5, we can see that a reduction to \$2.7/gal may not affect the industry. Most biorefineries would still be able to make at least a 10% return on investment to remain open, and biomass would still be utilized. An ethanol sale price below \$2.7/gal could affect the willingness of companies to invest in a biorefinery. Ideally, tax incentives that increase the ethanol sale price seen by the biorefinery would be stable across the facility lifetime as a sudden drop could cause biorefineries to scale down production.

When the biorefinery capital investment and operating costs are varied as shown in Figure 3.6, the number of installed biorefineries is unchanged until costs rise about 10%. There is enough economic incentive before that point to utilize almost all the available biomass for a developed cellulosic ethanol industry, but the industry would develop more rapidly if incentives lowered capital costs. Similarly, increasing the conversion efficiency $\beta_{b,1}$ from biomass to ethanol as shown in Figure 3.7 greatly increases the IRR.

3.6.3 Monte Carlo analysis

Monte Carlo based random sampling of the parameter space can give insights into the system robustness in two ways. After determining the optimum supply chain for the base case, random sampling of the parameter space and recalculation of the economics can determine how good the choice was. If companies had indeed decided to place

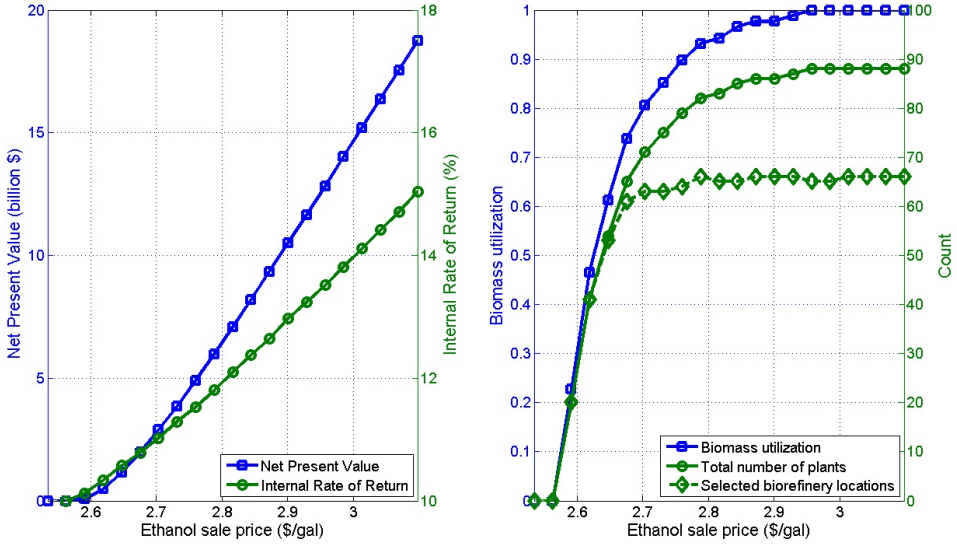

Figure 3.5: Effect of varying ethanol sale price with other base case parameters fixed.

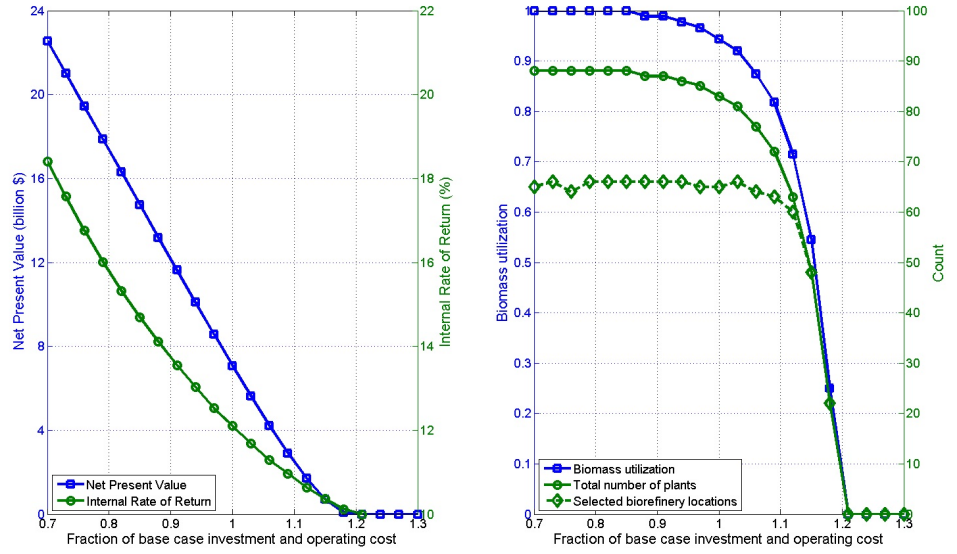

Figure 3.6: Effect of varying biorefinery capital investment and operating cost with other base case parameters fixed.

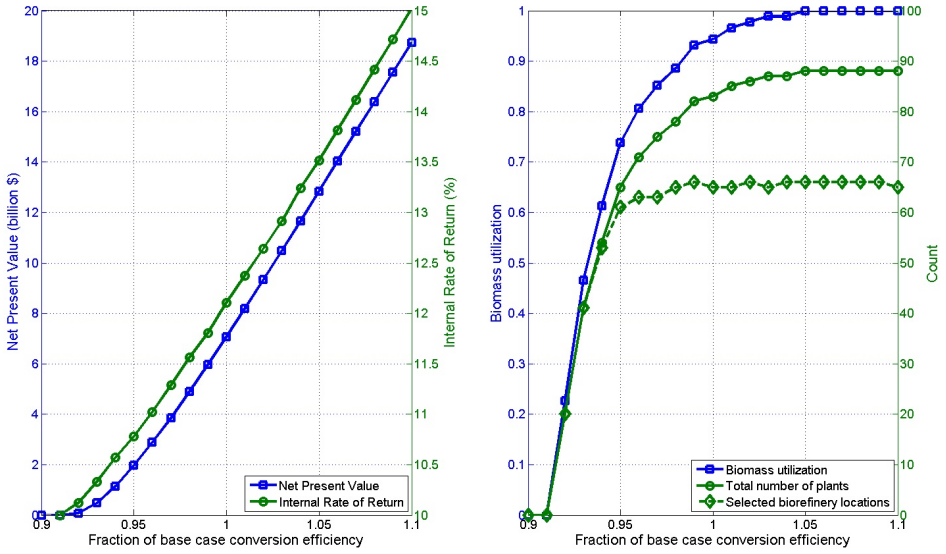

Figure 3.7: Effect of varying conversion efficiency with other base case parameters fixed.

biorefineries there and create long-term contracts with the local farmers to provide them with agricultural residues, an estimate of the probability of meeting their 10% annual rate of return could be determined. A second analysis of robustness could find the most robust supply chain choices. For each set of randomly sampled parameters, the supply chain would be re-optimized and the results compared.

For the first analysis, each parameter was sampled from a triangle distribution having the variability shown in Table 3.12. The parameter variability is similar to that used in [89]. Figure 3.8 shows the variability in IRR for the base case optimum supply chain when the parameter space is sampled for 10,000 parameter sets. With the assumed parameter variability, the biorefinery supply chain investments will fall short of a 10% rate of return, and thus have negative NPV, about 15% of the time.

For the second analysis of robustness, the model was optimized for 200 independently drawn parameter sets. An indication of the favorability of each candidate biorefinery location considering the parameter variability is shown in Figure 3.9. The fraction of trials in which a biorefinery of any size was placed at each location was calculated. Locations chosen least frequently are not surrounded by biomass producing counties included in the model. If more biomass producing counties were included in the model,

Table 3.12: Variability of model parameters.

Parameter		Variability
σ_p	unit sale price for product p (\$/gal)	± 20%
ρ_b	unit feedstock cost for biomass b (\$/dt)	± 30%
$\tau_{n,r}$	unit biomass transportation cost from n to r (\$/dt)	± 10%
ϕ_l	investment and lifetime operating cost for a biorefinery of size l (\$)	± 20%
$\lambda_{n,b}$	amount of biomass b harvestable at n annually (dt/y)	± 15%
$\beta_{b,p}$	biorefinery conversion of biomass b to product p (gal/dt)	± 10%

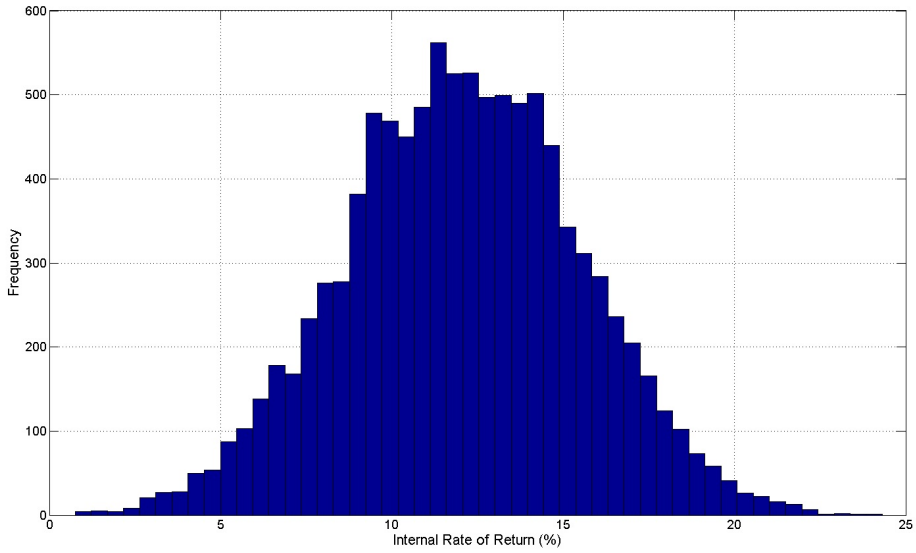

Figure 3.8: Monte Carlo method sampling of the parameter space for the base case optimum supply chain configuration.

these locations might be able to support a biorefinery economically.

It was not economical to construct any biorefineries in 21.5% of the trials. A large spread of total system IRR is observed as shown in Figure 3.10. The number of installed biorefineries (NREL SOT 2008 biochemical benchmark) is high as shown in Figure 3.11, such that 53.5% of trials had biomass utilization of 95% or higher.

3.7 Conclusions

The methodology proposed in this chapter provides an assessment of the maximum profit supply chain for lignocellulosic biomass-to-ethanol conversion technology systems when accounting for the spatial distribution of biomass. There is considerable potential for cellulosic ethanol production in the Midwest U.S. due to high biomass availability. Once the technology has been proven and n^{th}-plant economics evolve, and economic parameters stabilize, there is enough incentive for a 4.7 BGY cellulosic ethanol industry to develop in the region.

With the current estimated parameter variability of the system, there is a 21.5% chance this industry will not develop. If the industry did develop, it could become uneconomical approximately 15% of the time. An ethanol sale price seen by the biorefinery including tax incentives below \$2.7/gal could affect the willingness of companies to invest in biorefineries. There are various approaches to curb the risks associated with this non-commercialized technology. The cellulosic ethanol sale price seen by the biorefinery could be stabilized up to at least \$2.99/gal by continuing the Volumetric Ethanol Excise Tax Credit, or similar incentive. Incentive programs that lower first-of-kind biorefinery capital investment allow for convergence to the n^{th}-plant economics assumed in this study.

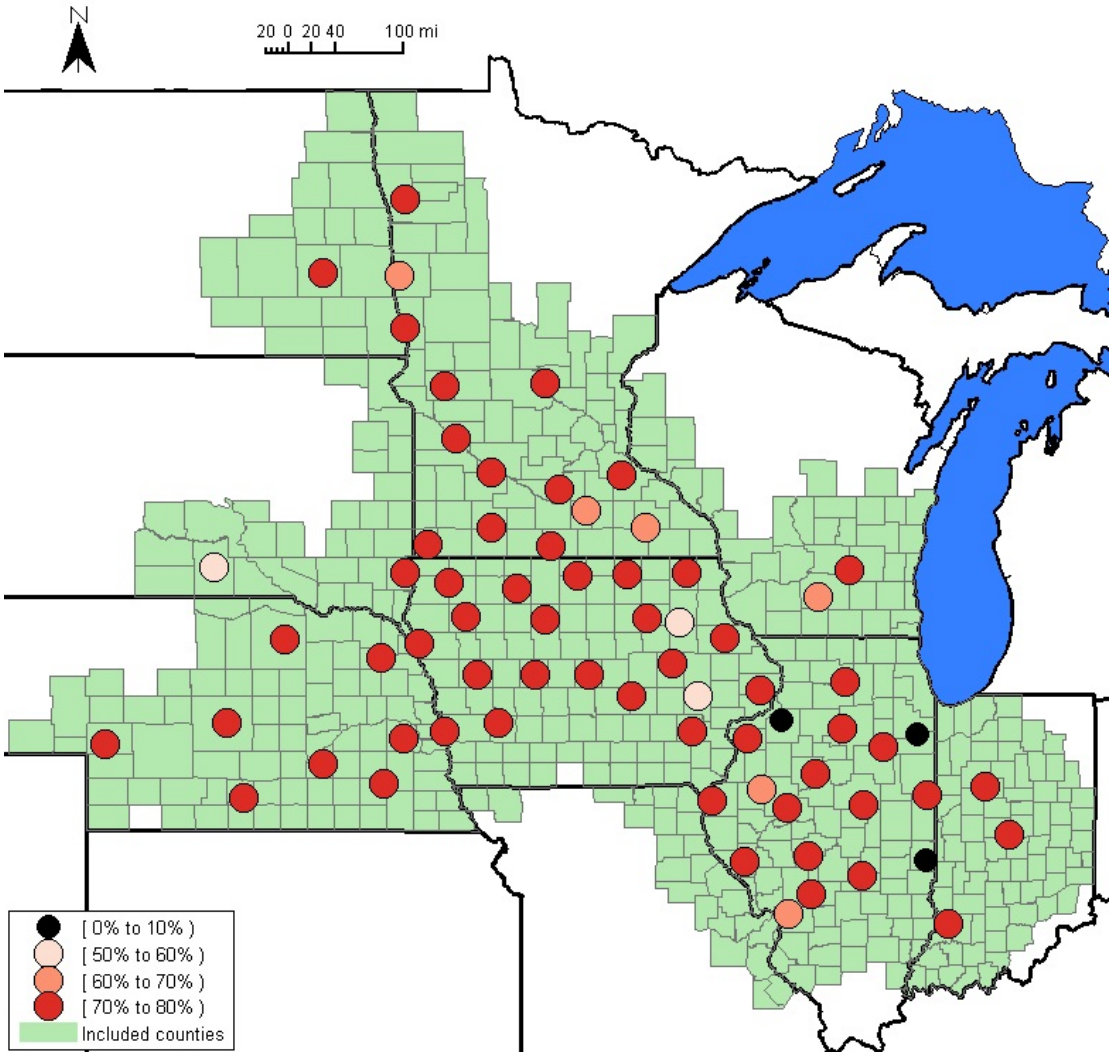

Figure 3.9: Percentage of trials in which each candidate biorefinery location was selected in 200 model runs, each using a randomly sampled parameter set. Biomass producing counties are shaded.

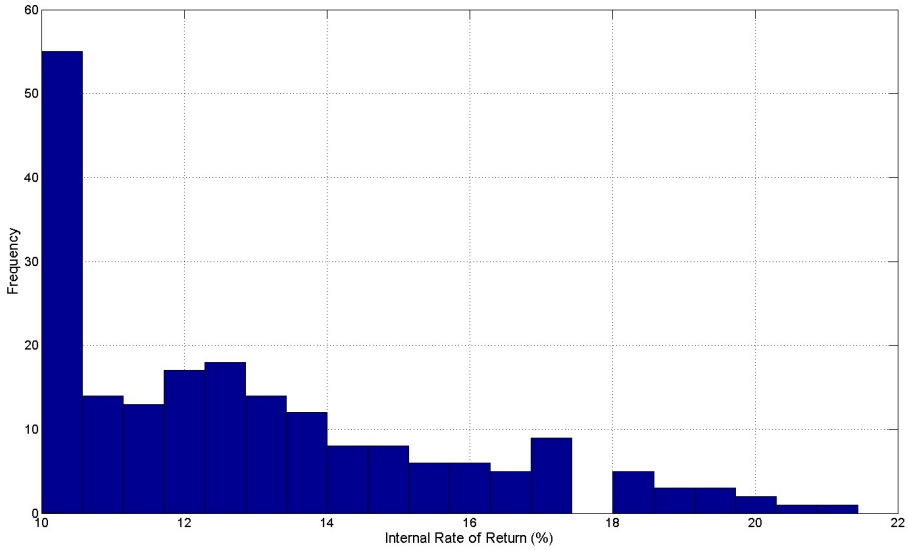

Figure 3.10: Internal Rate of Return for 200 model optimization trials sampled from the parameter space.

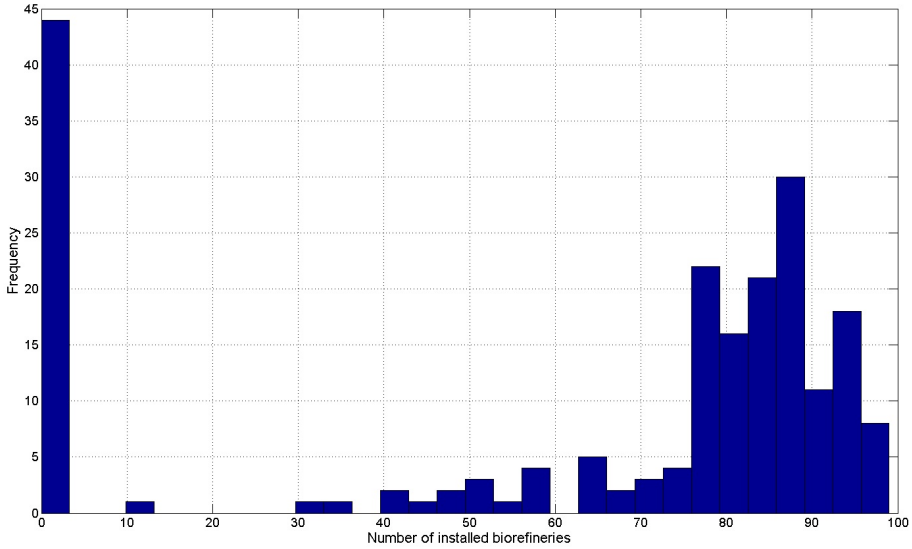

Figure 3.11: Total number of installed NREL SOT 2008 biochemical benchmark biorefineries for 200 model optimization trials sampled from the parameter space.

CHAPTER 4

Economic Supply Chain Optimization with Competing Biorefinery Technologies and Diverse Biomass Feedstocks*

4.1 Summary

In Chapter 3, we examined cellulosic ethanol production in the Midwest as a MILP with supply chain uncertainty estimated using Monte Carlo sampling. This chapter expands upon that idea, with a focus on accessing the feasibility of meeting governmental biofuel mandates (i.e. RFS) in 2015. This is done by including a broader set of biomass feedstocks and biofuel production technologies, along with a more detailed economic analysis. Facility capacity is now allowed to take continuous values (instead of discrete values, as in Chapter 3), by including piecewise-linear functions. Existing corn ethanol facilities and new candidate facility sites are considered for biofuel production by utilizing eight types of biomass. The spatial distribution and farmgate cost of biomass is accessed from a recently updated U.S. Department of Energy database. Seven biomass processing technologies that are expected to be commercialized in the near-term are available for construction at each candidate facility site. A detailed cash flow analysis that includes capital depreciation and taxation is embedded into the model formulation

*Reprinted with permission from W. Alex Marvin, Lanny D. Schmidt, and Prodromos Daoutidis, *Industrial & Engineering Chemistry Research*, 52(9):3192–3208, 2013 [21]. Copyright © 2013 American Chemical Society.

to give insights into the minimum biofuel selling price for each facility site. Equilibrium market cost for each of the Renewable Fuel classifications (renewable fuel, advanced biofuel and cellulosic biofuel), that is directly related to the Renewable Identification Number market price, is determined through sensitivity analysis of the delivered biofuel price.

4.2 Supply chain overview

This study considers the biofuel supply chain as a network of biomass producers, conversion facilities and markets that performs the functions of biomass production, harvesting, storage, processing and transportation, and biofuel distribution to markets. The optimization problem is to determine how to utilize the biomass resources to satisfy the market demand such that an objective function is maximized.

Each *biomass producer* $n \in \mathbf{N}$ resides at a geographic location and may have multiple *biomass types* available for farmgate purchase (at the roadside). Biomass types are differentiated by category (crops, grasses, agricultural waste, wood, municipal waste or landfill gas), species (e.g. animal products, barley, cotton, corn, hay, oats, perennial grasses, rice, sugarcane, soybeans or wheat) and state (e.g. loose, shredded, baled, pelleted, pyrolyzed or torrefied). In general, the maximum amount of a biomass type available at a biomass producer is a function of the farmgate price offered. As a simplifying assumption, each biomass producer has a fixed farmgate price for each of their available biomass types.

Each *facility site* $r \in \mathbf{R}$ resides at a geographic location, may purchase and process biomass, and produce and sell biofuels. The site is either a *candidate site* $\mathbf{R}^{\text{Candidates}} \subset \mathbf{R}$ for facility constructions or is an *existing site* $\mathbf{R}^{\text{Existing}} \subset \mathbf{R}$ of an operational facility. A number of *biomass processing technologies* $l \in \mathbf{L}$ can be installed at each candidate site. A facility site is defined by:

- a set of allowed transportation methods $v \in \mathbf{V}$ (e.g. rail, semi-truck, tank truck) for each biomass type and biofuel;
- a maximum capacity for biomass processing and biofuel production;
- a process yield from biomass to biofuel;
- a function that determines economic and environmental performance indexes for the facility based on supply chain decisions.

Each *market* $m \in \mathbf{M}$ resides at a geographic location and may purchase biofuels. Each biofuel, referred to as a *biofuel type* $p \in \mathbf{P}$, has a defined composition (e.g. ethanol, biodiesel, bio-gasoline), RFS2 fuel classification (cellulosic biofuel, biomass-based diesel, advanced biofuel or renewable fuel) and state (gas, liquid or solid). A market is defined by:

- a set of allowed transportation methods $v \in \mathbf{V}$ for each biofuel type;
- a demand for each biofuel type (may be zero);
- a purchase price for each biofuel type.

4.3 Mathematical formulation

We formulate the SCO problem as a MILP. The objective function, equations, parameters and decision variables are described in the following subsections.

4.3.1 Objective function

Total net present value (TNPV) for the entire supply chain, a measure of profitability, is chosen as the economic objective function. It is the sum of the net present value (NPV) corresponding to each of the facility sites ($r \in \mathbf{R}$):

$$\text{TNPV} = \sum_{r} \text{NPV}_r \tag{4.1}$$

NPV is calculated as the sum of a time series of cash flows, determined through engineering economic analysis [90], that have been discounted back to the present. This requires introducing a set $t \in \mathbf{T}$ of time periods that includes the years of facility construction and operational lifetime. Each facility site r in our study has cash flows during those time periods for:

- Revenue
  - Biofuel sales $\text{CT}_{r,t}^{\text{Biofuel}}$
  - Co-product sales $\text{CT}_{r,t}^{\text{Coproducts}}$
- Expenses

  - Variable costs
    * Biomass purchasing $\mathrm{CT}_{r,t}^{\mathrm{Biomass}}$
    * Equipment and parts replacement $\mathrm{CT}_{r,t}^{\mathrm{Parts}}$
    * Other variable costs $\mathrm{CT}_{r,t}^{\mathrm{Other\,Variable}}$ (non-biomass raw materials, fuels and waste disposal)
  - Fixed costs $\mathrm{CT}_{r,t}^{\mathrm{Fixed}}$ (labor, maintenance and insurance)
  - Fixed capital investment $\mathrm{CT}_{r,t}^{\mathrm{FCI}}$ (installed equipment cost, engineering, construction, legal and contractors fees, project contingency, and land)
  - Working capital $\mathrm{CT}_{r,t}^{\mathrm{WC}}$

- Income tax $\mathrm{CT}_{r,t}^{\mathrm{Taxes}}$

Income tax is paid on taxable income (revenue minus the sum of expenses and capital depreciation $d_{r,t}$) at tax rate TR. Expenses before facility start-up (fixed capital investment and working capital) are not taxable. We assume that losses after start-up are taxed and cannot be forwarded. This is a good assumption for most facility sites with positive NPV (the case for facility sites in this study) or when the facility site is owned by a profitable parent company with other revenue streams. Thus, the income tax paid can be written as:

$$\begin{aligned}\mathrm{CT}_{r,t}^{\mathrm{Taxes}} = \mathrm{TR} \cdot \Big[& \Big(\mathrm{CT}_{r,t}^{\mathrm{Biofuel}} + \mathrm{CT}_{r,t}^{\mathrm{Coproducts}} \Big) \\ & - \Big(\mathrm{CT}_{r,t}^{\mathrm{Biomass}} + \mathrm{CT}_{r,t}^{\mathrm{Parts}} + \mathrm{CT}_{r,t}^{\mathrm{Other\,Variable}} + \mathrm{CT}_{r,t}^{\mathrm{Fixed}} \Big) \\ & - d_{r,t} \Big] \end{aligned} \tag{4.2}$$

Cash flows in time period t are discounted to the present using the discounting factor $\theta_t = (1+i)^{-t}$ with discount rate i. The NPV for each facility site then takes the form:

$$\begin{aligned}\mathrm{NPV}_r = \sum_t \theta_t \Big[& \Big(\mathrm{CT}_{r,t}^{\mathrm{Biofuel}} + \mathrm{CT}_{r,t}^{\mathrm{Coproducts}} \Big) \\ & - \Big(\mathrm{CT}_{r,t}^{\mathrm{Biomass}} + \mathrm{CT}_{r,t}^{\mathrm{Parts}} + \mathrm{CT}_{r,t}^{\mathrm{Other\,Variable}} + \mathrm{CT}_{r,t}^{\mathrm{Fixed}} + \mathrm{CT}_{r,t}^{\mathrm{FCI}} + \mathrm{CT}_{r,t}^{\mathrm{WC}} \Big) \\ & - \mathrm{CT}_{r,t}^{\mathrm{Taxes}} \Big] \end{aligned} \tag{4.3}$$

Furthermore, it is reasonable to assume that cash flows for parts and capital depreciation are proportional to fixed capital investment. Pieces of equipment (that cost a

known fraction of the fixed capital investment) need replacement periodically during a facility lifetime. Capital depreciation is recorded for tax purposes as a fraction of the fixed capital investment by following an Internal Revenue Service (IRS) schedule. With these assumptions, the NPV for each facility site can be written as:

$$
\begin{aligned}
\mathrm{NPV}_r = & \left(\sum_t \theta_t \cdot \alpha_t^{\mathrm{Biofuel}}\right) \cdot (1-\mathrm{TR}) \cdot \mathrm{CF}_r^{\mathrm{Biofuel}} \\
& - \left(\sum_t \theta_t \cdot \alpha_t^{\mathrm{Biomass}}\right) \cdot (1-\mathrm{TR}) \cdot \mathrm{CF}_r^{\mathrm{Biomass}} \\
& + \sum_l \left[\left(\sum_t \theta_t \cdot \alpha_{l,t}^{\mathrm{Revenue}}\right) \cdot (1-\mathrm{TR}) \cdot \mathrm{CF}_{r,l}^{\mathrm{Coproducts}} \right. \\
& - \left(\sum_t \theta_t \cdot \alpha_{l,t}^{\mathrm{Variable}}\right) \cdot (1-\mathrm{TR}) \cdot \mathrm{CF}_{r,l}^{\mathrm{Other\,Variable}} \\
& - \left(\sum_t \theta_t \cdot \alpha_{l,t}^{\mathrm{Parts}}\right) \cdot (1-\mathrm{TR}) \cdot \mathrm{CF}_{r,l}^{\mathrm{FCI}} \\
& - \left(\sum_t \theta_t \cdot \alpha_{l,t}^{\mathrm{Fixed}}\right) \cdot (1-\mathrm{TR}) \cdot \mathrm{CF}_{r,l}^{\mathrm{Fixed}} \\
& - \left(\sum_t \theta_t \cdot \alpha_{l,t}^{\mathrm{FCI}}\right) \cdot \mathrm{CF}_{r,l}^{\mathrm{FCI}} \\
& - \left(\sum_t \theta_t \cdot \alpha_{l,t}^{\mathrm{WC}}\right) \cdot \mathrm{CF}_{r,l}^{\mathrm{WC}} \\
& \left. + \left(\sum_t \theta_t \cdot \alpha_{l,t}^{d}\right) \cdot \mathrm{TR} \cdot \mathrm{CF}_{r,l}^{\mathrm{FCI}} \right]
\end{aligned}
\tag{4.4}
$$

where biofuel sales and biomass purchasing are independent of the technology installed.

The terms within parentheses are summations of known parameters, and thus can be

aggregated to simplify the expression to the form used in our optimization formulation:

$$\begin{aligned}\mathrm{NPV}_r = {} & \sigma^{\mathrm{Biofuel}} \cdot \mathrm{CF}_r^{\mathrm{Biofuel}} - \sigma^{\mathrm{Biomass}} \cdot \mathrm{CF}_r^{\mathrm{Biomass}} \\ & + \sum_l \Big[\sigma_l^{\mathrm{Revenue}} \cdot \mathrm{CF}_{r,l}^{\mathrm{Coproducts}} \\ & - \sigma_l^{\mathrm{Variable}} \cdot \mathrm{CF}_{r,l}^{\mathrm{Other\,Variable}} \\ & - \sigma_l^{\mathrm{Fixed}} \cdot \mathrm{CF}_{r,l}^{\mathrm{Fixed}} - \sigma_l^{\mathrm{WC}} \cdot \mathrm{CF}_{r,l}^{\mathrm{WC}} \\ & - \left(\sigma_l^{\mathrm{Parts}} + \sigma_l^{\mathrm{FCI}} - \sigma_l^{d} \right) \cdot \mathrm{CF}_{r,l}^{\mathrm{FCI}} \Big] \end{aligned} \tag{4.5}$$

by introducing the parameters: $\sigma^{\mathrm{Biofuel}}$, $\sigma^{\mathrm{Biomass}}$, $\sigma_l^{\mathrm{Revenue}}$, $\sigma_l^{\mathrm{Variable}}$, $\sigma_l^{\mathrm{Parts}}$, $\sigma_l^{\mathrm{Fixed}}$, σ_l^{FCI}, σ_l^{WC}, and σ_l^{d}. These parameters are described in more detail in the notation section (Section 4.8) and their calculation is shown in the Supporting Information (Section 4.7).

4.3.2 Material flow constraints

The supply chain structure near a biomass producer is shown in Figure 4.1. The decision variables $f_{n,r,v,b}^{NR}$ are the amount of biomass type b delivered annually from biomass producer n to facility site r via transportation method v. Biomass sold from the biomass producer cannot exceed the maximum available $\beta_{n,b}^{N}$:

$$\sum_{r,v} f_{n,r,v,b}^{NR} \leq \beta_{n,b}^{N}, \quad \forall n, b \tag{4.6}$$

In the case of edible biomass resources $\mathbf{B}^{\mathrm{Food}} \subset \mathbf{B}$, a maximum fraction τ_b of the total available biomass can be sold to produce biofuels:

$$\sum_{n,r,v} f_{n,r,v,b}^{NR} \leq \tau_b \sum_{n} \beta_{n,b}^{N}, \quad \forall b \in \mathbf{B}^{\mathrm{Food}} \tag{4.7}$$

As a remark, we avoid introducing redundant or unneeded set combinations for all the decision variables and constraints to reduce memory usage and computation time. For example, $f_{n,r,v,b}^{NR}$ decision variables are introduced for only the combinations of (n, r, v, b) that correspond to: (i) a biomass producer n with biomass type b available ($\beta_{n,b}^{N} > 0$), (ii) a facility site r that can utilize biomass type b, (iii) an allowed method v to transport biomass type b and (iv) a biomass producer n that is no further than 200 miles from facility site r. Similarly, constraints from equation (4.6) are not introduced

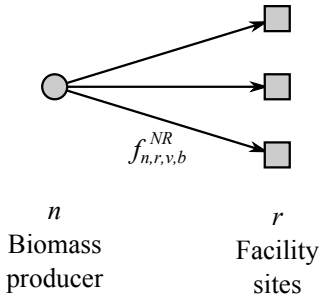

Figure 4.1: Simplified supply chain schematic for a biomass producer.

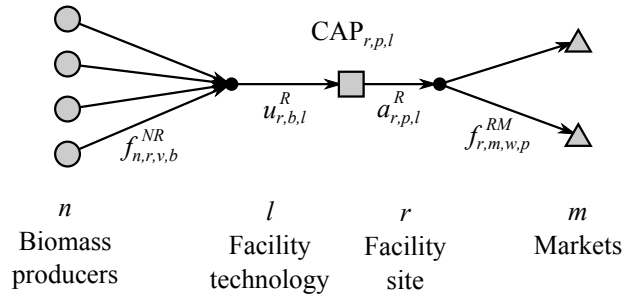

Figure 4.2: Simplified supply chain schematic for a facility site.

for combinations of (n, b) such that $\beta^{N}_{n,b} = 0$. This is accomplished through the use of tuple and tuple set data structures available in IBM ILOG CPLEX Optimization Studio, the optimization software package used in this study. A similar approach was used by Ferrio and Wassick [91] to define decision variables in GAMS for only the "valid transportation lanes" in a chemical supply chain network. These set details are not shown in an effort to avoid needlessly complicated notation.

The supply chain structure near a facility site is shown in Figure 4.2. Biomass delivered to the facility site must be used by a biomass processing technology:

$$\sum_{n,v} f^{NR}_{n,r,v,b} = \sum_{l} u^{R}_{r,b,l}, \quad \forall r, b \tag{4.8}$$

where $u^{R}_{r,b,l}$ is the amount of biomass b used at r by technology l.

Process yield for each biomass processing technology is incorporated by the parameter $\eta^{R}_{b,p,l}$. The amount of biofuel type p produced at facility site r by technology l, $a^{R}_{r,p,l}$, is then:

$$a^{R}_{r,p,l} = \sum_{b} \eta^{R}_{b,p,l} \cdot u^{R}_{r,b,l}, \quad \forall r, p, l \tag{4.9}$$

Some biomass processing technologies are designed for a specific mixture of multiple feedstocks. This can be accounted for by introducing the parameter $\mu_{b,l}$ that represents the fraction of biofuel produced from biomass type b using technology l:

$$\mu_{b,l} \cdot a^R_{r,p,l} = \eta^R_{b,p,l} \cdot u^R_{r,b,l}, \quad \forall r, b, p, l \tag{4.10}$$

The installed facility capacity $\mathrm{CAP}_{r,p,l}$ determines the maximum biofuel production:

$$a^R_{r,p,l} \leq \delta \cdot \mathrm{CAP}_{r,p,l}, \quad \forall r, p, l \tag{4.11}$$

where the capacity factor parameter δ accounts for fractional capacity utilization due to inherent facility downtime and maintenance. We assume 8,410 operating hours per year or $\delta \approx 0.959$.

All biofuels produced at the facility are sold to markets:

$$\sum_l a^R_{r,p,l} = \sum_{m,v} f^{RM}_{r,m,v,p}, \quad \forall r, p \tag{4.12}$$

where the decision variables $f^{RM}_{r,m,v,p}$ are the amount of biofuel p delivered annually from facility site r to market m via transportation method v.

The supply chain structure near a market is shown in Figure 4.3. Biofuel delivered to the market must be within a demand satisfaction window for each of the RFS2 biofuel classifications $k \in \mathbf{K} = \{\mathrm{RF}, \mathrm{AB}, \mathrm{CB}\}$. This is incorporated by the parameters $\beta^{M,\min}_{m,k}$ and $\beta^{M,\max}_{m,k}$, and can be accounted for by:

$$\beta^{M,\min}_{m,k} \leq \sum_{p \in \mathbf{P}^{\mathrm{Class}}_k} \sum_{r,v} f^{RM}_{r,m,v,p} \leq \beta^{M,\max}_{m,k}, \quad \forall m, k \tag{4.13}$$

where $\mathbf{P}^{\mathrm{Class}}_k \subset \mathbf{P}$ is the subset of biofuel types that can be counted for RFS2 biofuel classification k. Note that these RFS2 biofuel classifications are nested (e.g. cellulosic biofuels can also be counted as renewable biofuels for mandate satisfaction).

All shipments, usages, productions and installed capacities must be non-negative quantities:

$$f^{NR}_{n,r,v,b},\ f^{RM}_{r,m,v,p},\ u^R_{r,b,l},\ a^R_{r,p,l},\ \mathrm{CAP}_{r,p,l} \geq 0 \tag{4.14}$$

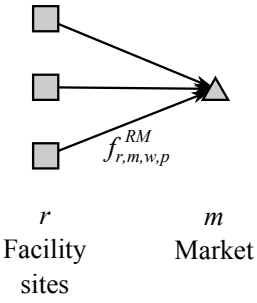

Figure 4.3: Simplified supply chain schematic for a market.

4.3.3 Cash flow and facility capacity constraints

The cash flow for biofuel sales at each facility site is proportional to biofuel deliveries:

$$\mathrm{CF}_r^{\mathrm{Biofuel}} = \sum_{m,v,p} C_{r,m,v,p}^{\mathrm{Biofuel}} \cdot f_{r,m,v,p}^{RM}, \quad \forall r \tag{4.15}$$

where a facility-gate biofuel sale price of $C_{r,m,v,p}^{\mathrm{Biofuel}}$ is paid for each unit of biofuel type p shipped from facility site r to market m via method v. This allows for the accounting of a surprising diversity of logistical costs. The facility-gate biofuel sale price is the unit price the market offers minus logistical costs associated with the specific delivery option, as long as those costs can be found on a per unit of biofuel basis. Transportation cost (determined by the travel distance between r and m), and loading and unloading costs are common logistical costs.

Similarly, the cash flow for biomass purchasing is proportional to biomass deliveries:

$$\mathrm{CF}_r^{\mathrm{Biomass}} = \sum_{n,v,b} C_{n,r,v,b}^{\mathrm{Biomass}} \cdot f_{n,r,v,b}^{NR}, \quad \forall r \tag{4.16}$$

where a delivered biomass price of $C_{n,r,v,b}^{\mathrm{Biomass}}$ is paid for each unit of biomass type b shipped from biomass producer n to facility site r via method v. The delivered biomass price is the sum of the farmgate price demanded by the biomass producer and any logistical costs associated with the specific delivery option, as long as those costs can be found on a per unit of biomass basis. Transportation cost (determined by the travel distance between n and r), loading and unloading costs and preprocessing costs (e.g. method v could involve baling, densification or pyrolysis of the biomass) are common logistical costs.

Existing facilities

Technology selection, capacity and costs are known for operational facilities. Thus the facility capacity is equal to the known value of $R_{r,p,l}^{\text{Existing,CAP}}$ for each biofuel type p and technology l:

$$\text{CAP}_{r,p,l} = R_{r,p,l}^{\text{Existing,CAP}}, \quad \forall r, p, l : \; r \in \mathbf{R}^{\text{Existing}} \tag{4.17}$$

Cash flows that depend on the biofuel production level (coproduct sales and other variable costs) are proportional to their known value if the existing facility were operating at full capacity:

$$\text{CF}_{r,l}^{\text{Coproducts}} = \frac{a_{r,p,l}^{R}}{R_{r,p,l}^{\text{Existing,CAP}}} \cdot R_{r,l}^{\text{Existing,Coproducts}}, \quad \forall r, l : \; r \in \mathbf{R}^{\text{Existing}} \tag{4.18}$$

$$\text{CF}_{\text{r,l}}^{\text{Other Variable}} = \frac{a_{r,p,l}^{R}}{R_{r,p,l}^{\text{Existing,CAP}}} \cdot R_{r,l}^{\text{Existing,Other Variable}}, \quad \forall r, l : \; r \in \mathbf{R}^{\text{Existing}} \tag{4.19}$$

Similarly, cash flows that are independent of capacity utilization are set to their known values:

$$\text{CF}_{r,l}^{\text{Fixed}} = R_{r,l}^{\text{Existing,Fixed}}, \quad \forall r, l : \; r \in \mathbf{R}^{\text{Existing}} \tag{4.20}$$

$$\text{CF}_{r,l}^{\text{FCI}} = R_{r,l}^{\text{Existing,FCI}}, \quad \forall r, l : \; r \in \mathbf{R}^{\text{Existing}} \tag{4.21}$$

$$\text{CF}_{r,l}^{\text{WC}} = R_{r,l}^{\text{Existing,WC}}, \quad \forall r, l : \; r \in \mathbf{R}^{\text{Existing}} \tag{4.22}$$

Note that only unresolved fixed capital cost can be depreciated at existing facilities. Similarly, only unresolved working capital can be recovered. Unless the facility recently began operations, it is expected that $R_{r,l}^{\text{Existing,FCI}}$ and $R_{r,l}^{\text{Existing,WC}}$ are zero.

Candidate sites

Each candidate site may be developed by constructing facilities using the biomass processing technologies. Capacity for the installed technology is desired to be a continuous variable, requiring knowledge of the facility costs as a function of facility capacity. In general, these functions may be nonlinear (e.g. fixed capital investment is often related to capacity using a power law to capture economies of scale). We approximate each nonlinear function with a piecewise linear function to avoid introducing nonlinear equations into the formulation. Similar strategies have been widely used in literature (e.g.

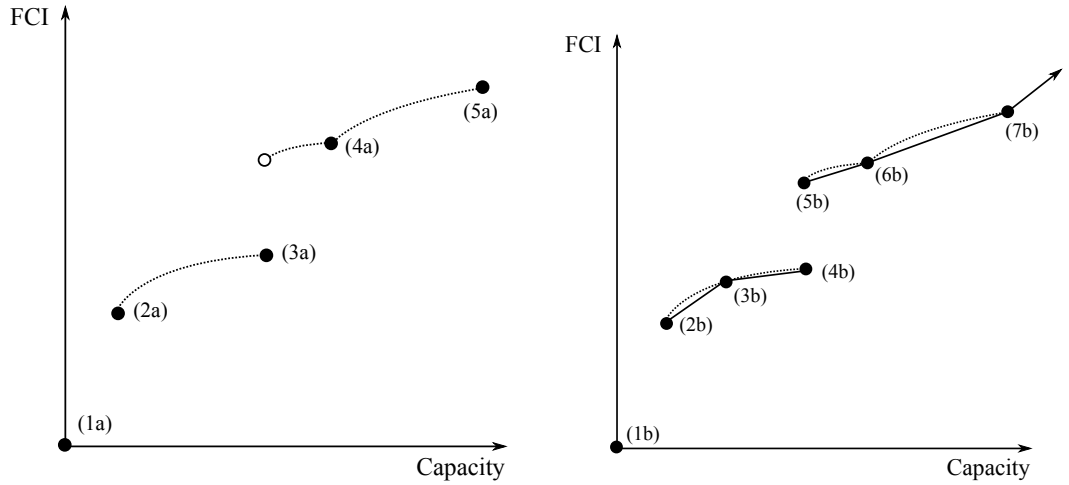

(a) True nonlinear function. Notable points have these facilities installed: (1a) none, (2a) one minimum capacity, (3a) one maximum capacity, (4a) one max and one min, (5a) two max.

(b) Piecewise linear approximation with $J = 8$ points. The final point is at high capacity and is not shown.

Figure 4.4: Piecewise linearization of fixed capital investment (FCI).

optimization of polygeneration systems [92] and biomass supply chains with multiple stages of processing [93]).

Our technique accounts for multiple technology options, and nonlinear relationships with discontinuity and step changes. These features are important for this study, as multiple facilities of the same technology can be installed at each facility site. A minimum and maximum capacity for each facility leads to a discontinuity at zero and a step at the maximum capacity, as shown in Figure 4.4 for fixed capital investment. The step is due to the loss of economies of scale when two smaller facilities are installed.

The piecewise linear functions are defined by a set of discrete points $j \in \{1, \ldots, J\}$, with corresponding capacity $\mathrm{CAP}^{\mathrm{linear}}_{p,l,j}$ for each biofuel type and technology. Note that $\mathrm{CAP}^{\mathrm{linear}}_{p,l,j} = 0$, if technology l cannot produce biofuel type p. We calculate the corresponding facility costs at each facility capacity using the (linear or nonlinear) functions

$f_l^{\text{Fixed}}(\cdot)$, $f_l^{\text{FCI}}(\cdot)$ and $f_l^{\text{WC}}(\cdot)$:

$$\text{CF}_{l,j}^{\text{linear,Fixed}} = f_l^{\text{Fixed}}\left(\text{CAP}_{p_l^{\text{major}},l,j}^{\text{linear}}\right), \quad \forall l, j \tag{4.23}$$

$$\text{CF}_{l,j}^{\text{linear,FCI}} = f_l^{\text{FCI}}\left(\text{CAP}_{p_l^{\text{major}},l,j}^{\text{linear}}\right), \quad \forall l, j \tag{4.24}$$

$$\text{CF}_{l,j}^{\text{linear,WC}} = f_l^{\text{WC}}\left(\text{CAP}_{p_l^{\text{major}},l,j}^{\text{linear}}\right), \quad \forall l, j \tag{4.25}$$

where the major biofuel product of each technology is $p_l^{\text{major}} \in \mathbf{P}$.

We introduce continuous decision variables $\lambda_{r,l,j}^R$ (where $r \in \mathbf{R}^{\text{Candidates}}$) that completely determine the installed capacity and associated costs using the discrete points. The $\lambda_{r,l,j}^R$ decision variables represent how similar the installed facility is to each discrete point, and so must sum to one and be non-negative:

$$\sum_j \lambda_{r,l,j}^R = 1, \quad \forall r, l : r \in \mathbf{R}^{\text{Candidates}} \tag{4.26}$$

$$\lambda_{r,l,j}^R \geq 0, \quad \forall r, l, j : r \in \mathbf{R}^{\text{Candidates}} \tag{4.27}$$

The installed capacity is then:

$$\text{CAP}_{r,p,l} = \sum_j \text{CAP}_{p,l,j}^{\text{linear}} \cdot \lambda_{r,l,j}^R, \quad \forall r, p, l : r \in \mathbf{R}^{\text{Candidates}} \tag{4.28}$$

Similarly, the associated costs for that installed capacity are:

$$\text{CF}_{r,l}^{\text{Fixed}} = \sum_j \text{CF}_{l,j}^{\text{linear,Fixed}} \cdot \lambda_{r,l,j}^R, \quad \forall r, l : r \in \mathbf{R}^{\text{Candidates}} \tag{4.29}$$

$$\text{CF}_{r,l}^{\text{FCI}} = \sum_j \text{CF}_{l,j}^{\text{linear,FCI}} \cdot \lambda_{r,l,j}^R, \quad \forall r, l : r \in \mathbf{R}^{\text{Candidates}} \tag{4.30}$$

$$\text{CF}_{r,l}^{\text{WC}} = \sum_j \text{CF}_{l,j}^{\text{linear,WC}} \cdot \lambda_{r,l,j}^R, \quad \forall r, l : r \in \mathbf{R}^{\text{Candidates}} \tag{4.31}$$

At most two adjacent discrete points (e.g. j and $j+1$) can have non-zero $\lambda_{r,l,j}^R$. Thus, for a fixed r and l, the set of $\lambda_{r,l,j}^R$ is a special ordered set of type 2. This property is accomplished by introducing binary decision variables $y_{r,l,j}^R$ for each $r \in \mathbf{R}^{\text{Candidates}}$,

$l \in \mathbf{L}$ and $j \in \{1, \ldots, J-1\}$, and adding the following constraints:

$$\lambda^R_{r,l,1} - y^R_{r,l,1} \leq 0, \quad \forall r, l : r \in \mathbf{R}^{\text{Candidates}} \tag{4.32}$$

$$\lambda^R_{r,l,j} - y^R_{r,l,j} - y^R_{r,l,j-1} \leq 0, \quad \forall r, l, j : j \in \{2, \ldots, J-1\}, r \in \mathbf{R}^{\text{Candidates}} \tag{4.33}$$

$$\lambda^R_{r,l,J} - y^R_{r,l,J-1} \leq 0, \quad \forall r, l : r \in \mathbf{R}^{\text{Candidates}} \tag{4.34}$$

$$\sum_{j=1}^{J-1} y^R_{r,l,j} = 1, \quad \forall r, l : r \in \mathbf{R}^{\text{Candidates}} \tag{4.35}$$

thus when $y^R_{r,l,j}$= true, the facility installed at r using technology l has capacity for biofuel type p between $\text{CAP}^{\text{linear}}_{p,l,j}$ and $\text{CAP}^{\text{linear}}_{p,l,j+1}$.

The discontinuity at zero capacity is enforced by the constraint:

$$\lambda^R_{r,l,1} = y^R_{r,l,1}, \quad \forall r, l : r \in \mathbf{R}^{\text{Candidates}} \tag{4.36}$$

At most one technology with nonzero capacity is allowed per candidate site, thus:

$$\sum_{l} y_{r,l,1} \geq |\mathbf{L}| - 1, \quad \forall r \in \mathbf{R}^{\text{Candidates}} \tag{4.37}$$

where $|\mathbf{L}|$ is the cardinality or number of technologies considered.

The piecewise segment between discrete points 4 and 5 is removed from consideration, due to the step discontinuity there, by adding the constraint:

$$y^R_{r,l,4} = 0, \quad \forall r, l : r \in \mathbf{R}^{\text{Candidates}} \tag{4.38}$$

The remaining cash flows of coproduct sales and other variable costs are proportional to major biofuel production for each technology, thus:

$$\text{CF}^{\text{Coproducts}}_{r,l} = \text{C}^{\text{Coproducts}}_{l} \cdot a^R_{r,p^{\text{major}}_l,l}, \quad \forall r, l : r \in \mathbf{R}^{\text{Candidates}} \tag{4.39}$$

$$\text{CF}^{\text{Other Variable}}_{\text{r,l}} = \text{C}^{\text{Other Variable}}_{l} \cdot a^R_{r,p^{\text{major}}_l,l}, \quad \forall r, l : r \in \mathbf{R}^{\text{Candidates}} \tag{4.40}$$

where the parameter $\text{C}^{\text{Coproducts}}_{l}$ is the coproduct revenue per unit of biofuel produced. Similarly, $\text{C}^{\text{Other Variable}}_{l}$ is the other variable expenses per unit of biofuel produced.

The resulting mixed integer linear program takes the form:

maximize	TNPV
subject to	equations (4.1), (4.5)–(4.22), (4.26)–(4.40)

4.4 Case study parameters

The mathematical formulation was applied to a case study for biofuel production in the 12-state region of the Midwestern United States to meet the Renewable Fuel Standards (RFS2) mandates for 2015. There are 3,109 biomass producers (each corresponding to a county in the contiguous U.S.), 159 existing facilities, 98 candidate sites, 3 markets, 8 biomass types, 4 biofuel types, 3 RFS2 biofuel classifications, 7 biomass processing technologies and 2 transportation methods.

4.4.1 Biomass resources

This case study utilizes the U.S. Department of Energy biomass resource database [94] that was made available online with the August 2011 update of the billion ton study (BT2) [95]. For each county in the contiguous U.S., this database includes the price and available quantities for individual biomass feedstocks. This information is the result of a substantial effort involving the U.S. Department of Energy, U.S. Department of Agriculture (USDA), USDA Forest Service, academic researchers and industry experts to quantify U.S. biomass resources with annual projections through 2030. A complete list of the assumptions for determining this removable biomass can be found in the BT2 report [95]. The potential biomass inventory at a given location is available at farmgate and has a defined biomass type (form and quality are defined by the production system). There are additional costs to preprocess, handle, and transport the biomass to a facility.

The biomass resource data used in this case study are year 2015 projections of the baseline scenario. The baseline scenario involves a continuation of the USDA 10-year forecast for the major food and forage crops, a 1% per annum average yield increase for energy crops, and a continuation of tillage practices (no large trend towards no-till cultivation). Specifically, the following biomass types are included in this case study:

- Conventional crops
  - Corn (available as kernels)

- Agricultural crop residues
  - Corn-stvr: corn stover (the stalks and leaves of corn; available as bales)
- Forest biomass and wood waste (all available as wood chips)
  - LOGP: conventionally sourced wood used for bioenergy (e.g. small-diameter pulpwood)
  - LOGRLOGT: integrated operations (removal of logging residues when merchantable timber is harvested)
  - LOGO: other removal residue (residues from cultural operations, such as precommercial thinnings or from timberland clearing)
  - Woody: coppice woody crops (species that regrow after harvest, such as poplar, willow and eucalyptus) and non-coppice woody crops (e.g. southern pine)
  - LOGTOF: treatment thinnings (removal of excess biomass to reduce fire hazards) from other forest lands (lands incapable to produce industrial wood in a commercially viable density)
- Energy crops
  - Perngrass: perennial grasses including switchgrass, bluestem and Indian grass (available as bales)

The maximum biomass availability $\beta^N_{n,b}$ is shown in Figure 4.5. Forest biomass and wood waste resources are combined together for display purposes. The associated farmgate price differs from county-to-county, but is not shown for simplicity. The only edible biomass type $\mathbf{B}^{\text{Food}}$ considered is Corn, and it's percentage use for biofuels is projected by the USDA to be stable between 33% and 35% through 2021 [96]. For this study, τ_{Corn} is fixed at 0.34.

4.4.2 Existing facilities

All facilities involved in the renewable fuels program (e.g. biofuel producers, biofuel importers, refiners, oxygenate blenders, fuel pipeline terminals and vehicle loading terminals) are obligated to maintain current registration with the U.S. EPA, and this database is available online (updated daily) [97]. When accessed on March 2012, the

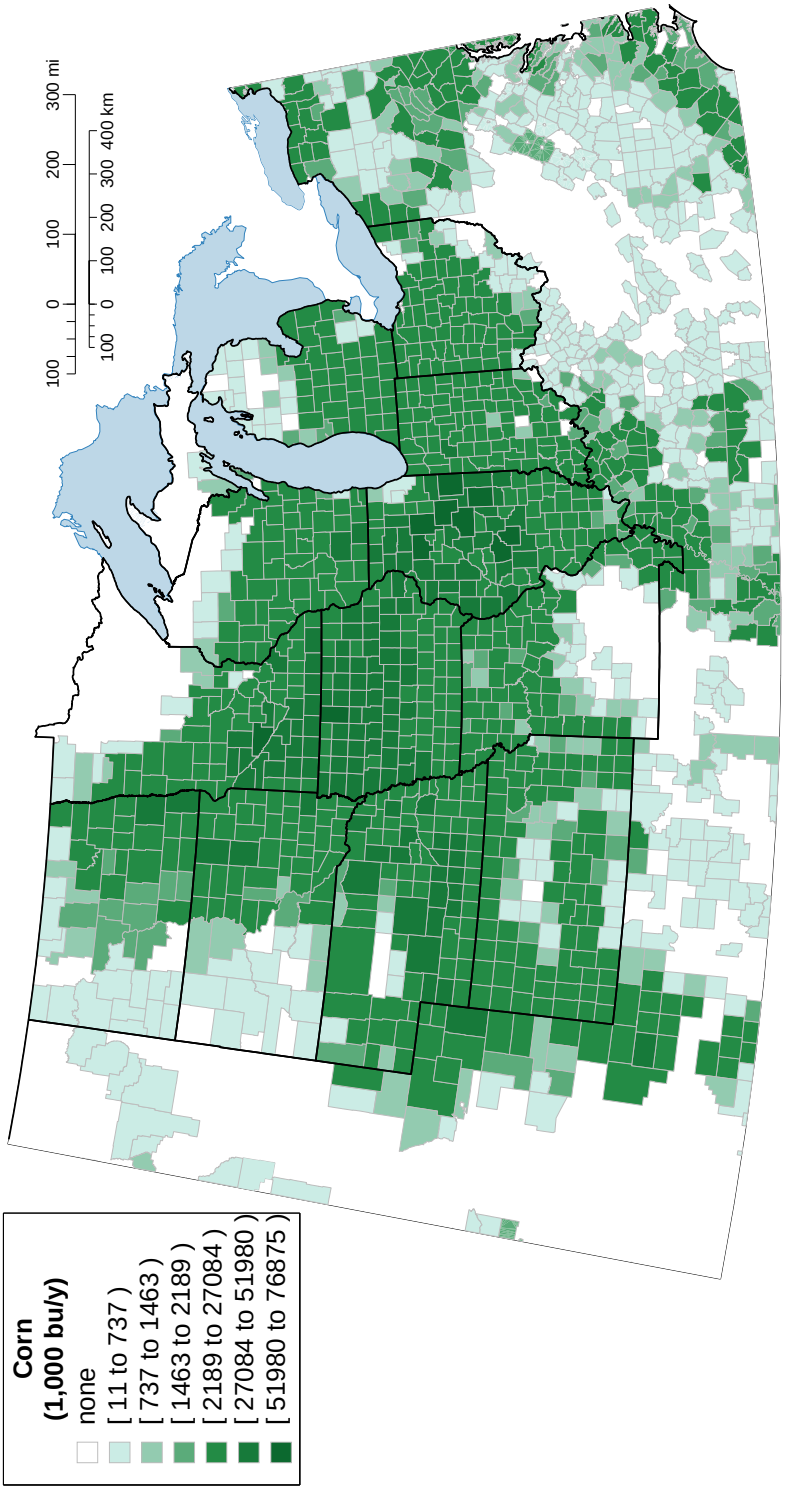
300 mi
200
100
0
100
100
0
100
200
300
400 km
Corn
(1,000 bu/y)
none
[11 to 737)
[737 to 1463)
[1463 to 2189)
[2189 to 27084)
[27084 to 51980)
[51980 to 76875]

(a) Corn grain

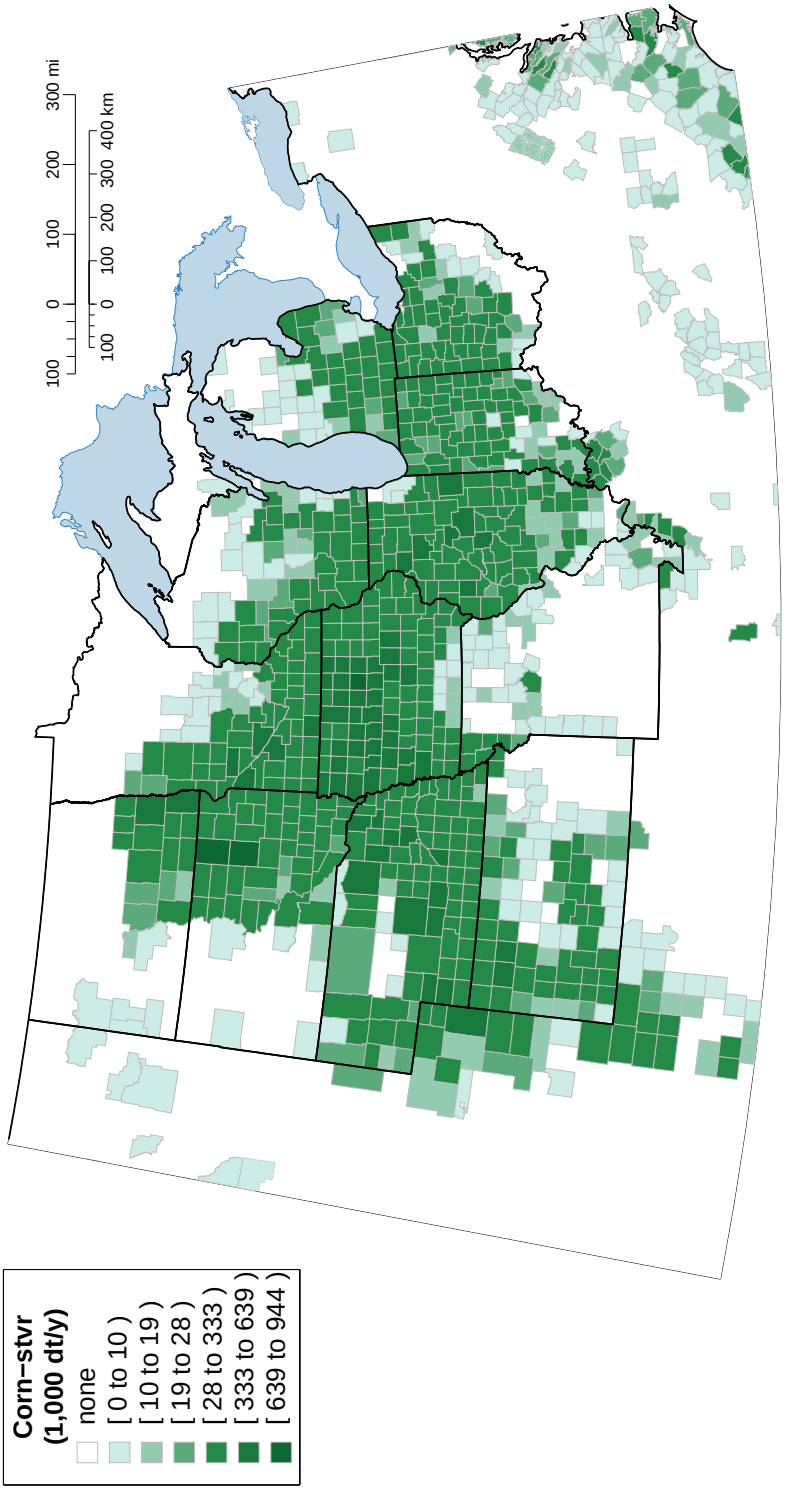

(b) Corn stover

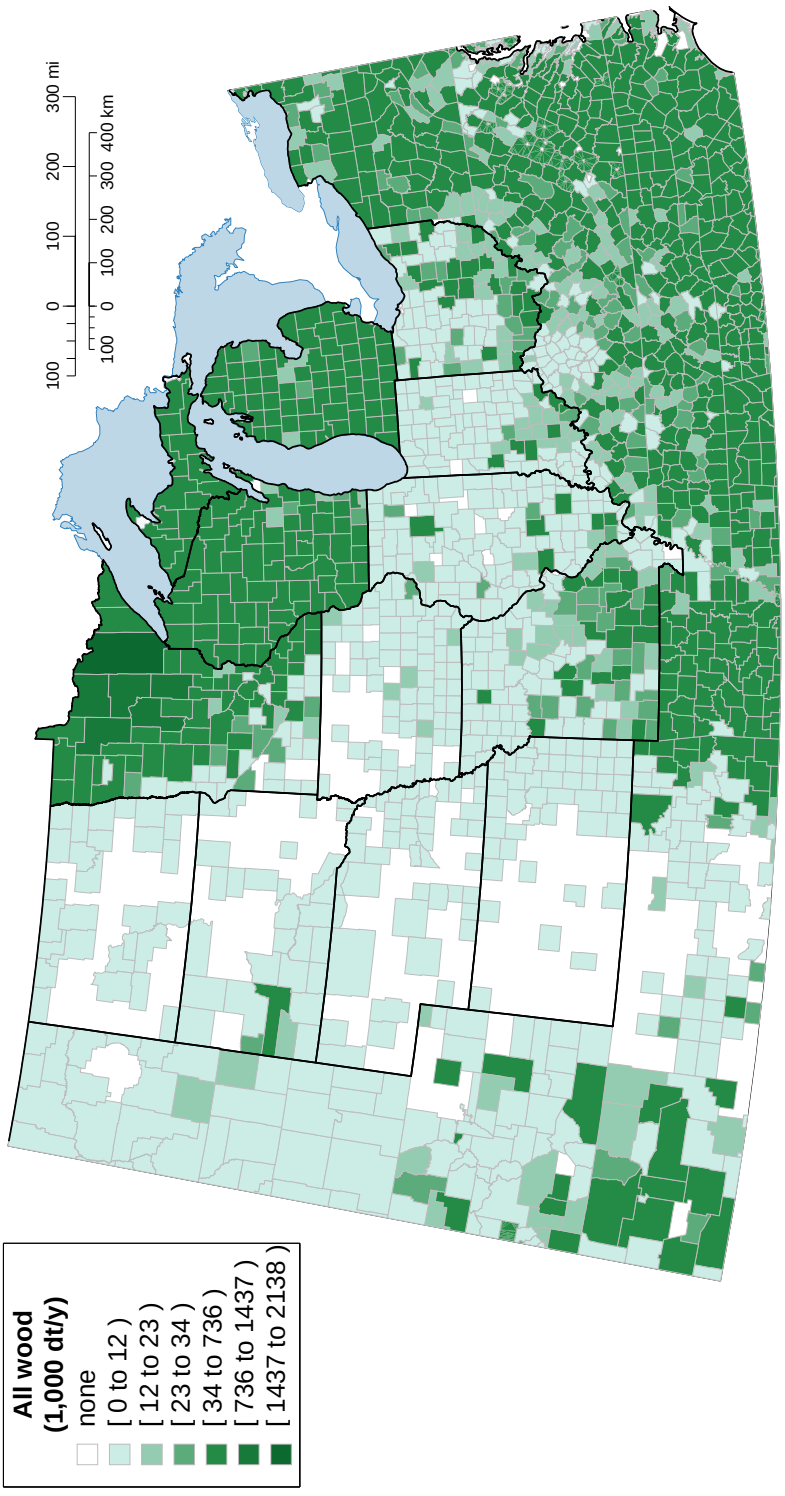

(c) Aggregated forest biomass and wood waste

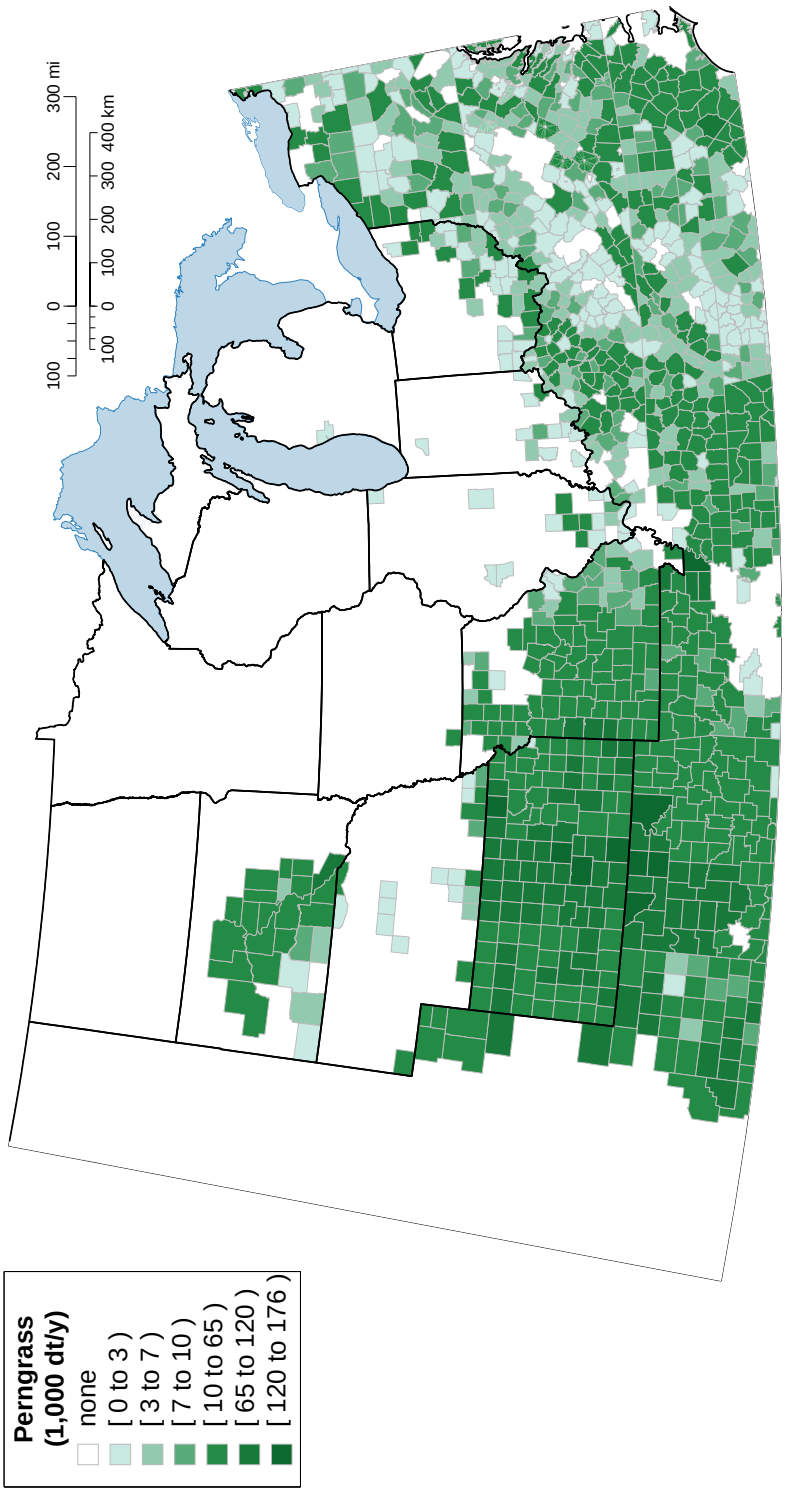

(d) Perennial grasses (switchgrass, big bluestem, Indian grass)

Figure 4.5: Maximum biomass resource availability. Farmgate price for each county not shown.

registered biofuel producing facilities included: 3 for cellulosic biofuel, 0 for cellulosic diesel, 187 for biodiesel, 28 for advanced biofuel (not including 119 foreign facilities) and 207 for renewable fuel (not including 5 foreign facilities). This database did not include biomass feedstock, biofuel capacity or cost information. Required biomass feedstocks and biofuel capacities of only the renewable fuel (RF) producing facilities was available through the Renewable Fuels Association [98].

This case study considers the 159 corn starch ethanol facilities located in the Midwest, shown in Figure 4.6, as existing facilities. Other biofuel producing facilities in the Midwest were not considered due to lack of operating cost information. The corn starch ethanol facilities are included by assuming variable and fixed costs proportional (based on capacity) to a 50 million gallon dry grind process (DGP) technoeconomic model [99]. Fixed capital investment and working capital are assumed to be zero (i.e. fully recovered).

4.4.3 Candidate sites

Candidate sites were identified as towns and cities in the Midwestern U.S. that have proper transportation infrastructure and workforce. U.S. 2000 Census geospatial data was accessed from National Atlas [100]. Only cities with populations between 10,000 and 50,000 were allowed. Nearby cities were aggregated and represented by the largest city within 50 miles. This resulted in the 98 candidate sites that are shown in Figure 4.7.

4.4.4 Biomass processing technologies

Seven biomass processing technologies, shown in Table 4.1, are included in this case study. Together, they can produce four unique biofuel types from eight unique biomass types (including five forest biomass and wood waste resources). This set of technologies is intended to be representative of the diversity seen in biomass processing.

Technoeconomic models from National Renewable Energy Laboratory (NREL) reports and publications [99, 101–105] are used for each technology. In these analyses, proven technology, as opposed to first-of-kind economics and operation is assumed. These NREL process models are backed by pilot and laboratory experimental data, and have been updated to reflect the state of technology. The process model capacity and economic information, shown in Table 4.2, defines the reference facility of each technology in this case study. The coproduct and other variable costs from the reports are shown in Table 4.3 per gallon of biofuel produced.

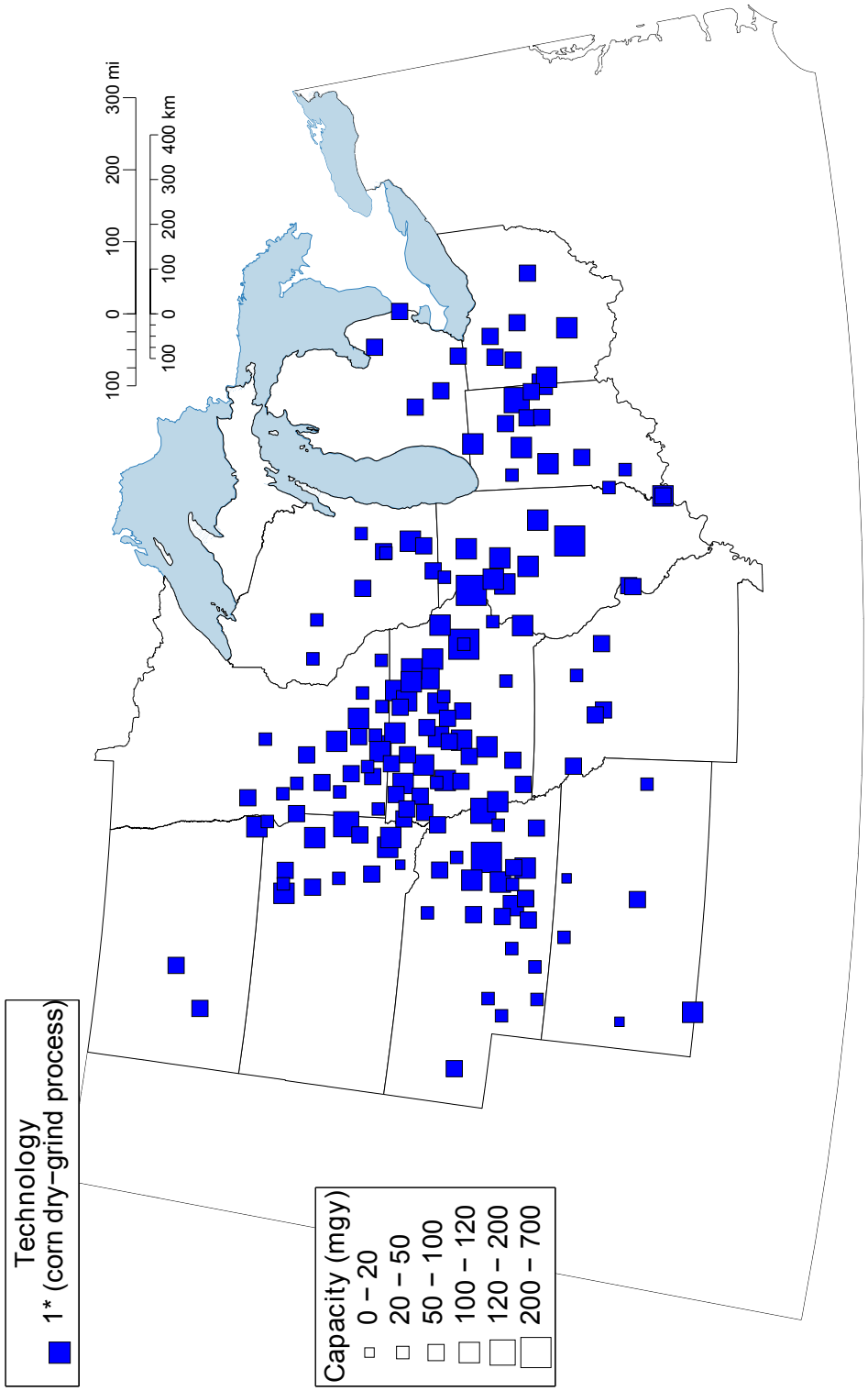

Figure 4.6: The 159 existing facilities considered in the case study. Installed capacity in million gallons per year (mgy).

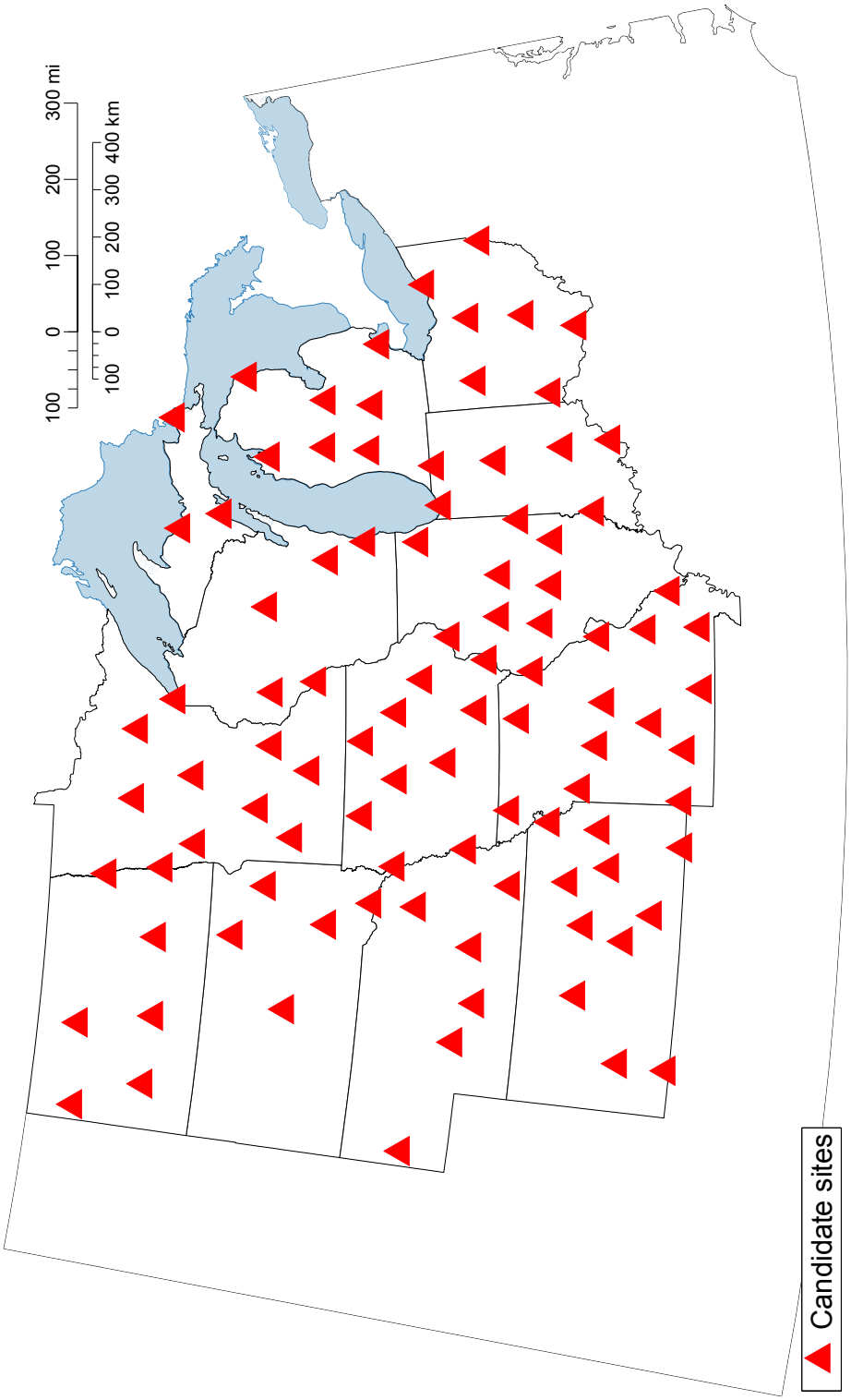

Figure 4.7: The 98 candidate sites with none nearer than 50 miles.

Table 4.1: Biomass processing technologies

Technology $l \in \mathbf{L}$	Description	Biomass feedstock b	Major biofuel product [a] p_l^{major}	Yield $\eta^R_{b,p_l^{\text{major}},l}$
1	Dry grind starch fermentation [99]	Corn	RF ethanol	2.84 gal/bu
2	Integrated corn and stover process [99]	Corn, Corn-stvr [b]	AB ethanol	2.84 gal/bu corn, 79.5 gal/dt corn-stvr
3	Dilute acid pretreatment and C5+C6 cofermentation [101]	Corn-stvr	CB ethanol	79 gal/dt
4	Indirect gasification and syngas upgrading to mixed alcohols [102]	All wood [c]	CB ethanol	83.75 gal/dt
5	Direct gasification and syngas upgrading to mixed alcohols [103]	All wood [c]	CB ethanol	65.27 gal/dt
6	Fast pyrolysis and bio-oil upgrading [104]	Corn-stvr	CB naphtha and diesel [d]	53.47 gal/dt
7	AFEX pretreatment and C5+C6 cofermentation [105]	Perngrass	CB ethanol	65.8 gal/dt

[a] Renewable fuel (RF), advanced biofuel (AB), cellulosic biofuel (CB) RFS2 biofuel classifications.

[b] 70.8% of AB ethanol is produced from Corn-stvr and 29.2% is from Corn.

[c] All wood includes LOGP, LOGRLOGT, LOGO, Woody and LOGTOF.

[d] This process produces a mixture of naphtha-range and diesel-range products.

Table 4.2: Reference facility capacity and economics

Technology $l \in \mathbf{L}$	Reference capacity in mgy [a]	Reference coproduct sales in \$M/y	Reference other variable costs in \$M/y	Reference fixed costs in \$M/y	Reference FCI [b] in \$M
1	50	13.2	13.3	3.2	74.9
2	50	9.4	17.1	12.4	241
3	61	6.57	26.7	10.7	401
4	64.7	15.4	3.32	23.2	490
5	50.4	10.5	2.80	14.6	254
6	58.2	5.92	32.1	8.98	176
7	50.8	5.47	22.2	10.7	432

[a] Million gallons per year (mgy) for major biofuel.
[b] Working capital is 5% of FCI.

Table 4.3: Coproduct and other variable costs

Technology $l \in \mathbf{L}$	Coproduct sales $C_l^{\text{Coproducts}}$ in \$/gal	Other variable costs $C_l^{\text{Other Variable}}$ in \$/gal
1	0.264	0.266
2	0.188	0.342
3	0.108	0.438
4	0.238	0.051
5	0.209	0.056
6	0.102	0.552
7	0.108	0.438

Table 4.4: Economic analysis assumptions

Assumption	Value
Discount rate (after-tax) i	10%
Debt/equity	0%/100%
General plant depreciation	200% DB [a]
General plant recovery period	7 years
Steam plant depreciation	150% DB [a]
Steam plant recovery period	20 years
Construction period	2.5 years
1st 6 months expenditures	8% of FCI
Next 12 months expenditures	60% of FCI
Last 12 months expenditures	32% of FCI
Start-up time	6 months
Revenues	50%
Variable costs	75%
Fixed costs	100%
Working capital	5% of FCI
Land	6% of total purchased equipment cost

[a] IRS Modified Accelerated Cost Recovery System (MACRS) using the 200% Declining Balance (DB) or 150% DB depreciation method provide the shortest recovery period and the largest tax deductions. IRS requires that steam production plants use a 20-year recovery period and other property use a 7-year recovery period.

Economic analysis

Each technology was analyzed with the same set of economic assumptions, shown in Table 4.4. This was done to standardize the discounted cash flow analysis, as described in Subsection 4.3.1, between the technologies. Time periods for the economic analysis are thus $t = \{-2, -1, 0, \ldots, 20\}$, where land is purchased in $t = -2$ and the working capital expense occurs in $t = 0$. General plant and steam plant value (as a fraction of total FCI) and required parts replacement schedules (with associated costs as a fraction of FCI) were obtained from the NREL technoeconomic models.

These economic assumptions allow for the time dependence of cash flows for each technology to be separated following Subsection 4.3.1. The tax rate (TR) is 39%. Revenue cash flows are constant during facilities operation ($t > 1$) and are 75% as high during year 1 due to start-up. Thus, the NPV scaling factors for revenue are $\sigma^{\text{Biofuel}} =$

Table 4.5: NPV scaling factors

Technology $l \in \mathbf{L}$	σ_l^{Parts}	σ_l^{FCI}	σ_l^d
1	0	1.100	0.2814
2	0	1.100	0.2814
3	0.001449	1.082	0.2633
4	0.04671	1.081	0.2814
5	0.005939	1.098	0.2828
6	0	1.099	0.2950
7	0.001449	1.082	0.2633

$5.055 = \sigma_l^{\text{Revenue}}, \forall l$, using a discount factor $i = 10\%$. Similarly, variable costs have NPV scaling factors $\sigma^{\text{Biomass}} = 5.124 = \sigma_l^{\text{Variable}}, \forall l$, fixed costs have NPV scaling factor $\sigma_l^{\text{Fixed}} = 5.193, \forall l$, and working capital has NPV scaling factor $\sigma_l^{\text{WC}} = 0.8514, \forall l$. The scaling factors for parts replacement, fixed capital investment and depreciation differ between technologies, as shown in Table 4.5. This is due to differing parts replacement schedules, cost of land, and steam plant cost relative to general plant cost.

Piecewise linearization

The relationship between costs and installed capacity is determined for each technology using the NREL technoeconomic models as reference capacities. It is assumed that single facilities can have capacity within 50% and 150% of the reference capacity for each technology. Thus, the discrete points $j = \{1, \ldots, 8\}$ are:

1. Zero capacity with zero costs
2. One facility at 50% of reference capacity
3. One facility at reference capacity with reference costs
4. One facility at 150% of reference capacity
5. One facility at 50% of reference capacity and one facility at reference capacity
6. One facility at 50% of reference capacity and one facility at 150% of reference capacity
7. Two facilities, each at 150% of reference capacity

Table 4.6: FCI linearization parameters $CF_{l,j}^{\text{linear,FCI}}$ in \$M

Technology $l \in \mathbf{L}$	1	2	3	4	5	6	7	8
1	0	46.1	74.9	99.5	121	146	199	398
2	0	148	241	320	389	468	639	1,280
3	0	251	401	529	652	780	1,060	2,120
4	0	301	490	650	791	952	1,300	2,600
5	0	156	254	337	411	494	675	1,350
6	0	108	176	233	284	342	467	934
7	0	266	432	573	697	839	1,150	2,290

8. Four facilities, each at 150% of reference capacity

Linearization parameters determining costs at each discrete point are calculated from the installed capacity. Coproduct revenues and other variable costs are proportional to installed capacity. Fixed costs are equal for discrete points 2-4 and double for discrete points 5-7, because they depend on number of equipment more strongly than capacity. Fixed capital investment (FCI) is shown in Table 4.6, and follows a 0.7 power law scaling to account for economies of scale. Working capital is proportional to the FCI.

4.4.5 Markets

Biofuel blending facilities, accessed from the U.S. EPA Fuels Reporting Registration website [97], are the end-users of biofuel produced at the facility sites. We assume that each facility site will sell its biofuel to the nearest biofuel blender. This allows us to reduce the number of biofuel flow decision variables by only considering three markets corresponding to each of the three RFS2 fuel classifications (RF, AB and CB). These markets represent the national demand for each fuel classification and offer a constant delivered biofuel price. However, each facility site receives the facility-gate sale price $C_{r,m,v,p}^{\text{Biofuel}}$ per unit of biofuel sold, which depends on the distance to the nearest biofuel blending facility. Biofuel sales to these markets thus maintain the proper logistics costs associated with biofuel transportation to an existing biofuel blending facility.

The Renewable Identification Number (RIN) system that was created by the U.S. EPA to facilitate compliance with RFS2 mandates is intended to make this a reality [10]. This system creates a market where biofuel blenders can trade RINs (numeric codes corresponding to volumes of produced or imported renewable fuel) to meet their RFS2

requirement. The delivered biofuel price is equal to the demand price (the price blenders are willing to pay with no RFS2 mandate) plus the value of the RIN. Thus, at market equilibrium, the delivered biofuel price will be sufficient to cover biofuel production costs.

We assume delivered biofuel prices $C^{M}_{m,p}$ that are sufficiently high to meet the RFS2 mandate in 2015. They are \$1.775/gal at the RF market, \$2.25/gal at the AB market and \$2.45/gal at the CB market. We will also determine the minimum biofuel prices required to satisfy the 2015 mandates. In ethanol equivalent gallons, the 2015 mandates are for 3.0 billion of cellulosic biofuel, 5.5 billion of advanced biofuel and 20.5 billion of renewable fuel. A gallon of non-ester renewable diesel (e.g. CB naphtha & diesel) is 1.7 ethanol-equivalent gallons. Unless otherwise specified, all liquid volumes in the following are in ethanol-equivalent gallons.

4.4.6 Transportation

Biomass and biofuel transportation costs depend on the distance traveled and the method of transportation. Distance variable costs (DVC) and distance fixed costs (DFC), as shown in Table 4.7, account for these costs. This assumes that corn stover is transported as large round bales using a 20 metric ton (t) capacity flatbed truck, woodchips using a 40 t chip van, and liquids (ethanol, naphtha and diesel) using a 40 t tanker [106].

The distance for biomass transportation includes an intra-county (collection) component and delivery component. This intra-county component is the mean travel distance from land area within the county to the center of the county, and is estimated as the mean distance to the center of a circle with area equal to the county's land area. The delivery component is the distance from the county center to the facility site. Biofuel transportation distance from facility sites is the distance to the nearest blending facility, and is equal for all markets. Point-to-point aerial transit distances are computed from the location coordinates and winding factors are used to account for the non-direct transportation. A 30% winding is assumed for roads and 79% for rail, that is common for the U.S. [40].

The delivered biomass price parameters $C^{\text{Biomass}}_{n,r,v,b}$ are calculated as the farmgate price at biomass producer n for biomass type b, plus the transportation costs from n to r via method v. Facility-gate biofuel price parameters $C^{\text{Biofuel}}_{r,m,v,p}$ are calculated as the delivered biofuel price at market m for biofuel type p, minus the transportation costs from r to

Table 4.7: Transportation parameters: distance variable and fixed cost

Mode	Item transported	DVC	DFC
Truck	Corn stover and perennial grasses [a]	0.227 $/dt/mile (0.12 $/t/km)	5.16 $/dt (4.39 $/t)
	All wood [b]	0.205 $/dt/mile (0.07 $/t/km)	5.47 $/dt (3.01 $/t)
	Ethanol	0.00024 $/gal/mile (0.05 $/t/km)	0.0115 $/gal (3.86 $/t)
	Naphtha & diesel	0.00024 $/gal/mile (0.05 $/t/km)	0.0115 $/gal (3.86 $/t)
Rail	Corn	0.00094 $/bu/mile (0.023 $/t/km)	-

[a] Transported as 15% moisture large round bales. Perennial grasses assumed the same costs as corn stover bales.

[b] All wood includes LOGP, LOGRLOGT, LOGO, Woody and LOGTOF, and is transported as 45% moisture wood chips.

m via method v.

4.5 Results

The MILP model was coded in IBM ILOG CPLEX Optimization Studio v12.2 [64], and has 154,765 continuous variables, 5,488 binary variables and 39,482 constraints. The results from two scenarios (no RFS2 mandates and strict mandates) will be discussed. Sensitivity to biofuel price is also presented for the case of no RFS2 mandates.

4.5.1 No RFS2 mandates

The RFS2 mandates aim to increase biofuel production levels each year by setting requirements on biofuel blenders, and do not directly put production requirements on biofuel producers. Biofuel producers will seek to make a profit, regardless if the RFS2 mandate has been met or not. This makes it important to examine the case where RFS2 mandates are not strictly enforced. For this, we remove equation (4.13) from the MILP formulation. An optimality gap of 0.50% was obtained after 8.4 hours, and the corresponding supply chain with TNPV of 21.3 $B is shown in Figure 4.8. During this run, 1% gap was obtained after 24 minutes and 0.75% gap after 2.1 hours.

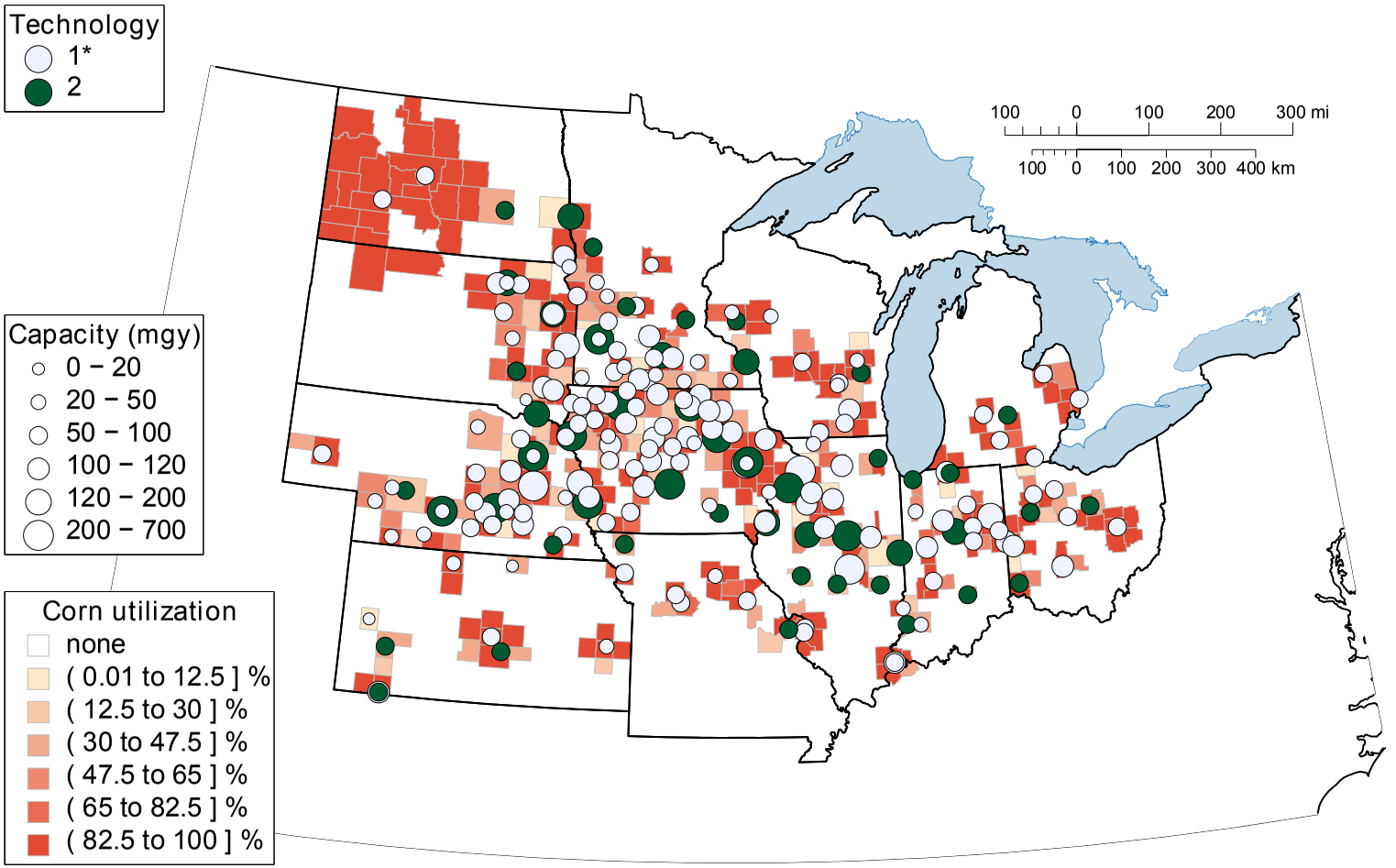

(a) Corn grain utilization with corn-utilizing facilities shown. RF and AB ethanol are produced from corn using technology 1 and 2, respectively. Existing facilities are denoted with an asterisk (*). Maximum corn utilization is 34%.

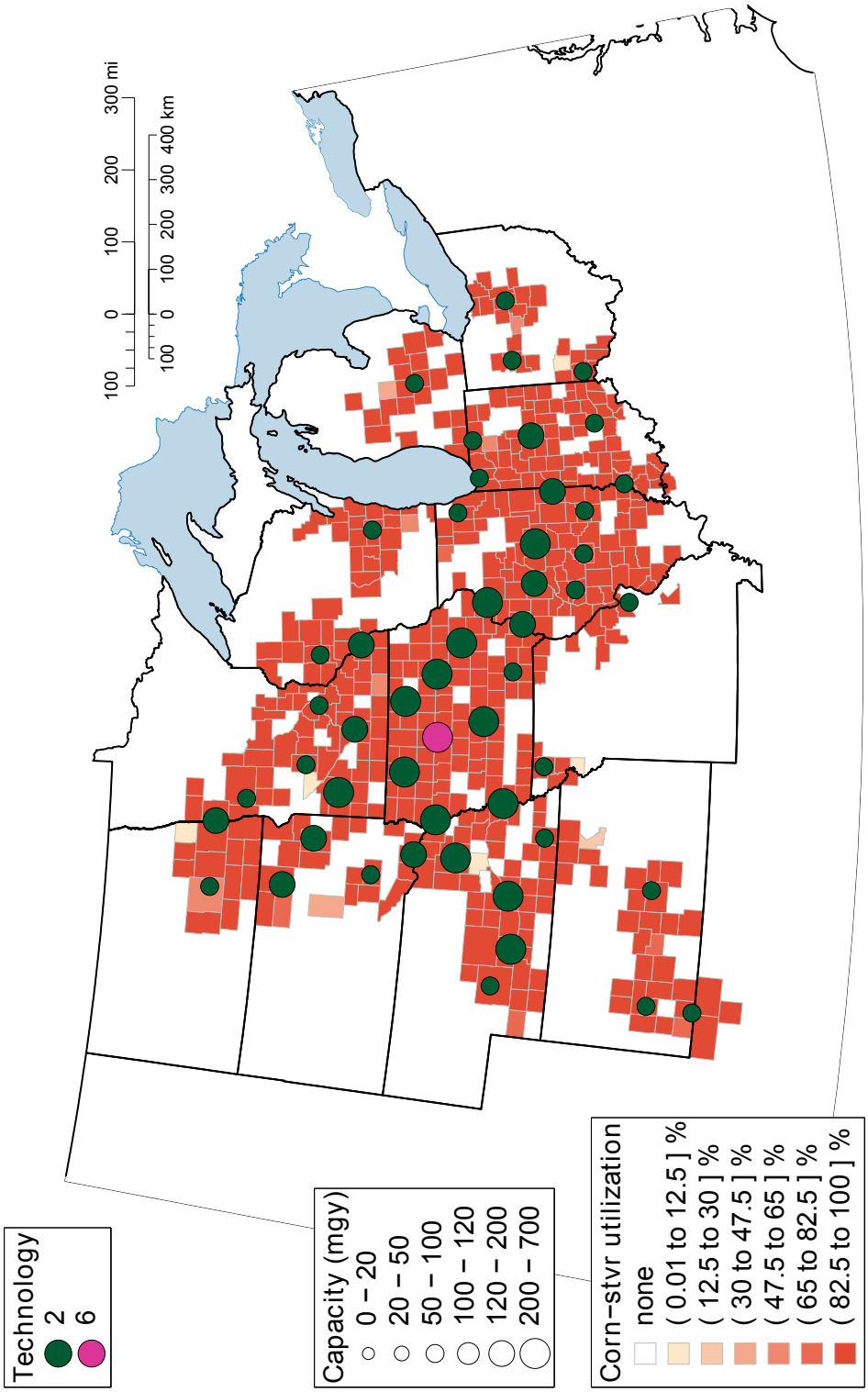

(b) Corn stover utilization with associated facilities shown. AB and CB ethanol, and CB naphtha & diesel are produced from corn stover.

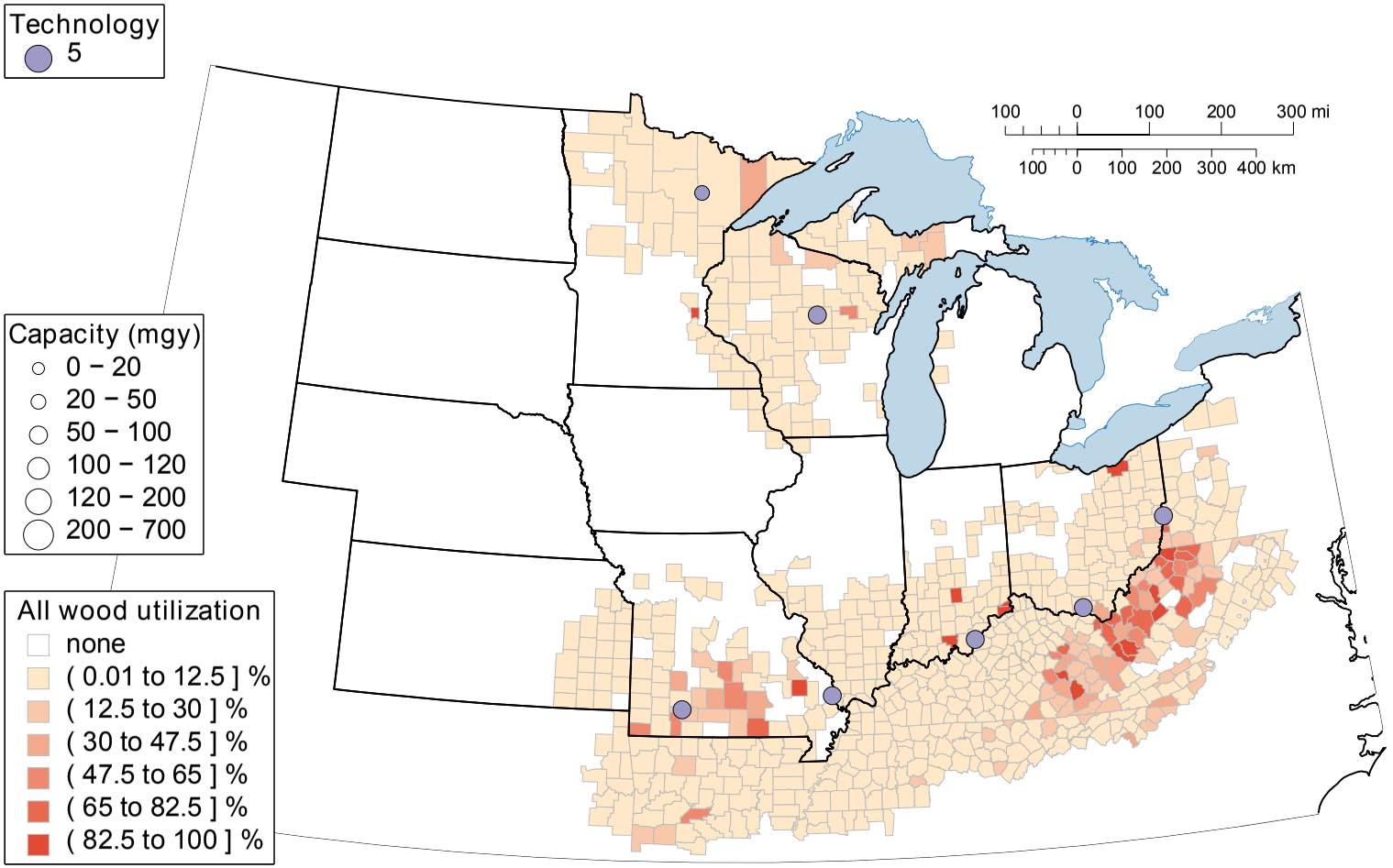

(c) Aggregated forest biomass and wood waste utilization with associated facilities shown. CB ethanol is produced from all wood.

Figure 4.8: Optimum supply chain configuration for the case of no RFS2 mandates. Installed facility capacity shown in million gallons per year (mgy). Renewable fuel (RF), advanced biofuel (AB) and cellulosic biofuel (CB) are produced. Perennial grasses were available but were not utilized in the optimum supply chain.

Table 4.8: Fraction of feedstock used by each technology for the case of no RFS2 mandates.

Technology	Unit	1	2	5	6
Corn	bu	1	0.9203	-	-
Corn-stvr	dt	-	0.0797	-	1
LOGP	dt	-	-	0.0284	-
LOGRLOGT	dt	-	-	0.4036	-
LOGO	dt	-	-	0.5678	-
Woody	dt	-	-	0	-
LOGTOF	dt	-	-	0.0001	-
Perngrass	dt	-	-	-	-

Table 4.9: Total biomass utilization and costs for the case of no RFS2 mandates.

Biomass type b	Total used	Unit	Average farmgate price in $/unit	Average delivered price in $/unit
Corn	4,816,582,732	bu	3.935	3.973
Corn-stvr	66,931,010	dt	49.47	66.58
LOGP	291,700	dt	74.82	109.5
LOGRLOGT	2,981,870	dt	54.32	83.58
LOGO	4,194,600	dt	32.15	68.84
Woody	0	dt	-	-
LOGTOF	1,000	dt	67.00	96.59
Perngrass	0	dt	-	-

In the solution, four of the seven biomass processing technologies are installed. Multiple technologies are competitive due to the diversity of biomass available. The average feedstock ratio for each technology is shown in Table 4.8. Corn grain and corn stover utilizing technologies ($l = \{1, 2, 6\}$) are prevalent due to the significant amount of corn grown in the Midwestern U.S.. A few wood chip processing facilities ($l = 5$) are also installed. No perennial grass facilities ($l = 7$) are installed. Only one of the 159 existing facilities are operating below nameplate capacity and none are idled. Of the 98 candidate sites considered, 58 are developed. Total utilization and average prices paid for biomass types are shown in Table 4.9. Total installed capacity for each biofuel type is shown in Table 4.10 along with associated average prices.

Our detailed economic analysis allows us to calculate the average distribution of

Table 4.10: Total biofuel production and costs for the case of no RFS2 mandates.

Biofuel type p	Total produced in M gal	Average facility-gate price in \$/gal	Average delivered price in \$/gal
RF ethanol	11,640	1.7515	1.775
AB ethanol	6,984	2.2280	2.25
CB ethanol	482	2.4299	2.45
CB naphtha & diesel	253	2.4199	2.45

discounted costs for each installed technology, as shown in Figure 4.9. Only real cash flows are shown; cash is not transferred due to depreciation, although it does effect taxes (an important cost source for each technology). Both biomass farmgate purchasing and logistics are important costs. Technology 5 has a proportionally higher variable transportation cost as it is the only installed technology to utilize wood, a more distributed resource in the Midwest when compared to Corn or Corn-stvr.

The minimum biofuel selling price at each facility site was also calculated, and is shown in Figure 4.10 for candidate sites only. These prices are the facility-gate biofuel price that corresponds with an NPV of zero (e.g. the facility has an internal rate of return equal to the discount rate of 10%). The price does not include biofuel transportation costs, which are approximately 1% of the facility-gate price as shown in Table 4.10. Most of the facilities installed at candidate sites have a minimum biofuel selling price between 1.97 and 2.23 \$/gal. Minimum biofuel selling price for existing facilities varies between 1.48 and 1.57 \$/gal.

Sensitivity to biofuel selling price

Biofuel production and technology selection are sensitive to biofuel selling price. Previous studies have acknowledged this when a single RFS2 biofuel classification is considered [51, 107], but we will demonstrate an added layer of complexity when multiple classifications are considered. This complexity arises from competition for biomass resources. To probe these effects, we determine the optimum supply chain for a series of biofuel selling prices. This allows us to generate the biofuel production curve, shown in Figure 4.11. Note that the added value of advanced and cellulosic biofuels over renewable fuel is fixed.

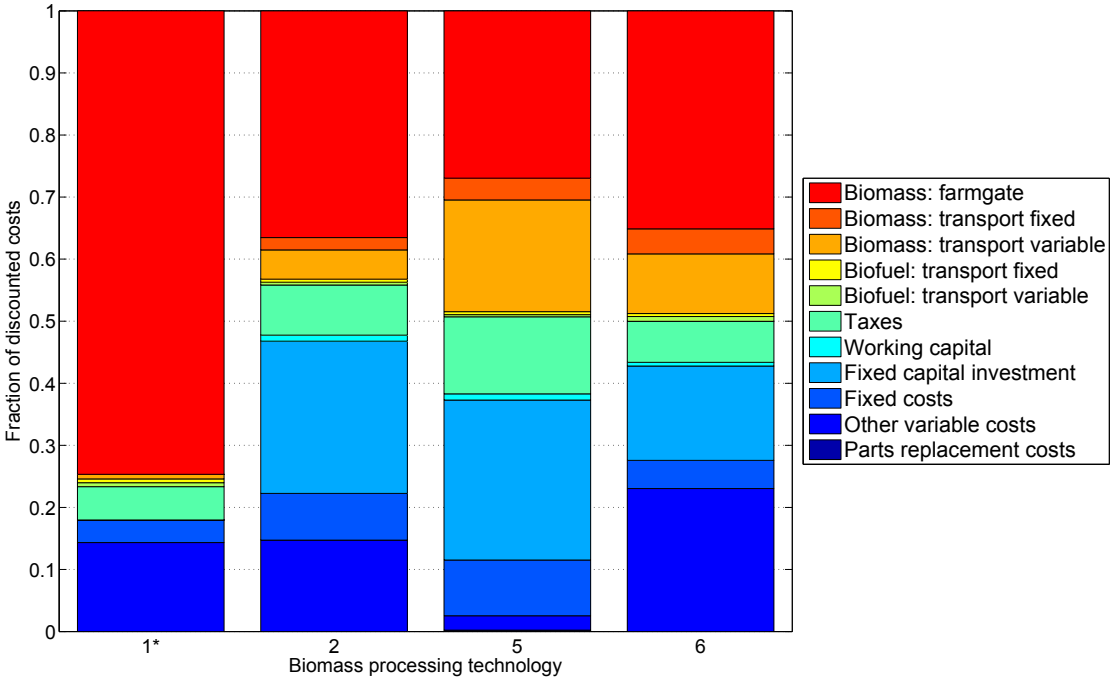

Figure 4.9: Breakdown of cost sources for installed technologies. Existing facilities are denoted by an asterisk (*). New facilities of technologies $l = \{1, 3, 4, 7\}$ were not constructed in the optimum supply chain.

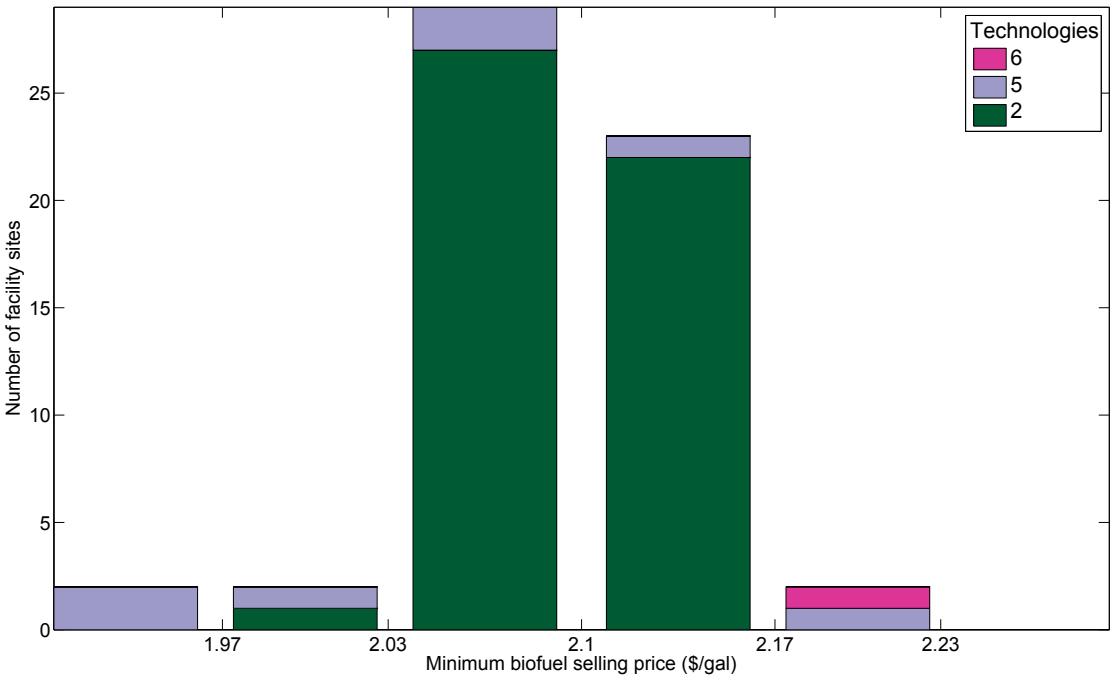

Figure 4.10: Minimum biofuel selling price.

Total biofuel production increases with selling price as expected, but some surprising changes in technology occur due to competition for biomass resources. With the seven technologies considered, RF ethanol (technology $l = 1$) and AB ethanol ($l = 2$) production compete for the available corn grain. Similarly, AB ethanol ($l = 2$), CB ethanol ($l = 3$) and CB naphtha & diesel ($l = 6$) production compete for the available corn stover. These two effects cause low AB ethanol ($l = 2$) production to increase with biofuel prices. At high biofuel prices, it becomes economical to utilize corn stover for cellulosic biofuels as well as for AB ethanol. At low biofuel prices, technology 6 is able to utilize corn stover in high density areas.

The two wood utilizing technologies ($l = \{4, 5\}$) compete for wood resources to produce CB ethanol. Technology 5 becomes more dominant at high biofuel prices due to larger facility capacity allowing it to access higher volumes of wood. A few facilities utilizing technology 5 are economical at a very low biofuel price, due to a small availability of cheap removable wood residues (LOGO).

We see the importance of the Midwest for biofuel production by displaying the cellulosic biofuel production separately in Figure 4.12. At approximately 2.7 $/gal, enough

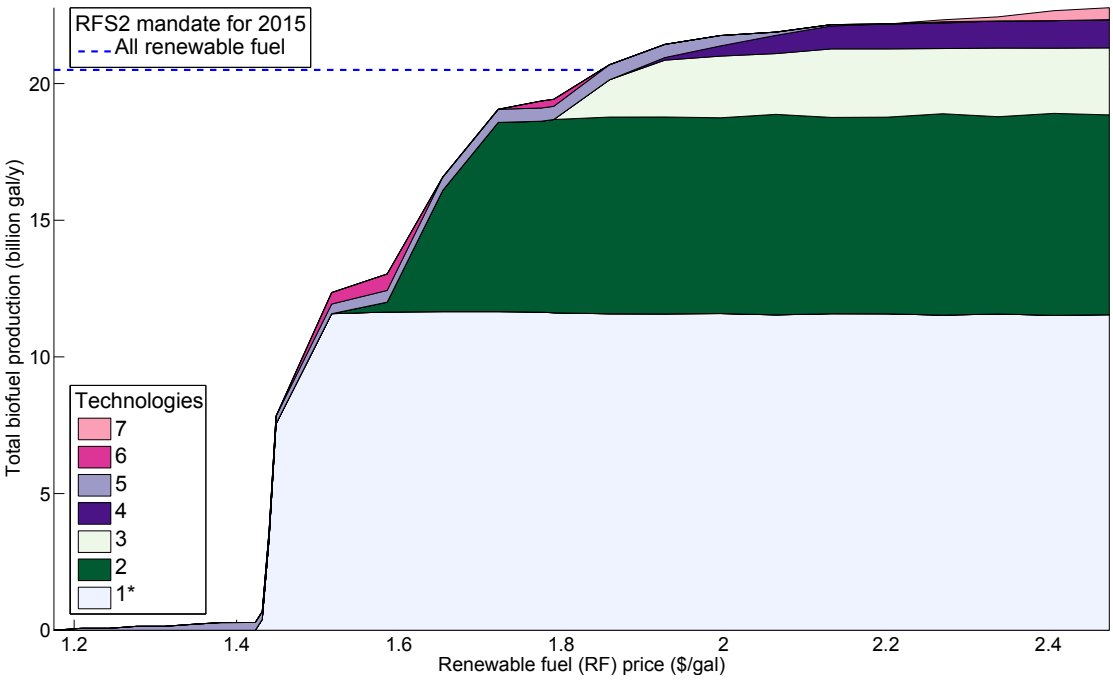

Figure 4.11: Biofuel production curve. Advanced biofuel (AB) price and cellulosic biofuel (CB) price are 0.475 and 0.675 $/gal higher than the RF price, respectively.

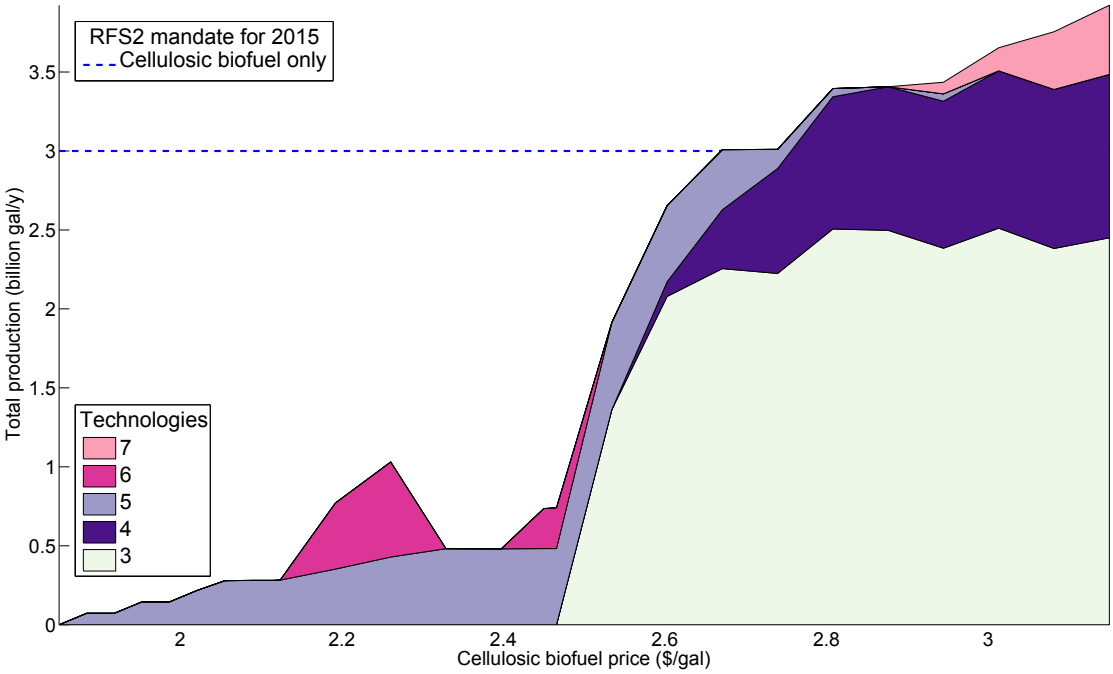

Figure 4.12: Biofuel production curve for cellulosic biofuel only. The national RFS2 mandate for 2015 is also shown.

cellulosic biofuel is produced in the Midwest to satisfy the national RFS2 mandate for 2015.

4.5.2 Mandated biofuel production

By enforcing the market demand constraints in equation (4.13), we have probed the effects of a strict biofuel mandate. Recall that the RFS2 biofuel classifications (RF, AB and CB) are nested, so blending a gallon of cellulosic biofuel is counted towards the RF, AB and CB mandated volumes. The national RFS2 mandate for 2015 requires 3 billion gallons of cellulosic biofuel, 2.5 billion gallons of other advanced biofuels and 15 billion gallons of implicit nonadvanced biofuels, for a total of 20.5 billion gallons of renewable fuel.

The optimum supply chain configuration that produces that distribution of biofuels was found in 14 hours with a 0.75% gap and is shown in Figure 4.13. Five of the seven biomass processing technologies are installed by developing 59 of the 98 candidate sites. Total utilization and average prices paid for biomass types are shown in Table 4.11.

Table 4.11: Total biomass utilization and costs for the case of strict biofuel mandates.

Biomass type b	Total used	Unit	Average farmgate price ($/unit)	Average delivered price ($/unit)
Corn	4,816,582,732	bu	3.935	3.975
Corn-stvr	61,526,786	dt	49.06	65.93
LOGP	209,900	dt	66.51	99.57
LOGRLOGT	3,025,270	dt	54.22	83.75
LOGO	4,341,800	dt	32.06	70.70
Woody	0	dt	-	-
LOGTOF	1,000	dt	67.00	96.59
Perngrass	0	dt	-	-

Table 4.12: Total biofuel production and costs for the case of strict biofuel mandates.

Biofuel type p	Total produced (M gal)	Average facility-gate price ($/gal)	Average delivered price ($/gal)
RF ethanol	12,949	1.977	2.0
AB ethanol	2,500	2.477	2.5
CB ethanol	1,751	2.982	3.0
CB naphtha & diesel	1,249	2.974	3.0

New technology 1 facilities are installed to expand corn ethanol production. A total of 26 technology 2 facilities are installed to meet the mandate for other advanced biofuels. Corn stover and wood utilizing technologies are installed to produce the mandated cellulosic biofuel. Total installed capacity for each biofuel type is shown in Table 4.12 along with associated average prices.

Biofuel prices required to economically meet the RFS2 mandates can then be found from the minimum biofuel selling prices for each facility. For all facilities to be profitable (NPV>0) while meeting the RFS2 mandates, the facility-gate biofuel prices for each biofuel classification must be at least the highest minimum biofuel selling price found in the optimum supply chain. The 24 facilities producing cellulosic biofuels have minimum prices between 1.96 and 2.39 $/gal, the 26 facilities producing other advanced biofuels are between 2.04 and 2.13 $/gal, and the 168 facilities producing implicit nonadvanced

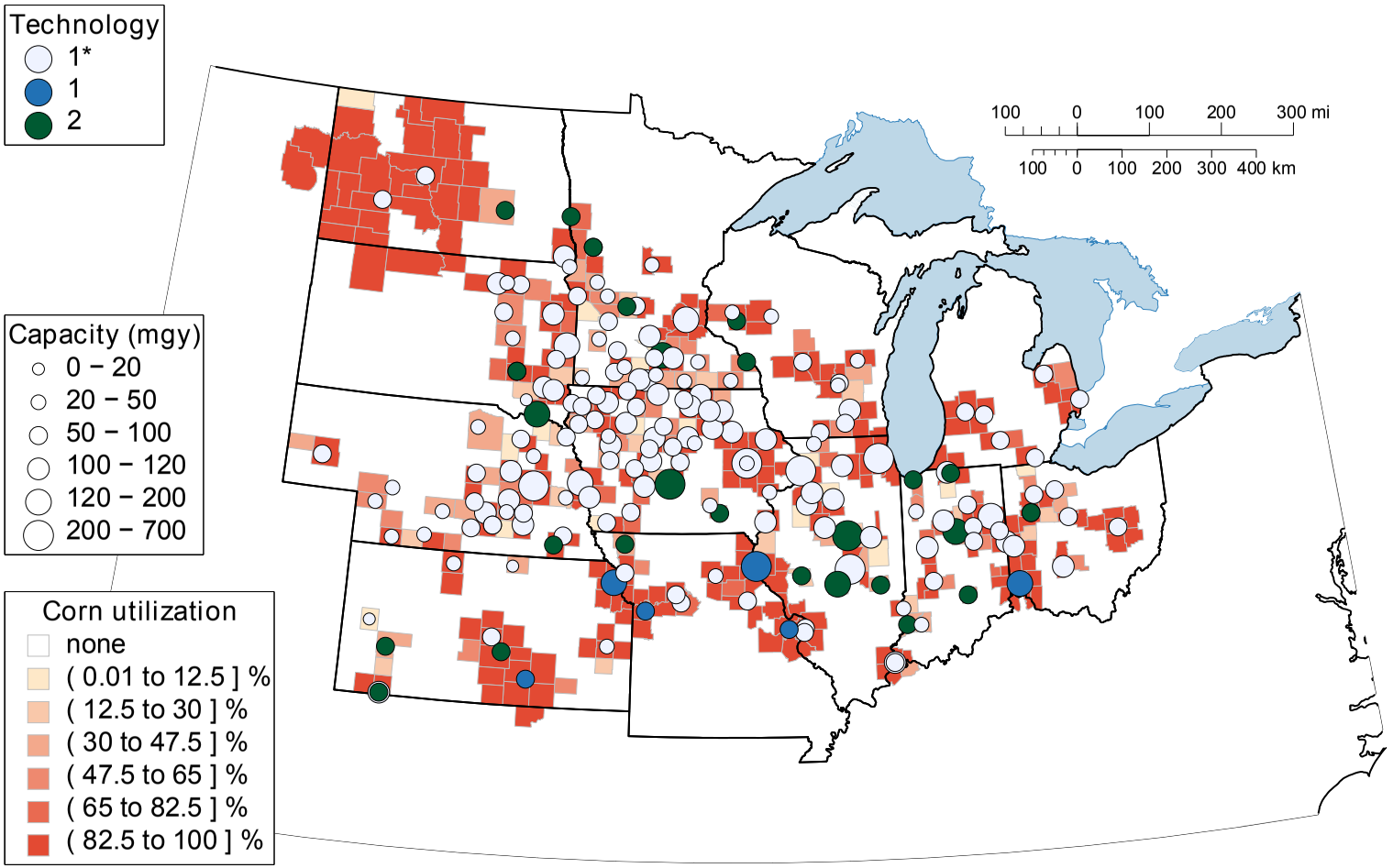

(a) Corn grain utilization with corn-utilizing facilities shown. RF and AB ethanol are produced from corn using technology 1 and 2, respectively. Existing facilities are denoted with an asterisk (*). Maximum corn utilization is 34%.

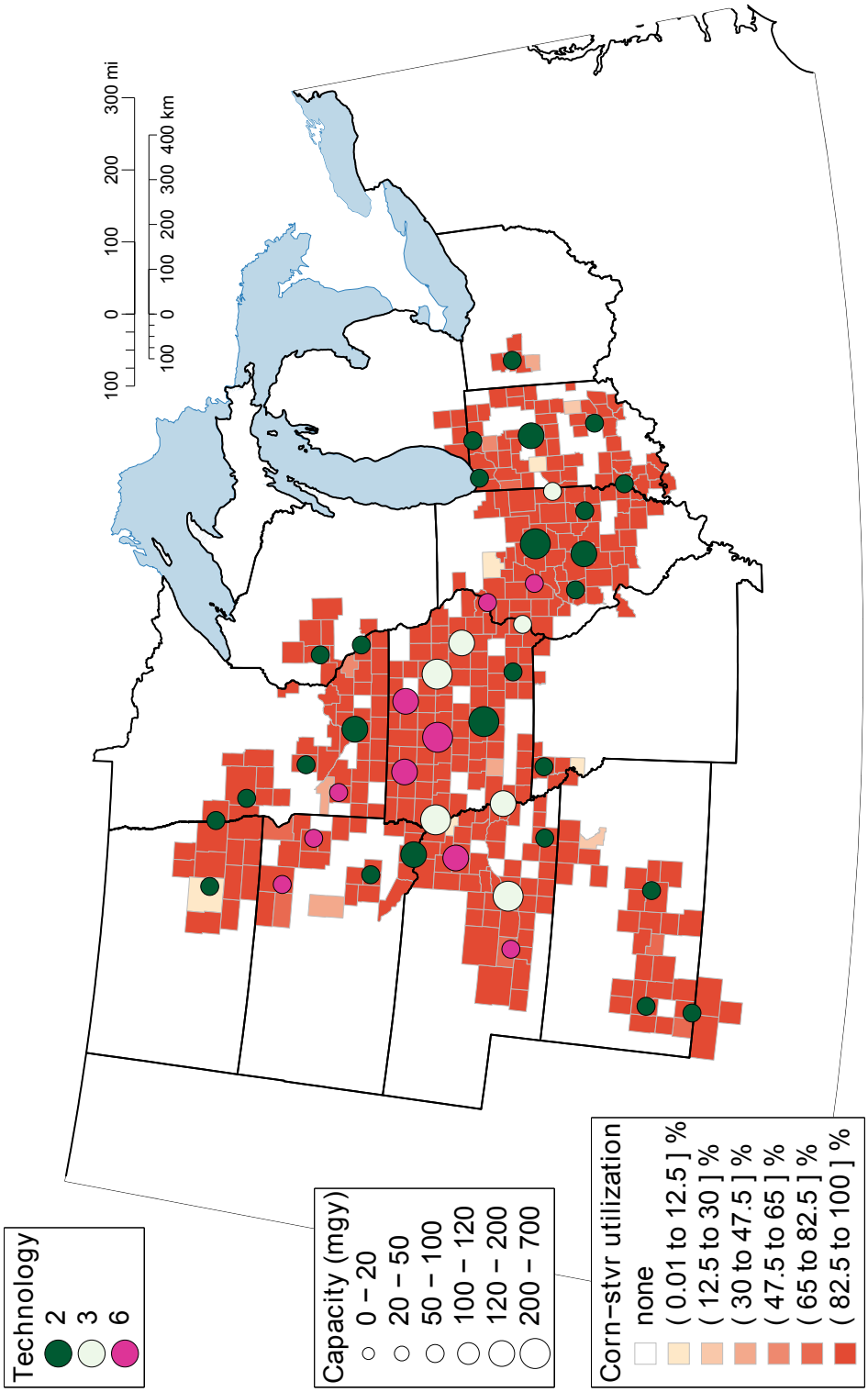

(b) Corn stover utilization with associated facilities shown. AB and CB ethanol, and CB naphtha & diesel are produced from corn stover.

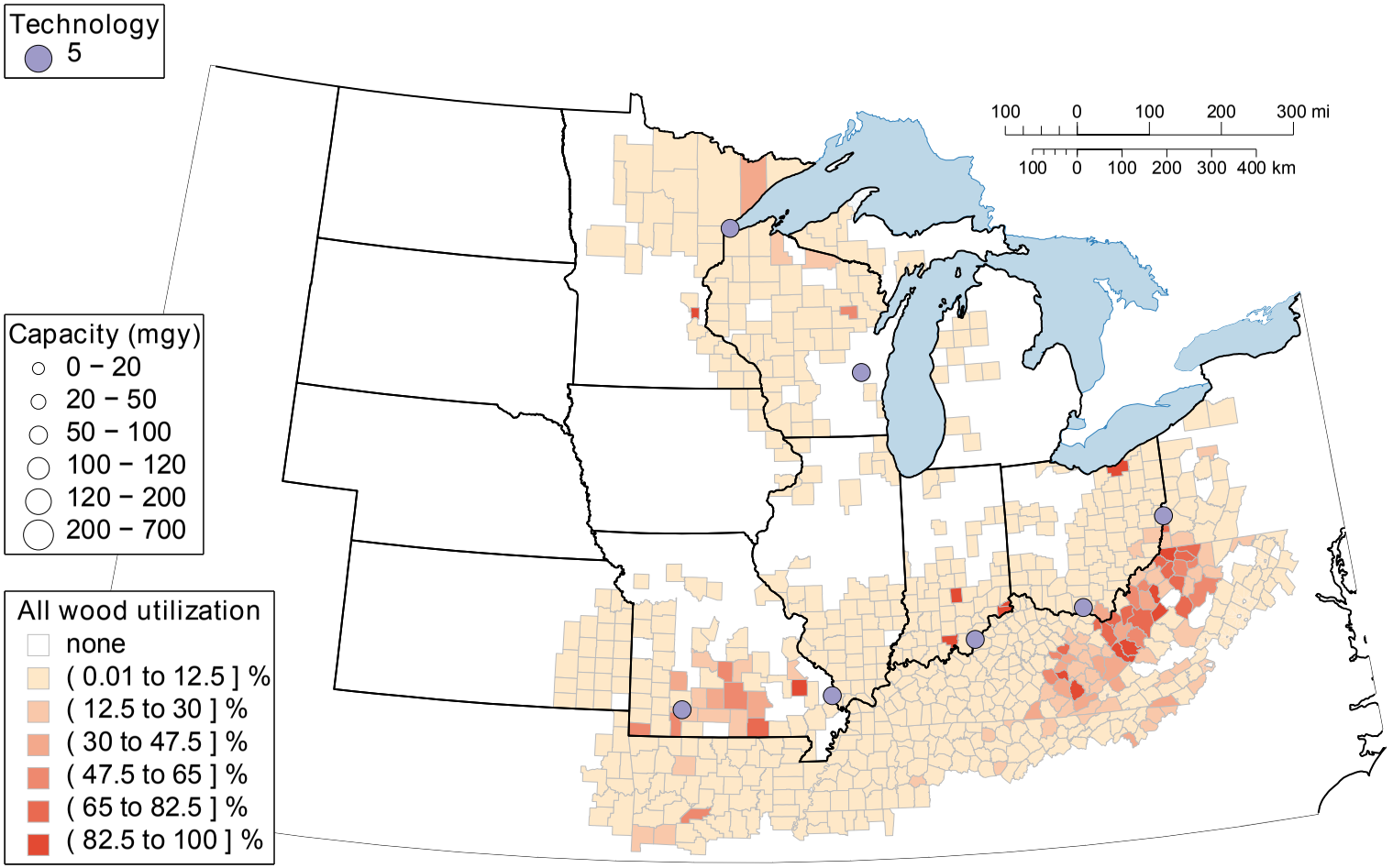

(c) Aggregated forest biomass and wood waste utilization with associated facilities shown. CB ethanol is produced from all wood.

Figure 4.13: Optimum supply chain configuration for the case of strict biofuel mandates. Installed facility capacity shown in million gallons per year (mgy). Renewable fuel (RF), advanced biofuel (AB) and cellulosic biofuel (CB) are produced. Perennial grasses were available but were not utilized in the optimum supply chain.

biofuels are between 1.48 and 1.71 $/gal. All facilities are then economical for facility-gate prices of 2.39, 2.13 and 1.71 $/gal for CB, AB and RF, respectively. Thus, the RIN values are estimated to be worth 0.68 $/gal for CB and 0.42 $/gal for AB.

4.6 Conclusions

We proposed a mixed integer linear program to determine facility location, capacity and technology selection for biomass to biofuel supply chains. By applying it to the Midwestern U.S., we found that Renewable Fuel Standard mandates for 2015 could be met. The Midwest case study included the existing corn ethanol facilities, new candidate sites, eight types of biomass, 4 types of biofuel and seven biomass processing technologies. A spatial distribution of biomass with county-level resolution with associated farmgate biomass cost at each producer was used. From this analysis, it is estimated that the Midwest can produce enough cellulosic and other advanced biofuel to meet the 2015 mandate for the entire United States. Producing this much biofuel is economical for all facilities involved if cellulosic biofuel, advanced biofuel and renewable fuel are worth 2.39, 2.13 and 1.71 $/gal, respectively.

4.7 Supporting information

4.7.1 Objective function parameters

This section gives more detailed information on the parameters used in the objective function, namely θ, TR, α and σ.

The economic analysis assumptions used include a discount rate $i = 0.1$ and a tax rate TR $= 0.39$. Recall that the discounting factor $\theta_t = (1+i)^{-t}$ is used to discount a cash flow from year t to the present.

Fixed Capital Investment

Each facility is assumed to be 100% equity financed with a construction period of 2.5 years. Construction begins halfway through year $t = -2$ and finishes at the end of year $t = 0$. The fixed capital investment (excluding land) paid during these years is as follows: 8% for $t = -2$, 60% for $t = -1$ and 32% for $t = 0$. Land is paid for at the beginning of year $t = -2$. Thus the fraction of FCI paid during each time period for

technology l is:

$$\alpha_{l,t}^{\mathrm{FCI}} = \begin{cases} 0.08 + \frac{\mathrm{L}_l}{\mathrm{FCI}_l}, & t = -2 \\ 0.60, & t = -1 \\ 0.32, & t = 0 \\ 0, & \text{else} \end{cases} \tag{4.41}$$

where L_l is the cost of land and FCI_l is the fixed capital investment of the reference capacity facility.

The expected discounted impact of fixed capital investment on facility NPV is then:

$$\begin{aligned} \sigma_l^{\mathrm{FCI}} &= \sum_t \theta_t \cdot \alpha_{l,t}^{\mathrm{FCI}} \\ &= 1.077 + 1.21 \frac{\mathrm{L}_l}{\mathrm{FCI}_l} \end{aligned} \tag{4.42}$$

Working capital

Working capital is paid during the last year of construction and is recovered at the end of the 20 year facility lifetime. Thus the fraction of WC paid during each time period is:

$$\alpha_{l,t}^{\mathrm{WC}} = \begin{cases} 1, & t = 0 \\ -1, & t = 20 \\ 0, & \text{else} \end{cases} \tag{4.43}$$

The expected discounted impact of working capital on facility NPV is then:

$$\begin{aligned} \sigma_l^{\mathrm{WC}} &= \sum_t \theta_t \cdot \alpha_{l,t}^{\mathrm{WC}} \\ &\approx 0.8514 \end{aligned} \tag{4.44}$$

Fixed costs

Fixed costs are constant during the operational lifetime of the facility and zero otherwise:

$$\alpha_{l,t}^{\mathrm{Fixed}} = \begin{cases} 1, & 1 \leq t \leq 20 \\ 0, & \text{else} \end{cases} \tag{4.45}$$

The expected discounted impact of the annual fixed cost of operating the facility is

then:

$$\sigma_l^{\text{Fixed}} = \left(\sum_l \theta_t \cdot \alpha_{l,t}^{\text{Fixed}} \right) \cdot (1 - \text{TR}) \approx 5.193 \tag{4.46}$$

Revenue: biofuel and coproduct sales

Revenue cash flows include biofuel and coproduct sales, and are constant during steady facility operation ($t > 1$) and are 75% as high during $t = 1$ due to start-up. We assume that each technology follows this assumption, thus:

$$\alpha_t^{\text{Biofuel}} = \alpha_{l,t}^{\text{Revenue}} = \begin{cases} 0.75, & t = 1 \\ 1, & t > 1 \\ 0, & \text{else} \end{cases} \tag{4.47}$$

The expected discounted impact of the annual revenue cash flows is then:

$$\sigma^{\text{Biofuel}} = \sigma_l^{\text{Revenue}} = \left(\sum_t \theta_t \cdot \alpha_{l,t}^{\text{Revenue}} \right) \cdot (1 - \text{TR}) \approx 5.055 \tag{4.48}$$

Variable costs: biomass purchasing and other variable costs

Variable Costs include biomass purchasing and other variable costs, and are constant at a rate proportional to biofuel production during steady facility operation ($t > 1$) and are 87.5% as high during $t = 1$ due to start-up. Note that the first half of $t = 1$ is start-up and variable costs are at 75% during those 6 months. We assume that each technology follows this assumption, thus:

$$\alpha_t^{\text{Biomass}} = \alpha_{l,t}^{\text{Variable}} = \begin{cases} 0.875, & t = 1 \\ 1, & t > 1 \\ 0, & \text{else} \end{cases} \tag{4.49}$$

The expected discounted impact of the annual variable cost cash flows is then:

$$\begin{aligned}\sigma^{\text{Biomass}} &= \left(\sum_t \theta_t \cdot \alpha_t^{\text{Biomass}}\right) \cdot (1 - \text{TR}) \\ &\approx 5.124\end{aligned} \tag{4.50}$$

$$\begin{aligned}\sigma_l^{\text{Variable}} &= \left(\sum_t \theta_t \cdot \alpha_{l,t}^{\text{Variable}}\right) \cdot (1 - \text{TR}) \\ &\approx 5.124\end{aligned} \tag{4.51}$$

Parts replacement

The cash flow for parts replacement is determined by the technoeconomic model for each biofuel technology. If no parts are expected to need replacement during the facility lifetime, $\alpha_{l,t}^{\text{Parts}}$ and σ_l^{Parts} are zero. The value of $\alpha_{l,t}^{\text{Parts}}$ corresponds to the fraction of FCI expected to be spent during t to replace parts for technology l. Those costs are described in Subsection 4.7.2.

The expected discounted impact of parts replacement on facility NPV is then:

$$\sigma_l^{\text{Parts}} = \left(\sum_t \theta_t \cdot \alpha_{l,t}^{\text{Parts}}\right) \cdot (1 - \text{TR}) \tag{4.52}$$

Depreciation

Capital depreciation is recorded for tax purposes by following requirements of the U.S. Internal Revenue Service (IRS). In particular, the IRS Modified Accelerated Cost Recovery System (MACRS) with either 200% or 150% declining balance (DB) can be applied to industrial equipment to provide the shortest recovery period and the largest tax deduction. We assume that facilities for each technology fall into an IRS Asset Class that uses a 7-year general plant and a 20-year steam plant recovery periods. This assumption is adopted from the NREL technoeconomic models.

The 7-year recovery period with 200% DB depreciates faster, thus giving a larger tax deduction than 150% DB. A 20-year recovery with 150% DB is faster than 200% DB, however. The depreciation schedule for both are shown in Table 4.13. Both schedules begin and end with a half year of recorded depreciation. The $\alpha_{l,t}^{d}$ values are determined

Year t	Percent of capital depreciated: General plant 7-year, 200% DB $\alpha_t^{d,\text{General}}$	Steam plant 20-year, 150% DB $\alpha_t^{d,\text{Steam}}$
1	14.29%	3.75%
2	24.49%	7.22%
3	17.49%	6.68%
4	12.49%	6.18%
5	8.93%	5.71%
6	8.93%	5.28%
7	8.93%	4.89%
8	4.46%	4.52%
9		4.46%
10		4.46%
11		4.46%
12		4.46%
13		4.46%
14		4.46%
15		4.46%
16		4.46%
17		4.46%
18		4.46%
19		4.46%
20		4.46%
21		2.23%

Table 4.13: MACRS depreciation schedules

from these percentages using the fraction of total FCI corresponding to the general plant and steam plant:

$$\alpha_{l,t}^{d} = \upsilon_l \cdot \alpha_t^{d,\text{General}} + (1 - \upsilon_l) \cdot \alpha_t^{d,\text{Steam}} \tag{4.53}$$

where υ_l is the fraction of FCI for the general plant, $\alpha_t^{d,\text{General}}$ is the 7-year 200% DB schedule and $\alpha_t^{d,\text{Steam}}$ is the 20-year 150% DB schedule.

The expected discounted impact of depreciation on facility NPV is:

$$\sigma_l^{d} = \left[\sum_t \theta_t \cdot \left(\upsilon_l \cdot \alpha_t^{d,\text{General}} + (1 - \upsilon_l) \cdot \alpha_t^{d,\text{Steam}}\right)\right] \cdot \text{TR} \tag{4.54}$$

4.7.2 Biofuel technology parameters

Dry grind starch fermentation

This technology ($l = 1$) converts shelled "Corn" to "RF ethanol" and is based on a joint study [99] by U.S. Department of Agriculture (Agricultural Research Service) and U.S. Department of Energy (National Bioenergy Center - National Renewable Energy Laboratory). The 50 mgy facility has FCI of 74.88 $M (total installed capital cost of 48.0 $M) with land cost of 1.44 $M. Thus:

$$\begin{aligned}\sigma_1^{\text{FCI}} &= 1.077 + 1.21\frac{1.44}{74.88} \\ &\approx 1.100\end{aligned} \tag{4.55}$$

There are no significant parts replacement, thus $\sigma_1^{\text{Parts}} = 0$. The entire plant follows the 7-year MACRS 200% DB depreciation ($\upsilon_1 = 1$):

$$\sigma_1^d \approx 0.2814 \tag{4.56}$$

Integrated corn and stover process

This technology ($l = 2$) converts "Corn" and "Corn-stvr" to "AB ethanol" and is based on a joint study [99] by U.S. Department of Agriculture (Agricultural Research Service) and U.S. Department of Energy (National Bioenergy Center - National Renewable Energy Laboratory). In particular, this technology has parallel shelled corn and corn stover fermentation, but share ethanol separation and purification capital. This is scenario 3 from Wallace et al. (2005) [99]. The 50 mgy facility has FCI of 240.8 $M (total installed capital cost of 154.3 $M) with land cost of 4.63 $M. Thus:

$$\begin{aligned}\sigma_2^{\text{FCI}} &= 1.077 + 1.21\frac{4.63}{240.8} \\ &\approx 1.100\end{aligned} \tag{4.57}$$

There are no significant parts replacement, thus $\sigma_2^{\text{Parts}} = 0$. The entire plant follows the 7-year MACRS 200% DB depreciation ($\upsilon_2 = 1$):

$$\sigma_2^d \approx 0.2814 \tag{4.58}$$

Dilute acid pretreatment and C5+C6 cofermentation

This technology ($l = 3$) converts "Corn-stvr" to "CB ethanol" and is based on an ongoing study by U.S. Department of Energy (National Renewable Energy Laboratory). The technoeconomic model has been updated multiple times since 2002 [75, 79], with the most recent in 2011 [101]. The 61 mgy facility has FCI of 400.6 \$M with land cost of 1.85 \$M. Thus:

$$\begin{aligned}\sigma_3^{\mathrm{FCI}} &= 1.077 + 1.21\frac{1.85}{400.6} \\ &\approx 1.082\end{aligned} \tag{4.59}$$

Baghouse bags are replaced every 5 years at a cost of 0.466 \$M, thus:

$$\alpha_{3,t}^{\mathrm{Parts}} = \begin{cases} \frac{0.466}{400.6} \approx 0.001164, & t = \{1, 6, 11, 16\} \\ 0, & \text{else} \end{cases} \tag{4.60}$$

and

$$\sigma_3^{\mathrm{Parts}} \approx 0.001449 \tag{4.61}$$

The general plant FCI is 334.6 \$M ($\upsilon_3 = \frac{334.6}{400.6} \approx 0.8354$), thus:

$$\sigma_3^d \approx 0.2633 \tag{4.62}$$

Indirect gasification and syngas upgrading to mixed alcohols

This technology ($l = 4$) converts woody biomass to "CB ethanol" and mixed alcohols, and is based on an ongoing study by U.S. Department of Energy (National Renewable Energy Laboratory). Specifically, biomass is converted to syngas via indirect steam gasification and is upgraded to mixed alcohols over a solid catalyst. The technoeconomic model was first published in 2007 [81] and was updated most recently in 2011 [102]. The 64.7 mgy facility has FCI of 489.7 \$M with land cost of 1.60 \$M. Thus:

$$\begin{aligned}\sigma_4^{\mathrm{FCI}} &= 1.077 + 1.21\frac{1.60}{489.7} \\ &\approx 1.081\end{aligned} \tag{4.63}$$

Parts replacement includes all catalyst purchasing. The tar reforming catalysts

(Ni/Mg/K supported on alumina) are regenerated and have an initial cost of 3.59 $M, and the mixed alcohol catalysts (metal-sulfide type) are replaced every 2 years at a cost of 8.87 $M. Thus:

$$\sigma_4^{\text{Parts}} \approx 0.04671 \tag{4.64}$$

The entire plant follows the 7-year MACRS 200% DB depreciation ($\upsilon_4 = 1$):

$$\sigma_4^d \approx 0.2814 \tag{4.65}$$

Direct gasification and syngas upgrading to mixed alcohols

This technology ($l = 5$) converts woody biomass to "CB ethanol" and mixed alcohols, and is based on an ongoing study by U.S. Department of Energy (National Renewable Energy Laboratory) [103]. It differs from technology 4 by using a high-pressure oxygen-blown direct gasifier to convert biomass to syngas, rather than external heating. Most of the assumptions are similar to the indirect gasification process as reported in 2007 [81]. The 50.4 mgy facility has FCI of 254.1 $M with land cost of 4.44 $M. Thus:

$$\begin{aligned} \sigma_5^{\text{FCI}} &= 1.077 + 1.21\frac{4.44}{254.1} \\ &\approx 1.098 \end{aligned} \tag{4.66}$$

Parts replacement includes all catalyst purchasing and baghouse bags. The tar reforming catalysts are regenerated and have an initial cost of 0.987 $M, and the mixed alcohol catalysts are replaced every 5 years at a cost of 0.357 $M. Thus:

$$\sigma_5^{\text{Parts}} \approx 0.04671 \tag{4.67}$$

The general plant FCI is 226.9 $M ($\upsilon_5 = \frac{226.9}{254.1} \approx 0.8928$), thus:

$$\sigma_5^d \approx 0.2828 \tag{4.68}$$

Fast pyrolysis and bio-oil upgrading

This technology ($l = 6$) converts "Corn-stvr" to "CB diesel & naphtha", and is based on a study by U.S. Department of Energy (National Renewable Energy Laboratory) [104]. Specifically, biomass is converted to bio-oil via fast pyrolysis, and is upgraded by hydrotreating and hydrocracking to a mixture of naphtha-range and diesel-range products.

The more economical hydrogen purchasing, as opposed to onsite hydrogen production, scenario is considered. The 58.2 mgy facility has FCI of 175.8 $M with land cost of 3.16 $M. Thus:

$$\begin{aligned}\sigma_5^{\mathrm{FCI}} &= 1.077 + 1.21\frac{3.16}{175.8} \\ &\approx 1.099\end{aligned} \tag{4.69}$$

There are no significant parts replacement, thus $\sigma_6^{\mathrm{Parts}} = 0$. Catalysts are replaced annually and recorded as a variable operating cost. The entire plant follows the 7-year MACRS 200% DB depreciation ($\upsilon_6 = 1$):

$$\sigma_6^d \approx 0.2814 \tag{4.70}$$

AFEX pretreatment and C5+C6 cofermentation

This technology ($l = 7$) converts "Perngrass" to "CB ethanol", and is based on a study in 2011 [105] that expanded the technoeconomic report on corn stover cofermentation (technology 3) from 2002 [79]. This expanded study considered six options for biomass preprocessing that are compatible with switchgass, a common perennial grass. The most economical option (without considering fermentable oligomer sugars), ammonia fiber expansion (AFEX) pretreatment, is considered here. The process is nearly identical to technology 3 downstream of pretreatment, so those parameters were used. FCI was increased by 31 $M to account for the additional pretreatment capital.

4.7.3 Facility capacities

Existing facilities

The 159 existing corn ethanol facilities are shown in Table 4.14. Each facility is registered with the U.S. EPA as part of the Renewable Fuels Program. Their location and nameplate capacity was accessed through the Renewable Fuels Association [98]. In a few cases, companies did not disclose individual facility capacity, so the total capacity was distributed evenly to their facilities with unknown capacity. Each existing facility is assumed to utilize technology 1.

Operating capacity is also shown in Table 4.14 corresponding to the optimal supply chain when the RFS2 mandates are strictly enforced. Note that almost all plants operate

at the maximum, assuming 8,410 operating hours per year (0.959 capacity factor).

Table 4.14: Biofuel production in mgy at existing facilities

Company	Facility location	Nameplate capacity	Operating capacity
Advanced BioEnergy, LLC (ABE)	Fairmont, NE	110.0	105.5
	Aberdeen, SD	46.0	44.1
	Huron, SD	32.0	30.7
Abengoa Bioenergy Corp.	Madison, IL	88.0	84.4
	Mount Vernon, IN	88.0	84.4
	Ravenna, NE	88.0	84.4
	York, NE	56.0	53.7
Absolute Energy, LLC	Saint Ansgar, IA	115.0	110.3
ACE Ethanol, LLC	Stanley, WI	41.0	39.3
Adkins Energy, LLC	Lena, IL	45.0	43.2
Ag Processing Inc. (AGP)	Hastings, NE	52.0	49.9
Al-Corn Clean Fuel	Claremont, MN	45.0	43.2
AltraBiofuels Inc.	Coshocton, OH	60.0	57.6
Amaizing Energy, LLC	Denison, IA	55.0	52.8
Archer Daniels Midland (ADM)	Cedar Rapids, IA	695.0	666.8
	Clinton, IA	237.0	227.4
	Columbus, NE	300.0	287.8
	Decatur, IL	290.0	278.2
	Marshall, MN	40.0	38.4
	Peoria, IL	100.0	95.9
Arkalon Energy, LLC	Liberal, KS	110.0	105.5
Aventine Renewable Energy, LLC	Aurora East, NE	45.0	43.2
	Mount Vernon, IN	110.0	105.5
Badger State Ethanol, LLC	Monroe, WI	50.0	48.0
Big River Resources, LLC	Boyceville, WI	40.0	38.4
	Galva, IL	100.0	95.9
	West Burlington, IA	100.0	95.9
	Dyersville, IA	110.0	105.5

Company	Facility location	Nameplate capacity	Operating capacity
BioFuel Energy Corp.	Fairmont, MN	115.0	110.3
	Wood River, NE	115.0	110.3
Blue Flint Ethanol	Underwood, ND	50.0	48.0
Bridgeport Ethanol	Bridgeport, NE	54.0	51.8
Bushmills Ethanol, Inc.	Atwater, MN	50.0	48.0
Carbon Green Bioenergy	Lake Odessa, MI	50.0	48.0
Cardinal Ethanol	Union City, IN	100.0	95.9
Cargill, Inc.	Blair, NE	195.0	187.1
	Eddyville, IA	35.0	33.6
Center Ethanol Co., LLC	Sauget, IL	54.0	51.8
Central Indiana Ethanol, LLC	Marion, IN	50.0	48.0
Central MN Ethanol Co-op	Little Falls, MN	21.5	20.6
Chief Ethanol Fuels, Inc.	Hastings, NE	62.0	59.5
Chippewa Valley Ethanol Co. (CVEC)	Benson, MN	45.0	43.2
Corn Plus, LLP	Winnebago, MN	49.0	47.0
Corn, LP	Goldfield, IA	60.0	57.6
Cornhusker Energy Lexington, LLC	Lexington, NE	40.0	38.4
Dakota Ethanol, LLC	Wentworth, SD	50.0	48.0
DENCO II, LLC	Morris, MN	24.0	23.0
Didion Ethanol	Cambria, WI	40.0	38.4
E Energy Adams, LLC	Adams, NE	50.0	48.0
East Kansas Agri-Energy, LLC	Garnett, KS	35.0	33.6
ESE Alcohol, Inc.	Leoti, KS	1.5	1.4
Flint Hills Resources, LP	Fairbank, IA	115.0	110.3
	Iowa Falls, IA	105.0	100.7
	Menlo, IA	110.0	105.5
	Shell Rock, IA	110.0	105.5
Gevo	Luverne, MN	21.0	20.1
Glacial Lakes Energy, LLC	Mina, SD	107.0	102.7

Company	Facility location	Nameplate capacity	Operating capacity
	Watertown, SD	100.0	95.9
Golden Grain Energy, LLC	Mason City, IA	115.0	110.3
Grain Processing Corp.	Muscatine, IA	20.0	19.2
	Washington, IN	20.0	19.2
Granite Falls Energy, LLC	Granite Falls, MN	52.0	49.9
Green Plains Renewable Energy	Blissfield, MI	60.0	57.6
	Bluffton, IN	120.0	115.1
	Central City, NE	100.0	95.9
	Fergus Falls, MN	60.0	57.6
	Lakota, IA	100.0	95.9
	Ord, NE	55.0	52.8
	Shenandoah, IA	65.0	62.4
	Superior, IA	60.0	57.6
Guardian Energy, LLC	Janesville, MN	110.0	105.5
Guardian Energy Holdings, LLC	Lima, OH	54.0	51.8
Hankinson Renewable Energy, LLC	Hankinson, ND	110.0	105.5
Heartland Corn Products	Winthrop, MN	100.0	95.9
Heron Lake BioEnergy, LLC	Heron Lake, MN	50.0	48.0
Highwater Ethanol, LLC	Lamberton, MN	55.0	52.8
Homeland Energy	New Hampton, IA	100.0	95.9
Husker Ag, LLC	Plainview, NE	75.0	72.0
Illinois River Energy, LLC	Rochelle, IL	100.0	95.9
Iroquois Bio-Energy Company, LLC	Rensselaer, IN	40.0	38.4
KAAPA Ethanol, LLC	Minden, NE	60.0	57.6
Kansas Ethanol, LLC	Lyons, KS	55.0	52.8
Life Line Foods, LLC	Saint Joseph, MO	50.0	48.0
Lincolnland Agri-Energy, LLC	Palestine, IL	48.0	46.1
Lincolnway Energy, LLC	Nevada, IA	55.0	52.8

Company	Facility location	Nameplate capacity	Operating capacity
Little Sioux Corn Processors, LP	Marcus, IA	92.0	88.3
Louis Dreyfus Commodities	Grand Junction, IA	100.0	95.9
	Norfolk, NE	45.0	43.2
Marquis Energy, LLC	Necedah, WI	50.0	48.0
	Hennepin, IL	100.0	95.9
Marysville Ethanol, LLC	Marysville, MI	50.0	48.0
Mid America Agri Products/Wheatland, LLC	Madrid, NE	44.0	42.2
Mid-Missouri Energy, Inc.	Malta Bend, MO	50.0	48.0
Midwest Renewable Energy, LLC	Sutherland, NE	25.0	24.0
Nebraska Corn Processing, LLC	Cambridge, NE	45.0	43.2
NEDAK Ethanol	Atkinson, NE	44.0	42.2
Nesika Energy, LLC	Scandia, KS	10.0	9.6
New Energy Corp.	South Bend, IN	102.0	97.9
North Country Ethanol, LLC	Rosholt, SD	20.0	19.2
NuGen Energy	Marion, SD	110.0	105.5
One Earth Energy, LLC	Gibson, IL	100.0	95.9
Patriot Renewable Fuels, LLC	Annawan, IL	100.0	95.9
Penford Products	Cedar Rapids, IA	45.0	43.2
Pine Lake Corn Processors, LLC	Steamboat Rock, IA	31.0	29.7
Platinum Ethanol, LLC	Arthur, IA	110.0	105.5
Plymouth Ethanol, LLC	Merrill, IA	50.0	48.0

Company	Facility location	Nameplate capacity	Operating capacity
POET Biorefining	Alexandria, IN	68.0	65.2
	Ashton, IA	56.0	53.7
	Big Stone City, SD	79.0	75.8
	Bingham Lake, MN	35.0	33.6
	Caro, MI	53.0	50.8
	Chancellor, SD	110.0	105.5
	Cloverdale, IN	92.0	88.3
	Coon Rapids, IA	54.0	51.8
	Corning, IA	65.0	62.4
	Emmetsburg, IA	55.0	52.8
	Fostoria, OH	68.0	65.2
	Albert Lea, MN	42.0	40.3
	Gowrie, IA	69.0	66.2
	Hanlontown, IA	56.0	53.7
	Hudson, SD	56.0	53.7
	Jewell, IA	69.0	66.2
	Laddonia, MO	50.0	48.0
	Lake Crystal, MN	56.0	53.7
	Leipsic, OH	68.0	65.2
	Macon, MO	46.0	44.1
	Marion, OH	68.0	65.2
	Mitchell, SD	68.0	65.2
	North Manchester, IN	68.0	65.2
	Portland, IN	68.0	65.2
	Preston, MN	46.0	44.1
	Scotland, SD	11.0	10.6
	Groton, SD	53.0	50.8
Prairie Horizon Agri-Energy, LLC	Phillipsburg, KS	40.0	38.4
Quad County Corn Processors	Galva, IA	30.0	28.8
Red Trail Energy, LLC	Richardton, ND	50.0	48.0

Company	Facility location	Nameplate capacity	Operating capacity
Redfield Energy, LLC	Redfield, SD	50.0	48.0
Show Me Ethanol, LLC	Carrollton, MO	55.0	52.8
Siouxland Energy & Livestock Co-op	Sioux Center, IA	60.0	57.6
Siouxland Ethanol, LLC	Jackson, NE	50.0	48.0
Southwest Iowa Renewable Energy, LLC	Council Bluffs, IA	110.0	105.5
Spectrum Business Ventures, Inc.	Mead, NE	25.0	24.0
The Andersons Ethanol, LLC	Albion, MI	55.0	52.8
	Clymers, IN	110.0	105.5
	Greenville, OH	110.0	105.5
Trenton Agri Products, LLC	Trenton, NE	40.0	38.4
United Ethanol, LLC	Milton, WI	52.0	49.9
United Wisconsin Grain Producers, LLC	Friesland, WI	53.0	50.8
Utica Energy, LLC	Oshkosh, WI	48.0	46.1
Valero Renewable Fuels	Albert City, IA	110.0	105.5
	Albion, NE	110.0	105.5
	Aurora, SD	120.0	115.1
	Bloomingburg, OH	110.0	105.5
	Charles City, IA	110.0	105.5
	Fort Dodge, IA	110.0	105.5
	Hartley, IA	110.0	105.5
	Jefferson Junction, WI	110.0	105.5
	North Linden, IN	110.0	105.5
	Welcome, MN	110.0	105.5

Installed facilities for the case of strict biofuel mandates

The optimum supply chain for strict RFS2 mandates also involved developing 59 of the 98 candidate sites, as shown in Table 4.15. At least one facility was constructed for

each technology excluding $l = \{4, 7\}$. Note that large nameplate capacities correspond to installing multiple facilities at one candidate site.

Table 4.15: Biofuel production in mgy at candidate sites

Location	Technology installed	Nameplate capacity	Operating capacity
Superior, WI	5	75.6	72.5
Moorhead, MN	2	75.0	72.0
Jamestown, ND	2	75.0	72.0
Fergus Falls, MN	2	75.0	72.0
Fond du Lac, WI	5	62.0	59.4
Edina, MN	1	150.0	143.9
Aberdeen, SD	6	87.3	83.8
Menomonie, WI	2	75.0	72.0
Willmar, MN	2	75.0	72.0
Watertown, SD	6	87.3	83.8
Marshall, MN	6	87.3	83.8
Mankato, MN	2	199.0	190.9
Mitchell, SD	2	75.0	72.0
Winona, MN	2	75.0	72.0
Kentwood, MI	1	75.0	72.0
Hoffman Estates, IL	1	300.0	287.8
Mason City, IA	6	189.1	181.4
Spencer, IA	6	174.6	167.5
Lima, OH	2	75.0	72.0
Mishawaka, IN	2	75.0	72.0
Cedar Falls, IA	3	231.1	221.7
Steubenville, OH	5	75.6	72.5
Fort Dodge, IA	6	239.5	229.8
South Sioux City, NE	3	249.8	239.6
Kokomo, IN	2	150.0	143.9
Marion, IA	3	183.0	175.6
Portage, IN	2	75.0	72.0

Location	Technology installed	Nameplate capacity	Operating capacity
Norfolk, NE	6	174.6	167.5
Moline, IL	6	87.3	83.8
West Des Moines, IA	2	255.3	245.0
Normal, IL	2	201.5	193.3
Fairfield, OH	1	150.0	143.9
Bellevue, NE	3	183.0	175.6
Ottumwa, IA	2	75.0	72.0
Burlington, IA	3	91.5	87.8
Canton, IL	6	87.3	83.8
Grand Island, NE	3	280.0	268.6
Columbus, IN	2	75.0	72.0
Danville, IL	3	91.5	87.8
Lexington, NE	6	87.3	83.8
Maryville, MO	2	75.0	72.0
Beatrice, NE	2	75.0	72.0
Quincy, IL	1	296.2	284.2
Jacksonville, IL	2	75.0	72.0
Charleston, IL	2	75.0	72.0
Taylorville, IL	2	150.0	143.9
Portsmouth, OH	5	75.6	72.5
Blue Springs, MO	1	75.0	72.0
Vincennes, IN	2	75.0	72.0
Chesterfield, MO	1	75.0	72.0
New Albany, IN	5	75.6	72.5
Cape Girardeau, MO	5	75.6	72.5
Hutchinson, KS	2	75.0	72.0
Garden City, KS	2	75.0	72.0
Derby, KS	1	75.0	72.0
Nixa, MO	5	75.6	72.5
Liberal, KS	2	75.0	72.0
Atchison, KS	1	150.0	143.9

Location	Technology installed	Nameplate capacity	Operating capacity
Yankton, SD	2	150.0	143.9

4.8 Notation

Sets

Index or subset	Description
$n \in \mathbf{N}$	biomass producers
$r \in \mathbf{R}$	facility sites
$\mathbf{R}^{\text{Candidates}} \subset \mathbf{R}$	candidate facility sites
$\mathbf{R}^{\text{Existing}} \subset \mathbf{R}$	existing facility sites
$m \in \mathbf{M}$	markets
$b \in \mathbf{B}$	biomass types
$\mathbf{B}^{\text{Food}} \subset \mathbf{B}$	edible biomass types
$p \in \mathbf{P}$	biofuel types
$k \in \mathbf{K}$	RFS2 biofuel classifications $\mathbf{K} = \{\text{RF}, \text{AB}, \text{CB}\}$
$\mathbf{P}_k^{\text{Class}} \subset \mathbf{P}$	biofuel types of RFS2 biofuel classification k
$p_l^{\text{major}} \in \mathbf{P}$	major biofuel product of technology l
$l \in \mathbf{L}$	biomass processing technologies
$v \in \mathbf{V}$	transportation (and preprocessing) methods
$t \in \mathbf{T}$	time periods (includes facility construction and operational lifetime)
$j \in \{1, \ldots, J\}$	discrete points for piecewise linear approximations

Parameters

i	discount rate
θ_t	discounting factor $(1+i)^{-t}$
TR	tax rate
$\alpha_t^{\text{Biofuel}}$	fraction of biofuel revenue expected during time period t
$\alpha_t^{\text{Biomass}}$	fraction of biomass purchasing expected during time period t

$\alpha_{l,t}^{\text{Revenue}}$ fraction of coproduct revenue expected during time period t for technology l

$\alpha_{l,t}^{\text{Variable}}$ fraction of variable costs expected during time period t for technology l

$\alpha_{l,t}^{\text{Parts}}$ fraction of FCI paid for parts replacement during time period t for technology l

$\alpha_{l,t}^{\text{Fixed}}$ fraction of fixed costs expected during time period t for technology l

$\alpha_{l,t}^{\text{FCI}}$ fraction of FCI paid during time period t for technology l

$\alpha_{l,t}^{\text{WC}}$ fraction of WC paid during time period t for technology l

$\alpha_{l,t}^{d}$ fraction of FCI depreciation during time period t for technology l

σ^{Biofuel} $= \left(\sum_t \theta_t \cdot \alpha_t^{\text{Biofuel}}\right) \cdot (1 - \text{TR})$; expected discounted impact of annual biofuel revenue on facility NPV

σ^{Biomass} $= \left(\sum_t \theta_t \cdot \alpha_t^{\text{Biomass}}\right) \cdot (1 - \text{TR})$; expected discounted impact of annual biomass purchasing on facility NPV

$\sigma_l^{\text{Revenue}}$ $= \left(\sum_t \theta_t \cdot \alpha_{l,t}^{\text{Revenue}}\right) \cdot (1 - \text{TR})$; expected discounted impact of annual coproduct revenue on facility NPV for technology l

$\sigma_l^{\text{Variable}}$ $= \left(\sum_t \theta_t \cdot \alpha_{l,t}^{\text{Variable}}\right) \cdot (1 - \text{TR})$; expected discounted impact of annual variable costs on facility NPV for technology l

σ_l^{Parts} $= \left(\sum_t \theta_t \cdot \alpha_{l,t}^{\text{Parts}}\right) \cdot (1 - \text{TR})$; expected discounted impact of parts replacement on facility NPV for technology l

σ_l^{Fixed} $= \left(\sum_t \theta_t \cdot \alpha_{l,t}^{\text{Fixed}}\right) \cdot (1 - \text{TR})$; expected discounted impact of annual fixed cost on facility NPV for technology l

σ_l^{FCI} $= \sum_t \theta_t \cdot \alpha_{l,t}^{\text{FCI}}$; expected discounted impact of fixed capital investment on facility NPV for technology l

σ_l^{WC} $= \sum_t \theta_t \cdot \alpha_{l,t}^{\text{WC}}$; expected discounted impact of working capital on facility NPV for technology l

σ_l^{d} $= \left(\sum_t \theta_t \cdot \alpha_{l,t}^{d}\right) \cdot \text{TR}$; expected discounted impact of depreciation on facility NPV for technology l

$\beta^{N}_{n,b}$ amount of biomass type b available at biomass producer n

τ_b fraction of biomass type b that can be used for biofuel production

$\eta^{R}_{b,p,l}$ yield of biofuel type p per unit of biomass type b using biomass processing technology l

$\mu_{b,l}$ fraction of biofuel produced from biomass type b using technology l

δ capacity factor

$\beta^{M,\min}_{m,k}$ minimum amount of RFS2 biofuel classification k demanded at market m

$\beta^{M,\max}_{m,k}$ maximum amount of RFS2 biofuel classification k demanded at market m

$C^{\text{Biofuel}}_{r,m,v,p}$ facility-gate biofuel sale price per unit of biofuel type p at facility site r sold to market m and transported via method v

$C^{\text{Biomass}}_{n,r,v,b}$ delivered biomass price per unit of biomass type b shipped from biomass producer n to facility site r and transported via method v

$\text{CAP}_{r,p,l}$ ($r \in \mathbf{R}^{\text{Existing}}$) maximum production capacity for biofuel p of the facility at existing site r using technology l

$R^{\text{Existing,CAP}}_{r,p,l}$ equal to $\text{CAP}_{(r,p,l)}$ if $(r,p,l) \in a^{R,\text{set}}$ and zero otherwise

$R^{\text{Existing,Coproducts}}_{r,l}$ ($r \in \mathbf{R}^{\text{Existing}}$) annual cash flow for coproducts at existing site r using technology l

$R^{\text{Existing,Other Variable}}_{r,l}$ ($r \in \mathbf{R}^{\text{Existing}}$) annual cash flow for other variable costs at existing site r using technology l

$R^{\text{Existing,Fixed}}_{r,l}$ ($r \in \mathbf{R}^{\text{Existing}}$) annual cash flow for fixed costs at existing site r using technology l

$R^{\text{Existing,FCI}}_{r,l}$ ($r \in \mathbf{R}^{\text{Existing}}$) fixed capital investment at existing site r using technology l

$R^{\text{Existing,WC}}_{r,l}$ ($r \in \mathbf{R}^{\text{Existing}}$) working capital at existing site r using technology l

$\text{CAP}^{\text{linear}}_{p,l,j}$ capacity of discrete point j for biofuel type p using technology l

$\text{CF}^{\text{linear,Fixed}}_{l,j}$ annual cash flow for fixed costs of discrete point j using technology l

$\mathrm{CF}_{l,j}^{\mathrm{linear,FCI}}$ fixed capital investment of discrete point j using technology l

$\mathrm{CF}_{l,j}^{\mathrm{linear,WC}}$ working capital of discrete point j using technology l

$\mathrm{C}_{l}^{\mathrm{Coproducts}}$ coproduct revenue per unit of biofuel produced by technology l

$\mathrm{C}_{l}^{\mathrm{Other\,Variable}}$ other variable expenses per unit of biofuel produced by technology l

Continuous decision variables

TNPV total new present value for the entire supply chain

NPV_{r} net present value for facility site r

$\mathrm{CF}_{r}^{\mathrm{Biofuel}}$ annual cash flow for biofuel sales at r

$\mathrm{CF}_{r}^{\mathrm{Biomass}}$ annual cash flow for biomass purchasing at r

$\mathrm{CAP}_{r,p,l}$ $\left(r \in \mathbf{R}^{\mathrm{Candidates}}\right)$ maximum production capacity for biofuel p of the facility at site r using technology l

$\mathrm{CF}_{r,l}^{\mathrm{Coproducts}}$ $(r \in \mathbf{R}^{\mathrm{Candidates}})$ annual cash flow for coproducts at candidate site r using technology l

$\mathrm{CF}_{r,l}^{\mathrm{Other\,Variable}}$ $(r \in \mathbf{R}^{\mathrm{Candidates}})$ annual cash flow for other variable costs at candidate site r using technology l

$\mathrm{CF}_{r,l}^{\mathrm{Fixed}}$ $(r \in \mathbf{R}^{\mathrm{Candidates}})$ annual cash flow for fixed costs at candidate site r using technology l

$\mathrm{CF}_{r,l}^{\mathrm{FCI}}$ $(r \in \mathbf{R}^{\mathrm{Candidates}})$ fixed capital investment at candidate site r using technology l

$\mathrm{CF}_{r,l}^{\mathrm{WC}}$ $(r \in \mathbf{R}^{\mathrm{Candidates}})$ working capital at candidate site r using technology l

$f_{n,r,v,b}^{NR}$ flow of biomass type b from biomass producer n to facility site r via transportation method v

$f_{r,m,v,p}^{RM}$ flow of biofuel type p from facility site r to market m via transportation method v

$u^R_{r,b,l}$ amount of biomass type b used at facility site r using biomass processing technology l

$a^R_{r,p,l}$ amount of biofuel type p produced at facility site r using biomass processing technology l

$\lambda^R_{r,l,j}$ ($r \in \mathbf{R}^{\text{Candidates}}$) fraction of discrete point j using technology l installed at r

Binary decision variables

$y^R_{r,l,j}$ ($r \in \mathbf{R}^{\text{Candidates}}$, $j \in \{1, \ldots, J-1\}$) binary variable: equal to true if the facility installed at r using technology l has capacity for biofuel type p between $\text{CAP}^{\text{linear}}_{p,l,j}$ and $\text{CAP}^{\text{linear}}_{p,l,j+1}$

CHAPTER 5

Multiobjective Supply Chain Optimization for Biofuels

5.1 Summary

Both environmental and economic performance are critical in the development of the biofuel industry for it to truly be a sustainable alternative to petroleum-based transportation fuels. In this chapter, the supply chain optimization problem described in Chapter 4 has been expanded as a multiobjective optimization problem with a competing objective of minimizing greenhouse gas emissions. Recent life cycle analysis literature on biofuels is leveraged to quantify the impact of each activity in the biofuel supply chain. The resulting multiobjective mixed integer linear program is solved using an ε-constraint approach that yields the Pareto Frontier of efficient supply chain designs. This allows for the identification of supply chain decisions that greatly reduce greenhouse gas emissions for minimal economic losses.

5.2 Multiobjective optimization and Pareto optimality

Economic gain is not the only objective of biofuels production and use. Many biorefinery technologies are designed specifically to reduce emissions, water use or land use. Multiobjective optimization seeks to identify one or a set of Pareto optimal solutions

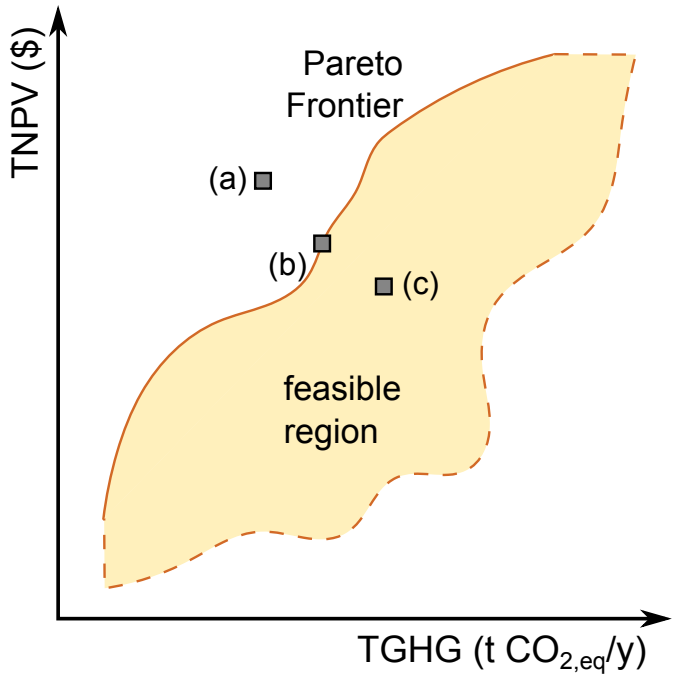

Figure 5.1: Example Pareto Frontier for maximization of TNPV and minimization of TGHG. The feasible region for the optimization problem is shown with its efficient boundary being the Pareto Frontier. Point (a) is infeasible, point (b) is a Pareto point, and point (c) is feasible but is dominated by point (b).

(Pareto points) [108]. Pareto points are solutions that are non-inferior to all other feasible solutions. This is shown in Figure 5.1 for the two objectives of maximizing TNPV and minimizing total greenhouse gas emissions (TGHG) for the entire supply chain. Point (b) is a Pareto point because there is no feasible solution that simultaneously improves both objectives. There are usually many Pareto points, and the whole set of them is referred to as the Pareto Frontier or surface. Recall that it is desirable to lower TGHG and raise TNPV, so the upper left boundary in Figure 5.1 is the Pareto Frontier. Each solution along the Pareto Frontier is mathematically equal (i.e. a solution that is better for one objective cannot be found without necessarily worsening at least one other objective) and thus depend on the preference of a decision maker to select a "right" solution.

The general form of a multiobjective optimization problem involving K objectives

to be minimized is

$$\begin{aligned} \min \quad & (f_1(x), \ldots, f_K(x)) \\ \text{s.t.} \quad & x \in X \end{aligned}$$

where x is the vector of decision variables with feasible set X defined by constraints.

Multiobjective optimization techniques vary in how a decision maker may express their preference, and the techniques fall into three major groups [109–111]:

- A priori methods
- A posteriori methods
- Interactive methods

A priori methods require preference information to be specified before finding a solution. The solution returned is a Pareto point that best satisfies the decision makers preference. Examples include scalarization (agglomeration), no-preference methods and utility function methods, and are shown in Table 5.1. Applying a so-called carbon tax to greenhouse gas emissions is a common example of linear scalarization to convert a multiobjective problem involving emissions and economics into a single-objective problem. In general, the weights assigned to the objectives convert them into uniform units (e.g. dollars) and represent the relative importance for each objective. Minimizing the Euclidean norm (L_2) from an ideal state for all the objectives is an example of a no-preference method.

A posteriori methods generate a representative set of Pareto points that the decision makers can then evaluate based on their preferences. These methods require additional computational effort, as determining each Pareto point may require as much time as an a priori method. For example, many well-known a posteriori methods (e.g. normal-boundary intersection [112] and successive pareto optimization [113]) construct and solve several scalarization problems. Metaheuristics, such as simulated annealing, particle swarm optimization and evolutionary algorithms, generate a representative set of solutions by searching the feasible region quickly, but Pareto optimality of the solutions is not guaranteed. The ε-constraint method is the most widely applied a posteriori method in multiobjective optimization. In this method, single-objective problems are solved where one of the original objectives is minimized while the other objectives are

Table 5.1: A priori methods for multiobjective optimization problems.

Method	Form
Linear scalarization	min $\sum_{k=1}^{K} w_k \cdot f_k(x)$ s.t. $x \in X$ where w_k are the non-negative weights of the objectives.
No-preference (e.g. global criterion)	min $\left\|\left\|f(x) - f^{\text{ideal}}\right\|\right\|$ s.t. $x \in X$ where $f(x)$ is the vector of objectives, f^{ideal} is some target, and $\|\cdot\|$ can be any L_p norm.
Utility function	min $u(f(x))$ s.t. $x \in X$ where the utility function $u(\cdot)$ represents the preference of the decision maker.

constrained:

$$\begin{aligned} \min \quad & f_1(x) \\ \text{s.t.} \quad & x \in X \\ & f_k(x) \leq \varepsilon_k, \quad \forall\, k \neq 1 \end{aligned}$$

where the parameters ε_k are varied between ε_k^L and ε_k^U. These bounds are determined by solving the K single-objective problems for each objective function separately. Thus,

$$\begin{aligned} \varepsilon_k^L = \min \quad & f_k(x) \\ \text{s.t.} \quad & x \in X \end{aligned}$$

and ε_k^U is the maximum value of $f_k(x)$ among the solutions when minimizing the other objectives.

Solution filtering ensures that the ε-constraint method returns Pareto points, as the solved single-objective problems themselves do not ensure feasibily or that they dominate the solutions with other $\{\varepsilon_k\}$ values. The advantages of the ε-constraint method are that it (i) obtains a representation of the Pareto Frontier that can be quickly improved with a finer grid of $\{\varepsilon_k\}$ values, (ii) doesn't suffer from scaling problems of scalarization (e.g. numerical precision and comparable order of magnitude), and (iii) can identify islanded (unsupported) Pareto points that are common to integer and mixed

integer problems [114].

Interactive methods require that the decision maker is continuously interacting with the method while searching for the most preferred Pareto point [115, 116]. Instead of the method converging mathematically, these methods end when the decision maker has psychologically converged on a desirable solution. At each iteration of the method, the decision maker can modify their preferences in a number of ways. Some methods allow for tradeoff information, where the decision maker ranks objective trade-offs for a number of possible search directions. Other methods allow for modifying the target objectives f^{ideal} within a no-preference method search for Pareto points. Classification of objective functions is another approach in which the objectives are ranked at the current Pareto point, then the method seeks to find a better Pareto point. Although intuitive and transparent for the decision maker, iterative methods suffer from the drawbacks of requiring constant decision maker attention and limiting the decision maker to seeing only a subset of the whole range of possibilities available along the Pareto Frontier.

5.3 Mathematical formulation

The mathematical formulation from Chapter 4, described in Section 4.3, was expanded to incorporate an environmental objective function. Thus, the multiobjective optimization problem examined in this chapter has the objectives to (i) maximize total net present value and (ii) minimize total greenhouse gas emissions.

TGHG for the entire supply chain is the sum of the greenhouse gas emissions corresponding to each of the facility sites:

$$\text{TGHG} = \sum_{r} \text{GHG}_r \tag{5.1}$$

Each facility site r in the study has emissions associated with:

- Biomass production, $\text{EF}_r^{\text{Biomass}}$
  - Fertilizer production
  - Fertilizer N_2O
  - Farming
  - Land use change

- Biomass transportation, $\mathrm{EF}_r^{\mathrm{TransportBiomass}}$
- Biorefinery, $\mathrm{EF}_r^{\mathrm{Biorefinery}}$
  - Operations
  - Coproduct credit
- Biofuel transportation, $\mathrm{EF}_r^{\mathrm{TransportProducts}}$
- Market, $\mathrm{EF}_r^{\mathrm{Market}}$
  - Biofuel combustion
  - Fuel credit

The greenhouse gas emission for each facility is then:

$$\begin{aligned}\mathrm{GHG}_r = \mathrm{EF}_r^{\mathrm{Biomass}} + \mathrm{EF}_r^{\mathrm{TransportBiomass}} + \mathrm{EF}_r^{\mathrm{Biorefinery}} \\ + \mathrm{EF}_r^{\mathrm{TransportProducts}} + \mathrm{EF}_r^{\mathrm{Market}}, \quad \forall\, r\end{aligned} \tag{5.2}$$

Emissions from each of these sources are assumed proportional to the corresponding supply chain activity, as described in the following equations:

$$\mathrm{EF}_r^{\mathrm{Biomass}} = \sum_{n,v,b} E_b^N \cdot f_{n,r,v,b}^{NR}, \quad \forall\, r \tag{5.3}$$

where E_b^N is the amount of emissions associated with producing a unit of biomass type b (e.g. t $\mathrm{CO}_{2,\mathrm{eq}}$/dt):

$$\mathrm{EF}_r^{\mathrm{TransportBiomass}} = \sum_{n,v,b} E_{b,v}^{NR} \cdot D_{n,r}^{NR} \cdot f_{n,r,v,b}^{NR}, \quad \forall\, r \tag{5.4}$$

where $D_{n,r}^{NR}$ is the round-trip distance between biomass producer n and facility site r, and $E_{b,v}^{NR}$ is the amount of emissions associated with transporting a unit of biomass type b via method v per unit distance (e.g. t $\mathrm{CO}_{2,\mathrm{eq}}$/mi/dt):

$$\mathrm{EF}_r^{\mathrm{Biorefinery}} = \sum_{b,l} E_{b,l}^{RB} \cdot u_{r,b,l}^{R}, \quad \forall\, r \tag{5.5}$$

where $E_{b,l}^{RB}$ is the amount of emissions associated with converting a unit of biomass type b using biorefinery technology l (e.g. t $\mathrm{CO}_{2,\mathrm{eq}}$/dt):

$$\mathrm{EF}_r^{\mathrm{TransportProducts}} = \sum_{m,v,p} E_{p,v}^{RM} \cdot D_{r,m}^{RM} \cdot f_{r,m,v,p}^{RM}, \quad \forall\, r \tag{5.6}$$

where $D_{r,m}^{RM}$ is the round-trip distance between facility site r and market m, and $E_{p,v}^{RM}$ is the amount of emissions associated with transporting a unit of product p via method v per unit distance (e.g. t $CO_{2,eq}$/mi/gal):

$$\mathrm{EF}_r^{\mathrm{Market}} = \sum_{m,v,p} E_p^M \cdot f_{r,m,v,p}^{RM}, \quad \forall\, r \tag{5.7}$$

where E_p^M is the amount of emissions associated with the market/customer use of a unit of product p (e.g. t $CO_{2,eq}$/gal).

The multiobjective mixed integer linear program is then:

$$\begin{aligned} &\text{maximize} && (\mathrm{TNPV}, -\mathrm{TGHG}) \\ &\text{subject to} && \text{equations (4.1), (4.5)–(4.22), (4.26)–(4.40), (5.1)–(5.7)} \end{aligned} \tag{MoMP}$$

5.4 Solution strategy

Problem (MoMP) is solved by transforming it into the single-objective mixed integer linear program:

$$\begin{aligned} &\text{maximize} && \varepsilon_1 \cdot \mathrm{TNPV} - (1-\varepsilon_1) \cdot \mathrm{TGHG} \\ &\text{subject to} && \text{equations (4.1), (4.5)–(4.22), (4.26)–(4.40), (5.1)–(5.7)} \\ & && \mathrm{TGHG} \leq \varepsilon_2 \end{aligned} \tag{SoMP}$$

Pareto points are found by solving problem (SoMP) iteratively in the following ε-constraint strategy:

Step 1: Maximize TNPV without considering TGHG by solving problem (SoMP) with $\varepsilon_1 = 1$ and $\varepsilon_2 = \inf$. Store the solution value of TGHG as the highest TGHG along the Pareto Frontier $\mathrm{TGHG}^{\max}$.

Step 2: Minimize TGHG without considering TNPV by solving problem (SoMP) with $\varepsilon_1 = 0$ and $\varepsilon_2 = \inf$. Store the solution value for all decision variables as the initial guess for the next problem. Store the solution value of TGHG as the lowest TGHG along the Pareto Frontier $\mathrm{TGHG}^{\min}$.

Step 3: Maximize TNPV while constraining TGHG by solving problem (SoMP) with

$\varepsilon_1 = 1$ and $\varepsilon_2 = \text{TGHG}^{\min}$. Store the solution value of all decision variables as the initial guess for the next problem.

Step K $(K \geq 4)$**:** Maximize TNPV while constraining TGHG by solving problem (SoMP) with $\varepsilon_1 = 1$ and $\varepsilon_2 \in [\text{TGHG}^{\min}, \text{TGHG}^{\max}]$. Store the solution value of all decision variables as the initial guess for the next problem. Note that this initial guess is only a feasible solution if the next problem has a higher value for ε_2, therefore there is an advantage to monotonically increasing ε_2 in the search for Pareto points.

End when the desired number of Pareto points (e.g. resolution of the Pareto Frontier) have been obtained. Solution filtering is required to confirm that each step returned a feasible solution that is not dominated by any other solution, and is thus Pareto optimal.

5.5 Life cycle analysis

Biofuels are promoted as alternatives to petroleum-based transportation fuels, in part, for their reduced greenhouse gas emissions, determined by thorough life cycle analysis. This attribute of biofuels has been recognized in policies aimed at reducing the transportation sector's GHG emissions (e.g., the Low-Carbon Fuel Standard in California [117], the U.S. Renewable Fuel Standard program [11], and the Renewables Directive in the European Union [118]). However, there is still active debate and research over the emissions of biofuels. The emissions of the widespread corn ethanol dry-grind process are even disputed, with some authors concluding that it offers lower emissions when compared with gasoline [119,120], some authors concluding the opposite [121], and others concluding that emissions are nearly equal [122]. Most studies agree that cellulosic biofuels offer lower emissions when compared with gasoline [123–127]. Such life cycle analysis studies differ in their system boundary assumptions for biofuels or petroleum fuels (e.g. including land use change, coproduct credits, petroleum supply defense via military actions), and in their parameter values (e.g. biorefinery technology updates, better estimates).

This chapter utilizes results for the life cycle analysis of select biofuels performed using the GREET (Greenhouse gases, Regulated Emissions, and Energy Use in Transportation) model. The GREET model was developed at Argonne National Laboratory and is a trusted tool for researchers and politicians to examine greenhouse gas emissions from vehicles and transportation fuels on a consistent basis [128]. Parameters and assumptions are continuously updated as the biofuel technologies develop, small-scale

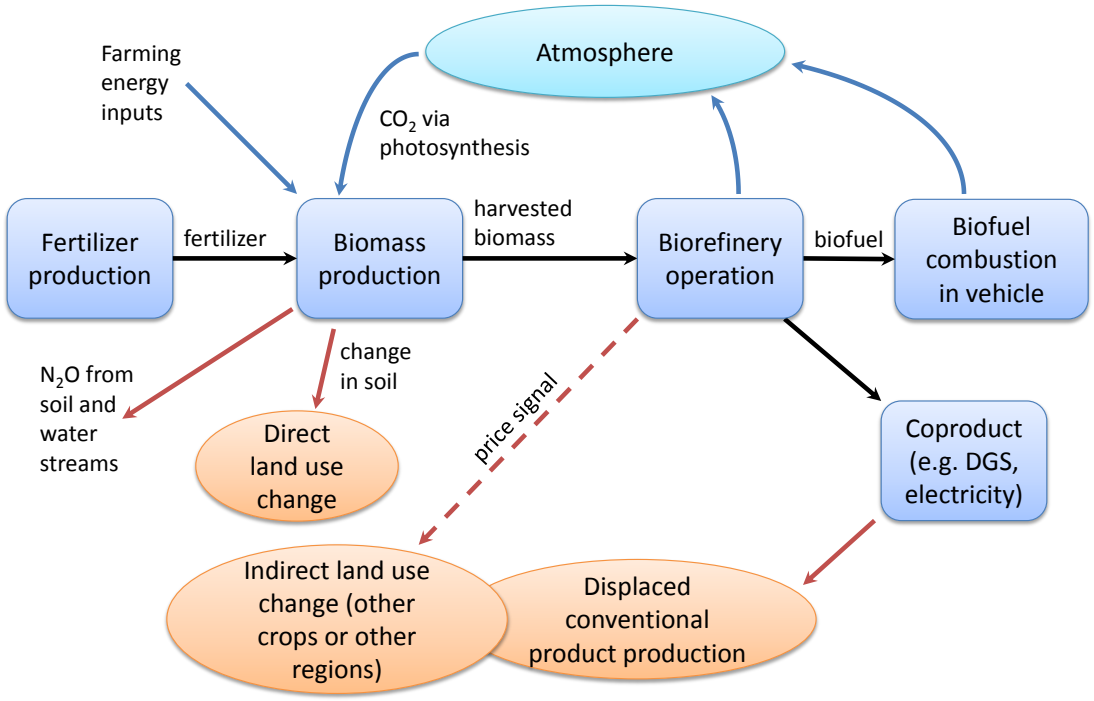

Figure 5.2: System boundary of the biofuel life cycle analysis (inspired by [123, Figure 2]).

experiments are performed, and large-scale field trials are completed. Furthermore, numerous national laboratory reports and papers have been published on biofuel life cycle analysis using GREET, with some based on technoeconomic models corresponding to the seven biorefinery technologies considered in this thesis (see Subsection 4.4.4).

The system boundary considered for the biofuel life cycle analysis is shown in Figure 5.2. Greenhouse gases considered here are measured in CO_2-equivalent tonnes (t $CO_{2,eq}$). This measure is an aggregation of emissions of CO_2, CH_4 and N_2O, weighted by their 100 year global warming potentials of 1, 25 and 298, respectively. In other words, 1 unit of CH_4 is predicted to have the same global warming potential as 25 units of CO_2 over a 100 year time horizon. These global warming potentials are as specified by the International Panel on Climate Change's 2007 assessment [129].

Table 5.2: Emission parameter values for biomass production.

Biomass type b	E_b^N
Corn	0.00916 t $CO_{2,eq}$/bu
Corn-stvr	0.0636 t $CO_{2,eq}$/dt
All wood	0.111 t $CO_{2,eq}$/dt
Perngrass	0.111 t $CO_{2,eq}$/dt

5.6 Emission parameters

Emission parameters introduced in Section 5.3 are determined from the Argonne GREET model [128] and associated literature [123, 125, 126], using process data from the technoeconomic models corresponding to each of the seven considered biorefinery technologies. Many values are obtained from a report by Wang et al. [123], which summarizes the recent GREET model updates and performs life cycle analysis on a number of biorefinery technologies along with gasoline. This is the 2012 update of their earlier study from 2006 [125]. Transportation emission values for biomass and biofuels are taken from [56]. The emission parameters are shown in Tables 5.2, 5.3, 5.4, 5.5 and 5.6.

Comparisons of two competing products (e.g. a biofuel and gasoline) requires a choice of functional unit. Functional unit options for fuels include volume or mass basis, energy equivalence, and end use equivalence. Conclusions depend on the choice of functional unit. For example, comparing ethanol and gasoline using a volume functional unit (i.e. per gallon) leads to the conclusion that ethanol is cheaper, which may not be the case considering its lower energy density compared to gasoline. In this chapter, I will consider the functional unit of gasoline equivalent gallon (i.e. volumes with equal energy content). Thus, the effect of lower energy density in some biofuels is removed. Additionally, the market/customer product use in Table 5.6 accounts for the biofuel offsetting an equal energy volume of gasoline. A value of 94 g $CO_{2,eq}$/MJ, found by Wang et al. [123], was assumed for gasoline.

It should also be noted that end use equivalence functional units may be appropriate in some cases. Most notably, miles per gallon of gasoline equivalent gallon is useful for vehicles designed to take advantage of the properties of ethanol (e.g. higher compression ratio and different fuel-air mixture) to extract additional engine performance. As the gasoline equivalent gallon functional unit does not depend on particular vehicle design or performance, it is more suitable for the present supply chain optimization.

Table 5.3: Emission parameter values for biomass transportation.

Biomass type b	Method v	$E^{NR}_{b,v}$
Corn	Rail	8.58E-7 t $CO_{2,eq}$/mi/bu
All biomass	Truck	1.98E-4 t $CO_{2,eq}$/mi/dt

Table 5.4: Emission parameter values for biorefinery operation.

Biomass type b	Technology l	$E^{RB}_{b,l}$
Corn	1	0.00389 t $CO_{2,eq}$/bu
Corn	2	0.00389 t $CO_{2,eq}$/bu
Corn-stvr	2	–0.0557 t $CO_{2,eq}$/dt
Corn-stvr	3	–0.0557 t $CO_{2,eq}$/dt
All wood	4	0.145 t $CO_{2,eq}$/dt
All wood	5	0.145 t $CO_{2,eq}$/dt
Corn-stvr	6	0.145 t $CO_{2,eq}$/dt
Perngrass	7	–0.0477 t $CO_{2,eq}$/dt

Table 5.5: Emission parameter values for biofuel transportation.

Product p	Method v	$E^{RM}_{p,v}$
RF ethanol	Truck	5.91E-7 t $CO_{2,eq}$/mi/gal
AB ethanol	Truck	5.91E-7 t $CO_{2,eq}$/mi/gal
CB ethanol	Truck	5.91E-7 t $CO_{2,eq}$/mi/gal
CB Naphtha & diesel	Truck	5.54E-7 t $CO_{2,eq}$/mi/gal

Table 5.6: Emission parameter values for market/customer product use (e.g. biofuel combustion).

Product p	E^{M}_{p}
RF ethanol	–0.00746 t $CO_{2,eq}$/gal
AB ethanol	–0.00746 t $CO_{2,eq}$/gal
CB ethanol	–0.00746 t $CO_{2,eq}$/gal
CB naphtha & diesel	–0.0112 t $CO_{2,eq}$/gal

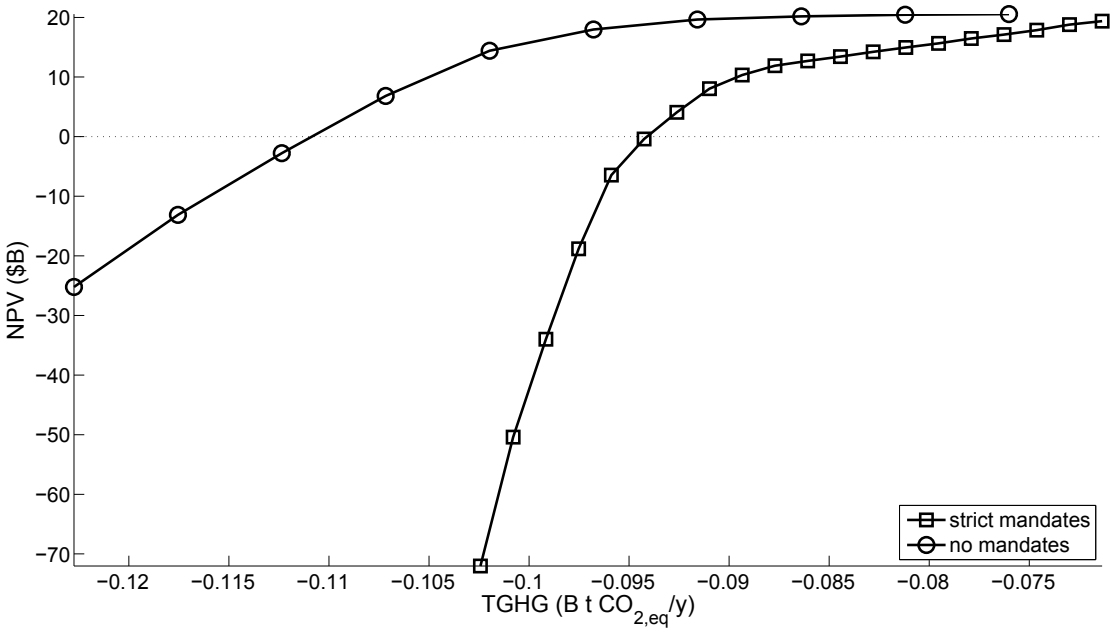

Figure 5.3: Pareto Frontiers for the scenarios of no biofuel mandates and strict mandates.

5.7 Results

The MILP model was coded in IBM ILOG CPLEX Optimization Studio v12.2 [64], and has 156,947 continuous variables, 5,488 binary variables and 40,982 constraints. The Pareto Frontier of supply chains is presented along with some notable Pareto points, with an evaluation of the tradeoff between economic and environmental performance.

5.7.1 Pareto Frontiers

The two scenarios of no biofuel mandates and strict mandates were considered, and their corresponding Pareto Frontiers are shown in Figure 5.3. The Pareto points are identified using the ε-constraint approach described in Section 5.4. Each of the single-objective problems are solved with a target optimality gap of 0.5% and a time limit of 10 hours. Most of the Pareto points are identified to an optimality gap less than 2.0% in 10 hours.

The addition of the biofuel mandate constraints reduces the size of the feasible region, thus the Pareto Frontier for the no biomass mandates scenario dominates the Pareto Frontier of the strict mandates scenario. This is largely the result of the strict

mandate scenario hitting the upper bound on production of biofuels, whereas the no mandates scenario can improve both economics and emission objectives by producing more biofuel than is truly demanded. For this reason, the remainder of this section will focus on results for the strict mandates scenario.

The effect of constraining TGHG can be seen by plotting the total biofuel production for each Pareto point, as shown in Figure 5.4. Recall that the 2015 RFS2 mandates are for the production of 3 B gal/y cellulosic biofuel, 2.5 B gal/y of other advanced biofuel and 15 B gal/y of implicit non-advanced biofuel. Cellulosic biofuels (CB) produced by technologies $l = \{3, 4, 5, 6, 7\}$ may be sold in each of those three categories, whereas advanced biofuel (AB) produced by technology $l = 2$ may be sold in the latter two categories, and renewable fuel (RF) produced by technology $l = 1$ may only be sold in the last category. Much of the biofuel demand is satisfied then by CB for low TGHG Pareto points. Limited cellulosic biomass availability prevents all of the demand to be satisfied this way, and thus AB and RF are also produced. As the ε-constraint is relaxed, an increasing amount of the biofuel demand is satisfied by RF. Also, recall that technology 2 competes for corn (also a RF feedstock) and corn stover (also a CB feedstock) as feedstocks, thus AB production from technology 2 remains relatively constant. CB naphtha & diesel-range is produced in small amounts from technology 6, as it competes for corn stover with technologies that typically have lower greenhouse gas emissions.

5.7.2 Key Pareto points

This section will provide some analysis of the strict mandates scenario Pareto Frontier, by examining key Pareto points. The goal is to identify modest supply chain changes that may lead to large emission gains for a small loss of profit.

Highest TNPV

It turns out that the same supply chain configuration identified in Chapter 4 for the strict mandates scenario is a Pareto point for the multiobjective problem. For simplicity, those results are summarized here. In the solution, five different technologies are installed with a total of 168 facilities producing RF (15,000 M gal/y), 26 producing AB (2,500 M gal/y) and 24 producing CB (3,000 M gal/y). All produced biofuels are sold in their highest RFS fuel classification. By examining the breakeven prices for each facility, it

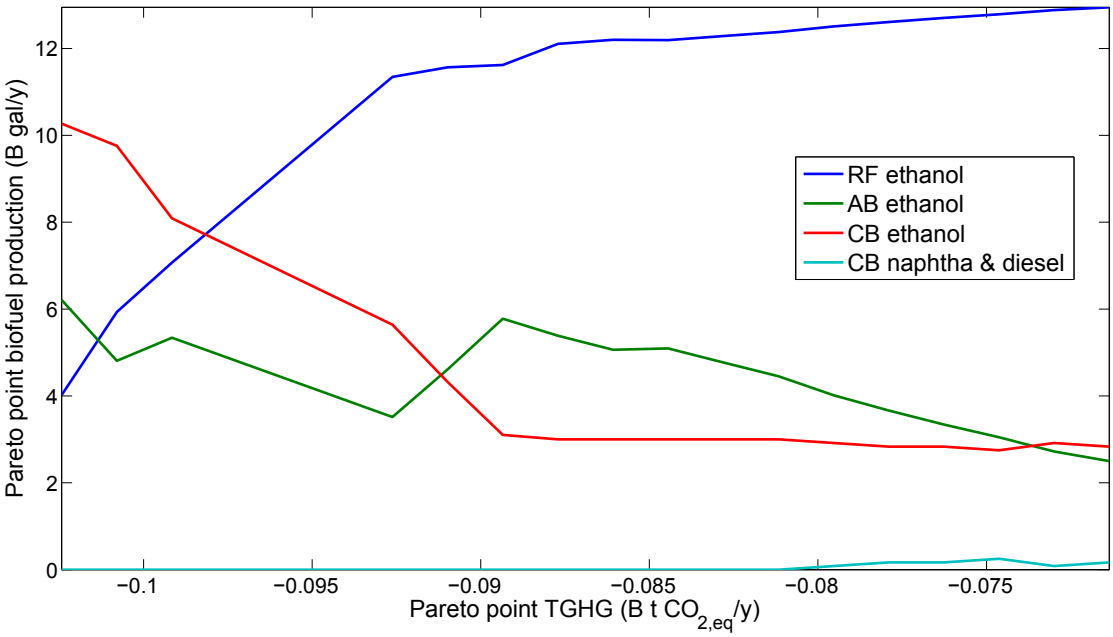

Figure 5.4: Total biofuel production for each Pareto point.

was found that all facilities are economical for facility-gate prices of 2.39, 2.13 and 1.71 $/gal for CB, AB and RF, respectively.

Lowest TGHG

The Pareto point with the lowest TGHG is found by first minimizing TGHG without considering TNPV, then maximizing TNPV while constraining TGHG to be less than the previous solution value. Recall that the previous solution is used as an initial guess to expedite the solution of the second problem. This Pareto point is shown in Figure 5.6. Five of the seven technologies are installed by developing 90 of the 98 candidate sites, with a total of 60 facilities producing RF (4,020 M gal/y), 33 producing AB (6,211 M gal/y) and 57 producing CB (10,269 M gal/y). CB and AB are produced far in excess of the RFS mandates for their classifications, so they are sold at lower fuel classifications. Limited supply of cellulosic material in 2015 prohibits CB from dominating the biofuel markets, although that would have resulted in a lower TGHG. Technology 4 (indirect gasification) is favored over technology 5 (direct gasification), which was installed in the highest TNPV Pareto point, for production of CB ethanol from all-wood, because it has higher product yield for nearly identical emissions.

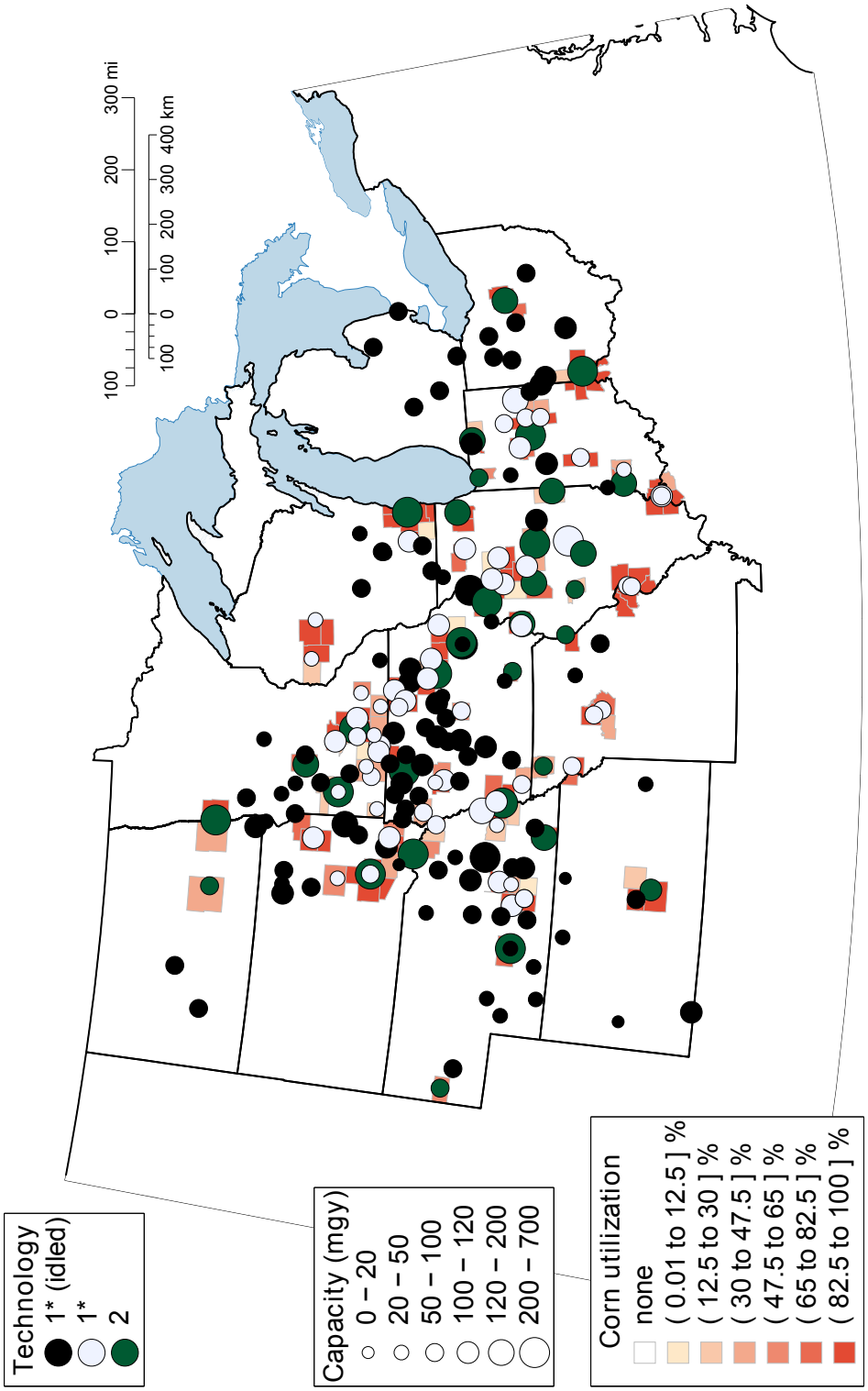

(a) Corn grain utilization with corn-utilizing facilities shown. RF and AB ethanol are produced from corn using technology 1 and 2, respectively. Existing facilities are denoted with an asterisk (*). Maximum corn utilization is 34%. In this Pareto point, many existing facilities are idled (zero production) in favor of lower emission biofuel technologies.

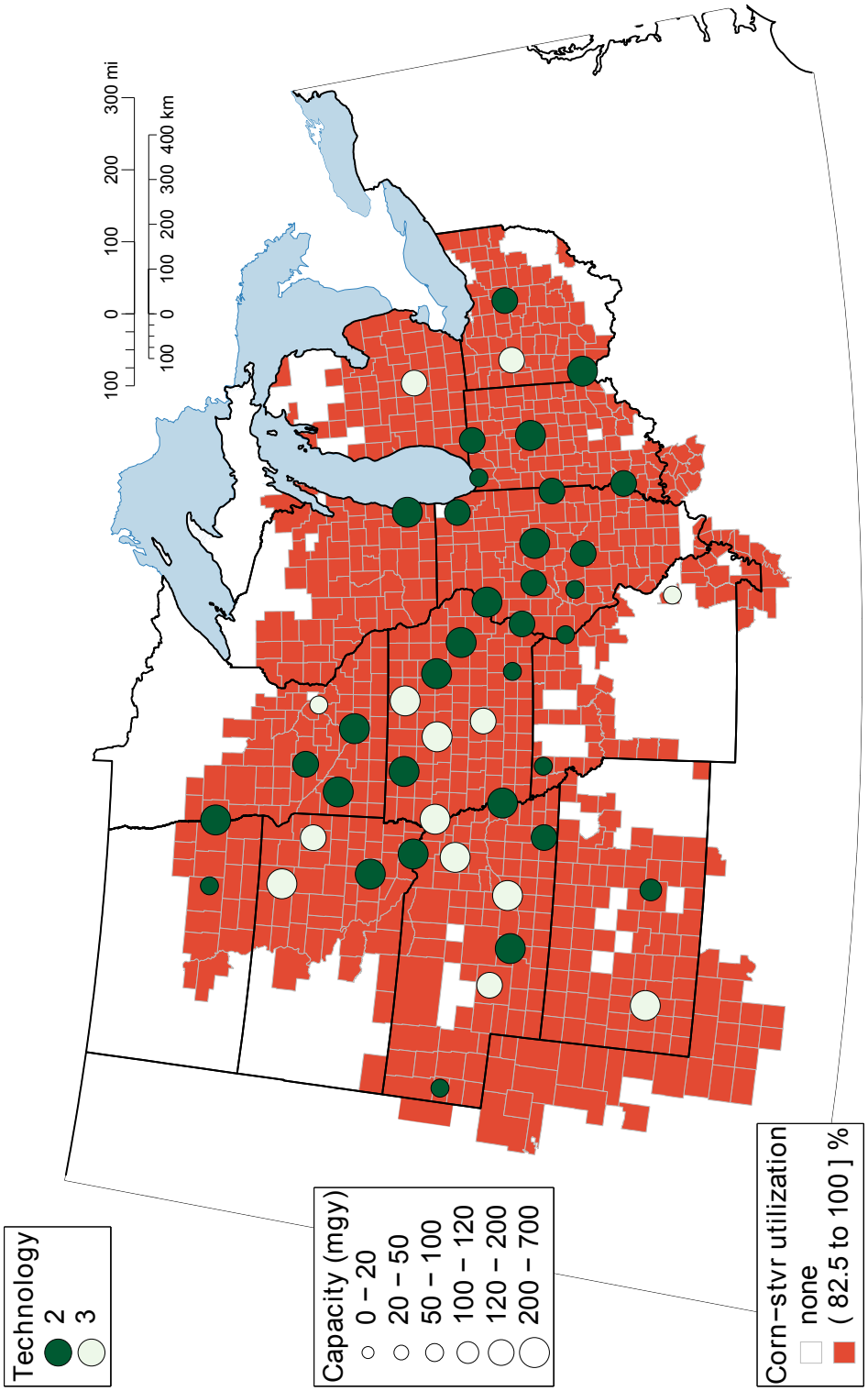

(b) Corn stover utilization with associated facilities shown. AB and CB ethanol, and CB naphtha & diesel are produced from corn stover.

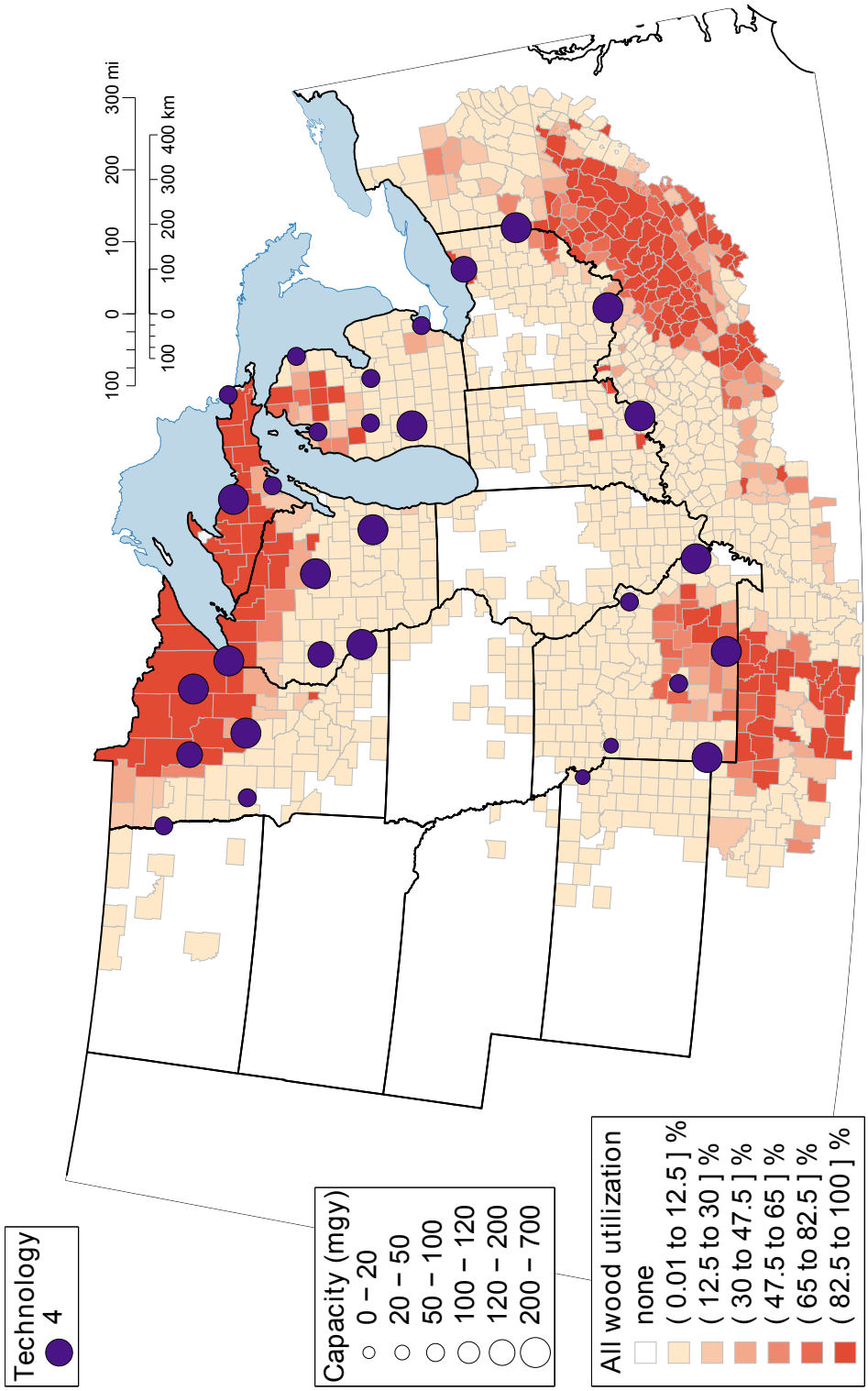

(c) Aggregated forest biomass and wood waste utilization with associated facilities shown. CB ethanol is produced from all wood.

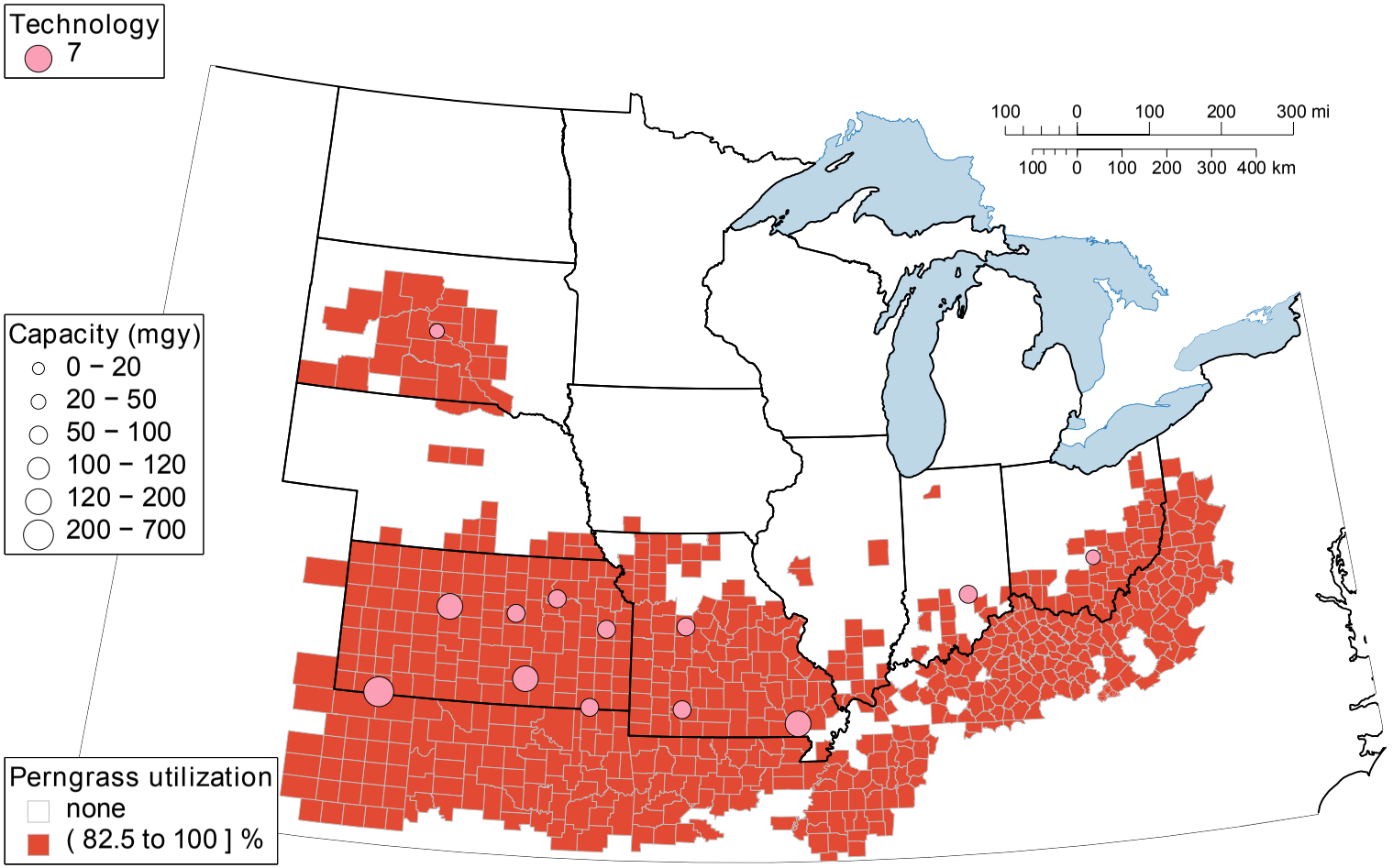

(d) Perennial grass utilization with associated facilities shown. CB ethanol is produced from perennial grasses.

Figure 5.5: Optimum supply chain configuration for the lowest TGHG Pareto point in the case of strict biofuel mandates with fuel credits. Installed facility capacity shown in million gallons per year (mgy). Renewable fuel (RF), advanced biofuel (AB) and cellulosic biofuel (CB) are produced.

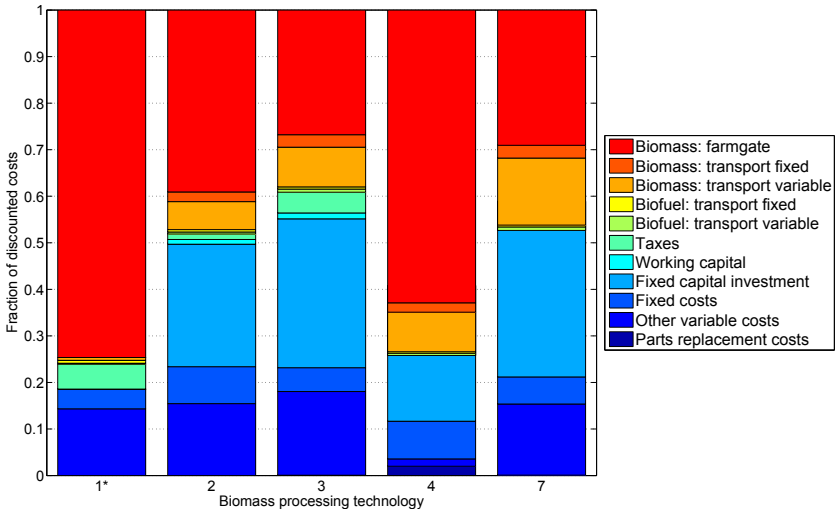

Figure 5.6: Breakdown of cost sources for installed technologies for the lowest TGHG Pareto point in the case of strict biofuel mandates with fuel credits. Existing facilities are denoted by an asterisk (*). New facilities of technologies $l = \{5, 6\}$ were not constructed in the optimum supply chain.

The average distribution of discounted costs for each installed technology is shown in Figure 5.6. By examining the breakeven prices for each facility, it was found that all facilities are economical for facility-gate prices of 4.18, 2.28 and 1.74 \$/gal for CB, AB and RF, respectively. Thus, CB costs are 75% higher for this Pareto point than the highest TNPV Pareto point, while the costs of AB and RF are equivalent. The average distribution of emissions is shown in Figure 5.7. Technologies 2, 3 and 7 have lower net emissions than technology 1 in the solution due to lower emission biomass feedstock(s) and emission-negative biorefinery operation (the result of emission credits for coproducts like electricity). Compressor operation in the high pressure gasification of technology 4, along with no turbine installation for possible electricity generation, leads it to have emission-positive biorefinery operation. Technology 4 still has lower emissions than technology 1 due to wood being a lower emission biomass feedstock than corn.

Balanced

The "balanced" Pareto point described here offers large emissions gains for a small loss on profit, compared to the highest TNPV case. This point was chosen by examining

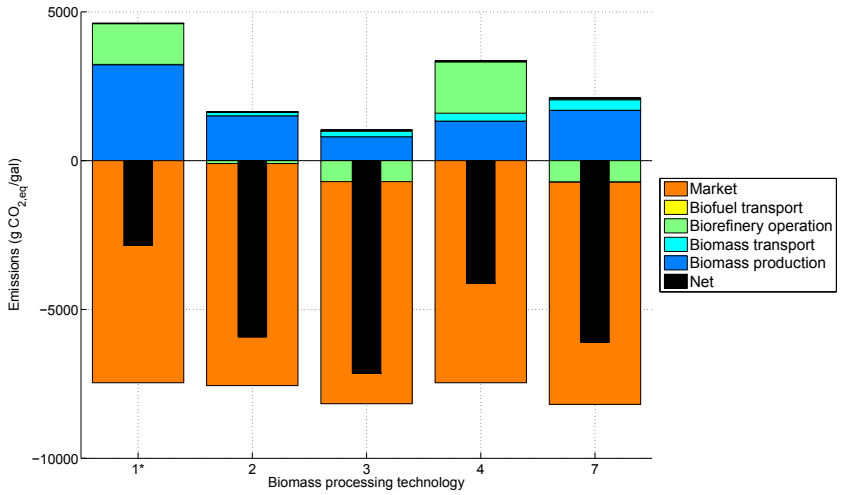

Figure 5.7: Breakdown of emission sources for installed technologies for the lowest TGHG Pareto point in the case of strict biofuel mandates with fuel credits. Net emissions per gallon of produced biofuel is also shown. Existing facilities are denoted by an asterisk (*). New facilities of technologies $l = \{5, 6\}$ were not constructed in the optimum supply chain.

the Pareto Frontier (see Figure 5.3) as a decision maker would. The highest TNPV Pareto point offered TNPV of 19.4 B$ and TGHG of -71.4 M t $CO_{2,eq}$/y, while the lowest TGHG Pareto point offered TNPV of -72.0 B$ and TGHG of -102 M t $CO_{2,eq}$/y. Thus there is an opportunity to reduce biofuel production emissions by nearly half, from the highest TNPV case. Presented here is the Pareto point that captures more than half of those emission reductions, with a TNPV of 11.3 B$ and a TGHG of -87.7 M t $CO_{2,eq}$/y. This Pareto point was found in 7.6 hours with a 0.50% gap and is shown in Figure 5.8. Three of the seven technologies are installed by developing 60 of the 98 candidate sites, with a total of 161 facilities producing RF (11,900 M gal/y), 43 producing AB (5,600 M gal/y) and 15 producing CB (3,000 M gal/y). Just enough CB is produced to satisfy the mandate, but excess AB is produced and sold as the lower classification (RF). This offsetting of some RF (produced from corn grain) with AB (produced from in an integrated process that utilizes corn and corn stover) is what gives this Pareto point improved emissions.

The average distribution of discounted costs for each installed technology is shown in Figure 5.9. By examining the breakeven prices for each facility, it was found that all facilities are economical for facility-gate prices of 2.47, 2.23 and 1.71 $/gal for CB,

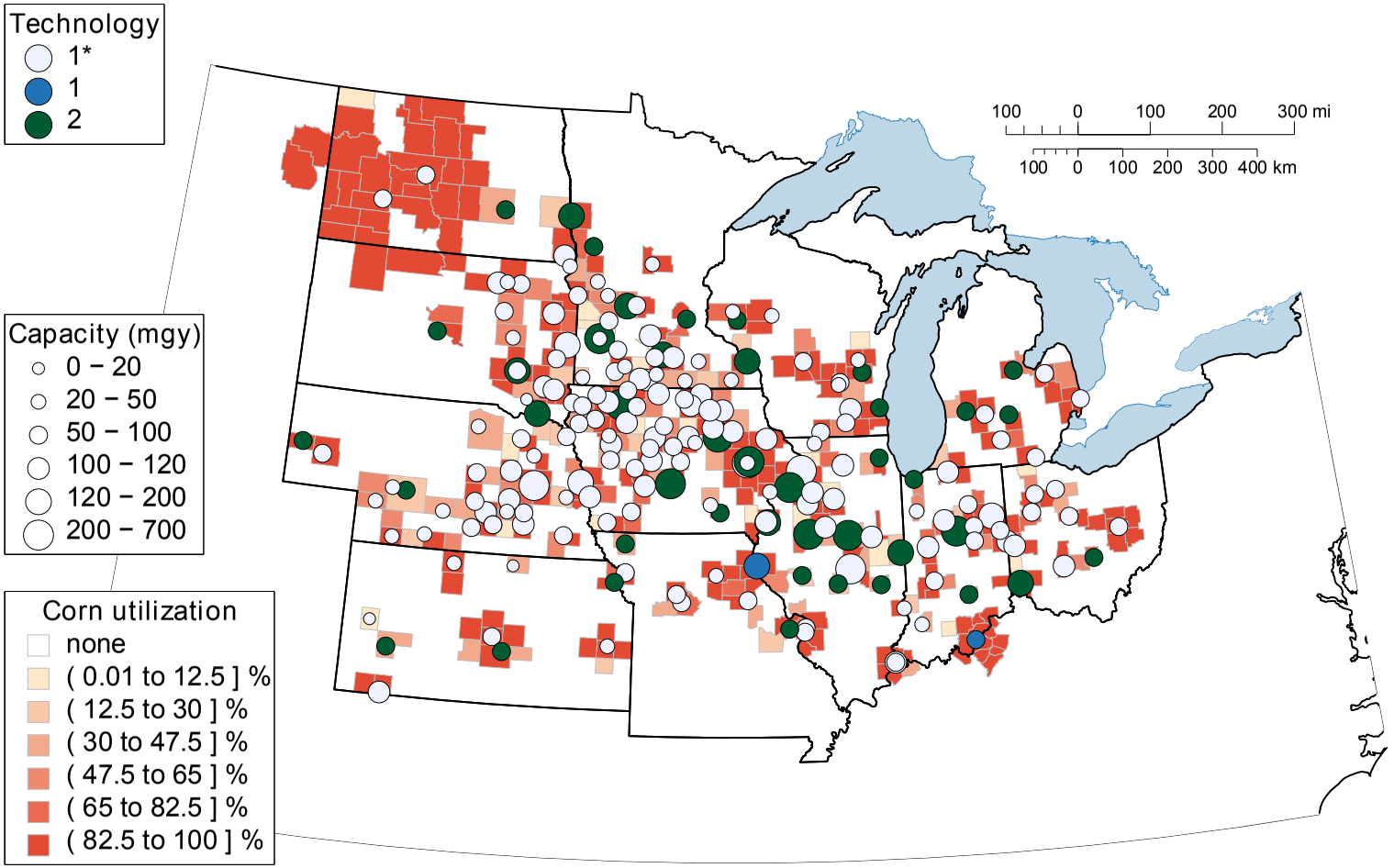

(a) Corn grain utilization with corn-utilizing facilities shown. RF and AB ethanol are produced from corn using technology 1 and 2, respectively. Existing facilities are denoted with an asterisk (*). Maximum corn utilization is 34%.

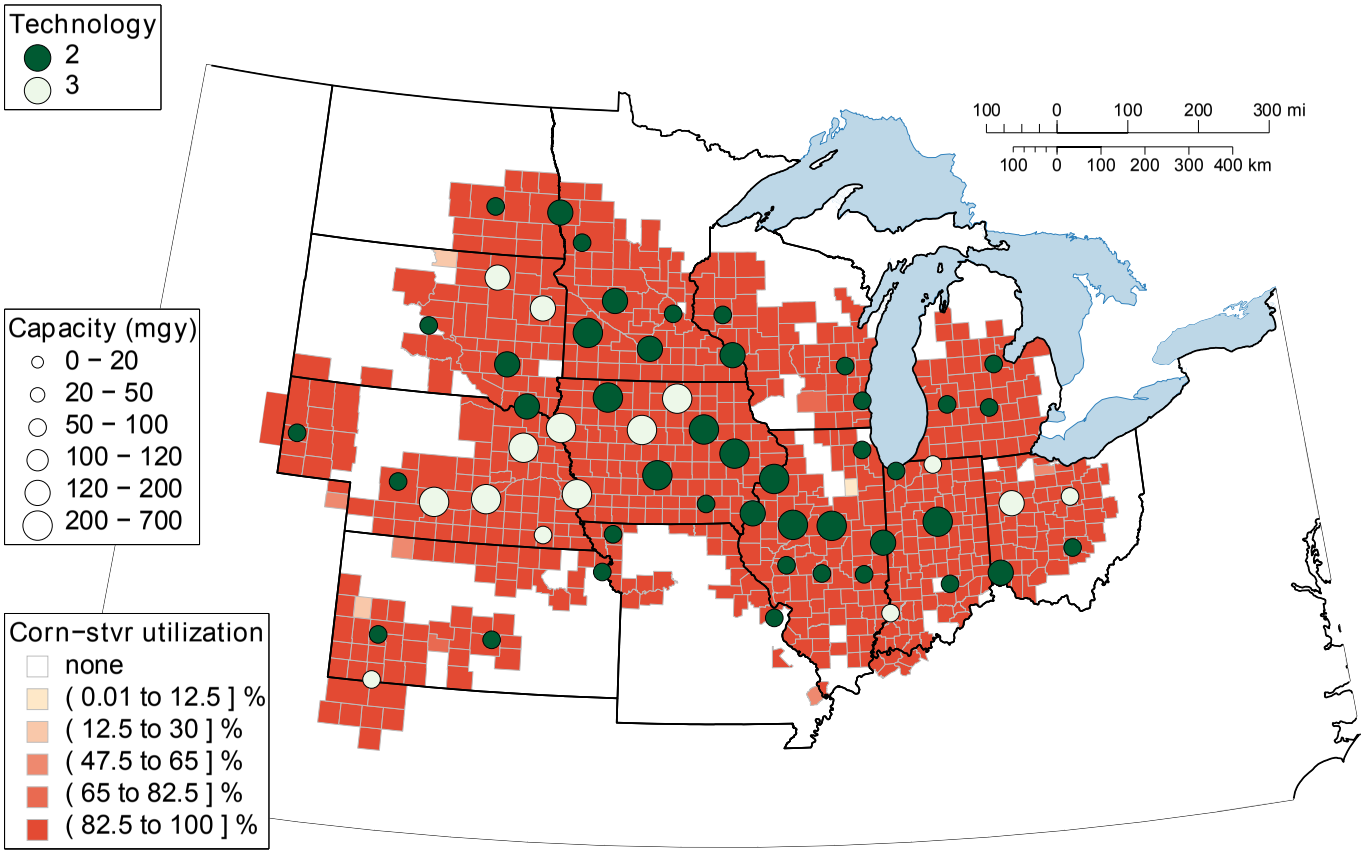

(b) Corn stover utilization with associated facilities shown. AB and CB ethanol, and CB naphtha & diesel are produced from corn stover.

Figure 5.8: Optimum supply chain configuration for the "Balanced" Pareto point in the case of strict biofuel mandates with fuel credits. Installed facility capacity shown in million gallons per year (mgy). Renewable fuel (RF), advanced biofuel (AB) and cellulosic biofuel (CB) are produced. Forestry resources and perennial grasses were available but were not utilized in the optimum supply chain.

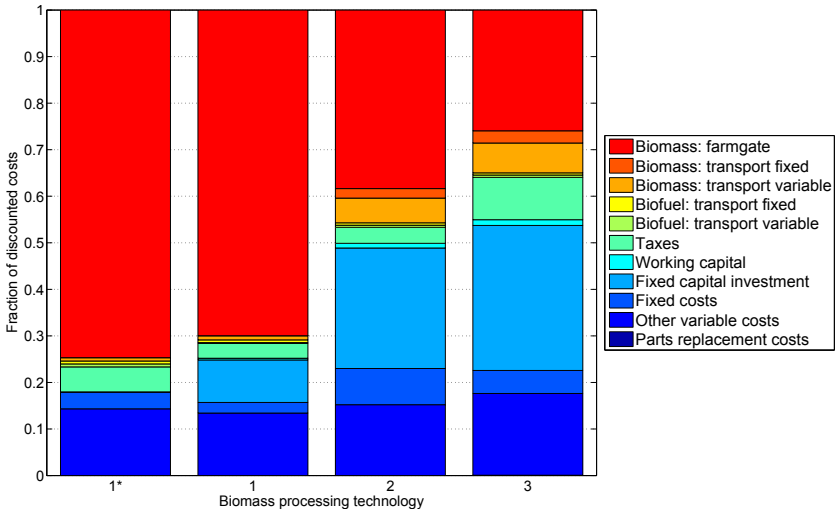

Figure 5.9: Breakdown of cost sources for installed technologies for the "Balanced" Pareto point in the case of strict biofuel mandates with fuel credits. Existing facilities are denoted by an asterisk (*). New facilities of technologies $l = \{4, 5, 6, 7\}$ were not constructed in the optimum supply chain.

AB and RF, respectively. Thus, the biofuels prices are at most only 0.10 \$/gal higher than in the Pareto point with highest TNPV. The average distribution of emissions is shown in Figure 5.10. As expected, the emissions distribution for technologies 1, 2 and 3 are similar to what was found in the other Pareto points, however there are small differences in the transportation emissions.

5.8 Conclusions

This chapter proposed a multiobjective mixed integer linear program to determine biofuel supply chain configurations that are Pareto optimal for profit and emissions. It was applied to the Midwestern U.S. 2015 case study introduced in Chapter 4 to determine facility location, capacity and technology selection. Pareto Frontiers were found for the two case studies of strict RFS mandates and no mandates. In the strict mandates case study, it was found that the lowest TGHG Pareto point offers an additional 50% reduction in emissions compared to the highest TNPV Pareto point. Unfortunately, the lowest TGHG Pareto point corresponds with a large negative TNPV. One of the Pareto points showed that half of these emission reductions are obtainable by shifting some renewable fuel production to advanced biofuel technologies, with biofuel prices

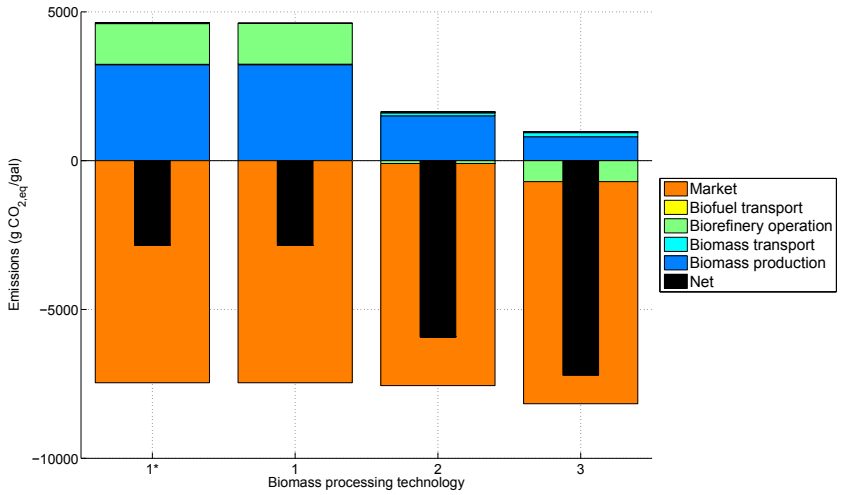

Figure 5.10: Breakdown of emission sources for installed technologies for the "Balanced" Pareto point in the case of strict biofuel mandates with fuel credits. Net emissions per gallon of produced biofuel is also shown. Existing facilities are denoted by an asterisk (*). New facilities of technologies $l = \{4, 5, 6, 7\}$ were not constructed in the optimum supply chain.

only 0.10 \$/gal higher than in the Pareto point with highest TNPV.

CHAPTER 6

Automated Generation and Optimal Selection of Biofuel-Gasoline Blends and Their Synthesis Routes*

6.1 Summary

Biomass can be converted into a plethora of compounds through different chemical transformations, thus leading to a complex network of possible synthesis steps. In this work, we propose a novel strategy that simultaneously identifies (a) the most desirable biomass-derived products for an application of interest, and (b) the corresponding synthesis routes. The strategy consists of i) constructing an exhaustive network of reactions consistent with an input set of chemistry rules and ii) using the network information to formulate and solve an optimization problem that yields an optimal product distribution and the sequence of reactions that synthesize them. We use this strategy to identify potential renewable oxygenates and hydrocarbons obtained from heterogeneous catalysis of biomass that can be blended with gasoline to satisfy ASTM specifications. Multiple objectives (energy loss, catalyst requirement and absolute heat duty) are considered and multiple alternative solutions are found in each case. We identified that both oxygenates and hydrocarbons are components of optimal blends for the energy loss objective, but the other two objectives produce only oxygenates. The proposed strategy is flexible

*Reprinted with permission from W. Alex Marvin, Srinivas Rangarajan, and Prodromos Daoutidis, *Energy & Fuels*, 27(6):3585–3594, 2013 [22].

enough to be applicable for any problem involving concurrent product and chemistry selection.

6.2 Introduction

Ethanol, produced from sugar and cellulose, is currently the predominant biomass-derived compound blended into gasoline. Ethanol, however, has several disadvantages as a fuel: its heating value is about 70% of that of gasoline, it is miscible in water, and ethanol-gasoline blends have a higher vapor pressure than unblended gasoline. Several oxygenates have therefore been proposed as potential alternative gasoline blend components, including higher alcohols such as 1-butanol and furans such as dimethylfuran (DMF) [130]. These molecules have been shown to be synthesized from cellulose and sugars through biochemical [131,132] and thermochemical routes [14,133]. Furthermore, catalytic routes have also been identified to produce hydrocarbons such as C_8 olefins and alkanes from biomass [134]. Indeed, the network of all possible reactions that can upgrade biomass to fuels is large and complex. Consequently, there are several potential biomass-derived compounds that can be blended with gasoline, and multiple chemical routes may exist to synthesize each one of them. This leads to two related problems: (a) the identification of optimal feasible biofuel-gasoline blends in terms of techno-economic objectives, and (b) the selection of efficient synthesis routes to produce renewable blend components in terms of kinetics, thermochemistry, selectivity, etc.

A number of computer-aided molecular design (CAMD) methods have been proposed to identify compounds for specific applications (fuels, solvents, polymers, and refrigerants). These include (a) "generate and test" explicit enumeration of molecules constructed from an allowed list of molecular groups [135], (b) evolutionary strategies to intelligently search the compound space [136], (c) inverse design strategies based on signature molecular descriptors [137,138], and (d) rigorous optimization [139–141]. These methods are computationally tractable while still being exhaustive in their search to identify the most desirable set of compounds for the chosen application. They, however, do not explicitly account for the feasibility of chemical synthesis of the particular compound. Molecular structural constraints can in principle be imposed in optimization-based approaches using available chemistry knowledge, however, this still cannot accurately capture the diversity of synthesis options. A method that explicitly takes into

account the synthesis feasibility was proposed and applied to identifying promising biofuels and their production routes by Marquardt and co-workers [142,143]. A network of biomass conversion reactions was first assembled from the literature. Then, the physical properties of each of the species in the network was calculated to identify those with satisfactory fuel properties. A pathway search then identified possible routes to synthesize the target compounds. The reaction network, in this method, was constructed manually and therefore was limited in size and not exhaustive in terms of accounting for all plausible reactions.

In this paper, we propose and apply a scalable strategy to identify optimal gasoline blends and synthesis routes to produce the renewable additives from biomass. The strategy involves combining rule-based network generation to construct an exhaustive network of reactions that upgrade biomass, with the formulation of a Mixed Integer Linear Programming (MILP) problem to identify the mix of renewable additives (to be blended with gasoline) and their synthesis routes from biomass that is optimal on the basis of thermochemistry, kinetics or economics. We specifically consider heterogeneous catalytic routes to convert biomass into oxygenates and hydrocarbons, while ensuring that the gasoline blends identified satisfy all ASTM specifications.

6.3 Product and chemistry selection strategy

Figure 6.1 shows the workflow of the strategy adopted. First, RING [144,145], a rule-based network generator developed in our group is used to construct the reaction network pertaining to upgrading biomass-derived platform oxygenates. Second, an optimization module accepts the generated network, thermochemistry of the species and kinetics of reactions in the network, and physical properties of possible products, and formulates a MILP with ASTM fuel specfications as constraints. The output of the optimization module is a list of alternative blends *and* synthesis routes that can then be explored manually. Below, we discuss these two steps in detail.

6.3.1 Reaction network construction

The inputs into RING for generating the reaction network include: (a) initial reactants, and (b) reaction rules describing the chemistry. The underlying principle of rule-based network generation is the recursive application of reaction rules to initial reactants and new species generated subsequently, until all possible reactions and species have been

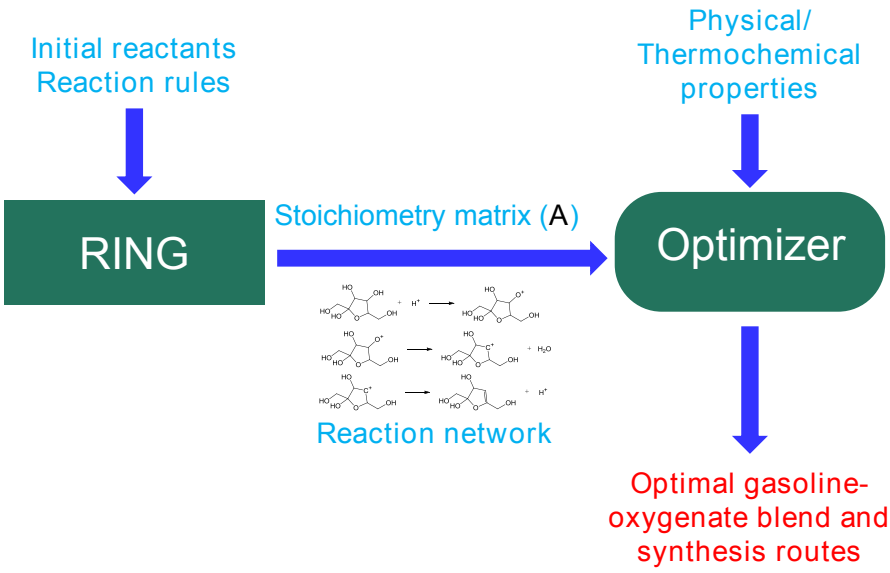

Figure 6.1: Proposed strategy for connecting automated network generation and optimization.

generated. RING thus generates an exhaustive network of reactions consistent with the specified rules from the initial reactants. For this work, the 14 oxygenates shown in Figure 6.2 were used as initial reactants. These compounds (other than hydrogen and water) were recognized as potential biomass-derived platform chemicals in a U.S. DOE report [2] and a subsequent study [146]. The reaction rules used herein are given in the Supporting Information, along with representative examples of the corresponding reactions. These rules correspond to heterogeneous acid, base, and metal catalysis comprising of C-C bond formation (e.g. aldol condensation, oligomerization, ketonization), removal of oxygen (e.g. dehydration, hydrogenolysis, esterification), atom/bond rearrangement (e.g. isomerization, cyclization), and saturation (hydrogenation). RING was constrained to limit the size of the molecules generated to have less than 10 heavy atoms (atoms other than hydrogen). Further, all rules were restricted to be applied only to those molecules that were generated in fifteen or fewer steps. The generated network had 8178 reactions and 2895 molecules including hydrocarbons and oxygenates.

The thermochemistry of all species was calculated on-the-fly using RING. Enthalpy, entropy, and free energy of formation at a given temperature for molecules in gas phase were estimated using the group additivity method [147–150]. The low heating value

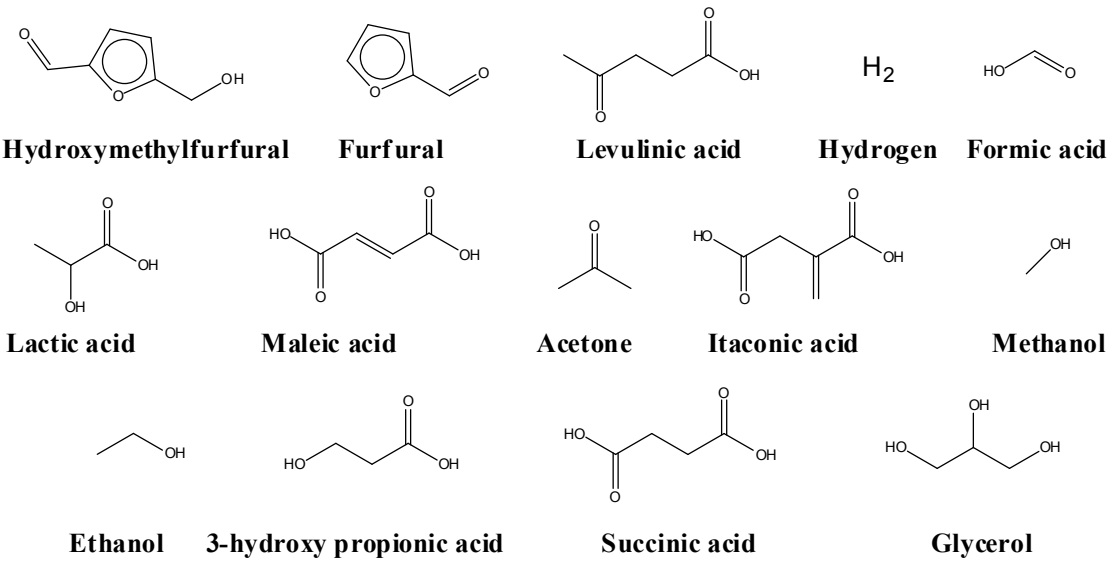

Figure 6.2: Initial reactants input into RING.

of oxygenates were taken from the literature [130], while that of hydrocarbons was estimated using the heat of formation values obtained using RING. Figure 6.3 shows a parity plot comparing the experimental and estimated values of the heat of formation or reaction for a dataset of 50 compounds and reactions. The compounds included are representative of the generated reaction network, and includes oxygenates and hydrocarbons up to 9 heavy atoms (the complete data are given in the Supporting Information). It can be seen that RING-estimated values are reasonably accurate.

Representative values of reaction rates were calculated for each rule from data reported in the literature. Specifically, a reported kinetic rate expression and the associated kinetic rate constants, activation energies, and equilibrium constants were identified for each rule and the maximum initial reaction rate at a given temperature and overall reactant composition was calculated. A uniform temperature of 500 K and overall gas phase reactant concentration of 1 mol/lit was used for all the calculations (see the Supporting Information for details). For each reaction in the network, the rate was assumed to be equal to the representative value of the underlying rule. This assumption is reasonable for two reasons. First, the representative values have been calculated for reactions with molecules of similar size and shape (linear, branched, or cyclic) as those in the network. Second, the representative values capture the relative rates of different rules well and hence can be used to compare and contrast multiple synthesis routes with

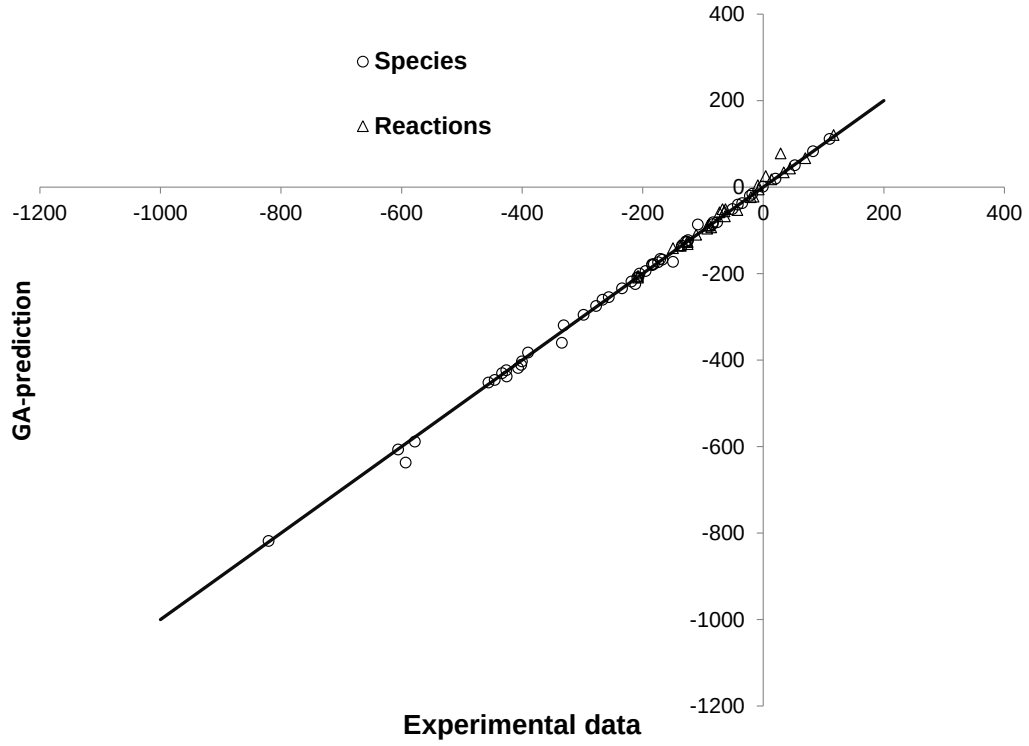

Figure 6.3: Parity plot of experimental and predicted heat of formation and reaction values of a representative set of hydrocarbons and oxygenates. All values are in kJ/mol. Prediction is based on group additivity method in RING. See Supporting Information for more details.

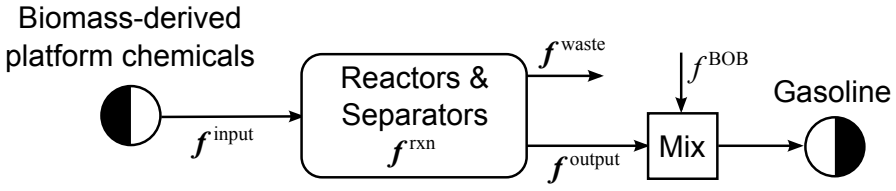

Figure 6.4: Chemical process envisioned to convert biomass-derived platform chemicals to gasoline. The decision variables for the optimization problem are shown.

different chemistries.

6.3.2 Optimization framework

The optimization framework focuses on a chemical process that will produce and mix gasoline blend components with Blendstock for Oxygenate Blending (BOB) to make gasoline, as shown in Figure 6.4. One particular BOB is considered due to data availability (BOB 2 from Christensen et al. [130]), which is intended for blending of 10 %vol ethanol to produce volatility class AA (lowest maximum allowable vapor pressure) gasoline for hot weather areas. The optimization problem is to determine the optimal inputs, reaction fluxes and blend composition, such that ASTM gasoline requirements are satisfied. Note that the Reactors and Separators section of the chemical process could be designed to perform any number of the 8178 reactions from the generated reaction network. Similarly, any number of the 2895 molecules from the reaction network could be used as input, waste or output. The decision variables for the optimization problem are the flowrates (in mol/min) of input ($\boldsymbol{f}^{\text{input}} = \{f_i^{\text{input}}\}$), waste ($\boldsymbol{f}^{\text{waste}} = \{f_i^{\text{waste}}\}$), output ($\boldsymbol{f}^{\text{output}} = \{f_i^{\text{output}}\}$) and BOB ($f^{\text{BOB}}$), and the flux (in extent/min) for each reaction ($\boldsymbol{f}^{\text{rxn}} = \{f_j^{\text{rxn}}\}$).

6.3.3 Objective functions

A number of objective functions (e.g. cost, environmental impact, efficiency) can be formulated to select for desirable chemical processes. This paper will present results for three objective functions (energy loss, catalyst requirement and heat duty), but a number of others (e.g. input cost, revenue, separability) could be constructed, if the required data were available.

Minimization of energy loss (ΔE) is an important objective, as it was found to be a better indicator of investment cost than even the facility size for a dataset of fuel and

chemical manufacturing plants [151]. In the paper, a regression was determined that equates investment cost (in million 1993 US$) with $3 \cdot (\Delta E)^{0.84}$, where ΔE (in MW) is the difference between the low heating values of the inputs (feed and fuel) and the product stream leaving the plant. Thermodynamics require that $\Delta E \geq 0$, and so the investment cost is a monotonically increasing function of ΔE. Thus, minimization of ΔE is equivalent to minimizing investment cost. The energy loss of the chemical process is:

$$\Delta E = \sum_i \Delta H^{\circ}_{\mathrm{c,i}} \cdot \left(f_i^{\mathrm{input}} - f_i^{\mathrm{output}} \right) \tag{6.1}$$

where $\Delta H^{\circ}_{\mathrm{c,i}}$ is the heat of combustion (low heating value) for molecule i.

Minimization of catalyst requirement R^{cat} is a useful objective to reduce catalyst costs and avoid slow reactions, which may require large reactors or high residence times. With the estimated reaction rates r_j (in extent/(min·$\mathrm{g_{cat}}$)) for each reaction j, the catalyst requirement is:

$$R^{\mathrm{cat}} = \sum_j \frac{f_j^{\mathrm{rxn}}}{r_j} \tag{6.2}$$

Minimization of absolute heat duty H^{abs} reduces the costs of heat transfer, by favoring energetically neutral reactions. This could lead to reductions in operating (e.g. less fuel and cooling water) and capital (e.g. smaller heat exchangers) expenses for utilities. The absolute heat duty for the chemical process is:

$$H^{\mathrm{abs}} = \sum_j \left| \Delta H_j^{\mathrm{rxn}} \right| \cdot f_j^{\mathrm{rxn}} \tag{6.3}$$

where $\Delta H_j^{\mathrm{rxn}}$ is the heat of reaction j calculated from the heat of formation values for each species in the reaction network.

In this chapter, we will consider each of the above objective functions separately, solving a single-objective optimization problem. However, a multiobjective optimization problem could also be formulated [111]. A weighted (aka agglomerated) approach could be used to combine objective functions into one, based on their relative importance. Non-dominated (Pareto) points could also be found by solving for one objective function, while constraining the others by an upper bound (ε-constraint method). In both of these cases, the multiobjective problem is simply reformulated in terms of single-objective problems.

6.3.4 Constraints

The steady-state molar balance around the Reactors and Separators section of the chemical process is:

$$f_i^{\text{input}} + \sum_j A_{i,j} \cdot f_j^{\text{rxn}} - f_i^{\text{waste}} - f_i^{\text{output}} = 0 \tag{6.4}$$

where $A_{i,j}$ is the stoichiometric coefficient of molecule i in reaction j in the reaction network.

Gasoline production of 1 g/min is taken as a basis:

$$M^{\text{BOB}} \cdot f^{\text{BOB}} + \sum_i M_i \cdot f_i^{\text{output}} = 1 \tag{6.5}$$

where M^{BOB} and M_i are the molecular weights of the BOB and molecule i, respectively. The molecular weight of the BOB is assumed to be 110 g/mol.

During network generation, reactions are identified that (i) must occur together or (ii) are related such that if the reaction occurs, some other reaction(s) must also occur. These two cases will be refered to as *joint* and *transform* sets of reactions, respectively, and they are accounted for in the optimization formulation. Joint sets of reactions (indexed by l) are defined by $\mathbf{J}_l^{\text{joint}} \subset \mathbf{J}$, which is the subset of reactions that must occur simultaneously. This is enforced by the constraint:

$$f_j^{\text{rxn}} = \frac{r_j}{r_{j^\star}} \cdot f_{j^\star}^{\text{rxn}}, \quad \forall\, l,\ j \in \mathbf{J}_l^{\text{joint}},\ j \neq j^\star \tag{6.6}$$

where $j^\star$ is the first reaction in joint set l. Note that if the reaction rates are equal, all reactions in a joint set will have equal reaction flux.

This set of constraints is equivalent (i.e. the two sets of equations share the same null basis) to:

$$f_j^{\text{rxn}} = \frac{r_j}{\sum_{j\prime \in \mathbf{J}_l^{\text{joint}}} r_{j\prime}} \cdot \sum_{j\prime \in \mathbf{J}_l^{\text{joint}}} f_{j\prime}^{\text{rxn}}, \quad \forall\, l,\ j \in \mathbf{J}_l^{\text{joint}} \tag{6.7}$$

which may be a more intuitive relation for reactions that occur simultaneously. Equation (6.6) is more efficient for optimization though, as it involves fewer (and more sparse) constraints.

An example of a joint set of reactions is the dehydration of a diol molecule (e.g. see Figure 6.5) – the reaction network will have two reactions that deydrate the alcohol

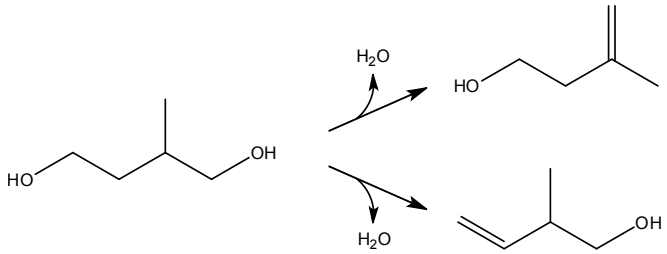

Figure 6.5: An example of reactions that must occur together – the dehydration of a diol molecule. These two reactions are $j = \{2396, 2397\}$ in the reaction network.

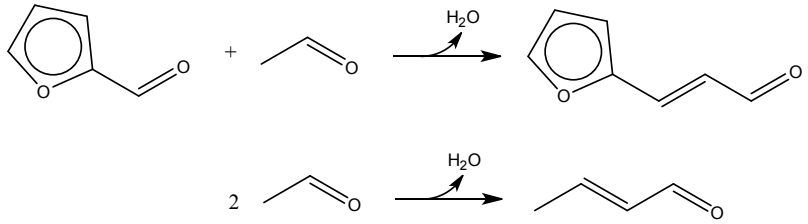

Figure 6.6: An example of reactions which are related such that if the reaction occurs, some other reaction(s) must also occur. If the top reaction (an aldol condensation) occurs, the bottom reaction (a self-condensation) must also occur, because the reactant molecule (acetaldehyde) can undergo self-condensation. These two reactions are $j = \{59, 62\}$ in the reaction network.

groups separately, but in practice both reactions will occur together with selectivity that depends on the relative reaction rates. This example joint set contains two reactions, but in general the joint sets may contain any number of reactions. In total, there are 1745 joint sets with each set involving between 2 and 16 reactions.

Transform sets of reactions are handled easily by editing the stoichiometry of the reactions. If a subset of reactions $\mathbf{J}_j^{\text{transform}} \subset \mathbf{J}$ also occur if reaction j occurs, then the stoichiometry of those reactions can be added to that of reaction j.

An example of a transform set of reactions is aldol condensation, where one of the molecules can undergo self-condensation (e.g. see Figure 6.6). In this case, the self-condensation reaction must occur if the aldol condensation reaction occurs. In total, there are 629 transform sets with each set involving between 2 and 3 reactions.

The 8 blend properties considered are anti-knock index (AKI), low heating value (LHV), oxygen content, water absorption, Reid vapor pressure (RVP) and three batch distillation temperatures (T_{10}, T_{50}, T_{90}). Octane rating is measured here using AKI,

equal to (RON+MON)/2, but both the research octane number (RON) and motor octane number (MON) are calculated and presented. All properties are predicted using linear mixing rules. This assumes that all the blended gasoline properties are proportional to the amount (volume, mass or mole fraction) of each component and BOB (taken as a single component). For RVP, T_{10}, T_{50}, and T_{90} of BOB-oxygenate blends, experimental data reported McCormick and co-workers [130, 152] show a linear dependence on volume fraction of the blend component up to 10 %vol. They also report that the octane rating of the blends follow linear mixing rules based on mole fraction of pure components (gasoline taken as a single component) in line with an earlier study [153]. Although the data reported is for binary mixtures (assuming BOB is a single component), we have assumed these mixing rules hold for multi-component blends (multiple oxygenates with a BOB). This assumption should be sufficiently accurate in this case, as the blend components are expected to be at low concentrations. In fact, the BOB is normally intended to be blended with 10 %vol ethanol. The minimum and maximum blend specifications, shown in Table 6.1, are enforced by

$$S_k^{\min} \cdot \left(f^{\mathrm{BOB}} + \sum_i f_i^{\mathrm{output}} \right) \leq P_k^{\mathrm{BOB}} \cdot f^{\mathrm{BOB}} + \sum_i P_{i,k} \cdot f_i^{\mathrm{output}}, \quad \forall\, k \in \mathbf{K} \tag{6.8}$$

$$S_k^{\max} \cdot \left(f^{\mathrm{BOB}} + \sum_i f_i^{\mathrm{output}} \right) \geq P_k^{\mathrm{BOB}} \cdot f^{\mathrm{BOB}} + \sum_i P_{i,k} \cdot f_i^{\mathrm{output}}, \quad \forall\, k \in \mathbf{K} \tag{6.9}$$

where $\mathbf{K}$ is the set of blend properties. BOB and each blend component contribute P_k^{BOB} and $P_{i,k}$, respectively, to the blend property. These are, therefore, the effective pure component property. For example, a blend that is entirely BOB will have properties equal to P_k^{BOB}.

The molecular inputs are limited to the set ($\mathbf{I}^{\mathrm{input}}$) of biomass-derived platform chemicals shown in Figure 6.2, with the addition of water. Similarly, the outputs are limited to the set ($\mathbf{I}^{\mathrm{output}}$) for reasons of data availability:

$$f_i^{\mathrm{input}} = 0, \quad \forall i \notin \mathbf{I}^{\mathrm{input}} \tag{6.10}$$

$$f_i^{\mathrm{output}} = 0, \quad \forall i \notin \mathbf{I}^{\mathrm{output}} \tag{6.11}$$

Experimental data from McCormick and co-workers [130, 152] for the blending of 11 oxygenate molecules with BOBs was available, and was used to determine the blend property parameters P_k^{BOB} and $P_{i,k}$. As discussed earlier the experimental data for

Table 6.1: Blend properties and required specifications

k	Property description	Unit	$S_k^{\min}$	$S_k^{\max}$
1	anti-knock index (AKI)	-	87	-
2	low heating value (LHV)	kJ/mL	30	33
3	oxygen content	wt%	-	3.7%
4	water absorbed by gasoline phase at saturation	wt%	-	5%
5	Reid vapor pressure (RVP)	kPa	-	54
6	distillation temp for T_{10}	°C	-	70
7	distillation temp for T_{50}	°C	77	121
8	distillation temp for T_{90}	°C	-	190

RVP and distillation temperatures of BOB-oxygenate blend varies linearly with volume fraction of the blend component; this linear trend was extrapolated to get the effective property ($P_{i,k}$) of the pure oxygenate. Experimental values of RON, MON, and LHV values of these molecules were also reported and were directly taken for this study. Properties for 4 additional oxygenate molecules were estimated from their structural isomer present in the original dataset. The data for 1-pentanol was used to estimate properties for 2-pentanol and 3-pentanol, and the data for 3-methyl-1-butanol was use to estimate properties for 2-methyl-1-butanol and 3-methyl-2-butanol. The total set of 15 oxygenate molecules is shown in Figure 6.7.

Group contribution methods were used to estimate the AKI and LHV property parameters for 157 hydrocarbon molecules, but RVP and the distillation temperatures could not be estimated. AKI values were estimated from RON and MON rules given by Ghosh et al. [154] for hydrocarbons depending on carbon number and type (paraffins, olefins, iso-paraffins, iso-olefins, naphthenes, and aromatics - collectively referred to as PIONA). LHV of a hydrocarbon is calculated from group addivity-based estimation of heat of combustion of that compound by assuming that the products of the combustion reaction (carbon monoxide and water) are in gaseous phase at 298 K. These hydrocarbons were identified in the reaction network by searching for PIONA compounds with eight or less carbons.

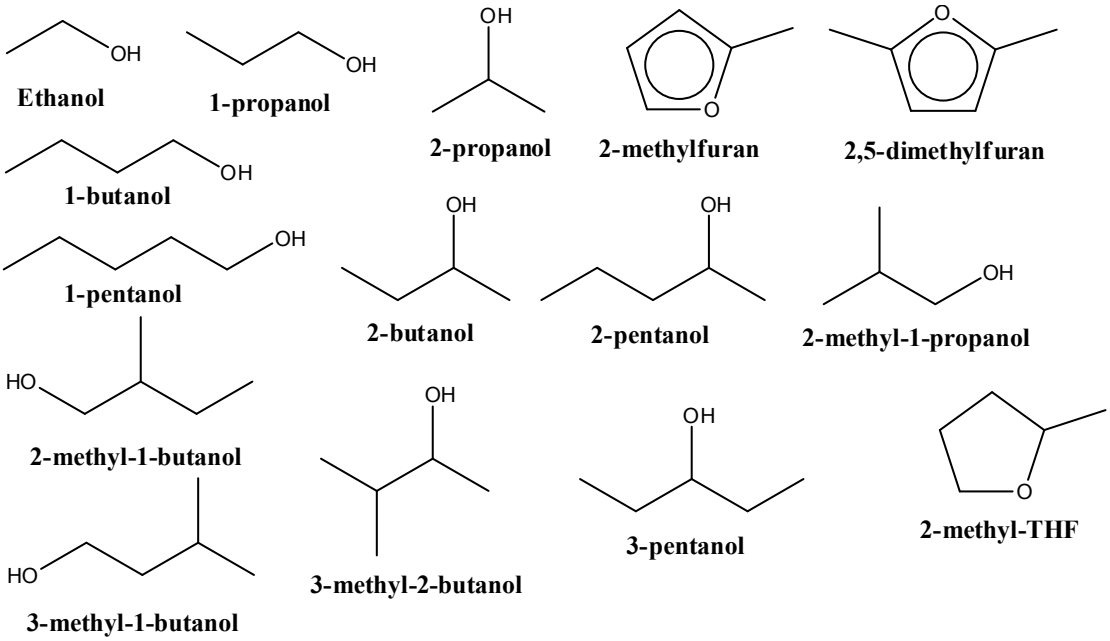

Figure 6.7: The 15 oxygenate molecules that are allowed outputs.

6.3.5 Optimization program and solution strategy

The linear program to find the optimal synthesis chemistry and blend composition is then:

$$\begin{aligned} &\text{minimize} && Z \\ &\text{subject to} && \text{equations (6.4)–(6.6), (6.8)–(6.11)} \end{aligned} \tag{LP}$$

where the objective function Z is either energy loss ΔE, catalyst requirement R^{cat} or absolute heat duty H^{abs}.

It is expected that there will be a large number of alternative solutions to (LP) with equal or nearly equal performance as the optimal solution. Enumerating these solutions is important, as they identify different blend compositions or different synthesis chemistry that are worth further investigation. Due to the nature of (LP), a linear interpolation between the alternative solutions is also optimal. An algorithm proposed by Lee et al. [155] was implemented to enumerate the alternative solutions. It involves introducing binary variables to (LP) that indicate which of the decision variables are non-zero. The resulting mixed integer linear program (MILP) is then solved iteratively, while adding integer cuts to avoid repeating previous solutions.

One advantage of the algorithm is that the introduced binary variables can easily be used to avoid reaction cycles, a major source of degeneracy in solutions to (LP). Note that the binary variables w_j^{rxn} indicate if each reaction is non-zero, due to

$$f_j^{\text{rxn}} \leq U \cdot w_j, \quad \forall\, j \tag{6.12}$$

where U is an upper bound.

Each cycle, indexed by m, is then defined by a subset of reactions $\mathbf{J}_m^{\text{cycle}}$. Cycles are avoided by requiring that at least one of the reactions in the cycle is forced to have zero flux. This is enforced by

$$\sum_{j \in \mathbf{J}_m^{\text{cycle}}} w_j \leq |\mathbf{J}_m^{\text{cycle}}| - 1, \quad \forall\, m \tag{6.13}$$

where $|\mathbf{J}_m^{\text{cycle}}|$ is the of number of reactions in the reaction cycle (i.e. ordinality of the set).

Avoiding cycles in solutions thus requires knowledge of the cycles present in the reaction network. Enumerating these cycles can be a challenge. Note that 2–reaction cycles are easily identified by searching for the negative stoichiometry of each reaction. Larger cycles can be identified by iteratively solving a linear program similar to (LP) that maximizes the sum of the w_j, while the inputs, outputs and waste is set to zero. Each solution of such a linear program will then identify one cycle. This reaction cycle enumeration algorithm is described in more detail in the Supporting Information.

The MILP to find alternative solutions, while avoiding reaction cycles, is then

$$\begin{aligned} &\text{minimize} && Z \\ &\text{subject to} && \text{equations (6.4)–(6.6), (6.8)–(6.13)} \end{aligned} \tag{MP}$$

where some additional constraints from the algorithm to enumerate the alternative solutions [155] are not shown for simplicity, but are discussed in the Supporting Information.

6.4 Results: gasoline blend alternatives

Problem (MP) was coded in GAMS v23.8 and solved using CPLEX v12.4. It has 28,525 variables (11,296 binary) and 17,402 constraints with 93,815 nonzero entries in the model coefficient matrix (0.019% sparsity). Presolving (examining the problem

for logical reduction opportunities with the goal of reducing the problem size before sending to the optimizer) significantly reduces the model size to 7,610 variables (182 binary) and 3,032 constraints with 24,622 nonzeros (0.11% sparsity). Solution time to find each alternative solution was less than 5 sec, with the first 10 alternative solutions normally returned in less than 30 sec. Finding additional alternative solutions requires slightly more time, such that the first 20 and 40 solutions can be found in 1 min and 3.5 min, respectively. The results from two scenarios (oxygenates with and without hydrocarbons) for the energy loss ΔE objective function will be discussed here; the results for the other objective functions are included in the Supporting Information.

6.4.1 Oxygenates

The first scenario considers only the 15 oxygenate molecules shown in Figure 6.7 as allowed outputs (i.e. the set I^{output}). Figure 6.8 displays some of the alternative solutions, with additional information presented in Table 6.2. The first solution (with outputs identified with dashed boxes) produces 2-methylfuran from furfural through successive hydrogenation steps, directly uses ethanol, and blends them with BOB to produce gasoline. Glycerol is used as the hydrogen source, but later solutions indicate that methanol is the next-best hydrogen source. The water gas shift reaction of carbon monoxide and water leads to additional production of hydrogen. Recall that ethanol can be used directly, as it is an allowed input and output. Later solutions suggest producing ethanol instead from lactic acid.

The second solution (with outputs identified with solid boxes) produces 1-propanol and ethanol from lactic acid and blends them with BOB to produce gasoline. Lactic acid decomposition leads to acetaldehyde as the major product which can subsequently be hydrogenated to ethanol. Dehydration of lactic acid produces acrylic acid that can be hydrogenated to 1-propanol. The required hydrogen is provided by glycerol while later solutions propose methanol.

These reactions or similar ones have been reported in the literature. Glycerol and methanol can be used as a hydrogen source. For example, glycerol has been shown to decompose to produce hydrogen and carbon monoxide in vapor phase [156] while methanol has been proposed as an in-situ source of hydrogen for fuel cell applications [157]. Hydrogenation and further hydrogenolysis of furfural to produce 2-methylfuran has been proposed by Resasco and co-workers [158]. Lactic acid decomposition to acetaldehyde and dehydration to acrylic acid have been reported to occur in almost equal selectivity

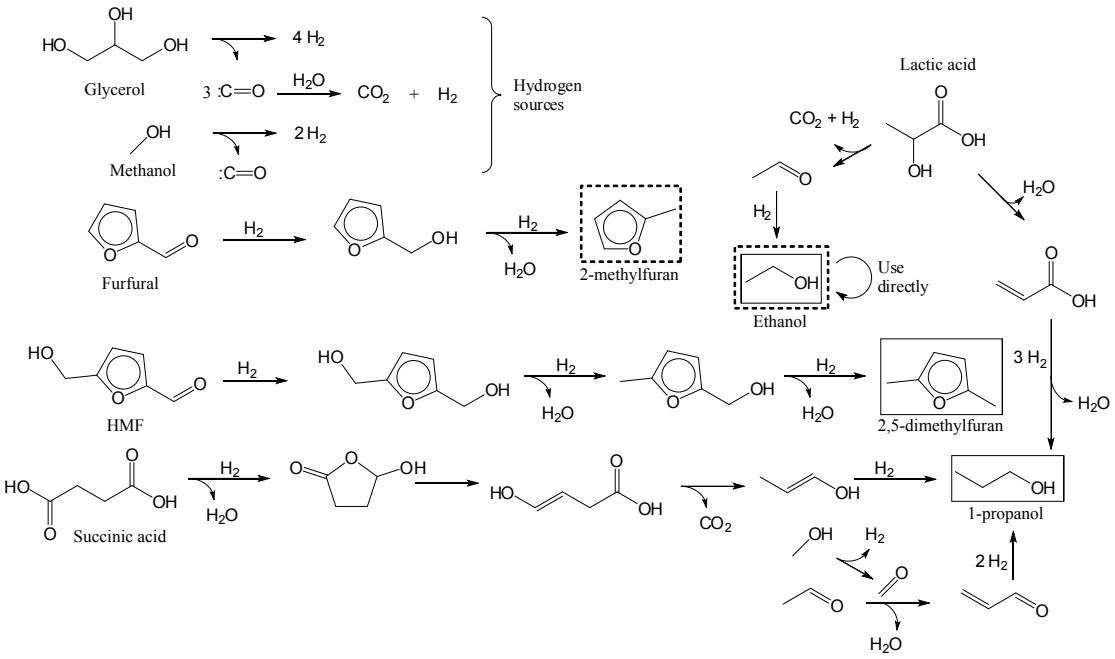

Figure 6.8: Some alternative solutions of (MP) with $Z = \Delta E$ when the set of allowed outputs are 15 oxygenate compounds.

on heterogeneous catalysts [159, 160]. Alcohols are common hydrogenation products of acids.

Table 6.2 shows the specific inputs, wastes, outputs and blend properties for each alternative solution. Note that the compositions of inputs (feedstock) and ouputs (blended gasoline) differs greatly between the two solutions. On the other hand, the physical properties of the resulting blends are similar. This highlights the importance of the proposed strategy to address problems where both the feedstock and product composition is entirely unknown, but there are desired product properties. Furthermore, alternative chemistries to synthesize a compound can also be identified with this strategy. Figure 6.8 shows two alternative routes for synthesizing 1-propanol (other than from lactic acid) – one starting with succinic acid, and the other involving ethanol and methanol. Interestingly, while ethanol-methanol condensation is a part of a general class of higher alcohol synthesis scheme called Guerbet synthesis that can occur on metal with metal-oxide bifunctional catalysts [161–163], succinic acid conversion involves a sequence identical to levulinic acid conversion to butene [164].

The limitation of this scenario is that it only has 15 molecules as allowed outputs, due

Table 6.2: Alternative solutions of (MP) with $Z = \Delta E$ when the set of allowed outputs are 15 oxygenate compounds.

		Solution	
		1	2
Input in 10^{-3} mol/min	ethanol	1.0	-
	furfural	0.61	0.40
	HMF	-	0.026
	lactic acid	-	1.45
	glycerol	0.17	0.43
Waste in 10^{-3} mol/min	H_2O	0.087	0.57
	CO_2	0.52	2.0
Output in 10^{-3} mol/min and (wt%)	ethanol	1.0 (4.58)	0.72 (3.33)
	2-methylfuran	0.61 (4.97)	0.4 (3.32)
	1-propanol	-	0.72 (4.34)
	BOB	8.2 (90.5)	8.0 (89.01)
Blend Property	AKI	87	87
	RON	90.7	90.8
	MON	83.3	83.2
	LHV (kJ/mL)	32	31
	oxygen content (wt%)	2.6	2.9
	water absorption (wt%)	5.0	5.0
	RVP (kPa)	42	41
	T_{10} (°C)	61	62
	T_{50} (°C)	98	94
	T_{90} (°C)	170	169

to availability of experimental data for blend properties. Furthermore, these molecules are all oxygenates, so that the possibility of blending renewable hydrocarbons is not allowed. Such hydrocarbons may be favorable, as they tend to have high energy density and low water solubility. Notice that the two alternative solutions are at the water absorption upper bound of 5%, largely due to ethanol in the blends.

6.4.2 Hydrocarbons and oxygenates

Hydrocarbons are included as allowed outputs in the second scenario by estimating the AKI and LHV property parameters using group contribution methods. However, these methods couldn't be used to estimate the parameters for RVP, T_{10}, T_{50} and T_{90}. Due to the first scenario's solutions having significant slack for these blend properties, it's assumed they can be removed. The remaining blend properties with specifications are AKI, LHV, oxygen content and water absorption.

Figure 6.9 displays some of the alternative solutions generated, with additional information presented in Table 6.3. The first solution (with outputs identified with solid boxes) produces 1-butene from ethanol, directly uses ethanol, and blends them with BOB to produce gasoline. Again, the required hydrogen is provided by glycerol, but some later solutions use methanol instead. The second solution is similar, but produces gasoline that contains only 1-butene and BOB. The third solution produces 1-butene from ethanol, 1-propanol from lactic acid, directly uses ethanol, and blends them with BOB. The fourth solution (with outputs identified with dashed boxes) produces ethanol, 1-butene and 2-pentene from lactic acid, and blends them with BOB. Note that producing 1-propanol from succinic acid instead of lactic acid, is observed in later solutions.

Ethanol conversion to 1-butanol is an example of Guerbet synthesis [161–163]. Dehydration of alcohols to alkenes has been studied extensively in the heterogeneous catalysis literature [165, 166]. 1-butene synthesis from lactic acid is different from above only in the step that produces acetaldehyde. 2-pentene from lactic acid involves dehydration to acrylic acid which is followed by ketonization of the acid. Dumesic and co-workers have shown that acids can be coupled together through ketonization to get a ketone over base catalysts [167]. The ketones thus formed are all converted into 3-pentanol as shown, which can then undergo dehydration to selectively produce 2-pentene.

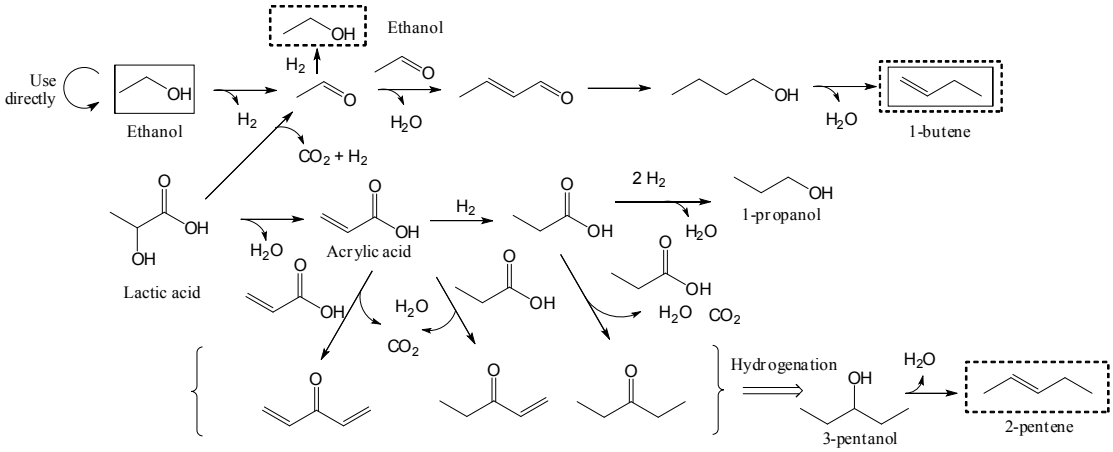

Figure 6.9: Alternative solutions of (MP) with $Z = \Delta E$ when the set of allowed outputs are 15 oxygenates and 157 hydrocarbons. Sources of hydrogen are not shown in the figure as they are identical to those in Figure 6.8.

Table 6.3: Alternative solutions of (MP) with $Z = \Delta E$ when the set of allowed outputs are 15 oxygenates and 157 hydrocarbons.

		Solution			
		1	2	3	4
Input in 10^{-3} mol/min	ethanol	3.8	5.4	-	-
	glycerol	-	-	0.61	0.51
	lactic acid	-	-	2.9	4.7
Waste in 10^{-3} mol/min	H_2O	2.7	5.4	2.0	4.5
	CO_2	-	-	3.3	5.1
Output in 10^{-3} mol/min and (wt%)	ethanol	1.1 (4.8)	-	0.48 (2.2)	1.1 (4.9)
	1-butene	1.4 (7.7)	2.7 (15)	0.47 (2.6)	0.65 (3.7)
	2-pentene	-	-	-	1.2 (8.3)
	1-propanol	-	-	1.4 (8.5)	-
	BOB	8.0 (87)	7.7 (85)	7.9 (87)	(83)
Blend Property	AKI	87	87	87	87
	RON	90.7	90.9	91.0	91.2
	MON	83.3	83.1	83.0	82.8
	LHV (kJ/mL)	32	32	31	32
	oxygen cont. (wt%)	1.7	-	3.0	1.7
	water abs. (wt%)	5.0	-	5.0	5.0

6.4.3 Other objective functions

Complete information about the results for the catalyst requirement and absolute heat duty objective functions can be found in the Supporting Information, but they are summarized here. Minimizing catalyst requirement favors fast reactions, thus hydrogenation and decomposition reactions are common in the alternate solutions. When only oxygenates are considered, the optimal blends are composed of ethanol, 2-methylfuran (from hydrogenating furfural) and 2,5-dimethylfuran (from hydrogenating HMF). Including hydrocarbons in the set of allowed inputs does not change the solutions – the same chemistries and blends are optimal. Producing hydrocarbons requires additional reactions to remove oxygen from the inputs, and thus they are unfavorable for this objective function.

Minimizing absolute heat duty favors energetically neutral reactions. This differs from the energy loss objective, where exothermic and endothermic reactions could be combined to produce an energetically neutral process. When only oxygenates are considered, the optimal blends are similar to those of the catalyst requirement objective, but with the addition of 1-propanol (from hydrogenating acetone). Similarly as before, including hydrocarbons as allowed inputs does not effect the optimal solutions.

The sensitivity of the optimal solutions to blend specifications was examined for the catalyst requirement objective function (see Supporting Information for complete information) to determine when hydrocarbons are favorable. When the water absorption specification is lowered to 2 wt%, the results did not qualitatively change. However, the composition did change to favor furans (2-methylfuran and 2,5-dimethylfuran) over ethanol, as they are less hygroscopic. When the low heating value specificiation is raised to 32 kJ/mL, 1-butene (from maleic acid or succinic acid) is blended with 2-methylfuran and 2,5-dimethylfuran. The amount of hydrocarbons blended increases as the LHV specification raises.

6.5 Discussion

The results given above clearly indicate that, for the given objective function (energy loss) and product constraints, both oxygenate and hydrocarbons can be components of optimal blends. This is expected because hydrocarbons have a higher LHV in comparison to oxygenates and thus producing them leads to a lower energy loss objective value. For stricter product constraints, the nature of solutions can differ. For example,

reducing the limit on water adsorption leads to solutions that involve a greater fraction of heavier oxygenates or hydrocarbons. As expected, hydrocarbons do not appear in the optimal blends of the other objective functions (catalyst requirement and absolute heat duty). These objectives favor having fewer reactions, and as such would avoid the increased processing to remove oxygen from the inputs.

The proposed strategy lends itself to several advantages. First, it allows for large reaction networks to be generated and considered for blend optimization in a fast, automated and scalable manner. It should be noted that because compounds from the generated reaction network (thus synthetically feasible) are considered for blend optimization, the number of compounds evaluated is a fraction of that explored in the molecular design methods discussed earlier. Second, this strategy has a significant potential for "discovering" new reaction routes. Several of the reactions identified in Figures 6.8 and 6.9 have a precedent in the literature. However, unexplored reactions can also be identified. For example, although acrylic acid conversion to 2-pentene involves reactions similar to those reported in the literature, the specific reactions haven't themselves been reported, and therefore constitute a potentially novel route to making hydrocarbons from biomass. The reactions identified by this method could be used to guide experimentation. Third, the strategy is generic and flexible enough to be applied to other combined product and chemistry selection problems involving different sets of chemistries, objectives, and physicochemical properties. For example, optimal diesel blends consisting of alkanes and oxygenates such as fatty esters and their synthesis routes from biomass can be identified subject to physical property constraints involving properties such as cetane index, density, cold flow properties, boiling point, etc.

In this study we have only considered chemistry routes and have ignored the associated utilities and separation steps. Further, although we include additional information and constraints such as joint reactions in our formulation, we do not explicitly take into consideration the selectivity of reactions. This would be specifically important in cases where the reaction system (such as pyrolysis of biomass) is too complex to be represented by a single rule. We also approximate property estimation methods and blending rules to ensure they are linear. Each of these three limitations can be effectively addressed. For example, separation and utility costs (either in energy or economic terms) can be estimated for each reaction. This will require the knowledge/assumption of process variables such as temperature and pressure, and the physical and chemical properties of

compounds such as relative volatility, boiling point, density, individual kinetic parameters, etc. Once available, all the information can be combined to formulate, in effect, a process synthesis problem. The only way selectivity can be efficiently handled is by creating an approximate kinetic model for each reaction by noting that the underlying mechanism can further involve several intermediates. For systems that are too complex, multiple reaction rules may have to be employed. Note that all these inclusions would make the problem nonlinear, making it necessary to use nonlinear programming (NLP) solvers and global optimizers.

6.6 Conclusions

We have developed a strategy for combined product and chemistry selection. This involves generating an exhaustive network of reactions based on a desired set of chemistry rules using our software RING, and formulating and solving an optimization problem with an appropriate objective while including the network stoichiometry information in the constraints. We use this strategy to identify potential renewable oxygenates and hydrocarbons that can be blended with gasoline in an optimal manner. In addition, we also identify the synthesis routes that convert biomass-derived oxygenates to these blend components using heterogeneous catalysis. As constraints we included, (a) the mass balance arising from the network stoichiometry and, (b) the desired range for different physical properties (based on ASTM requirements) such as octane rating, heating value, vapor pressure, etc. We considered three objectives - energy loss, catalyst requirement and absolute heat duty - and further found alternative solutions to get alternative optimal blends and chemistries. We identified that both oxygenates and hydrocarbons are components of optimal blends for the energy loss objective, but the other two objectives produce only oxygenates. Those objectives avoid the increased number of reactions required to remove oxygen from the inputs. However, raising the low heating value requirement leads to hydrocarbons being produced and included in the optimal blends. We posit that our strategy can be extended to solve broad classes of product and chemistry selection problems.

6.7 Supporting information

The Supporting Information contains information about the reaction network construction (reaction rates and rules, and group additivity estimates of heat of formation), reaction cycle enumeration algorithm, alternative solution algorithm, and other objective function (catalyst requirement and absolute heat duty) results. Some sensitivity analysis results are also presented for the catalyst requirement objective function. A complete set of GAMS files and parameter files are included to regenerate the presented results. An input file to RING with chemistry rules used is also included.

6.7.1 Reaction network construction

The software RING, developed in our research group, was used to generate the reaction network. Srinivas Rangarajan is acknowledged for his efforts in defining the reaction rules used for network generation, as well as for finding estimated reaction rates and rate laws from literature, and for group additivity estimation of standard heats of formation. Due to this collaboration, this section is not included in the present thesis. Interested readers can find the complete supporting information online at the journal website, for the paper presented in this chapter [22].

6.7.2 Reaction cycle enumeration algorithm

We propose the following algorithm for enumerating the reaction cycles in a reaction network. It involves iteratively solving the MILP:

$$
\begin{aligned}
\min \quad & Z = \sum_j w_j \\
\text{s.t.} \quad & \sum_j A_{i,j} \cdot f_j^{\text{rxn}} = 0 \\
& f_j^{\text{rxn}} = \frac{r_j}{r_{j^\star}} \cdot f_{j^\star}^{\text{rxn}}, \quad \forall\, l,\ j \in \mathbf{J}_l^{\text{joint}},\ j \neq j^\star \\
& f_j^{\text{rxn}} \leq U \cdot w_j, \quad \forall\, j \\
& f_j^{\text{rxn}} \geq L \cdot w_j, \quad \forall\, j \\
& \sum_{j \in \mathbf{J}_m^{\text{cycle}}} w_j \leq |\mathbf{J}_m^{\text{cycle}}| - 1, \quad \forall\, m \\
& Z \geq 2
\end{aligned}
\tag{MP2}
$$

Table 6.4: Cycles identified in the reaction network.

Size of cycle	Number of cycles identified of that size
2	140
4	60
5	2
6	6
32	1

where $j^\star$ is the first reaction in joint set l, and U and L are the upper and lower bounds for nonzero reaction fluxes, respectively. The set of identified cycles is indexed by m, and each cycle is defined by a subset of reactions $\mathbf{J}_m^{\text{cycle}}$. The objective function Z is the number of reactions in the identified reaction cycle. This is enforced using binary variables w_j that are 1, if reaction j has nonzero reaction flux f_j^{rxn}. We are interested in enumerating cycles, so the lower bound of $Z \geq 2$ makes the problem infeasible if no additional cycles can be identified.

The reaction cycles are found iteratively by solving problem (MP2) using the following algorithm:

Step 1: Set iteration counter $M = 1$. Solve problem (MP2) to find the first reaction cycle. If the problem was feasible and returns a solution, define the subset $\mathbf{J}_M^{\text{cycle}}$ as the subset of j such that $w_j = 1$. Set $M = M + 1$.

Step M $(M \geq 2)$**:** Solve problem (MP2) to find the M^{th} reaction cycle. If the problem was feasible and returns a solution, define the subset $\mathbf{J}_M^{\text{cycle}}$ as the subset of j such that $w_j = 1$. Set $M = M + 1$.

End if the MILP is infeasible.

This algorithm identified the cycles, shown in Table 6.4, for the reaction network presented in this chapter (i.e. generated by RING).

6.7.3 Alternative solution algorithm

An algorithm proposed by Lee et al. [155] was implemented to enumerate the alternative solutions of the fuel blending optimization problem. The algorithm is applicable

for identifying optimal points for any linear program. First, the linear program is transformed into the canonical form:

$$\begin{aligned} \min \quad & Z = \alpha^T z \\ \text{s.t.} \quad & B \cdot z = q \\ & z \geq 0 \end{aligned} \tag{LP2}$$

where $z = \{z_i\}$ is the vector of decision variables and slack variables.

Recall that if the feasible region is non-empty and the optimal solution is bounded, a linear program has a unique optimal objective function value. However, there may be one or infinitely many solutions that correspond with the optimal objective function value. These solutions lie at the intersection of the objective function hyperplane and the convex polytope defined by the linear constraints of the linear program. The extreme points of this intersection are the alternative solutions of the linear program.

The alternative solutions are found iteratively by constraining the decision variables to force a change in the basis set. This is accomplished by introducing vectors of binary variables $w = \{w_i\}$ and $y = \{y_i\}$ with constraints to create a mixed integer linear program. The algorithm from Lee et al. [155] is:

Step 1: Set iteration counted $K = 1$. Solve the linear program and store the optimal objective function value $(Z^1)^\star$. Define the set NZ^1 as the non-zero decision variables of the optimal solution. Set $K = K + 1$.

Step K $(K \geq 2)$**:**

(a) Solve the MILP:

$$\begin{aligned} \min \quad & Z = \alpha^T z \\ \text{s.t.} \quad & B \cdot z = q \\ & \sum_{i \in \text{NZ}^{K-1}} y_i \geq 1 \\ & \sum_{i \in \text{NZ}^k} w_i \leq |\text{NZ}^k| - 1, \quad \forall\, k = \{1, \ldots, K-1\} \\ & 0 \leq z_i \leq U \cdot w_i, \quad \forall\, i \\ & y_i + w_i \leq 1, \quad \forall\, i \in \text{NZ}^{K-1} \end{aligned} \tag{MP3}$$

(b) Store the optimal objective function value $(Z^K)^\star$.

(c) Define the set NZ^K as the non-zero decision variables of the optimal solution.

(d) Set $K = K + 1$.

End if $(Z^K)^\star > (Z^1)^\star$.

For our gasoline blending problem, we adjust the stopping criteria to be when $(Z^K)^\star > 1.5 \cdot (Z^1)^\star$. Thus, we find the true alternative optima of the linear program, and then some "nearly optimal" points within 50% of the optimal objective function value.

6.7.4 Other objective function results

Catalyst requirement, $R^{\mathbf{cat}}$

Figure 6.10 displays some of the alternative solutions, with additional information presented in Table 6.5. The first solution (with outputs identified with solid boxes) produces 2-methylfuran from furfural, directly uses ethanol, and blends them with BOB to produce gasoline. The required hydrogen is acquired directly as an input, but some later solutions use formic acid or glycerol to instead produce hydrogen. The second and third solutions are examples that use these alternative hydrogen sources. The fourth solution (with outputs identified with dashed boxes) produces 2,5-dimethylfuran from HMF, directly uses ethanol, and blends them with BOB to produce gasoline.

Including hydrocarbons as allowed inputs does not change the results for $Z = R^{\text{cat}}$. Producing a hydrocarbon requires additional reactions to remove oxygen from the inputs, and is thus unfavorable here.

Absolute heat duty, $H^{\mathbf{abs}}$

Figure 6.11 displays some of the alternative solutions, with additional information presented in Table 6.6. The first three solutions are very similar to the results from the catalyst requirement objective. However, the fourth solution is interesting as it produces 1-propanol from acetone.

Including hydrocarbons as allowed inputs does not change the results for $Z = H^{\text{abs}}$. Producing a hydrocarbon requires additional reactions to remove oxygen from the inputs. These oxygen removing reactions are often not energetically neutral, and thus hydrocarbons are not favored here.

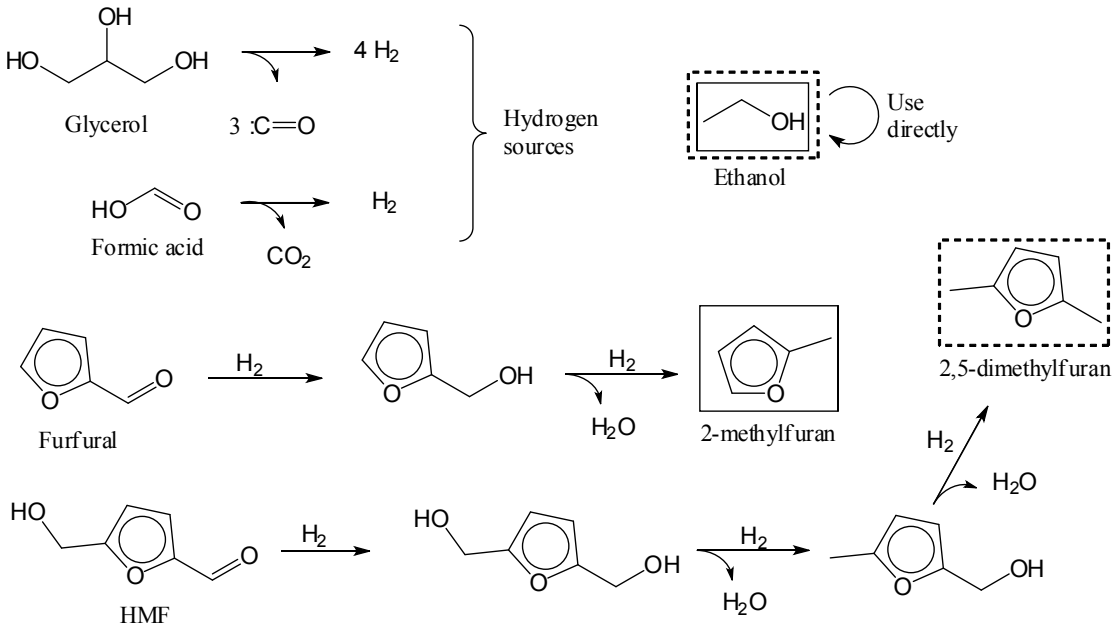

Figure 6.10: Some alternative solutions with $Z = R^{\text{cat}}$ when the set of allowed outputs are 15 oxygenate compounds.

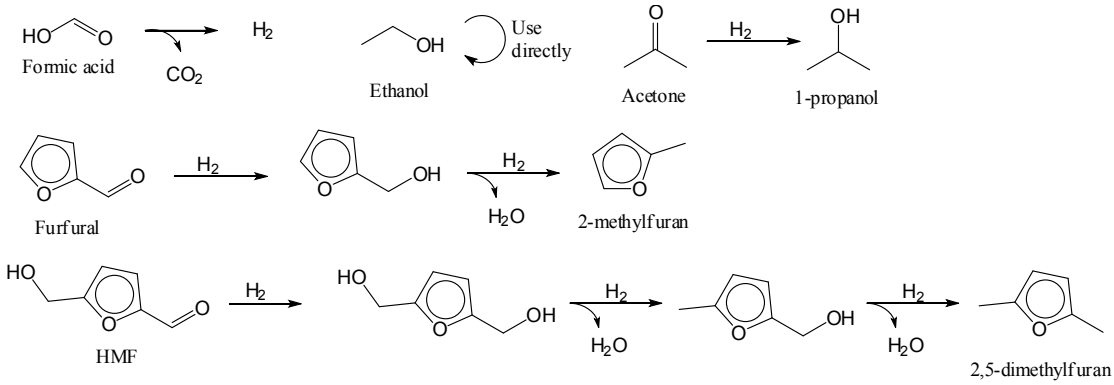

Figure 6.11: Some alternative solutions with $Z = H^{\text{abs}}$ when the set of allowed outputs are 15 oxygenate compounds.

Table 6.5: Alternative solutions with $Z = R^{\text{cat}}$ when the set of allowed outputs are 15 oxygenate compounds.

		Solution			
		1	2	3	4
Input 10^{-3} mol/min	ethanol	1.0	1.0	1.0	0.99
	furfural	0.61	0.61	0.61	-
	HMF	-	-	-	0.54
	hydrogen	1.2	-	-	1.6
	formic acid	-	1.2	-	-
	glycerol	-	-	0.3	-
Waste 10^{-3} mol/min	H_2O	0.61	0.61	0.61	1.1
	CO_2	-	1.2	-	-
	CO	-	-	0.91	-
Output 10^{-3} mol/min and (wt%)	ethanol	1.0 (4.6)	1.0 (4.6)	1.0 (4.6)	0.99 (4.5)
	2-methylfuran	0.61 (5.0)	0.61 (5.0)	0.61 (5.0)	-
	2,5-dimethylfuran	-	-	-	0.54 (5.2)
	BOB	8.2 (90.5)	8.2 (90.5)	8.2 (90.5)	8.2 (90.3)
Blend Property	AKI	87	87	87	87
	RON	90.7	90.7	90.7	90.8
	MON	83.3	83.3	83.3	83.2
	LHV (kJ/mL)	31.5	31.5	31.5	31.6
	oxygen (wt%)	2.6	2.6	2.6	2.4
	water abs. (wt%)	5.0	5.0	5.0	5.0
	RVP (kPa)	42	42	42	41
	T_{10} (°C)	61	61	61	63
	T_{50} (°C)	98	98	98	100
	T_{90} (°C)	170	170	170	170

Table 6.6: Alternative solutions with $Z = H^{\text{abs}}$ when the set of allowed outputs are 15 oxygenate compounds.

		Solution			
		1	2	3	4
Input 10^{-3} mol/min	ethanol	1.0	1.0	1.0	-
	furfural	0.61	0.61	-	0.32
	HMF	-	-	0.54	-
	acetone	-	-	-	1.6
	hydrogen	1.2	-	1.6	2.3
	formic acid	-	1.2	-	-
Waste 10^{-3} mol/min	H_2O	0.61	0.61	1.1	0.32
	CO_2	-	1.2	-	-
Output 10^{-3} mol/min and (wt%)	ethanol	1.0 (4.6)	1.0 (4.6)	1.0 (4.5)	-
	2-methylfuran	0.61 (5.0)	0.61 (5.0)	-	0.32 (2.6)
	2,5-dimethylfuran	-	-	0.54 (5.2)	-
	1-propanol	-	-	-	1.6 (9.8)
	BOB	8.2 (90.5)	8.2 (90.5)	8.2 (90.3)	8.0 (87.5)
Blend Property	AKI	87	87	87	87
	RON	90.7	90.7	90.9	90.8
	MON	83.3	83.3	83.2	83.2
	LHV (kJ/mL)	31.5	31.5	31.6	31.3
	oxygen (wt%)	2.6	2.6	2.4	3.1
	water abs. (wt%)	5.0	5.0	5.0	5.0
	RVP (kPa)	42	42	41	41
	T_{10} (°C)	61	61	63	61
	T_{50} (°C)	98	98	100	94
	T_{90} (°C)	170	170	170	169

Table 6.7: Alternative solutions with $Z = R^{\text{cat}}$ when the set of allowed outputs are 15 oxygenates and 157 hydrocarbons. Water absorption is limited to 2 wt%.

		Solution			
		1	2	3	4
Input 10^{-3} mol/min	ethanol	0.39	0.39	0.39	0.38
	furfural	0.92	0.92	0.92	-
	HMF	-	-	-	0.82
	hydrogen	1.8	-	-	2.5
	formic acid	-	1.8	-	-
	glycerol	-	-	1.4	-
Waste 10^{-3} mol/min	H_2O	0.92	0.92	0.92	1.6
	CO_2	-	1.8	-	-
	CO	-	-	1.4	-
Output 10^{-3} mol/min and (wt%)	ethanol	0.39 (1.8)	0.39 (1.8)	0.39 (1.8)	0.38 (1.7)
	2-methylfuran	0.92 (7.6)	0.92 (7.6)	0.92 (7.6)	-
	2,5-dimethylfuran	-	-	-	0.82 (7.9)
	BOB	8.2 (90.6)	8.2 (90.6)	8.2 (90.6)	8.2 (90.3)
Blend Property	AKI	87	87	87	87
	RON	90.8	90.8	90.8	90.9
	MON	83.2	83.2	83.2	83.1
	LHV (kJ/mL)	31.3	31.3	31.3	31.4
	oxygen (wt%)	2.1	2.1	2.1	1.9
	water abs. (wt%)	2.0	2.0	2.0	2.0

6.7.5 Sensitivity analysis

We were interested in the sensitivity of the optimal blends and chemistries to changes in the blend specifications. Presented here are the results for (i) decreasing the allowed water absorption and (ii) increasing the minimum allowed LHV.

Water absorption

For the $Z = R^{\text{cat}}$ objective with oxygenates and hydrocarbons as allowed outputs, the results did not qualitatively change when the water absorption require was lowered to 2 wt%. However, the composition did change to favor furans (2-methylfuran and 2,5-dimethylfuran) over ethanol, as they are less hygroscopic. The chemistry is the same as in Figure 6.10, but the composition and properties are shown in Table 6.7.

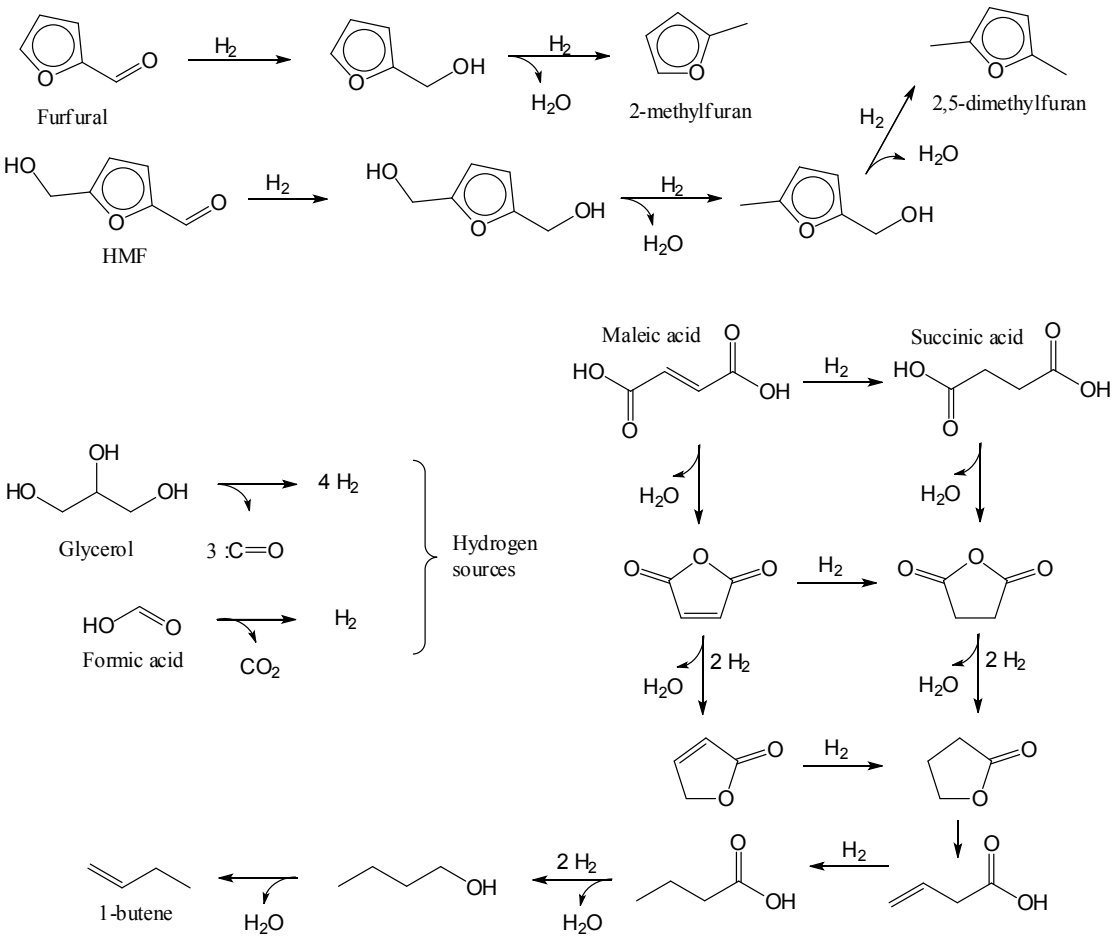

Figure 6.12: Some alternative solutions with $Z = R^{\text{cat}}$ when the set of allowed outputs are 15 oxygenates and 157 hydrocarbons. LHV must be higher than 32 kJ/mL.

Low heating value

For the $Z = R^{cat}$ objective with oxygenates and hydrocarbons as allowed outputs, a hydrocarbon (1-butene) appeared in the optimum solutions when the minimum LHV requirement was raised to 32 kJ/mL. Figure 6.12 displays some of the alternative solutions, with additional information presented in Table 6.8. The same chemistries seen previously produce 2-methylfuran from furfural, and 2,5-dimethylfuran from HMF. Either maleic acid or succinic acid is used to produce 1-butene.

Table 6.8: Alternative solutions with $Z = R^{\text{cat}}$ when the set of allowed outputs are 15 oxygenates and 157 hydrocarbons. LHV must be higher than 32 kJ/mL.

		Solution			
		1	2	3	4
Input 10^{-3} mol/min	succinic acid	1.6	-	1.6	1.7
	maleic acid	-	1.6	-	-
	HMF	0.40	0.40	0.40	-
	furfural	-	-	-	0.41
	hydrogen	9.2	11	-	9.3
	formic acid	-	-	9.2	-
Waste 10^{-3} mol/min	H_2O	7.2	7.2	7.2	7.2
	CO_2	-	-	9.2	-
Output 10^{-3} mol/min and (wt%)	1-butene	1.6 (9.0)	1.6 (9.0)	1.6 (9.0)	1.7 (9.5)
	2,5-dimethylfuran	0.40 (3.8)	0.40 (3.8)	0.40 (3.8)	-
	2-methylfuran	-	-	-	0.41 (3.4)
	BOB	7.9 (87.2)	7.9 (87.2)	7.9 (87.2)	7.9 (87.1)
Blend Property	AKI	87	87	87	87
	RON	90.9	90.9	90.9	90.9
	MON	83.1	83.1	83.1	83.1
	LHV (kJ/mL)	32	32	32	32
	oxygen (wt%)	0.64	0.64	0.64	0.66
	water abs. (wt%)	0.004	0.004	0.004	0.004

CHAPTER 7

Future Work

This research has addressed important practical questions related to the feasibility of converting biomass that is plentiful in the Midwest into valuable biofuels and co-products. However, there are still several open issues that need further investigation. These issues will be discussed as they relate to the supply chain optimization and product design problems.

7.1 Supply chain optimization future work

The variety of supply chain choices shown in this work demonstrate the ability of MILP formulations to capture the complex behavior of biofuel supply chains, but there are a number of possible expansions. The models in Chapters 3, 4 and 5 acknowledged that the cost of biofuel transportation is much less than biomass transportation. In general this is true, as the low energy density of biomass is significantly more costly to transport the same distance, but it may be the case that much longer transportation distances are required for biofuels to reach customers. Note that Chapters 4 and 5 accounted for an approximate cost of biofuel transportation, by assuming that produced biofuels are sold to the nearest biofuel blending terminal, but the transportation of blended fuels to fueling stations was not considered. State-level fuel demand is available from the U.S. Energy Information Administration [168] and could be disaggregated to the county-level

based on population, as an estimate of local fuel demand.

Although existing facilities for the most common biofuel (ethanol) were included, there are also existing facilities for other biofuels. Including the U.S. biodiesel industry at first seemed to be straightforward, but the individual facility capacities, feedstock information, installed technologies and biomass availabilities were unavailable. Agricultural crop oil availabilities could be determined per county by examining the crop production figures reported to the U.S. Department of Agriculture and available online on the National Agricultural Statistics Service website [65]. Waste cooking oil availability could be estimated from the number of restaurants located in each county. Animal fats availability could be estimated from livestock populations. The National Biodiesel Board (NBB) maintains a list of their members (146 facilities) that is available on their website [169] with some capacities listed, but no feedstock information. Biodiesel magazine maintains a list that currently contains 193 facilities [170]. The BioFuels Atlas interactive online GIS map (initially developed for biopower) displays the biodiesel plant locations available from the NBB [171]. Similarly, the interactive GIS map on the U.S. Department of Energy Bioenergy Knowledge Discovery Framework website (initially developed to visualize and distribute the findings of the Billion-Ton Update [95]) uses biodiesel facility data from the NBB, after verification of capacity, transportation modal access and location by Oak Ridge National Laboratory [172]. It may also be possible to get facility capacities from the U.S. EPA RFS Part 80 list of registered companies [97]. None of these options should be expected to yield perfect information, as companies avoid disclosing proprietary information, but it is possible to cross-reference them for estimates.

Competition between biofuel technologies for biomass was included, but there are other significant market forces that could be taken account of. Energy (fuel, power), food and land markets become intertwined with biofuels. Cellulosic biofuels seek to solve the food, energy and environment *trilemma* by utilizing non-food biomass to produce fuels with substantial greenhouse gas emission reductions and local societal benefits [124]. Land markets, however, could be effected, dependent on the expansion of biomass production. Market equilibrium models could be used to account for changes in prices (e.g. of crop land, corn, biofuels) as production increases. There is some preliminary work in this area for biofuel production in Illinois from corn, where the price of corn varied with ethanol production following a non-cooperative Stackelberg leader-follower game in which farms and the biofuel industry aim to maximize their

own profit objectives [52]. Simulation, rather than optimization, techniques are also being explored to account for market equilibrium. The National Renewable Energy Laboratory's Biomass Scenario Model is a systems dynamics model that accounts for a dispensing station owner's decision whether to offer biofuel and a consumer's choice whether to purchase that fuel [173]. Multi-agent simulation is another way to account for the intelligent adaptation of interacting stakeholders [174, 175].

Expanding the MILP to account for dynamic decisions is another option. In this research, the focus was on the near-term expansion of the biofuel industry, with facility operation beginning in 2015. It is also possible to write a dynamic supply chain optimization problem where facilities can be constructed in time periods along a time horizon. The intuitive time horizon would be today until 2022, the last year with RFS mandates. Mandates for each year could then be satisfied. Note, that this author greatly considered this expansion and made multiple efforts in that direction, but combinatorial explosion and the resulting extended computation times prevented any further study. This problem is feasible for smaller study regions with fewer candidate sites, and has been demonstrated in a number of studies [37, 176, 177] with some also considering monthly time periods to account for biomass storage inventory [53].

7.1.1 Optimization under uncertainty

This research has considered nominal economic and technological parameters, yet many of those are inherently uncertain. They specify volatile prices or characteristics of technology not demonstrated at commercial scales. For example, the national average price of corn grain used for ethanol varied from \$2/bushel in 2005 to \$4.2/bushel in 2007 [65]. Many studies have examined how biomass utilizing systems can be affected by economic parameter uncertainty. The logistic challenges for fossil fuel substitution with biomass for energy production were explored in [88]. The sensitivity of ethanol production cost was compared across multiple technologies in [82]. Techniques to examine the effect of parameter uncertainty include single parameter sensitivity, Monte Carlo parameter sampling and optimization under uncertainty. Chapter 3 included the first two methods, but the last is worth discussing here as future work.

A number of techniques exist in the literature for handling uncertain parameters in optimization models [109] and many have been applied to chemical engineering problems [178]. Often they can be categorized as *wait-and-see* or *here-and-now* problems. Wait-and-see problems, including the aforementioned Monte Carlo sampling, show the

effect of uncertainty by comparing optimum decisions for many realizations of the parameters (e.g. scenarios). Here-and-now problems, on the other hand, require decisions to be made before observation of the parameters using some probabilistic measure, such as expected value. Stochastic programming incorporates both wait-and-see and here-and-now problems together with the idea of recourse, where corrective action can be taken after parameter observation. In supply chain optimization, this often amounts to two-stage recourse where infrastructure decisions x are made before future prices are observed (first-stage) and logistics decisions y are made after the market develops (second-stage). The first-stage problem is to minimize the sum of infrastructure costs and the expected value of second-stage decisions made due to the choice of infrastructure:

$$\begin{aligned} \min \quad & J(x) = c^T x + E_\omega \left[Q(x, \omega) \right] \\ \text{s.t.} \quad & Ax \leq b \\ & x \geq 0 \end{aligned}$$

where ω is the vector of uncertain parameters and x normally includes discrete or binary decision variables, thus requiring MILP algorithms.

With infrastructure decisions fixed and uncertain parameters observed, the second-stage problem is to minimize logistical costs:

$$\begin{aligned} Q(x, \omega) = \min \quad & q(\omega)^T y \\ \text{s.t.} \quad & T(\omega)x + W(\omega)y \leq h(\omega) \\ & y \geq 0 \end{aligned}$$

where decision variables y are normally all continuous to allow for LP algorithm use.

The probability distribution for each uncertain parameter can be discretized to generate a matrix of parameter scenarios each with respective probability of occurring, greatly simplifying the expected value calculation $E_\omega \left[Q(x, \omega) \right]$ by reducing the number of second-stage optimizations. This allows for the first-stage and second-stage problems

to be combined into the two-stage stochastic programming model:

$$\begin{aligned} \min \quad & c^T x + \sum_s p_s q_s^T y_s \\ \text{s.t.} \quad & Ax \leq b \\ & x \geq 0 \\ & T_s x + W_s y_s \leq h_s, \quad \forall\, s \\ & y_s \geq 0, \quad \forall\, s \end{aligned}$$

where scenarios are indexed by s and have corresponding probability p_s, and y_s are the second-stage decisions for each scenario s.

This two-stage approach has been used to optimize a hybrid fuel cell Aspen process flow sheet [179], multi-product allocation to manufacturing facilities with uncertain demand [180], corn-ethanol supply chains in northern Italy [176], and cellulosic ethanol supply chains in Illinois [177]. Often the L-shaped decomposition method is used, which takes advantage of the special decomposable structure of the two-stage stochastic programming model [181]. Computational requirements may be too high to use this approach across the entire study region, but it can be applied in smaller regions with fewer decision variables.

7.2 Product design future work

The strategy of combining reaction network generation with optimization for product design, presented in Chapter 6, is flexible enough to be applicable for any problem involving concurrent product and chemistry selection. Examining other blended product design problems is a logical next step, including lubricants, surfactants and diesel. Our group has already examined fatty alcohol surfactant design without the optimization component to automate the process [182]. The aim would be to determine product molecules with desired properties and their synthesis routes, with these routes evaluated and ranked in terms of stoichiometric, energetics and physical parameters such as atom efficiency, enthalpy and free energy change of reactions, and aqueous-organic partition coefficients (Log P) of intermediates. Expanding the property prediction of the gasoline design problem is another possibility, so that less (if any) BOB is required. In this case, linear mixing rules are expected to be replaced with nonlinear functions,

making the problem a mixed integer nonlinear program and more difficult to solve. Lubricant design is a similar problem, in that a base oil is normally blended with small amounts of additives to modify performance. There may be physical property requirements for viscosity, elastohydrodynamic lubrication friction coefficient, density, thermal conductivity and heat capacity per unit volume. For low concentrations, a linear model may be appropriate for some blend property predictions.

Bibliography

[1] Prodromos Daoutidis, W Alex Marvin, Srinivas Rangarajan, and Ana I Torres. Engineering Biomass Conversion Processes: A Systems Perspective. *AIChE Journal*, 59(1):3–18, January 2013.

[2] Robert D Perlack, Lynn L Wright, Anthony F Turhollow, Bryce J Stokes, and Donald C Erbach. Biomass as Feedstock for a Bioenergy and Bioproducts Industry: The Technical Feasibility of a Billion-Ton Annual Supply. Technical Report April, ORNL/TM-2005/66. Oak Ridge National Laboratory, Oak Ridge, Tennessee, 2005.

[3] B Solomon, J Barnes, and K Halvorsen. Grain and cellulosic ethanol: History, economics, and energy policy. *Biomass and Bioenergy*, 31(6):416–425, June 2007.

[4] D D Songstad, P Lakshmanan, J Chen, W Gibbons, S Hughes, and R Nelson. Historical perspective of biofuels: learning from the past to rediscover the future. *In Vitro Cellular & Developmental Biology - Plant*, 45(3):189–192, May 2009.

[5] Alcohol for autos may displace gasoline. *The New York Times*, March 1906.

[6] Launching a great industry; the making of cheap alcohol. *The New York Times*, November 1906.

[7] Some of the Problems Awaiting Solution. *National Geographic Magazine*, pages 131–146, February 1917.

[8] Jason Hill, Erik Nelson, David Tilman, Stephen Polasky, and Douglas G Tiffany. Environmental, economic, and energetic costs and benefits of biodiesel and ethanol biofuels. *Proceedings of the National Academy of Sciences of the United States of America*, 103(30):11206–10, July 2006.

[9] U.S. Environmental Protection Agency. Regulation of Fuels and Fuel Additives: 2012 Renewable Fuel Standards; Final Rule. Technical Report 5, U.S. Environmental Protection Agency, 2012.

[10] Lihong McPhail, Paul Westcott, and Heather Lutman. The Renewable Identification Number System and U.S. Biofuel Mandates. Technical report, U.S. Department of Agriculture, Economic Research Service, BIO-3, 2011.

[11] U.S. Environmental Protection Agency. EPA Finalizes Regulations for the National Renewable Fuel Standard Program for 2010 and Beyond. Technical Report February, U.S. Environmental Protection Agency, 2010.

[12] Pamela P Peralta-Yahya, Fuzhong Zhang, Stephen B del Cardayre, and Jay D Keasling. Microbial engineering for the production of advanced biofuels. *Nature*, 488(7411):320–8, August 2012.

[13] Shota Atsumi, Taizo Hanai, and James C Liao. Non-fermentative pathways for synthesis of branched-chain higher alcohols as biofuels. *Nature*, 451(7174):86–9, January 2008.

[14] Avelino Corma, Sara Iborra, and Alexandra Velty. Chemical routes for the transformation of biomass into chemicals. *Chemical reviews*, 107(6):2411–502, June 2007.

[15] Ana Ines Torres, Prodromos Daoutidis, and Michael Tsapatsis. Continuous production of 5-hydroxymethylfurfural from fructose: a design case study. *Energy & Environmental Science*, 3(10):1560, 2010.

[16] A.I. Torres, M. Tsapatsis, and P. Daoutidis. Biomass to chemicals: Design of an extractive-reaction process for the production of 5-hydroxymethylfurfural. *Computers & Chemical Engineering*, 42:130–137, July 2012.

[17] Mark M Wright and Robert C Brown. Comparative economics of biorefineries based on the biochemical and thermochemical platforms. *Biofuels, Bioproducts and Biorefining*, 1(1):49–56, September 2007.

[18] Juan Carlos Serrano-Ruiz, Ryan M West, and James a Dumesic. Catalytic conversion of renewable biomass resources to fuels and chemicals. *Annual review of chemical and biomolecular engineering*, 1:79–100, January 2010.

[19] Joshua L Colby, Paul J Dauenhauer, and Lanny D Schmidt. Millisecond autothermal steam reforming of cellulose for synthetic biofuels by reactive flash volatilization. *Green Chemistry*, 10(7):773, 2008.

[20] W Alex Marvin, Lanny D Schmidt, Saif Benjaafar, Douglas G Tiffany, and Prodromos Daoutidis. Economic Optimization of a Lignocellulosic Biomass-to-Ethanol Supply Chain. *Chemical Engineering Science*, 67(1):68–79, January 2012.

[21] W Alex Marvin, Lanny D Schmidt, and Prodromos Daoutidis. Biorefinery Location and Technology Selection Through Supply Chain Optimization. *Industrial & Engineering Chemistry Research*, 52(9):3192–3208, October 2013.

[22] W Alex Marvin, Srinivas Rangarajan, and Prodromos Daoutidis. Automated Generation and Optimal Selection of Biofuel-Gasoline Blends and Their Synthesis Routes. *Energy & Fuels*, 27(6):3585–3594, June 2013.

[23] George B Dantzig and Mukund N Thapa. *Linear Programming: 2: Theory and Extensions*. Springer, 1997.

[24] Ronald L Rardin. *Optimization in Operations Research*. Prentice Hall, Inc., Upper Saddle River, NJ, 2000.

[25] Christodoulos A Floudas. *Nonlinear and Mixed-Integer Optimization*. Oxford University Press, New York, NY, 1995.

[26] Michael Wang, May Wu, and Hong Huo. Life-cycle energy and greenhouse gas emission impacts of different corn ethanol plant types. *Environmental Research Letters*, 2(2):024001, April 2007.

[27] Todd West, Katherine Dunphy-guzman, Amy Sun, Len Malczynski, David Reichmuth, Richard Larson, James Ellison, Robert Taylor, Vincent Tidwell, Lennie Klebanoff, Patricia Hough, Andrew Lutz, Christopher Shaddix, Norman Brinkman,

Candace Wheeler, and David O'Toole. Feasibility, economics, and environmental impact of producing 90 billion gallons of ethanol per year by 2030. Technical report, Sandia National Laboratories, Livermore, CA and Albuquerque, NM, 2009.

[28] Commission of the European Communities. Renewable Energy Road Map - Renewable energies in the 21st century: building a more sustainable future, 2007.

[29] Thomas D Foust, Robert Wooley, John Sheehan, Robert Wallace, Kelly Ibsen, David Dayton, Mike Himmel, John Ashworth, Robert McCormick, Margo Melendez, J Richard Hess, Kevin L Kenney, Christopher T Wright, Corey Radtke, Robert D Perlack, Jonathan Mielenz, Michael Wang, Seth Synder, and Todd Werpy. A National Laboratory Market and Technology Assessment of the 30x30 Scenario. Technical Report March, National Renewable Energy Laboratory, Golden, Colorado, 2007.

[30] Renewable Fuels Association. 2010 Ethanol Industry Outlook: Climate of Opportunity. Technical report, Renewable Fuels Association, August 2010.

[31] U.S. DOE Energy Efficiency & Renewable Energy. Integrated Biorefinery Project Locations, 2010.

[32] A Milbrandt. A Geographic Perspective on the Current Biomass Resource Availability in the United States. *National Renewable Energy Laboratory*, (December):70, 2005.

[33] R Vance Morey, Nalladurai Kaliyan, Douglas G Tiffany, and David R Schmidt. A Corn Stover Supply Logistics System. *Applied Engineering in Agriculture*, 26(3):455–461, 2010.

[34] Paul W Gallagher, Mark Dikeman, John Fritz, Eric Wailes, Wayne Gauthier, and Hosein Shapouri. Supply and Social Cost Estimates for Biomass from Crop Residues in the United States. *Environmental & Resource Economics*, 24(4):335–358, 2003.

[35] J Richard Hess, Christopher T Wright, and Kevin L Kenney. Cellulosic biomass feedstocks and logistics for ethanol production. *Biofuels, Bioproducts and Biorefining*, 1(3):181–190, November 2007.

[36] Marieke E Bruins and Johan P M Sanders. Small-scale processing of biomass for biorefinery. *Biofuels, Bioproducts and Biorefining*, 6(2):135–145, March 2012.

[37] Heungjo An, Wilbert E Wilhelm, and Stephen W Searcy. Biofuel and petroleum-based fuel supply chain research: A literature review. *Biomass and Bioenergy*, 35(9):3763–3774, July 2011.

[38] Christodoulos A Floudas, Josephine A Elia, and Richard C Baliban. Hybrid and single feedstock energy processes for liquid transportation fuels: A critical review. *Computers & Chemical Engineering*, 41:24–51, June 2012.

[39] William R Morrow, W Michael Griffin, and H Scott Matthews. Modeling Switchgrass Derived Cellulosic Ethanol Distribution in the United States. *Environmental Science & Technology*, 40(9):2877–2886, May 2006.

[40] K Suh, S Suh, B Walseth, J Bae, and R Barker. Optimal Corn Stover Logistics for Biofuel Production: A Case in Minnesota. *Transactions Of The ASABE*, 54(1):229–238, 2011.

[41] Josephine A Elia, Richard C Baliban, Xin Xiao, and Christodoulos A Floudas. Optimal energy supply network determination and life cycle analysis for hybrid coal, biomass, and natural gas to liquid (CBGTL) plants using carbon-based hydrogen production. *Computers & Chemical Engineering*, 35(8):1399–1430, August 2011.

[42] Richard C Baliban, Josephine A Elia, and Christodoulos A Floudas. Toward Novel Hybrid Biomass, Coal, and Natural Gas Processes for Satisfying Current Transportation Fuel Demands, 1: Process Alternatives, Gasification Modeling, Process Simulation, and Economic Analysis. *Industrial & Engineering Chemistry Research*, 49(16):7343–7370, August 2010.

[43] Josephine A Elia, Richard C Baliban, and Christodoulos A Floudas. Toward Novel Hybrid Biomass, Coal, and Natural Gas Processes for Satisfying Current Transportation Fuel Demands, 2: Simultaneous Heat and Power Integration. *Industrial & Engineering Chemistry Research*, 49(16):7371–7388, August 2010.

[44] Josephine A Elia, Richard C Baliban, and Christodoulos A Floudas. Nationwide energy supply chain analysis for hybrid feedstock processes with significant CO2 emissions reduction. *AIChE Journal*, 58(7):2142–2154, July 2012.

[45] Gelson Tembo, Francis M Epplin, and Raymond L Huhnke. Integrative Investment Appraisal of a Lignocellulosic Biomass-to-Ethanol Industry. *Journal of Agricultural and Resource Economics*, 28(3):611–633, 2003.

[46] Lawrence Daniel Mapemba. Herbaceous plant biomass harvest and delivery cost with harvest segmented by month and number of harvest machines endogenously determined. *Biomass and Bioenergy*, 32(11):1016–1027, November 2008.

[47] Yogendra Shastri, Alan Hansen, Luis Rodríguez, and K C Ting. Development and application of BioFeed model for optimization of herbaceous biomass feedstock production. *Biomass and Bioenergy*, 35(7):2961–2974, July 2011.

[48] Seungmo Kang, Hayri Önal, Yanfeng Ouyang, Jürgen Scheffran, and Ümit Deniz Tursun. *Handbook of Bioenergy Economics and Policy, chapter 10*. Springer New York, New York, NY, 2010.

[49] Sylvain Leduc, F Starfelt, Erik Dotzauer, Georg Kindermann, I McCallum, Michael Obersteiner, and J Lundgren. Optimal location of lignocellulosic ethanol refineries with polygeneration in Sweden. *Energy*, 35(6):2709–2716, June 2010.

[50] Nathan Parker, Peter Tittmann, Quinn Hart, Richard Nelson, Ken Skog, Anneliese Schmidt, Edward Gray, and Bryan Jenkins. Development of a biorefinery optimized biofuel supply curve for the Western United States. *Biomass and Bioenergy*, 34(11):1597–1607, November 2010.

[51] Jinkyung Kim, Matthew J Realff, and Jay H Lee. Optimal design and global sensitivity analysis of biomass supply chain networks for biofuels under uncertainty. *Computers & Chemical Engineering*, 35(9):1738–1751, September 2011.

[52] Yun Bai, Yanfeng Ouyang, and Jong-Shi Pang. Biofuel supply chain design under competitive agricultural land use and feedstock market equilibrium. *Energy Economics*, 34(5):1623–1633, February 2012.

[53] Fengqi You, Ling Tao, Diane J Graziano, and Seth W Snyder. Optimal design of sustainable cellulosic biofuel supply chains: Multiobjective optimization coupled with life cycle assessment and input-output analysis. *AIChE Journal*, 58(4):1157–1180, April 2012.

[54] Fengqi You and Belinda Wang. Life Cycle Optimization of Biomass-to-Liquid Supply Chains with DistributedCentralized Processing Networks. *Industrial & Engineering Chemistry Research*, 50(17):10102–10127, September 2011.

[55] Andrea Zamboni, Nilay Shah, and Fabrizio Bezzo. Spatially Explicit Static Model for the Strategic Design of Future Bioethanol Production Systems. 1. Cost Minimization. *Energy & Fuels*, 23(10):5121–5133, October 2009.

[56] Andrea Zamboni, Fabrizio Bezzo, and Nilay Shah. Spatially Explicit Static Model for the Strategic Design of Future Bioethanol Production Systems. 2. Multi-Objective Environmental Optimization. *Energy & Fuels*, 23(10):5134–5143, October 2009.

[57] Ozlem Akgul, Andrea Zamboni, Fabrizio Bezzo, Nilay Shah, and Lazaros G Papageorgiou. Optimization-Based Approaches for Bioethanol Supply Chains. *Industrial & Engineering Chemistry Research*, 50(9):4927–4938, May 2011.

[58] Sara Giarola, Andrea Zamboni, and Fabrizio Bezzo. Spatially explicit multi-objective optimisation for design and planning of hybrid first and second generation biorefineries. *Computers & Chemical Engineering*, 35(9):1782–1797, September 2011.

[59] Warren D Seider, J D Seader, Daniel R Lewin, and Soemantri Widagdo. *Product and Process Design Principles: Synthesis, Analysis and Evaluation.* John Wiley & Sons Inc., 3rd ed. edition, 2008.

[60] Susan Hesse Owen and Mark S Daskin. Strategic facility location: A review. *European Journal of Operational Research*, 111(3):423–447, December 1998.

[61] Mitsuo Gen and Runwie Cheng. *Genetic Algorithms and Engineering Design.* John Wiley & Sons, 1997.

[62] Jorge H. Jaramillo, Joy Bhadury, and Rajan Batta. On the use of genetic algorithms to solve location problems. *Computers & Operations Research*, 29(6):761–779, May 2002.

[63] Y. Hinojosa, J. Puerto, and F.R. Fernández. A multiperiod two-echelon multicommodity capacitated plant location problem. *European Journal of Operational Research*, 123(2):271–291, June 2000.

[64] IBM. IBM ILOG CPLEX Optimization Studio 12.2, 2011.

[65] U.S. Department of Agriculture. National Agricultural Statistics Service (NASS) Quick Stats, 2010.

[66] Daniel R Petrolia. The economics of harvesting and transporting corn stover for conversion to fuel ethanol: A case study for Minnesota. *Biomass and Bioenergy*, 32(7):603–612, 2008.

[67] W W Wilhelm, Jane M F Johnson, Douglas L Karlen, and David T Lightle. Corn Stover to Sustain Soil Organic Carbon Further Constrains Biomass Supply. *Agronomy Journal*, 99(6):1665, 2007.

[68] Lawrence Daniel Mapemba. *Cost to Deliver Lignocellulosic Biomass to a Biorefinery, PhD Thesis*. Phd thesis, Oklahoma State University, 2005.

[69] NationalAtlas.gov. Raw data download - 2001 County boundaries, 2010.

[70] Ümit Deniz Tursun, Seungmo Kang, Hayri Önal, Yanfeng Ouyang, and Jürgen Scheffran. Optimal Biorefinery Locations and Transportation Netowkr for the Future Biofuels Industry in Illinois. In Madhu Khanna, editor, *Environmental and Rural Development Impacts*, pages 149–166, St. Louis, Missouri, 2008.

[71] Sylvain Leduc, Erwin Schmid, Michael Obersteiner, and Keywan Riahi. Methanol production by gasification using a geographically explicit model. *Biomass and Bioenergy*, 33(5):745–751, May 2009.

[72] Johannes Schmidt, Sylvain Leduc, Erik Dotzauer, Georg Kindermann, and Erwin Schmid. Potential of biomass-fired combined heat and power plants considering the spatial distribution of biomass supply and heat demand. *International Journal of Energy Research*, 34:n/a–n/a, 2009.

[73] Google Inc. Google Maps, 2010.

[74] Burton C English, Cameron Short, and Earl O Heady. The Economic Feasibility of Crop Residues as Auxiliary Fuel in Coal-Fired Power Plants. *American Journal of Agricultural Economics*, 63(4):636–644, 1981.

[75] D Humbird and A Aden. Biochemical Production of Ethanol from Corn Stover: 2008 State of Technology Model. Technical Report August, National Renewable Energy Laboratory, Golden, Colorado, 2009.

[76] F Kabir Kazi, J Fortman, R Anex, G Kothandaraman, D Hsu, A Aden, and A Dutta. Techno-Economic Analysis of Biochemical Scenarios for Production of Cellulosic Ethanol Techno-Economic Analysis of Biochemical Scenarios for Production of Cellulosic Ethanol. Technical Report June, National Renewable Energy Laboratory, Golden, Colorado, 2010.

[77] U.S. DOE Energy Efficiency & Renewable Energy. Clean Cities Alternative Fuel Price Report for October 2010. Technical Report October, 2010.

[78] U.S. DOE Energy Efficiency & Renewable Energy: Alternative Fuels & Advanced Vehicles Data Center. Federal & State Incentives & Laws, 2010.

[79] A Aden, M Ruth, Kelly Ibsen, J Jechura, K Neeves, John Sheehan, B Wallace, L Montague, A Slayton, and J Lukas. Lignocellulosic Biomass to Ethanol Process Design and Economics Utilizing Co-Current Dilute Acid Prehydrolysis and Enzymatic Hydrolysis for Corn Stover. Technical Report June, National Renewable Energy Laboratory, Golden, Colorado, 2002.

[80] Lee R Lynd, Charles Wyman, M Laser, D Johnson, and R Landucci. Strategic Biorefinery Analysis: Analysis of Biorefineries. Technical Report October, National Renewable Energy Laboratory, Golden, Colorado, 2005.

[81] S D Phillips, A Aden, J Jechura, David Dayton, and T Eggeman. Thermochemical Ethanol via Indirect Gasification and Mixed Alcohol Synthesis of Lignocellulosic Biomass Thermochemical Ethanol via Indirect Gasification and Mixed Alcohol Synthesis of Lignocellulosic Biomass. Technical Report April, National Renewable Energy Laboratory, Golden, Colorado, 2007.

[82] Carlo N Hamelinck, Geertje Van Hooijdonk, and André PC Faaij. Ethanol from lignocellulosic biomass: techno-economic performance in short-, middle- and long-term. *Biomass and Bioenergy*, 28(4):384–410, April 2005.

[83] U.S. Environmental Protection Agency. Regulation of Fuels and Fuel Additives: 2011 Renewable Fuel Standards; Final Rule. Technical Report 236, U.S. Environmental Protection Agency, 2010.

[84] Lee R Lynd. Overview and Evalutation of Fuel Ethanol from Cellulosic Biomass: Technology, Economics, the Environment, and Policy. *Annual Review of Energy and the Environment*, 21(1):403–465, November 1996.

[85] C R Wilke, R D Yang, A F Sciamanna, and R P Freitas. Raw materials evaluation and process development studies for conversion of biomass to sugars and ethanol. *Biotechnology and Bioengineering*, 23(1):163–183, January 1981.

[86] DoKyoung Lee, Vance N. Owens, Arvid Boe, and Peter Jeranyama. Composition of Herbaceous Biomass Feedstocks. Technical Report June, Plant Science Department South Dakota State University, 2007.

[87] The MathWorks Inc. MATLAB R2009b 64bit, 2009.

[88] Antonio C Caputo, Mario Palumbo, Pacifico M Pelagagge, and Federica Scacchia. Economics of biomass energy utilization in combustion and gasification plants: effects of logistic variables. *Biomass and Bioenergy*, 28(1):35–51, January 2005.

[89] Douglas G Tiffany and Steven J Taff. Current and future ethanol production technologies: costs of production and Rates of Return on invested capital. *International Journal of Biotechnology*, 11(1/2):75, 2009.

[90] Richard Turton, Richard C Bailie, Wallace B Whiting, and Joseph A Shaeiwitz. *Analysis, Synthesis, and Design of Chemical Processes*. Prentice Hall, Upper Saddle River, N.J., 3rd edition, 2009.

[91] Jeff Ferrio and John M Wassick. Chemical supply chain network optimization. *Computers & Chemical Engineering*, 32(11):2481–2504, November 2008.

[92] Pei Liu, Dimitrios I Gerogiorgis, and Efstratios N Pistikopoulos. Modeling and optimization of polygeneration energy systems. *Catalysis Today*, 127(1-4):347–359, September 2007.

[93] Ian M. Bowling, Jose Maria Ponce-Ortega, and Mahmoud M. El-Halwagi. Facility Location and Supply Chain Optimization for a Biorefinery. *Industrial & Engineering Chemistry Research*, 50(10):6276–6286, May 2011.

[94] U.S. Department of Energy. U.S. Billion Ton Update: Complete Data Download, 2011.

[95] U.S. Department of Energy. U.S. Billion-Ton Update: Biomass Supply for a Bioenergy and Bioproducts Industry. Technical report, R.D. Perlack and B.J. Stokes (Leads), ORNL/TM-2011/224. Oak Ridge National Laboratory, Oak Ridge, Tennessee, 2011.

[96] U.S. Department of Agriculture. Office of the Chief Economist. World Agricultural Outlook Board. USDA Agricultural Projections to 2021. Technical report, 2012.

[97] U.S. Environmental Protection Agency. Part 80: EPA Fuels Programs Registered Company/Facility ID List, 2012.

[98] Renewable Fuels Association. Biorefinery locations, 2012.

[99] Robert Wallace, Kelly Ibsen, Andrew J McAloon, and Winnie Yee. Feasibility Study for Co-Locating and Integrating Ethanol Production Plants from Corn Starch and Lignocellulosic Feedstocks. Technical report, National Renewable Energy Laboratory, Golden, Colorado, 2005.

[100] National_Atlas. Raw Data Download, 2012.

[101] D Humbird, R Davis, L Tao, C Kinchin, D Hsu, Andy Aden, P Schoen, J Lukas, B Olthof, M Worley, D Sexton, and D Dudgeon. Process Design and Economics for Biochemical Conversion of Lignocellulosic Biomass to Ethanol: Dilute-Acid Pretreatment and Enzymatic Hydrolysis of Corn Stover. Technical Report May, National Renewable Energy Laboratory, 2011.

[102] Abhijit Dutta, Michael Talmadge, Jesse Hensley, Matt Worley, Doug Dudgeon, David Barton, Peter Groenendijk, Daniela Ferrari, Brien Stears, Erin M Searcy, Christopher T Wright, and J Richard Hess. Process Design and Economics for Conversion of Lignocellulosic Biomass to Ethanol: Thermochemical Pathway by Indirect Gasification and Mixed Alcohol Synthesis. Technical Report May 2011, National Renewable Energy Laboratory, 2011.

[103] A Dutta and S D Phillips. Thermochemical Ethanol via Direct Gasification and Mixed Alcohol Synthesis of Lignocellulosic Biomass. Technical Report July, National Renewable Energy Laboratory, Golden, Colorado, 2009.

[104] Mark M Wright, Justinus A Satrio, Robert C Brown, Daren E Daugaard, and David D Hsu. Techno-Economic Analysis of Biomass Fast Pyrolysis to Transportation Fuels. Technical Report November, National Renewable Energy Laboratory, NREL/TP-6A20-46586, 2010.

[105] Ling Tao, Andy Aden, Richard T Elander, Venkata Ramesh Pallapolu, Y Y Lee, Rebecca J Garlock, Venkatesh Balan, Bruce E Dale, Youngmi Kim, Nathan S Mosier, Michael R Ladisch, Matthew Falls, Mark T Holtzapple, Rocio Sierra, Jian Shi, Mirvat a Ebrik, Tim Redmond, Bin Yang, Charles E Wyman, Bonnie Hames, Steve Thomas, and Ryan E Warner. Process and technoeconomic analysis of leading pretreatment technologies for lignocellulosic ethanol production using switchgrass. *Bioresource technology*, 102(24):11105–14, December 2011.

[106] Erin Searcy, Peter Flynn, Emad Ghafoori, and Amit Kumar. The relative cost of biomass energy transport. *Applied biochemistry and biotechnology*, 137-140(1-12):639–52, April 2007.

[107] W Alex Marvin, Lanny D Schmidt, Saif Benjaafar, Douglas G Tiffany, and Prodromos Daoutidis. Optimizing the Lignocellulosic Biomass-to-Ethanol Supply Chain: A Case Study for the Midwestern United States. In *21st European Symposium on Computer Aided Process Engineering*, volume 29, pages 1728–1732. Computer Aided Chemical Engineering, 2011.

[108] Teofilo F Gonzalez. *Handbook of approximation algorithms and metaheuristics*. Chapman & Hall/CRC, Boca Raton, 2007.

[109] Ignacio E Grossmann and Gonzalo Guillén-Gosálbez. Scope for the application of mathematical programming techniques in the synthesis and planning of sustainable processes. *Computers & Chemical Engineering*, 34(9):1365–1376, September 2010.

[110] Yann Collette and Patrick Siarry. *Multiobjective Optimization: Principles and Case Studies*. Springer, 2003.

[111] Kaisa Miettinen. *Nonlinear Multiobjective Optimization*. Kluwer Academic Publishers, Boston, 1999.

[112] Indraneel Das and J E Dennis. Normal-Boundary Intersection: A New Method for Generating the Pareto Surface in Nonlinear Multicriteria Optimization Problems. *SIAM Journal on Optimization*, 8(3):631–657, August 1998.

[113] Daniel Mueller-Gritschneder, Helmut Graeb, and Ulf Schlichtmann. A Successive Approach to Compute the Bounded Pareto Front of Practical Multiobjective Optimization Problems. *SIAM Journal on Optimization*, 20(2):915–934, January 2009.

[114] George Mavrotas. Effective implementation of the ϵ-constraint method in Multi-Objective Mathematical Programming problems. *Applied Mathematics and Computation*, 213(2):455–465, July 2009.

[115] A M Geoffrion, J S Dyer, and A Feinberg. An Interactive Approach for Multi-Criterion Optimization, with an Application to the Operation of an Academic Department. *Management Science*, 19(4):357–368, 1972.

[116] Kaisa Miettinen, Francisco Ruiz, and Andrzej P Wierzbicki. Introduction to Multiobjective Optimization: Interactive Approaches. In *Multiobjective Optimization*, pages 27–57. Springer, 2008.

[117] CARB (California Air Resources Board). Low Carbon Fuel Standard (LCFS) regulation, 2010.

[118] European Parliament. Directive 2009/28/EC: on the promotion of the use of energy from renewable sources and amending and subsequently repealing Directives 2001/77/EC and 2003/30/EC, 2009.

[119] David D Hsu, Daniel Inman, Garvin a Heath, Edward J Wolfrum, Margaret K Mann, and Andy Aden. Life cycle environmental impacts of selected U.S. ethanol production and use pathways in 2022. *Environmental science & technology*, 44(13):5289–97, July 2010.

[120] Michael Q Wang, Jeongwoo Han, Zia Haq, Wallace E Tyner, May Wu, and Amgad Elgowainy. Energy and greenhouse gas emission effects of corn and cellulosic ethanol with technology improvements and land use changes. *Biomass and Bioenergy*, 35(5):1885–1896, May 2011.

[121] Timothy Searchinger, Ralph Heimlich, R a Houghton, Fengxia Dong, Amani Elobeid, Jacinto Fabiosa, Simla Tokgoz, Dermot Hayes, and Tun-Hsiang Yu. Use of U.S. croplands for biofuels increases greenhouse gases through emissions from land-use change. *Science (New York, N.Y.)*, 319(5867):1238–40, February 2008.

[122] Alexander E Farrell, Richard J Plevin, Brian T Turner, Andrew D Jones, Michael O'Hare, and Daniel M Kammen. Ethanol can contribute to energy and environmental goals. *Science (New York, N.Y.)*, 311(5760):506–8, January 2006.

[123] Michael Wang, Jeongwoo Han, Jennifer B Dunn, Hao Cai, and Amgad Elgowainy. Well-to-wheels energy use and greenhouse gas emissions of ethanol from corn, sugarcane and cellulosic biomass for US use. *Environmental Research Letters*, 7(4):045905, December 2012.

[124] David Tilman, Robert Socolow, Jonathan A Foley, Jason Hill, Eric Larson, Lee Lynd, Stephen Pacala, John Reilly, Tim Searchinger, Chris Somerville, and Robert Williams. Beneficial biofuels–the food, energy, and environment trilemma. *Science*, 325(5938):270–271, July 2009.

[125] May Wu, Michael Wang, and Hong Huo. Fuel-Cycle Assessment of Selected Bioethanol Production Pathways in the United States. Technical report, Argonne National Laboratory, 2006.

[126] Jeongwoo Han, Amgad Elgowainy, I Palou-Rivera, Jennifer B Dunn, and Michael Q Wang. Well-to-Wheels Analysis of Fast Pyrolysis Pathways with GREET. Technical report, Argonne National Laboratory, 2011.

[127] M R Schmer, K P Vogel, R B Mitchell, and R K Perrin. Net energy of cellulosic ethanol from switchgrass. *Proceedings of the National Academy of Sciences of the United States of America*, 105(2):464–9, January 2008.

[128] Argonne National Laboratory - Transportation Technology R&D Center. GREET Model: The Greenhouse Gases, Regulated Emissions, and Energy Use in Transportation Model, 2010.

[129] International Panel on Climate Change (IPCC). Climate Change 2007: Synthesis Report. Technical report, Geneva, Switzerland, 2007.

[130] Earl Christensen, Janet Yanowitz, Matthew Ratcliff, and Robert L McCormick. Renewable Oxygenate Blending Effects on Gasoline Properties. *Energy & Fuels*, 25(10):4723–4733, October 2011.

[131] Pamela P Peralta-Yahya and Jay D Keasling. Advanced biofuel production in microbes. *Biotechnology journal*, 5(2):147–62, February 2010.

[132] Yajun Yan and James C Liao. Engineering metabolic systems for production of advanced fuels. *Journal of industrial microbiology & biotechnology*, 36(4):471–9, April 2009.

[133] George W Huber, Sara Iborra, and Avelino Corma. Synthesis of transportation fuels from biomass: chemistry, catalysts, and engineering. *Chemical reviews*, 106(9):4044–98, September 2006.

[134] Jesse Q Bond, David Martin Alonso, Dong Wang, Ryan M West, and James A Dumesic. Integrated catalytic conversion of gamma-valerolactone to liquid alkenes for transportation fuels. *Science (New York, N.Y.)*, 327(5969):1110–4, February 2010.

[135] L Constantinou, K Bagherpour, R Gani, J A Klein, and D T Wu. Computer aided product design: problem formulations, methodology and applications. *Computers & Chemical Engineering*, 20(6-7):685–702, June 1996.

[136] Anantha Sundaram, Prasenjeet Ghosh, James M Caruthers, and Venkat Venkatasubramanian. Design of fuel additives using neural networks and evolutionary algorithms. *AIChE Journal*, 47(6):1387–1406, June 2001.

[137] Nishanth G. Chemmangattuvalappil, Charles C Solvason, Susilpa Bommareddy, and Mario R Eden. Reverse problem formulation approach to molecular design using property operators based on signature descriptors. *Computers & Chemical Engineering*, 34(12):2062–2071, December 2010.

[138] W Michael Brown, Shawn Martin, Mark D Rintoul, and Jean-Loup Faulon. Designing novel polymers with targeted properties using the signature molecular descriptor. *Journal of chemical information and modeling*, 46(2):826–35, 2006.

[139] Arunprakash T. Karunanithi, Luke E. K. Achenie, and Rafiqul Gani. A New Decomposition-Based Computer-Aided Molecular/Mixture Design Methodology

for the Design of Optimal Solvents and Solvent Mixtures. *Industrial & Engineering Chemistry Research*, 44(13):4785–4797, June 2005.

[140] Nor Alafiza Yunus, Krist V Gernaey, John M Woodley, and Rafiqul Gani. An Integrated Methodology for Design of Tailor-Made Blended Products. In *Proceedings of the 22nd European Symposium on Computer Aided Process Engineering*, number June, pages 752–756. Elsevier Science, 2012.

[141] Nikolaos V Sahinidis, Mohit Tawarmalani, and Minrui Yu. Design of alternative refrigerants via global optimization. *AIChE Journal*, 49(7):1761–1775, July 2003.

[142] Manuel Hechinger, Anna Voll, and Wolfgang Marquardt. Towards an integrated design of biofuels and their production pathways. *Computers & Chemical Engineering*, 34(12):1909–1918, December 2010.

[143] Anna Voll and Wolfgang Marquardt. Reaction network flux analysis: Optimization-based evaluation of reaction pathways for biorenewables processing. *AIChE Journal*, 58(6):1788–1801, June 2012.

[144] Srinivas Rangarajan, Aditya Bhan, and Prodromos Daoutidis. Rule-Based Generation of Thermochemical Routes to Biomass Conversion. *Industrial & Engineering Chemistry Research*, 49(21):10459–10470, November 2010.

[145] Srinivas Rangarajan, Aditya Bhan, and Prodromos Daoutidis. Language-oriented rule-based reaction network generation and analysis: Description of RING. *Computers & Chemical Engineering*, 45:114–123, October 2012.

[146] Joseph J. Bozell and Gene R. Petersen. Technology development for the production of biobased products from biorefinery carbohydratesthe US Department of Energys Top 10 revisited. *Green Chemistry*, 12(4):539, 2010.

[147] Maarten K Sabbe, Freija De Vleeschouwer, Marie-Françoise Reyniers, Michel Waroquier, and Guy B Marin. First principles based group additive values for the gas phase standard entropy and heat capacity of hydrocarbons and hydrocarbon radicals. *The journal of physical chemistry. A*, 112(47):12235–51, November 2008.

[148] Maarten K Sabbe, Mark Saeys, Marie-Françoise Reyniers, Guy B Marin, Veronique Van Speybroeck, and Michel Waroquier. Group additive values for

the gas phase standard enthalpy of formation of hydrocarbons and hydrocarbon radicals. *The journal of physical chemistry. A*, 109(33):7466–80, August 2005.

[149] Shumaila S Khan, Xinrui Yu, Jeffrey R Wade, R Dean Malmgren, and Linda J Broadbelt. Thermochemistry of radicals and molecules relevant to atmospheric chemistry: determination of group additivity values using G3//B3LYP theory. *The journal of physical chemistry. A*, 113(17):5176–94, April 2009.

[150] Sidney W Benson. *Thermochemical Kinetics: Methods for the Estimation of Thermochemical Data and Rate Parameters*. John Wiley & Sons, 1976.

[151] Jean-Paul Lange. Fuels and Chemicals Manufacturing; Guidelines for Understanding and Minimizing the Production Costs. *CATTECH*, 5(2):82–95, 2001.

[152] Janet Yanowitz, Earl Christensen, and Robert L Mccormick. Utilization of Renewable Oxygenates as Gasoline Blending Components Utilization of Renewable Oxygenates as Gasoline Blending Components. Technical Report August, 2011.

[153] J. E. Anderson, U. Kramer, S. a. Mueller, and T. J. Wallington. Octane Numbers of Ethanol and MethanolGasoline Blends Estimated from Molar Concentrations. *Energy & Fuels*, 24(12):6576–6585, December 2010.

[154] Prasenjeet Ghosh, Karlton J. Hickey, and Stephen B. Jaffe. Development of a Detailed Gasoline Composition-Based Octane Model. *Industrial & Engineering Chemistry Research*, 45(1):337–345, January 2006.

[155] Sangbum Lee, Chan Phalakornkule, Michael M Domach, and Ignacio E Grossmann. Recursive MILP model for finding all the alternate optima in LP models for metabolic networks. *Computers & Chemical Engineering*, 24(2-7):711–716, July 2000.

[156] D Simonetti, E Kunkes, and J Dumesic. Gas-phase conversion of glycerol to synthesis gas over carbon-supported platinum and platinumrhenium catalysts. *Journal of Catalysis*, 247(2):298–306, April 2007.

[157] J Brown. Hydrogen production from methanol decomposition over Pt/Al2O3 and ceria promoted Pt/Al2O3 catalysts. *Catalysis Communications*, 5(8):431–436, August 2004.

[158] Surapas Sitthisa, Tawan Sooknoi, Yuguang Ma, Perla B. Balbuena, and Daniel E. Resasco. Kinetics and mechanism of hydrogenation of furfural on Cu/SiO2 catalysts. *Journal of Catalysis*, 277(1):1–13, January 2011.

[159] Juan Carlos Serrano-Ruiz and James A Dumesic. Catalytic upgrading of lactic acid to fuels and chemicals by dehydration/hydrogenation and CC coupling reactions. *Green Chemistry*, 11(8):1101, 2009.

[160] Garry C. Gunter, Robert H. Langford, James E. Jackson, and Dennis J. Miller. Catalysts and Supports for Conversion of Lactic Acid to Acrylic Acid and 2,3-Pentanedione. *Industrial & Engineering Chemistry Research*, 34(3):974–980, March 1995.

[161] Marcelo J L Gines and Enrique Iglesia. Bifunctional Condensation Reactions of Alcohols on Basic Oxides Modified by Copper and Potassium. *Journal of Catalysis*, 176(1):155–172, May 1998.

[162] Wataru Ueda, Takuo Ohshida, Tetsuo Kuwabara, and Yutaka Morikawa. Condensation of alcohol over solid-base catalyst to form higher alcohols. *Catalysis Letters*, 12(1-3):97–104, 1992.

[163] Salvador Ordóñez, Eva Díaz, Marta León, and Laura Faba. Hydrotalcite-derived mixed oxides as catalysts for different CC bond formation reactions from bioorganic materials. *Catalysis Today*, 167(1):71–76, June 2011.

[164] Jesse Q Bond, David Martin Alonso, Ryan M West, and James a Dumesic. γ-Valerolactone ring-opening and decarboxylation over SiO2/Al2O3 in the presence of water. *Langmuir*, 26(21):16291–8, November 2010.

[165] Hsu Chiang and Aditya Bhan. Catalytic consequences of hydroxyl group location on the rate and mechanism of parallel dehydration reactions of ethanol over acidic zeolites. *Journal of Catalysis*, 271(2):251–261, May 2010.

[166] Helmut Knözinger, Horst Bühl, and Karel Kochloefl. The dehydration of alcohols on alumina XIV. Reactivity and mechanism. *Journal of Catalysis*, 24(1):57–68, January 1972.

[167] Christian A Gaertner, Juan Carlos Serrano-Ruiz, Drew J Braden, and James A Dumesic. Ketonization Reactions of Carboxylic Acids and Esters over CeriaZirconia as Biomass-Upgrading Processes. *Industrial & Engineering Chemistry Research*, 49(13):6027–6033, July 2010.

[168] U.S. Energy Information Association. U.S. States: State Profiles and Energy Estimates, 2013.

[169] National Biodiesel Board. Biodiesel Plants Listing, 2013.

[170] Biodiesel Magazine. USA Plants, 2013.

[171] National Renewable Energy Laboratory. BioFuels Atlas, 2013.

[172] U.S. Department of Energy. Bioenergy Knowledge Discovery Framework, 2013.

[173] Laura J Vimmerstedt, Brian Bush, and Steve Peterson. Ethanol distribution, dispensing, and use: analysis of a portion of the biomass-to-biofuels supply chain using system dynamics. *PloS one*, 7(5):e35082, January 2012.

[174] Anthony Halog and Nana Awuah Bortsie-Aryee. The Need for Integrated Life Cycle Sustainability Analysis of Biofuel Supply Chains. In Zhen Fang, editor, *Biofuels - Economy, Environment and Sustainability*, chapter 7. InTech, 2013.

[175] Oscar Van Vliet, Bert De Vries, André Faaij, Wim Turkenburg, and Wander Jager. Multi-agent simulation of adoption of alternative fuels. *Transportation Research Part D: Transport and Environment*, 15(6):326–342, August 2010.

[176] Matteo Dal Mas, Sara Giarola, Andrea Zamboni, and Fabrizio Bezzo. Capacity planning and financial optimization of the bioethanol supply chain under price uncertainty. In S. Pierucci and G. Buzzi Ferraris, editors, *20th European Symposium on Computer Aided Process Engineering - ESCAPE20*, volume 28, pages 97–102. Elsevier B.V., 2010.

[177] Berhane H Gebreslassie, Yuan Yao, and Fengqi You. Design under uncertainty of hydrocarbon biorefinery supply chains: Multiobjective stochastic programming models, decomposition algorithm, and a Comparison between CVaR and downside risk. *AIChE Journal*, 58(7):2155–2179, July 2012.

[178] Urmila M Diwekar. Optimization Under Uncertainty in Chemical Engineering. In *Proceedings of the Indian National Science Academy - Part A*, pages 267–284, 2003.

[179] Vira Chankong, Yacov Y Haimes, and David M Gemperline. A multiobjective dynamic programming method for capacity expansion. *IEEE Transactions on Automatic Control*, 26(5):1195–1207, October 1981.

[180] Anshuman Gupta and Costas D Maranas. Managing demand uncertainty in supply chain planning. *Computers & Chemical Engineering*, 27(8-9):1219–1227, September 2003.

[181] Fengqi You, John M Wassick, and Ignacio E Grossmann. Risk management for a global supply chain planning under uncertainty: Models and algorithms. *AIChE Journal*, 55(4):931–946, April 2009.

[182] Srinivas Rangarajan, Aditya Bhan, and Prodromos Daoutidis. Identification and analysis of synthesis routes in complex catalytic reaction networks for biomass upgrading. *Applied Catalysis B: Environmental*, February 2013.